DIPLOMA THESIS

Ground vibrations measurements during roadway drifting, propagation of ground vibrations and impact quantification in the surrounding rock mass of roadheader and drill & blast development

(Erschütterungsmessungen während des Streckenvortriebs unter Tage, Ausbreitung von Erschütterungen und Quantifizierung des Energieeintrages in das umgebende Gebirge durch Teilschnittmaschinenvortrieb und Bohr- und Sprengvortrieb)

Submitted to the
Department of Mineral Resources and Petroleum Engineering
Chair of Mining Engineering and Mineral Economics
at the
University of Leoben

by

Florian Georg Egger

Reviewer:
A.o.Prof. Dipl.-Ing. Dr.mont. Peter Moser
Dipl.-Ing. Christian Heiss

Assessor:
o.Univ. Prof. Dipl.-Ing. Dr.mont. Horst Wagner

Leoben, July 2006

Acknowledgement

First of all, I would like to thank the mining and tunneling companies RHI-Magnesite Mine Breitenau, VOEST ALPINE Iron Ore Mine and Wolfram Mine Mittersill for providing the sites for in-situ measurements.

I am deeply grateful for the support and help of the VOEST ALPINE Bergtechnik for providing the access to roadheader specific data and to rock testing facilities.

I would also like to thank all my colleagues of the Chair of Mining Engineering and Mineral Economics at the University of Leoben.

My cordial thanks go to Mr. Dipl.-Ing. Christian Heiss, who untiringly helped me to accomplish the underground measurements on which the thesis is based.

This work is dedicated to my father Georg. May he rest in peace.
(Diese Diplomarbeit ist meinem Vater Georg gewidmet. Möge er in Frieden ruhen.)

Erklärung

Ich erkläre an Eides statt, dass ich die vorliegende Diplomarbeit selbstständig und unter ausschließlicher Verwendung der angeführten Literaturstellen angefertigt habe.

I declare on oath to have made this Diploma Thesis self-dependently and to have used none but the stated literature and sources.

Leoben, July 2006 Florian Georg Egger

Abstract

Mechanical excavation as well as excavation by means of drilling and blasting (D&B) causes an impact of energy to the surrounding rock mass that generates ground vibrations. These vibrations are transmitted through the rock mass as seismic body and surface waves and may cause as a function of the distance damage to the surrounding rock mass.

To estimate the loss of energy along a certain distance from the drift face and to approximate the cumulated impact of energy as well as the cumulated vibrations, the following three main objectives were specified:

1. the examination of a measuring program to complete the existing ground vibration measurement data of roadheader and D&B development in different underground mines und tunnel sites during roadway drifting
2. the development of a model for the propagation of ground vibrations caused by roadheader development and D&B development along the sidewalls of drifts, that considers different surrounding conditions like rock and rock mass quality, geometrical conditions and impact parameters
3. the development of a model to quantify the cumulative impact during the excavation of 1m roadway along the roadway axis

In the present investigation more than 400 in situ measurements were performed in two underground mines, two tunnel sites and at a test rig on a one to one scale for roadheader development and in three underground mines for D&B development.
All roadheader development was done by the means of an ALPINE MINER ATM 105 manufactured by VOEST- ALPINE Bergtechnik Zeltweg.
Ground vibrations of full rounds as well as of single shots were measured for D&B development.
Triaxial geophones, which were either fixed in boreholes or on the roadway surface, were used to measure the ground motion. For further analysis the dominating frequencies of the ground vibrations and a number of statistical parameters were determined from the observed data.

Since the simulation of the intricate process of drifting and the complex form of seismic wave propagation in the rock mass partly rests on assumptions, it remains crucial to keep in mind that in spite of an extensive scale of data reality can never be strictly described. Hence the approximated data must be considered with caution.

Analysis and modelling had to deal with the problem of over-fitting of data. Dimensional analysis and regression analysis were used to determine a propagation function for ground vibrations considering different rock, rock mass and geometrical conditions.

The absorption factor was determined by performing an analysis using the measurement results of four drifts developed by means of roadheader. There the correlation coefficient, which was reached in the least squares analysis, was 0,69.

The parameters with the widest influence on the value of the absorption factor were:

- the rock mass rating
- the density
- the Young's Modulus
- the overburden
- the frequency.

The absorption coefficients varied from 10^{-7} m^{-1} to 10^{-1} m^{-1} for the test sites.

The parameter considering the wave type (spherical wave or plate wave) was the distance of the considered element to the next surface.

The following figure shows the propagation functions for ground vibrations in different distances in front and behind the drift face. The propagation functions are related to a depth of 0,3m in the sidewall of the roadways.

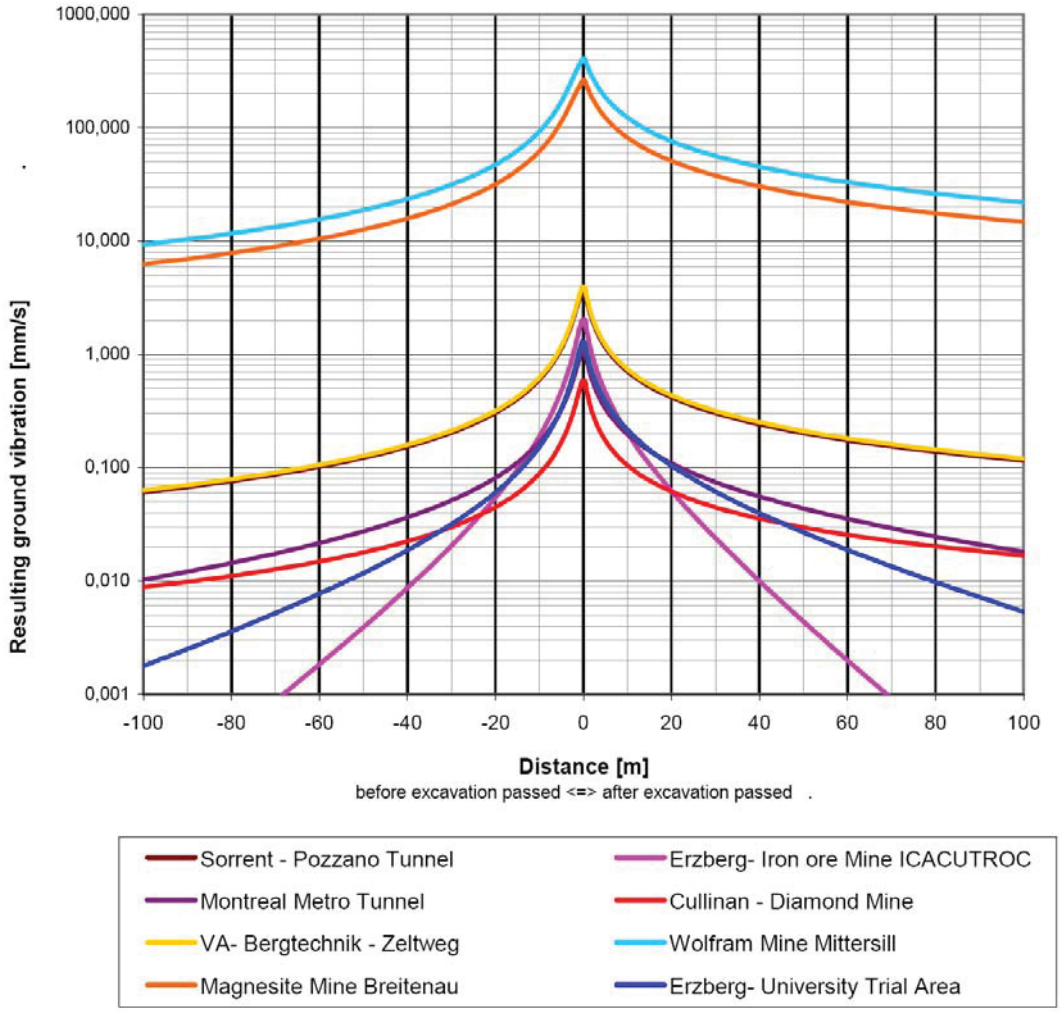

The third main objective was the quantification of the impact energy. As a result of the complex form of the propagation function an approximation solution was performed to quantify the impact of energy either per meter drift development or per m³ of excavated rock considering the following factors:

- the energy consumption of the excavation method E_{spec} (energy consumption of the cutting head, energy of the explosives)
- the radiated seismic energy ($E_{spec,rad}$) for one unit element at certain distances in the sidewall
- the cumulated radiated seismic energy E_{rad}
- the seismic efficiency factor η_{SE} (quotient of the cumulated radiated seismic energy and the energy consumption of the excavation method E_{rad} / E_{spec})
- the impact quantification number IQN, which is related to the cumulated movement of the unit element

On a *Microsoft Excel*® interface the different geometrical, rock and rock mass conditions as well as drifting specific parameters of the test sites were used to estimate the resulting ground vibrations at certain distances from the drift face and to estimate the impact of energy for a unit element in a certain depth of the sidewall of the roadway.

As only the cutting mode “horizontal slewing” was considered in this analysis, care has to be taken at the interpretation of the energy consumption of the roadheader.

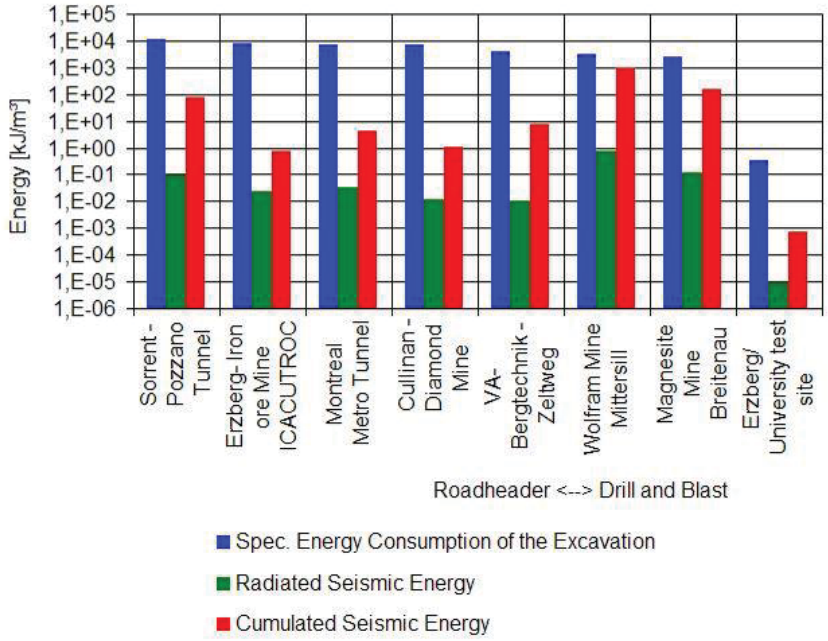

The simulation showed a higher energy consumption for roadheader development than for D&B development (full round of shots), whereas the radiated seismic energy for a unit element and the cumulated seismic energy was lower for roadheader development. Consequently, the seismic efficiency, which is the quotient of cumulated seismic energy and the energy of the excavation process, was smaller for roadheader development than for D&B development.

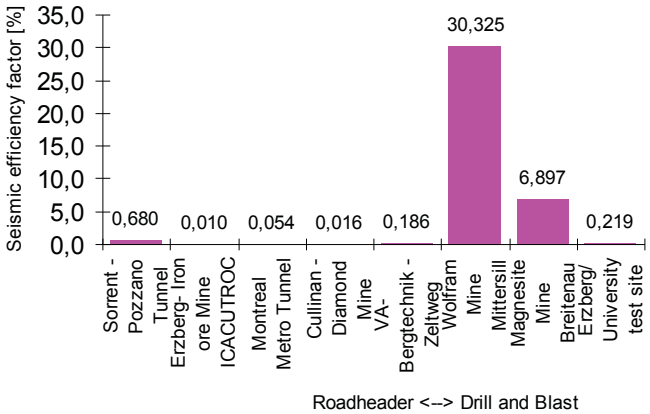

An impact quantification number was defined, which gives an indication of the cumulative oscillation movement of a unit element of rock for the whole excavation process, e.g. initially the element is ahead of the excavation, then the element is in the vicinity of the excavation and ultimately it is distance from the excavation face. The impact quantification number was higher for roadheader development than for D&B development, because in the case of a roadheader the unit element is permanently subjected to oscillations caused by the roadheading drum, whereas in D&B the unit element is only subjected to ground vibrations during blasting time. This means that in the case of a roadheader development the duration of excitation is about 10^5 times higher than that of D&B development.

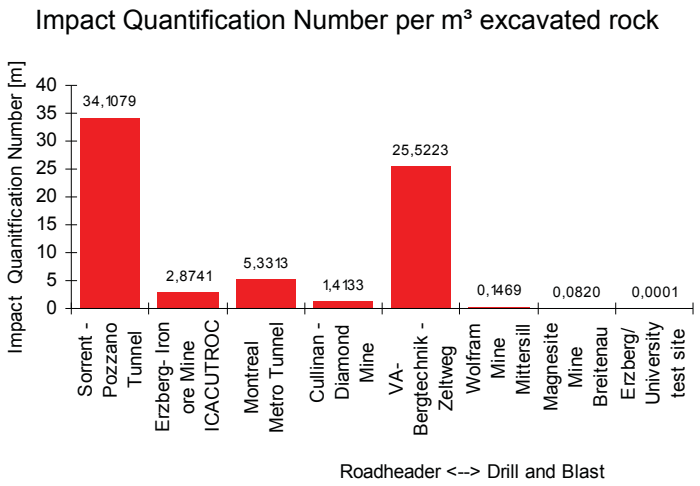

The estimation of the impact energy into the surrounding rock mass caused by different excavation methods could be a substantial help for a better understanding and approximation of the degree of rock disintegration around roadways, since the impact energy may be one of the main influencing variables on the genesis of the excavation damaged zone (EDZ).

Kurzfassung

Maschineller Vortrieb induziert, wie auch der Vortrieb durch Bohren und Sprengen, mechanische Energie ins umliegende Gebirge, die zum Teil in Vibration umgewandelt wird. Die Vibrationen während des Schneide- bzw. Sprengvorganges des Gesteins werden als Körper- oder Oberflächenwellen im Gebirge weitergeleitet und können zu Rissbildungen im Gestein und Auflockerung der umliegenden Gebirgsmasse führen.

Um den Verlust an seismischer Energie mit zunehmender Entfernung zur Vortriebstätigkeit zu bestimmen und den kumulierten Eintrag an seismischer Energie und die kumulierte Oszillation eines Volumselementes abschätzen zu können, wurden drei schwerpunktmäßige Arbeitsschritte festgelegt:

1. die Ausarbeitung eines Messprogramms zur Vervollständigung der vorhandenen Erschütterungsmessungen in verschiedenen untertägigen Bergwerken und Tunnelbauen mit Teilschnittmaschinen-, Bohr- und Sprengvortrieben
2. die Entwicklung einer Funktion der Ausbreitung von Erschütterungen entlang von Strecken, die unterschiedliche Gesteins- und Gebirgseigenschaften, sowie hohlraumspezifische Eigenschaften und vortriebsspezifische Parameter berücksichtigt
3. die Entwicklung eines Modells zur Abschätzung des kumulierten Eintrags an seismischer Energie und Vibration während der Dauer des gesamten Streckenvortriebes

Im ersten Arbeitsschritt fanden in-situ Messungen bei Vortrieben mit Teilschnittmaschinen in zwei untertägigen Bergbauen, zwei Tunneln und bei einem im Maßstab 1:1 durchgeführten Demonstrationsversuch an einem Betonblock statt. In drei untertägigen Bergbauen wurden Messungen bei Sprengvortrieben durchgeführt.
Alle maschinellen Vortriebe wurden mit der Teilschnittmaschine ALPINE MINER ATM105 der VOEST-ALPINE Bergtechnik Zeltweg ausgeführt. Bei den Sprengvortrieben wurden Erschütterungen kompletter Abschläge und von Einzelschüssen mit verschiedenen Sprengstoffen aufgezeichnet.

Digitale Messsysteme mit Triaxialgeophonen, die entweder bis 5m tief in die Streckenulme durch Horizontalbohrlöcher eingebracht oder an der Streckensohle verankert wurden, kamen zur Anwendung.

In der vorliegenden Diplomarbeit wurden Rohdaten von über 400 Erschütterungsmessungen mit *Diadem National Instruments*® automatisiert ausgewertet, um vornehmlich die resultierenden Schwinggeschwindigkeiten und die korrespondierenden Frequenzen, sowie eine Reihe statistischer Kenngrößen der einzelnen Messungen einheitlich zu bestimmen.

Da um den komplexen Vorgang der Vortriebstätigkeit, der Einleitung seismischer Wellen ins sowie deren Ausbreitung im Gebirge simulieren zu können, eine Reihe von Vereinfachungen und Approximationen gemacht werden mussten, ist trotz der großen Anzahl von Messdaten eine exakte Reproduktion der Bedingungen, welche zum Zeitpunkt der Messungen vorherrschten, nur sehr schwer möglich. Die ermittelten Kennzahlen und Parameter sind daher mit Vorsicht anzuwenden.

Um verschiedene Gesteins- und Gebirgseigenschaften sowie hohlraumspezifische Eigenschaften und vortriebsspezifische Parameter zu simulieren, wurde das mehrfach überbestimmte Gleichungssystem der Ausbreitungsfunktion seismischer Wellen mit Hilfe der Dimensionsanalyse, dem Buckingham Pi Theorem und einer Regressionsanalyse gelöst.
Die Ausbreitungsfunktion besteht, um die Abnahme der Energiedichte mit zunehmender Entfernung anhand der Wellenart zu berücksichtigen, aus einer Potentialfunktion und, da seismische Wellen in Festkörpern absorbiert werden, wobei durch innere Reibung seismische Energie hauptsächlich in Wärmeenergie umgewandelt wird, einer Exponentialfunktion.

Zur Bestimmung des Absorptionskoeffizienten wurden in der Analyse Daten aus vier verschiedenen Vortrieben mit Teilschnittmaschinen verwendet. Der damit erreichte Korrelationskoeffizient betrug 0,69.

Die Dimensionsanalyse verdeutlichte u. a. die Sensibilität des Absorptionskoeffizienten auf Änderung verschiedener Parameter: Auf Veränderungen der nachstehenden Parameter reagierte der Absorptionskoeffizient sehr sensibel:

- das Rock Mass Rating
- die Dichte des Gesteins
- das Elastizitätsmodul des Gesteins
- die Teufe des Hohlraumes
- die Frequenz der Erschütterung

Der Absorptionskoeffizient variierte zwischen 10^{-5} bis 10^{-1} m^{-1}. Als Parameter zur Berücksichtigung der Wellenform wurde die Tiefe der Geophone bzw. des betrachteten Volumselementes im Ulm bzw. in der Sohle herangezogen.

Das folgende Diagramm zeigt eine Übersicht über die Ausbreitungsfunktionen der resultierenden Erschütterungen für die verschiedenen Messorte. Die Ausbreitungsfunktion bezieht auf eine Tiefe von 0,3m im Ulm.

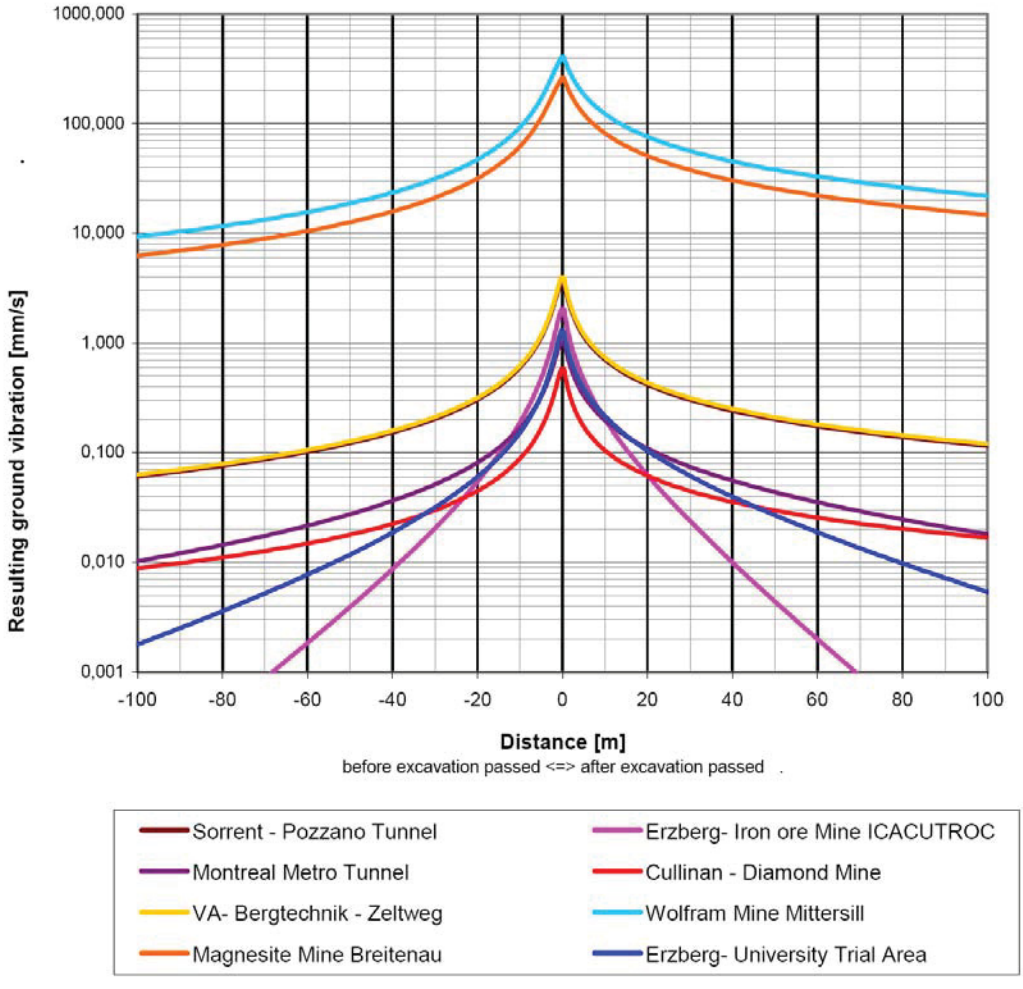

Der dritte Schwerpunkt dieser Arbeit lag in der Quantifizierung des Eintrages an seismischer Energie in das Gebirge. Aufgrund der komplexen Ausbreitungsfunktion seismischer Wellen wurde eine Approximationsrechnung entwickelt. Der Energieeintrag wurde durch folgende fünf Kennziffern beschrieben:

1. den Energieverbrauch der Vortriebsmethode (Energieverbrauch des Schneidkopfes bzw. spezifische Energie der Sprengstoffe)
2. den seismischen Energieeintrag in ein Volumselement von 1m³ in beliebiger Tiefe in der Ulme
3. die spezifische kumulierte seismische Energie
4. den seismischen Wirkungsgrad (Quotient aus kumulierter seismischer Energie und Energieverbrauch der Vortriebsmethode)
5. die Impakt-Quantifizierungs-Ziffer, die relativ zum kumulierten Weg eines Elements während der gesamten Vortriebsdauer ist.

Diese Kennziffern wurden jeweils auf 1m axialen Streckenvortrieb oder auf 1m³ hereingewonnenes Gebirge bezogen .

Anhand einer *Microsoft Excel*® Oberfläche konnten die verschiedenen Vortriebssituationen nachgestellt werden. Die Simulation erfolgte für ein Element der Streckenulme in 0,3m Tiefe. Der Energieverbrauch des Schneidkopfes bezog sich jeweils nur auf horizontales Schwenken.

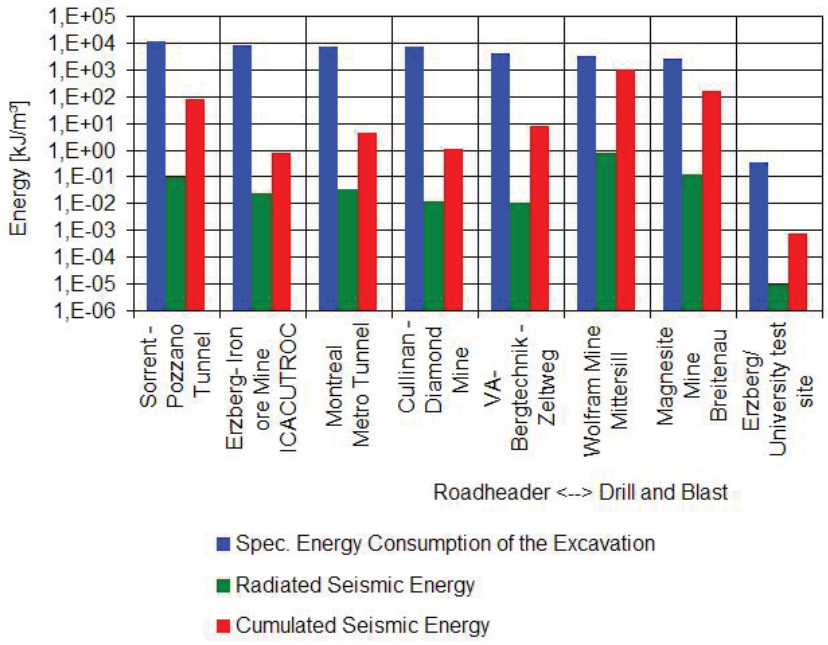

Die Simulation zeigte bei Vortrieben mit Teilschnittmaschinen einen höheren spezifischen Energieverbrauch als bei Bohr- und Sprengvortrieben, wobei aber der seismische Energieeintrag in ein betrachtetes Volumselement, sowie die spezifische kumulierte seismische Energie pro m³ hereingewonnenes Gebirge bei Bohr- und Sprengvortrieben höher war als bei Vortrieben mit Teilschnittmaschinen. Folglich waren auch die seismischen Wirkungsgrade für die Teilschnittmaschinenvortriebe geringer.

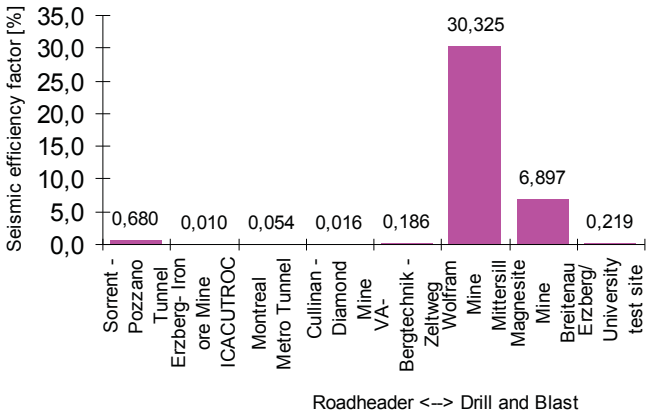

Da die ermittelte Netto-Ausbruchgeschwindigkeit für Sprengvortriebe etwa um den Faktor 10^5 höher war als jene der Teilschnittvortriebe, waren auch die Impakt-Quantifizierungs-Ziffern der untersuchten Vortriebe mit Teilschnittmaschinen im Bereich von 10 bis 400 mal größer als die der untersuchten Sprengvortriebe.

Impakt-Quantifizierungs-Ziffer pro m³ hereingewonnenes Gebirge

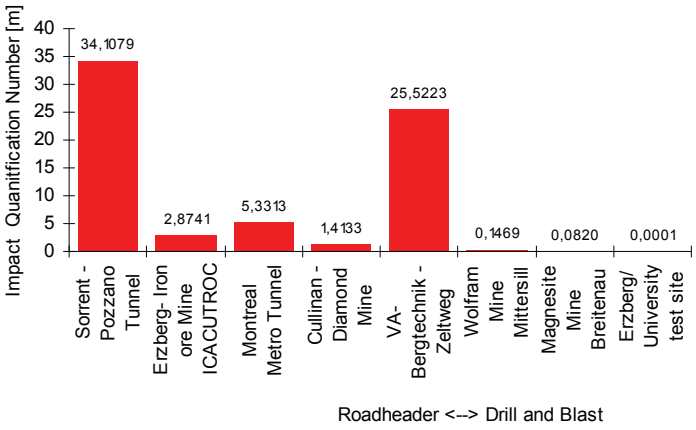

Auf Grund der Tatsache, dass der Energieeintrag verschiedener Vortriebsmethoden in das umliegende Gebirge eine wichtige Einflussgröße bei der Entstehung der Excavation Damaged Zone (EDZ, durch die Vortriebstätigkeit verursachte geschädigte Zone um eine Strecke) darstellen könnte, kann seine Ermittlung ein besseres Verständnis und eine bessere Abschätzung der geschädigten Zone und der Gebirgsauflockerung um Strecken bewirken.

Table of contents

List of Tables

List of Figures

1 General introduction

When an explosive detonates or the chisels of the cutting head of a roadheader are cutting rock, the impact generates waves in the surrounding media resulting in ground vibrations. The vibrations generated in blasting and cutting are transmitted through the rock mass as seismic body waves and surface waves. These waves can cause severe damage to the surrounding rock mass.

Hitherto functions to predict ground vibrations are mainly used for blasting operations in open pit mines. These relationships were determined iteratively, normally using one parameter for the rock mass conditions and one parameter for the impact of energy (e.g. mass of explosive). These functions are not satisfactory to predict ground vibrations along the sidewall of roadways for different rock conditions, rock mass conditions and geometrical conditions as well as different impacts of energy [14],[26].

In the present investigation a number of in situ measurements in different underground mines and tunnel sites using triaxial geophones, which were either fixed in boreholes or mounted on the surface of the roadway, were performed. The observed data was used for analysis and modelling. To deal with the problem of over fitting of data dimensional analysis and regression analysis were used to determine a propagation function for ground vibrations considering different:

- rock conditions
- rock mass conditions
- geometrical conditions
- impact parameters
- wave types

By knowing the propagation function, a model for the impact energy was set up and a *Microsoft Excel*® Interface was created to replicate different site conditions and to quantify the impact of energy.

2 Geophysical basics

Mechanical excavation as well as excavation by means of drilling and blasting (D&B) causes vibrations in the surrounding rock mass. However, it is important to explain the geophysical basics of wave types, wave propagation, reflection and refraction. Information for this Chapter was taken from the Non-Destructive-Research-Center at Iowa State University [28].

2.1 Wave propagation

Ground vibration measurements are based on the motion of particles in materials, which is generally referred to its acoustics. All materials consist of atoms, which may be forced into a vibrational motion around their equilibrium positions. Several patterns of vibrational motion exist at the atomic level, however, most are irrelevant to acoustics and ground vibrations. Acoustics is focused on particles that contain many atoms that move in unison to produce a mechanical wave. When a material is not stressed in tension or compression beyond its elastic limit, its individual particles perform elastic oscillations. When the particles of a medium are displaced from their equilibrium positions, internal restoration forces arise. These elastic restoring forces between particles, combined with inertia of the particles, lead to oscillatory motions of the medium.

In solids, sound waves can propagate in four principle modes that are based on the way the particles oscillate. Sound can propagate as longitudinal waves, shear waves, surface waves, and in thin materials as plate waves. The particle movement responsible for the propagation of longitudinal and shear waves is illustrated in Figure 2.1.

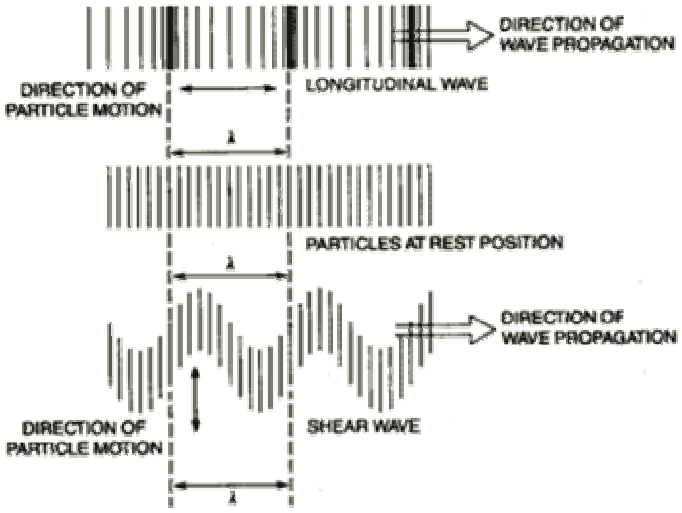

Figure 2.1: Propagation of longitudinal and shear waves

In longitudinal waves the oscillations occur in the longitudinal direction or the direction of wave propagation. Since compressional and dilational forces are active in these waves, they are also called pressure or compressional waves. They are also sometimes called density waves because their particle density fluctuates as they move. Compression waves can be generated in liquids as well as in solids because the energy travels through the atomic structure by a series of comparison and expansion movements.

In the transverse or shear wave the particles oscillate at a right angle or transverse to the direction of propagation. Shear waves require an acoustically solid material for effective propagation and, therefore, are not effectively propagated in materials such as liquids or gasses. Shear waves are relatively weak when compared to longitudinal waves. In fact, shear waves are usually generated in materials using some of the energy from longitudinal waves.

2.2 Modes of wave propagation

In solids molecules can support vibrations in all directions, hence a number of different types (modes) of sound waves are possible. However, at surfaces and interfaces various types of elliptical or complex vibrations of the particles make other wave modes possible.

Table 2.1 summarizes a number of possible wave modes in solids.

wave modes	*particle vibrations*
Longitudinal	parallel to wave direction
Transverse (Shear)	perpendicular to wave direction
Surface - Rayleigh	elliptical orbit - symmetrical mode
Plate Wave - Lamb	component perpendicular to surface (extensional wave)
Plate Wave - Love	parallel to plane layer, perpendicular to wave direction
Stoneley (Leaky Rayleigh Waves)	wave guided along interface

Table 2.1: Wave types in solids

Surface or Rayleigh waves travel along the surface of a relative thick solid material penetrating to a depth of one wavelength. The particle movement has an elliptical orbit as shown in Figure 2.2.

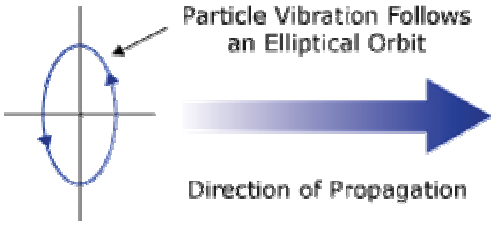

Figure 2.2: Particle movement in Rayleigh wave

2.3 Sound propagation in elastic material

Sound waves propagate due to the vibrations or oscillatory motions of particles within a material. Waves in the rock mass may be visualized as an infinite number of oscillating masses or particles connected by means of elastic springs. Each individual particle is influenced by the motion of its nearest neighbor and both inertial and elastic restoring forces act upon each particle.

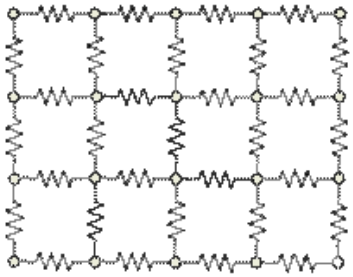

Figure 2.3: Spring model

A mass on a spring has a single resonant frequency determined by its spring constant **k** and its mass **m**. The spring constant is the restoring force of a spring per unit of length. Within the elastic limit of any material, there is a linear relationship between the displacement of a particle and the force attempting to restore the particle to its equilibrium position. This linear dependency is described by **Hooke's Law**.

In terms of the spring model, Hooke's Law says that the restoring force due to a spring is proportional to the length the spring is stretched to and acts in the opposite direction. Mathematically, Hooke's Law is written, **F =** $-\psi A_{PD}$, where **F** is the force, ψ is the spring constant, and A_{PD} is the amount of particle displacement. Hooke's law is represented graphically in Figure 2.4.

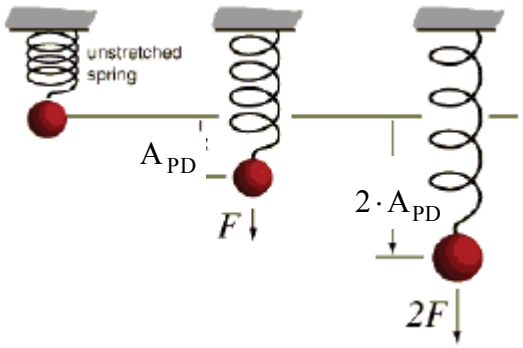

(1) $F = \psi \cdot A_{PD}$

Figure 2.4: Hooke's law

Note that the spring is applying a force to the particle that is equal and opposite to the force pulling down on the particle.

The mass of the particles is related to the density of the material, and the spring constant is related to the elastic constants of a material. The typical elastic constants of materials include:

- the Young's Modulus, Y_M: a proportionality constant between uniaxial stress and strain
- the Poisson's Ratio, ν: the ratio of radial strain to axial strain
- the Shear Modulus, G: also called rigidity, a measure of material´s resistance to shear

In isotropic materials, the elastic constants are the same for all directions within the material. However, rock is anisotropic and the elastic constants differ with each direction.

The motion of the particles causes a force F. When the force leads to a stress higher than the strength of the spring between the oscillating particles, the spring cracks. Thinking of a rock mass, this case results in rock disintegration caused by the forces of the motion of the particles.

2.4 Acoustic impedance, reflection, transmission and refraction

Sound waves travel through materials under the influence of sound pressure. Because molecules or atoms of a solid are bound elastically to one another, the excess pressure results in a wave propagating through the solid.

The acoustic impedance is important in:

- the determination of acoustic transmission and reflection at the boundary of two materials having different acoustic impedance
- the design of ultrasonic transducers
- assessing **absorption** of sound in a medium

Mechanical waves are reflected at boundaries where there are differences in acoustic impedance, Z. This is commonly referred to as an impedance mismatch. The fraction of the incident-wave intensity in reflected waves can be derived because particle

velocity and local particle pressures are required to be continuous across the boundary between materials.

The acoustic reflection and transmission coefficients (pressure) can be calculated using the following formulas:

(2) $Z_1 = \rho_1 \cdot v_1$

$Z_2 = \rho_2 \cdot v_2$

(3) $R = \left(\frac{Z_2 - Z_1}{Z_2 + Z_1} \right)^2$

(4) $TM = 1 - \left(\frac{Z_2 - Z_1}{Z_2 + Z_1} \right)^2$

Z_i... Accoustic impedance [kg/m²s]
ρ_i... Density [kg/m³]
v_i... Velocity of propagation [m/s]
R... Reflection coefficient [-]
TM... Transmission coefficient [-]

The acoustic impedance (Z) of a material is defined as the product of density (ρ) and acoustic velocity (v) of that material. The reflected energy is the square of the difference of the acoustic impedances of the two materials divided by their sum.

If reflection and transmission at interfaces are followed through the component and loss by attenuation is ignored, a small percentage of the original energy returns to the transducer.

Refraction takes place at an interface due to the different velocities of the acoustic waves within two materials. The velocity of sound in each material is determined by the material properties (Young's Modules and density) for that material, e.g. a series of plate waves travel in one material and enter a second material that has a higher acoustic velocity. Therefore, when the wave encounters the interface between these two materials, the portion of the wave in the second material is moving faster than the portion of the wave in the first material. That causes the wave to bend.

Snell's Law describes the relationship between the angles and the velocities of the waves. Snell's law equates the ratio of material velocities v_1 and v_2 to the ratio of the sins of incident (Θ_1) and refraction (Θ_2) angles, as shown in the following equation.

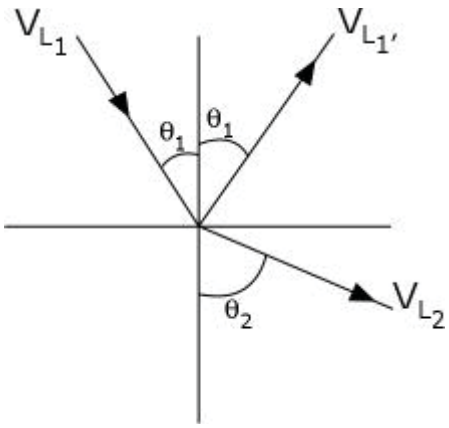

(5) $$\frac{\sin\theta_1}{V_{L_1}} = \frac{\sin\theta_2}{V_{L_2}}$$

Where: v_{L1} is the longitudinal wave velocity in material 1.

v_{L2} is the longitudinal wave velocity in material 2.

Figure 2.5: Snell´s Law

In Figure 2.5 a reflected longitudinal wave (v_{L1}) is also shown. This wave is reflected at the same angle as the incident wave, because the two waves are traveling in the same material and, therefore, have the same velocities. This reflected wave is unimportant in the explanation of Snell's Law.

3 Information about the applied measurement systems

In this work three different types of vibration measurement systems were used for investigations about sound propagation in hard rock:

- Ground vibration measurements close to the surface:
  1. Measurement system with triaxial geophones arranged close to the surface (VIBRAS 2004/3004)
- Ground vibration measurements in boreholes
  2. Measurement system with triaxial geophones - fixing with concrete
  3. Measurement system with triaxial geophones - mechanical mounting

3.1 Ground vibration measurements close to the surface

This system was also applied for measurements carried out by the Department of Mining Engineering at the University of Leoben in former projects. [22]
Thereby obtained data were compared to data of this work.

3.1.1 Measurement equipment

The VIBRAS 2004/3004 measurement system comprises two main devices: the measuring station and the evaluation device.

3.1.1.1 Measuring station

The measuring station is an analogue triaxial measuring device, which includes three geophone coils for absorbing vibrations in the x-, y- and z-axis. A circular spirit level on the case lid serves to control the correct set up. The measuring station holds a temporary buffer store, which serves as an interim store for the measured vibrations. As soon as the store is full, the oldest data are transmitted to the evaluation device for analysis.

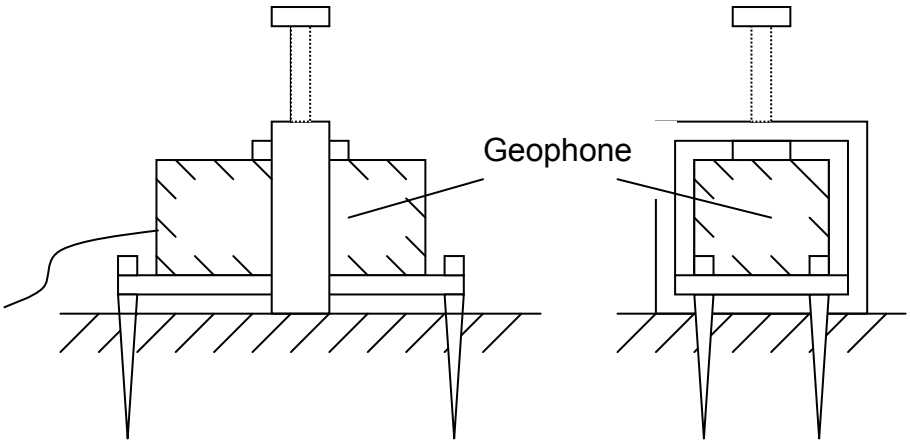

Figure 3.1: Mounting of geophone in footwall

For vibration measurements of good quality a perfect contact between geophone and rock is of greatest importance. Poor contact leads to falsified measuring results. For this reason a solid mounting of the geophones on the rock of the footwall is necessary. Mounting is done by an iron plate with 4 iron spikes of 10 cm length, which are driven into the rock by hammer strikes. The geophone is fixed on the plate with an iron screw-clamp (mounting of geophone is shown in Figure 3.1).

3.1.1.2 Evaluation device

The primary tasks of the evaluation device are to control the measuring stations, to collect and evaluate the delivered data.

The output of the analysis comprises:

- the components (peak particle velocity of the individual axis)
- the maximum peak particle velocity
- the vectorial graph (as graphical depiction)
- the frequency analysis (Fast Fourier Transformation) of the components x, y, z envelope (as graphical depiction)

Both, the device protocol and the measuring station protocol, can be printed out. During the investigations in Montreal an additional possibility, which subsequently should be processed further, was used to pass this evaluation onto a laptop.

VibModem is the software used for the recording and Vibchart is the software used for the evaluation.

An integral part of the measurement is the right choice of the operating mode of the evaluation device which must be selected according to the kind of the impact.
For the subscribed investigations two different operating modes were selected:

1. blast (single event)
2. impact driving (continuous measurement)

3.1.2 Operation mode

Actually, according to the kind of the impact, only the operating mode ‘impact driving’ would have been the right choice. However, since former measurements had always predefined the operating mode ‘blast’, for a direct comparison of the measuring results the operating mode ‘blast’ was chosen in the first measuring run and the operating mode ‘impact driving’ in the second run.

Operating mode – BLAST (single event)
In this setting single events are recorded and the analysis gives

- the components x, y, z
- the vectorial graph
- the frequency analysis of the components x, y, z

In principle, most different parameters can be freely defined for the particular operating mode. One of the important parameters is the ’time window around the highest peak value’ (or registration time). Then further evaluation, e.g. the frequency analysis, is carried out according to this predefined time window.

Operating mode – IMPACT DRIVING (continuous measurement)
This operating mode records on going events. Compared to the blast operation mode there is a difference in registration time and trigger threshold.

The evaluation provides information about the following parameters:

- the components x, y, z
- the envelope of the peak values
- the vectorial graph

The registration time includes the time window around the highest peak value within the ‘registration time of the envelope’. Following this, the predefined time window is stored and can be used for a frequency analysis.

3.2 Ground vibration measurements in boreholes

The measuring concept had to meet three prerequisites:

- the geophones should be positioned in a certain depth in the sidewall
- the geophones had to be in tight contact to the rock
- the geophones should be recovered after a measurement

In order to find out the expected peak particle velocities, test measurements were conducted at the test rig of the VOEST-ALPINE Bergtechnik in Zeltweg. According to the results of these measurements, the following sensors were selected to construct geophones, which meet the demand:

Input/Output Sensor SM-6 4.5 Hz (Sensor Nederland) see Figure 3.2
(The data sheet can be found in Appendix 1)

Figure 3.2: SM6 Sensor

3.2.1 Triaxial geophone construction

Two of three sensors were aligned horizontally and one vertically and encased in a rubber housing and positioned according to x,- y,- and z-axis.

- x- axis: horizontal and in the borehole- axis
- y- axis: horizontal and 90° to x-axis
- z- axis: vertical axis

A screened 3-twin twisted pair cable (AWG 24) should provide the connection to the measuring station. The triaxial geophone has a length of 17.5 cm and a diameter of 5 cm.

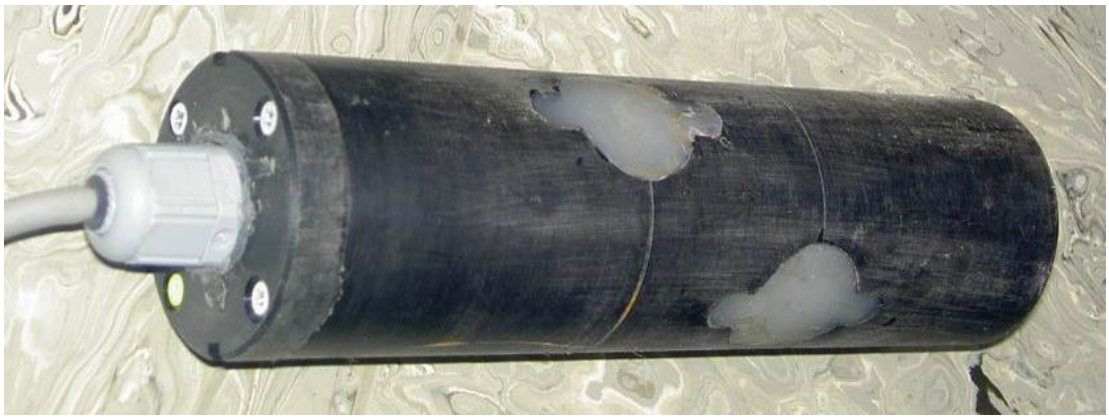

Figure 3.3: Triaxial geophone construction

In order to meet the three prerequisites mentioned above two different methods for fixing the geophone in the borehole were developed.

3.2.2 Triaxial geophone construction – fixing with concrete

This fixing method was used for measurements at the tunnel driving project of the Montreal Metro (Canada). There the measurements were accomplished by DI Sabine Leitgeb (Department of Mining and Tunneling at the University of Leoben) and Mag. Uwe Restner (VOEST ALPINE Bergtechnik) [9].

3.2.2.1 Information about the fixing method (fixing with concrete)

The triaxial-geophone was wrapped with a three-meter long lacing-wire and then inserted into a 2.5-metre long PE-pipe. The lacing-wire served the purpose to pull out the geophone after the measurement. Three wires of the length of the geophone were used to fix it in the PE-pipe. In order to avoid the seeping of concrete into the space between the PE-pipe and the geophone, the end of the pipe was sealed with silicone. This construction was concreted into the prepared borehole. By means of a marking on the geophone its orientation could be controlled.

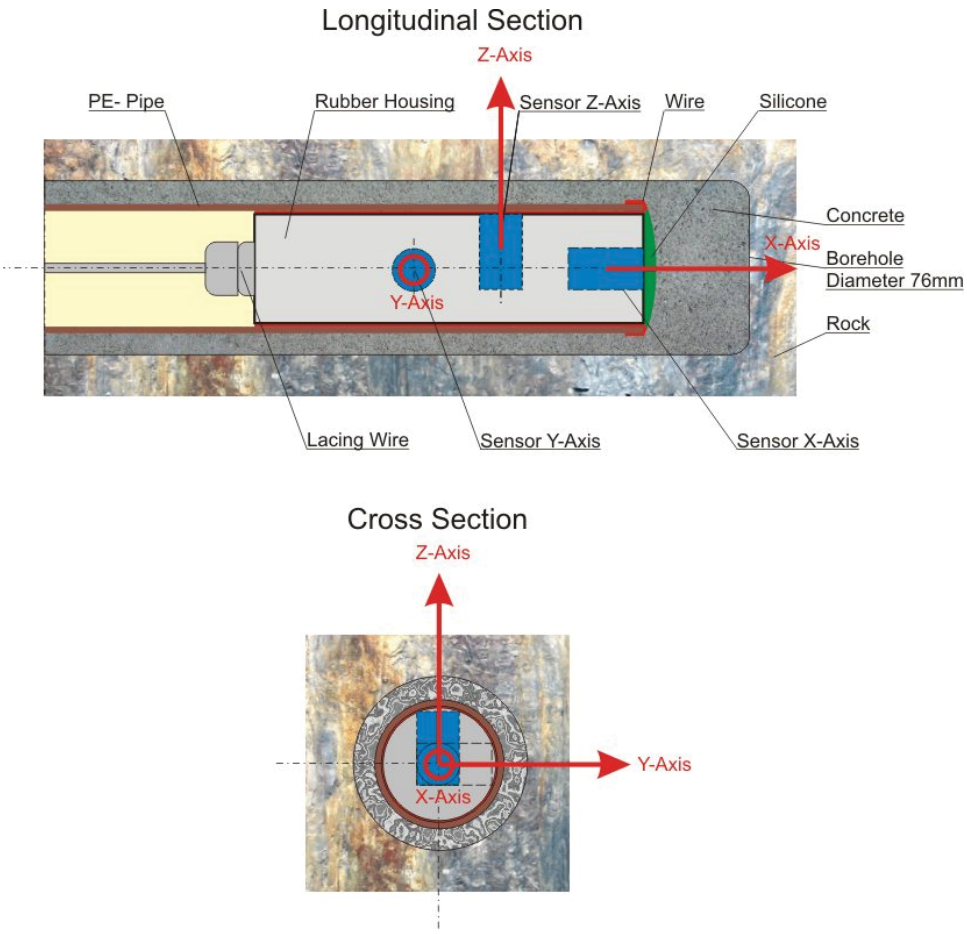

Figure 3.4: Sketch of the triaxial-geophone construction- fixing with concrete

3.2.2.2 Measurement equipment

This measuring system comprises the following elements:

- Input/Output sensor SM-6 4.5 Hz (Sensor Nederland)
- Triaxial-geophone construction
- Screened 3-twin twisted pair cable (AWG 24)
- DEWE rack 2000 with 6 x plug-in modules DAQP-V
- Laptop Panasonic CF–25
- DAQ – card AI-16E-4
- Software: Labview 6.02

3.2.2.3 Measurement signal chain

As shown in the survey in Figure 3.5, the SM-6 4.5 Hz sensor is at the top of the measurement signal chain. The sensor produces tension by motion caused by the arriving elastic waves which are passed on as electrical signals to the DEWE Rack 2000. If the distance between the encompassed geophones and the measuring station is longer than the appropriate cable, this distance has to be bridged with extension cables (cable drums with a shielded 6-pole cable with a cross section of 0.16 mm²).

This DEWE rack is equipped with 6 plug-in signal conditioners (2 geophones, 3 axes each) of the type DAQP-V (Appendix 2). At the beginning of a measurement the module's filter gradation is set to 10 kHz and the amplification to +/- 100 mV. The module converts the arriving signals into +/- 5 V voltage signals and passes them on to the Panasonic CF-25 laptop. By means of the analogue input card of the type DAQ-card AI-16E-4 (Appendix 3), which is installed on the laptop, these signals are sampled with 1 kHz and are available as discrete signals for further processing and depiction with the help of the Labview 6.02 software.

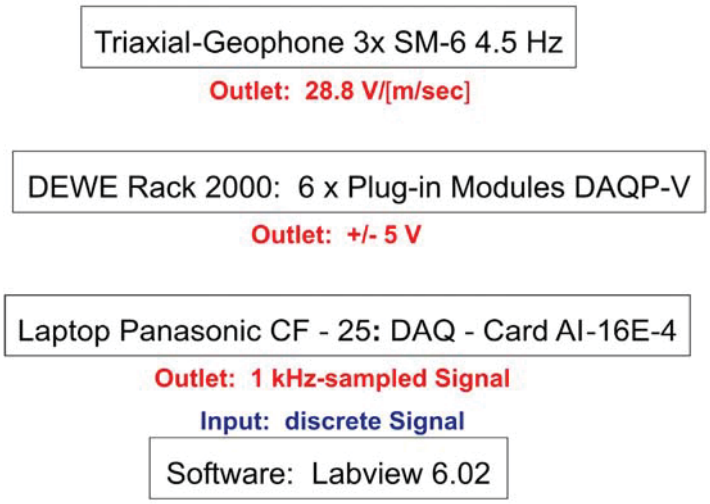

Figure 3.5: Graphical description of the measurement signal chain

3.2.3 Triaxial-geophone construction- mechanical mounting

The experience of the measurements carried out in Montreal (2003/04/28-2003/04/30) led to a further development of the fixing method of the triaxial geophones in boreholes at the Department of Mining and Tunneling at the University of Leoben in spring 2004 [3].

The following problems occurred by fixing a triaxial-geophone construction with concrete:

- the gap between the PE- pipe and the rubber housing absorbed vibrations
- a tight contact of the geophone to the concrete after its setting was not guaranteed
- the mounting and recovering of the geophones was very difficult

3.2.3.1 Information about the fixing method (mechanical mounting)

The mechanical mounting with bayonet coupling guarantees a rigid restraint and a tight contact of the geophone to the rock mass as well as an easy handling.

Test measurements in the Laboratory of the Department of Mining and Tunneling at the University of Leoben with a load cell showed a restraint force on the sliding wedge of more than 200 N.

The construction in Figure 3.6 shows the geophone housing with sliding wedge to mount the geophone tightly to the rock mass inside the boreholes.

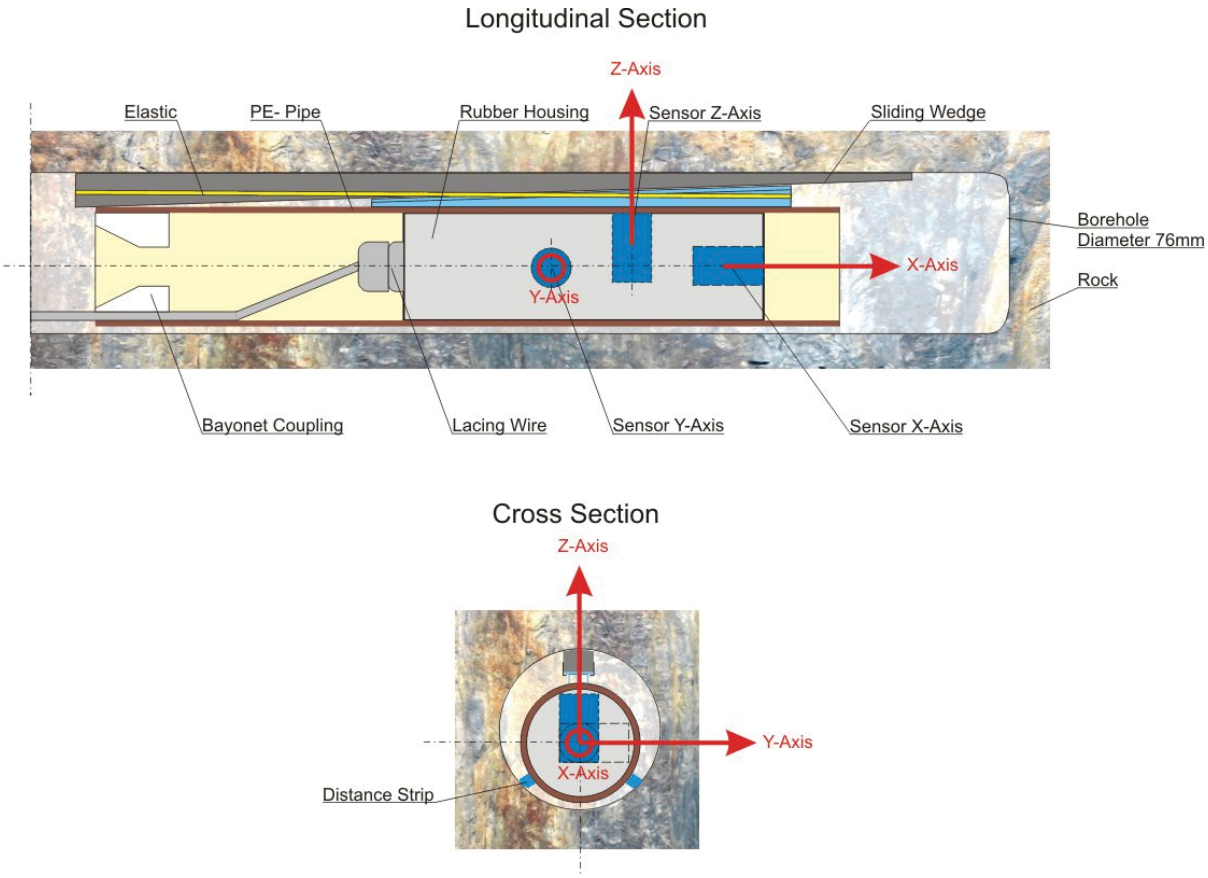

Figure 3.6: Sketch of the triaxial-geophone construction – mechanical fixing

The geophone can be fixed in a borehole and also recovered with a bayonet coupling on the forefront of an aluminum rod as can be seen in Figure 3.8.

Figure 3.7: Geophone housing with sliding wedge

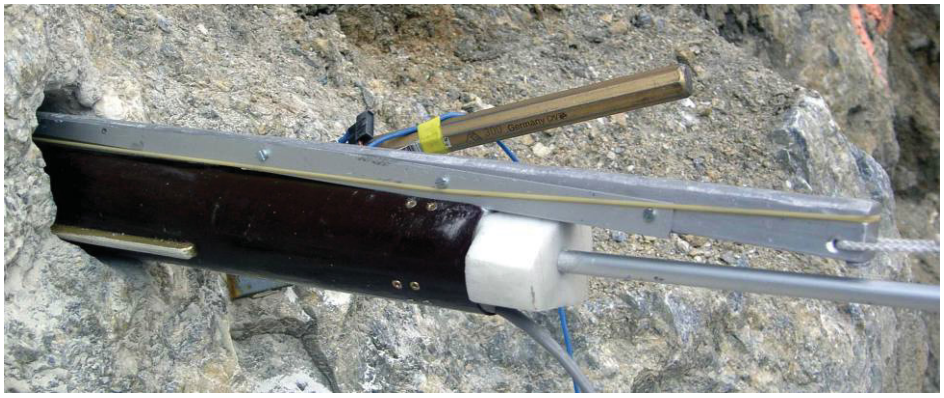

Figure 3.8: Detail of inserting the geophone

This kind of fixing guarantees a tight connection of the geophones with the rock mass and the possibility to recover them.

3.2.3.2 Measurement equipment

This measuring system consists of the following elements:

- Input/Output sensor SM-6 4.5 Hz (Sensor Nederland)
- Triaxial-geophone construction
- Screened 3-twin twisted pair cable (AWG 24)
- Junction box
- Analogue input card: DAQ AT-Mio-64E-3
- Software: Labview 6.02

3.2.3.3 Measurement signal chain

As shown in the survey in Figure 3.5, the sensor SM-6 4.5 Hz is at the top of the measurement signal chain. The sensor produces tension by motion caused by the arriving elastic waves which are passed on as electrical signals to the junction box. If the distance between the encompassed sensors and the measuring station is longer than the appropriate cable, this distance has to be bridged with extension cables (cable drums with a shielded 6-pole cable with a cross section of 0.16 mm²).

This junction box is equipped with 15 plug-in signal conditioners (5 geophones, 3 axes each). The junction box passes the signals to the analogue input card in the measuring computer. These signals are sampled with at least 10 kHz and are available as discrete signals for further processing and depiction with the help of the Labview software.

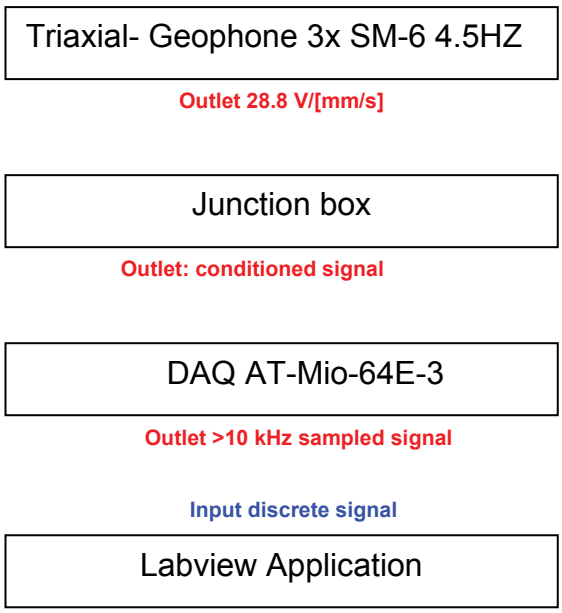

Figure 3.9: Graphical description of the measurement signal chain

4 Data analysis

The measurement system mentioned in Chapter 3.2.3 records a maximum of five triaxial-geophones that are switched parallel (in total 15 channels, each geophone x,-y,-z-axis for one individual measurement). For the present investigation the raw data were analyzed after converting with *Diadem*® 8.1 software of *National Instruments Corporation*® [4].

The following input parameters have been varied:

- Scan-Rate: 10000 / 15000 / 20000 / 30000 p/s
- Number of acquired scans: 100.000- 300.000
- Resulting scan time: 1 – 20 seconds.

Figure 4.1 shows the raw data of measurement No. 20 in Cullinan Diamond Mine.

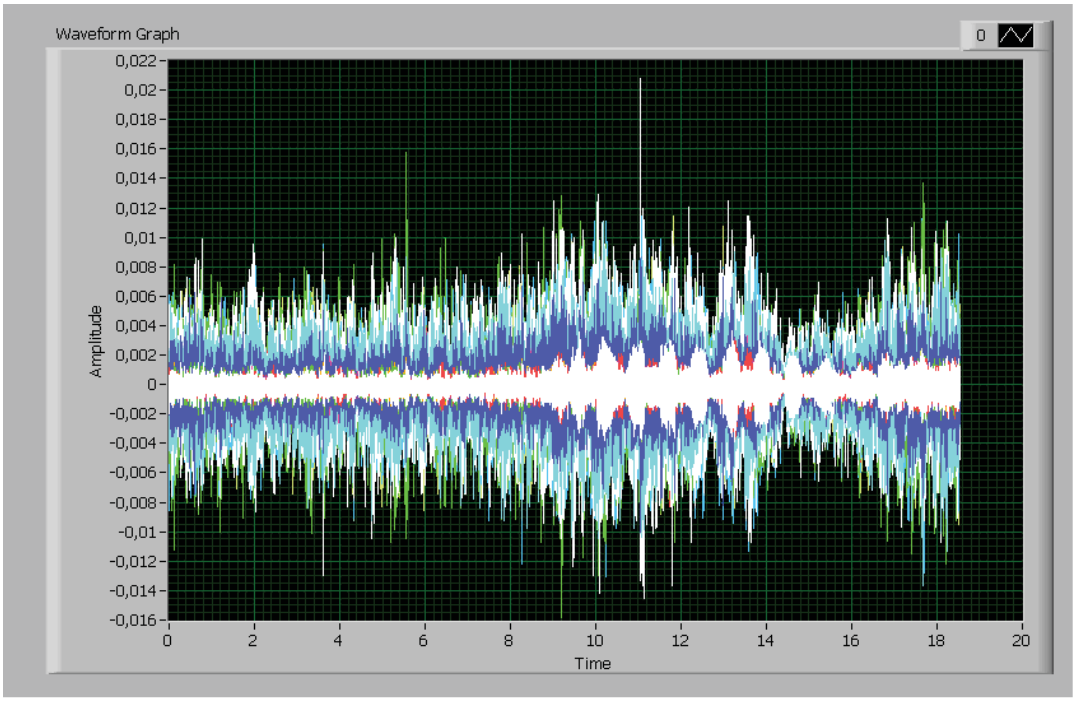

Figure 4.1: Amplitude [V] /time [s] - diagram, measurement 20 at Cullinan Diamond Mine

The ground vibration V_i [mm/s] is obtained by dividing the amplitude with the open circuit sensitivity.

(6) $$V_i = \frac{A_{rd,V,i}}{OCS}$$

i ... Data point number [-]
V_i ... Ground vibration at the data point i [mm/s]
$A_{rd,V,i}$ ... Amplitude of the signal at the data point i [V]
OCS ... Open Circuit Sensivity = 0,0288 $[\frac{V}{mm/s}]$

In the *Diadem*® software the resulting ground vibration RGV_i can be calculated using the following formula:

(7) $$RGV_i = \sqrt{\left(V_{x,i}{}^2 + V_{y,i}{}^2 + V_{z,i}{}^2\right)}$$

i ... Data point number [-]
$V_{x,i}$ ... Ground vibration of the x- axis at data point i [mm/s]
$V_{y,i}$ ... Ground vibration of the y- axis at data point i [mm/s]
$V_{z,i}$ ... Ground vibration of the z- axis at data point i [mm/s]
RGV_i ... Resulting ground vibration at data point i [mm/s]

It has to be noted that for this analysis the geophone orientations were determined by the borehole directions, whereas the direction of the arriving signal was determined by the position of the cutting head or the position of the round of shots relative to the position of the geophone.

Since the position of drift face relative to the independent geophone varies, care has to be taken at the interpretation of the magnitude of the components of the ground vibrations measured by individual geophones.

4.1 Signal analysis and statistical analysis

The ground vibration signals were analyzed in the *Diadem*® module “Analysis” by using the following basic mathematical functions: curve fitting functions, signal analysis functions, statistics and classification functions:

Smoothing of a channel:

In this function the channel is smoothed by a moving arithmetic means.

ChnSmooth(*Y*, *E*, SmoothWidth, SmoothType)

Y	Data channel of y- values
E	Result channel
SmoothWidth	Number of neighbored values taken into account for the moving arithmetic means
SmoothType	Number of values taken into account at the boundary points of the signal

Envelope curve calculation:

An upper and a lower envelope with a certain resolution of the original signal is calculated.

ChnEnvelopes(*X*, *Y*, *E1*, *E2*, *E3*, *E4*, DXPeak)

X	Data channel for the x- values (time)
Y	Data channel for the y- values (ground vibration)
E1	Result channel of the x- values of the upper envelope
E2	Result channel of the y- values of the upper envelope
E3	Result channel of the x- values of the lower envelope
E4	Result channel of the y- values of the lower envelope
DXPeak	Resolution of the envelope

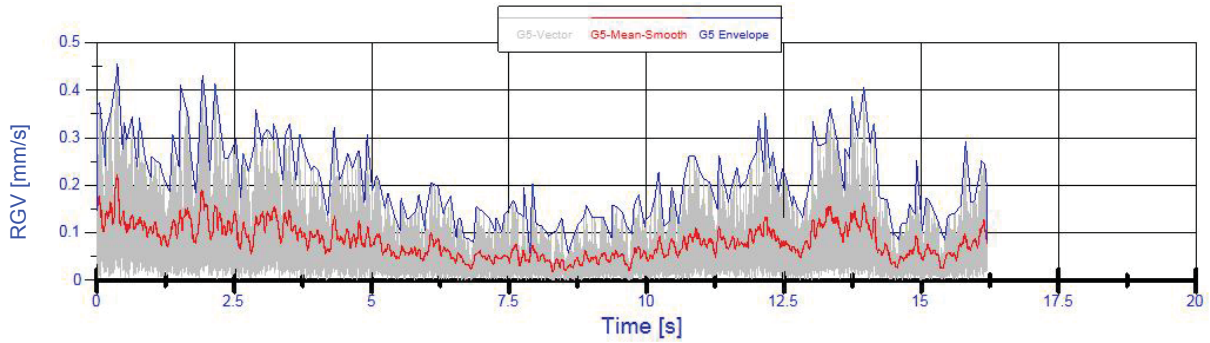

Figure 4.2: Resulting ground vibration diagram, smoothed signal and envelope, measurement 20 at Cullinan Diamond Mine

Normalization of a channel:

The original signal is normalized by setting the maximum value of the channel to a value of 1.

Y	Data channel of the y- values
E	Result channel

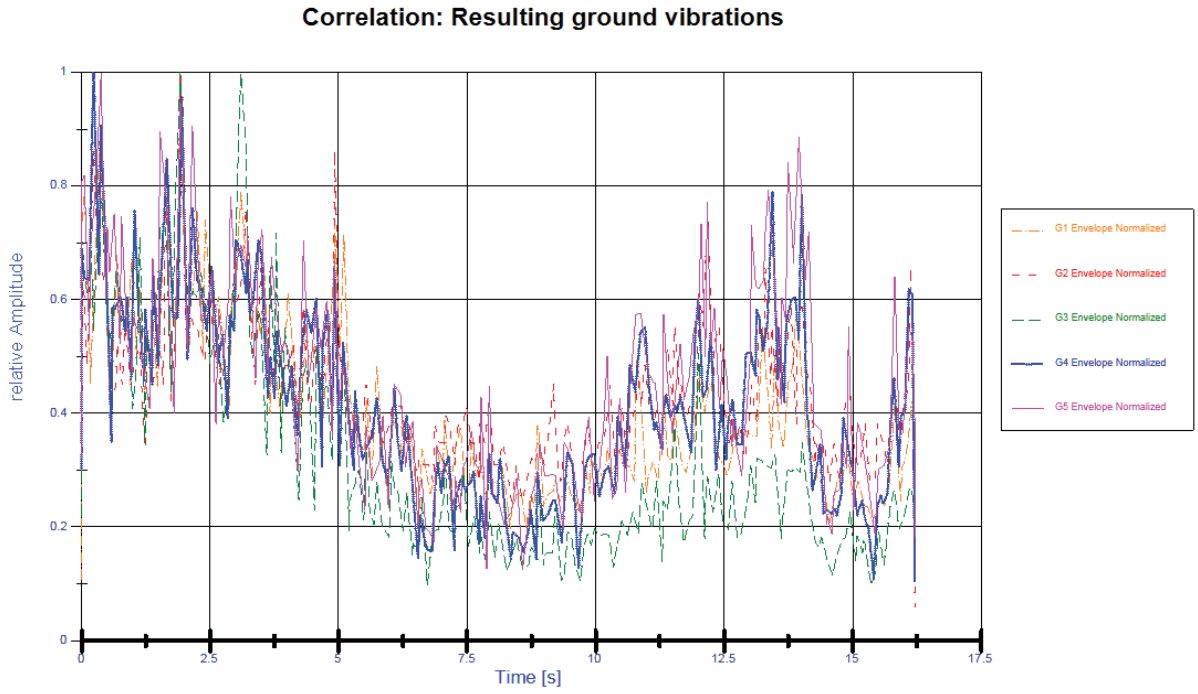

Figure 4.3: Correlation of the vibration signals of 5 geophones, measurement 20 at Cullinan Diamond Mine

Determination of statistical parameters:

StatBlockCalc(StatOrient, RowNoStr, ChnNoStr)

StatOrient	Defines the sequence of the statistical calculation
RowNoStr	Defines the channel rows for the determination
ChnNoStr	Data channels

For every geophone of every individual measurement of the resulting ground vibrations the following statistical parameters were determined for the ground vibrations and for the x, -y,- and z-axis:

- the minimum ground vibration of the axis (x,y,z)
- the maximum ground vibration of the axis (x,y,z)
- the maximum resulting ground vibration of the geophone
- the arithmetic mean of the resulting ground vibrations of the geophone
- the quadratic mean of the ground vibrations of the axis (x,y,z)
- the quadratic mean of the resulting ground vibrations of the geophone
- the standard deviation of the ground vibrations of the axis (x,y,z)
- the standard deviation of the resulting ground vibrations of the geophone
- the variation of the ground vibrations of the axis (x,y,z)
- the variation of the resulting ground vibrations of the geophone

Geo-phone	Axis	max. V [mm/s]	Arithm. Mean [mm/s]	Quadr. mean [mm/s]	Standard Deviation	Variation
1		0,088	0,015	0,017	0,008	0,000
2		0,071	0,011	0,013	0,007	0,000
3		0,234	0,023	0,029	0,017	0,000
4		0,362	0,057	0,068	0,036	0,001
5		0,458	0,081	0,097	0,053	0,003

Table 4.1: Overview of the statistical parameters determined for the resulting ground vibrations, measurement 20 at Cullinan Diamond Mine

FFT- Transformation:

The FFT (fast Fourier transformation) transfers a time domain function into a frequency domain function.

Call ChnFFT1(*X*, ChnNoStr)

X	Data channel of the x- values (time)
ChnNoStr	Data channels of the y- values (ground vibrations)

Determination of the x- values at maximum and minimum y- values:

This function was used to determine the frequencies at the maximum amplitude of the frequency spectra of the fast Fourier transformation.

ChnPeakFind(*X*, *Y*, *E1*, *E2*, PeakNo, PeakType, PeakSort)

Parameter

X	Data channel of x- values
Y	Data channel of y- values
E1	Result channel
E2	Result channel
PeakNo	Number of maximal of minimal peak values
PeakType	Defines if *Diadem*® is searching for minima or maxima
PeakSort	Defines the sequence for searching the minima and maxima

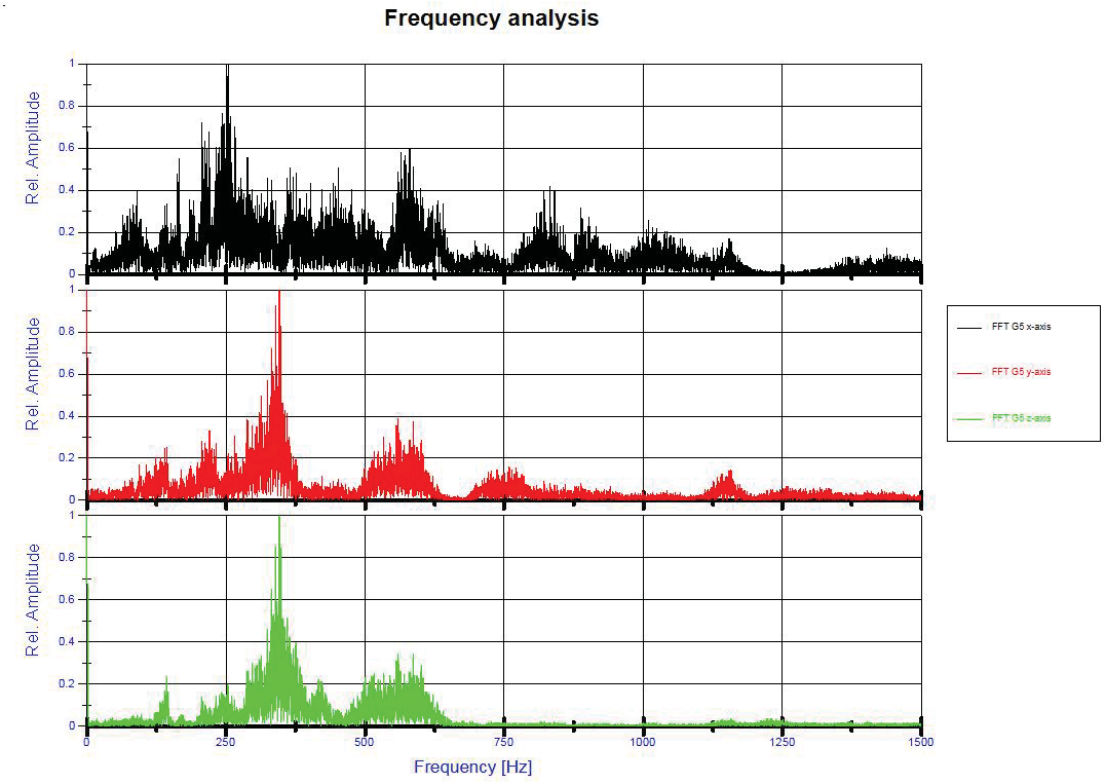

Figure 4.4: Frequency analysis, geophone 5, measurement 20 at Cullinan Diamond Mine

Figure 4.4 shows the dominating frequencies for the three axis. The frequency with the highest relative amplitude of each axis was taken for further analysis.

4.1.1 Individual analysis of signals resulting from roadheader operations

As a part of the vibration measurements at the test rig of VOEST-ALPINE Bergtechnik in Zeltweg the power consumption of the cutting head of the roadheader was also measured by the University of Leoben.

(8) $$P = \frac{\left(A_{rd,P,i} - 0,2\right) \cdot P_{CM}}{0,8}$$

P_i ... Power consumption of the cutting head [kW]
$A_{rd,P,i}$ ... Amplitude raw data [V]
P_{CM} ... Power cutter motor 300kW
I_L ... Lower current limit of the sensor 4mA
I_U ... Upper current limit of the sensor 20mA
R ... Resistance 50Ω
U_L ... Lower voltage limit 0,2V
U_U ... Upper voltage limit 0,8V

According to the equation above the raw data was analyzed and furthermore the smoothed curve, the envelope curve and the normalized curve were calculated and the statistical parameters from Chapter 4.1 (Signal analysis and statistical analysis) were determined.

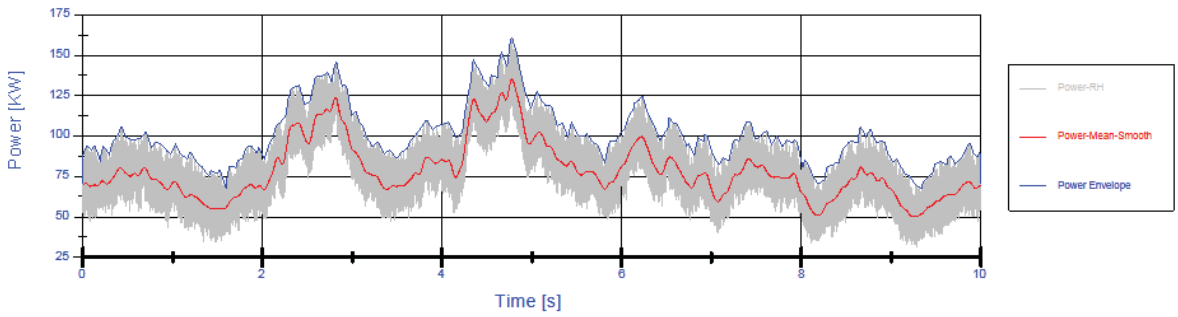

Figure 4.5: Power cutting head of the roadheader, measurement 32 at VOEST-ALPINE Bergtechnik trial site

The script file for the automated analysis of ground vibrations caused by roadheader operations and the calculation of statistical parameters can be found in Appendix 4.

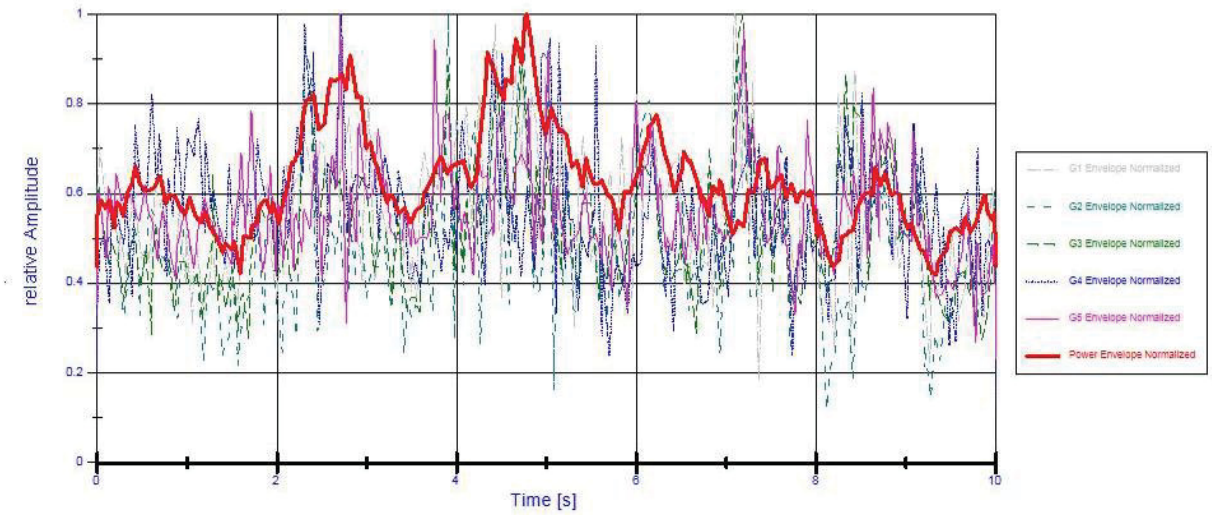

Figure 4.6: Correlation between relative amplitudes of the power and resulting ground vibrations

Figure 4.6 shows the high correlation between power or energy consumption of the cutting head and the ground vibration signals.

4.1.2 Individual analysis of signals resulting from blasting operations

At blasting operations only a part of the measured vibration signals are caused by the blasting itself. The other part of the signal is caused by working activities in the mine or in the tunnel - the so called “background noise”. When statistical parameters are calculated, this background noise influences the analysis and leads to a falsification of the results.

The following Figure shows an original signal of a ground vibration measurement caused by a round of shots.

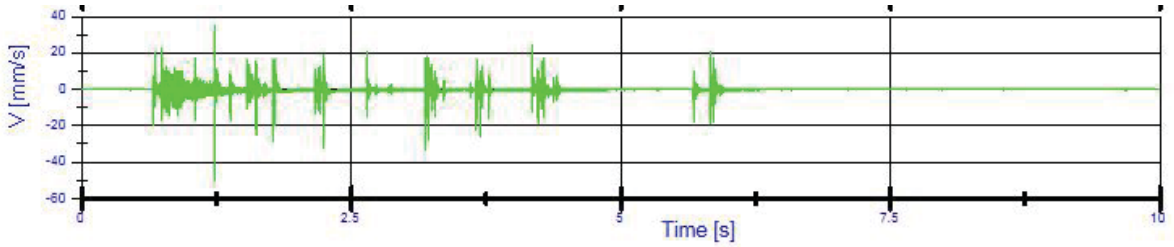

Figure 4.7: Original signal of ground vibrations of a round of shots

To determine the threshold of the background noise, the maximum and minimum value of the pre-trigger time were calculated. All data points that were lower than the maximum threshold and higher than the minimum threshold of the background noise of the ground vibration signals were set as NOVALUE as well as the related data points of the time channel.

The following example of a script file of *Diadem*® shows three commands:

- the determination of the threshold values of the background noise
- the setting of data points to NOVALUE
- the elimination of the NOVALUES for the ground vibration signal and the time signal for the x- axis of Geophone 1

```
   STATSEL(4)        ="Yes"    … Determination of Minima
   STATSEL(5)        ="Yes"    … Determination of Maxima
   STATCLIPCOPY      =0
   STATCLIPVALUE     =0
   STATFORMAT        =""
Call STATBLOCKCALC("Channel","1-8000", "G1 x-axis")
8000 … Number of pretrigger scans

Call FormulaCalc("Ch('G1 x-axis Filtered') :=
      Ch(G1x)+(Ch(G1 x-axis) >= Chd(1,Minima) and
      ch(G1 x-axis) <= Chd(1,Maxima))*NoValue")

Call ChnNovHandle("Time G1 x-axis","G1 x-axis filtered", "Delete", "X", 1)
```

When the signals were filtered, the statistical parameters and the exposed time were calculated. The exposed time was determined by dividing the channel length with the scan rate of the measurement.

```
CHD(1,"Exposed Time")=(CHNLENGTH("G1 x-axis filtered"))/15000
15000 … Scan Rate
```

Figure 4.8 shows the modified signal of a round of shots. The duration of the measurement was 10 seconds. The exposed time was 3,6 seconds after filtering the signal. That means that only 36% of the original data points were higher than the threshold and further used for the statistical analysis.

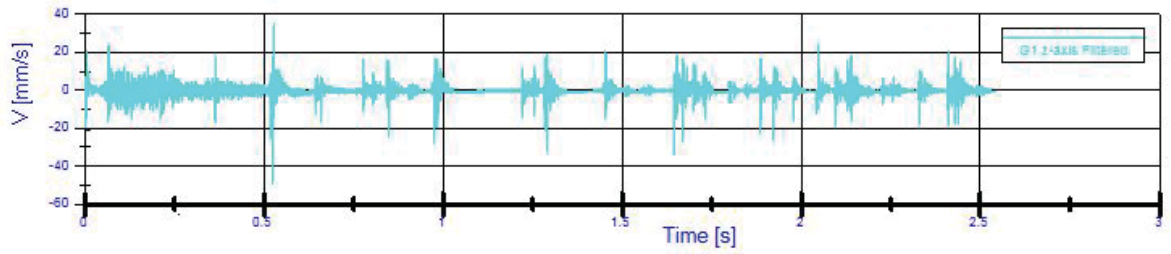

Figure 4.8: Modified signal of ground vibrations of a round of shots

The entire script file for the automated analysis in *Diadem*® of ground vibrations caused by blasting operations and the calculation of statistical parameters can be found in Appendix 5.

Since the boreholes, in which the geophones were installed, were not tamped, the sound wave caused by the blasting and propagated through the air also induced vibrations in the geophones. Therefore, for further processing, the exposed time of an individual measurement for drill and blast development was determined from the detonation speed of the explosives.

5 Vibration measurements in tunnels developed by means of a roadheader

To obtain data of drifts developed by the means of roadheader, measurements were performed in four different underground mines and tunnel sites and at the test rig of VOEST-ALPINE Bergtechnik on a concrete block.

The main objective to perform these measurements was the evaluation of data under different rock and impact conditions to determine a function for the propagation of ground vibrations.

Table 5.1 shows the different conditions of the rock and the rock mass as well as the geometrical parameters.

Parameter	Index	Unit	Location					Boundaries	
			Sorrent	Erzberg	Montreal	Cullinan	VAB	min	max
Overburden	OV	[m]	250	50	20	717	2,5	2,5	717
Depth Geophone	DG	[m]	0,1	0,1	2	0,9-3,5	0,3	0,1	2
Mean Distance of the geophones	D_{mean}	[m]	14,0	17,3	15,6	11,8	7,8	7,8	17,3
Cross Section	CS	[m²]	42,0	28,8	46,0	25,0	33,1	25,0	46,0
Density	ρ	[kg/m³]	2720	2630	2640	2698	2250	2250	2720
Uniaxial Compressive Strength	UCS	[Mpa]	188,0	152,0	94,4	79,4	32,3	32,3	188
Brazilian Tensile Strength	BTS	[Mpa]	7,7	11,0	6,4	6,6	3,1	3,1	11,0
Young's Modulus	Y_M	[Mpa]	47083	22550	10374	13704	10047	10047	47083
Fracture Energy	E_f	[J]	41	25	24	7,5	12	7,5	41
Mean Frequency	φ_{mean}	[1/s]	48	74	236	299	7	7	299
Rock Mass Rating (Bieniawski)	RMR	[-]	54	46	64	55	89	44	90
Mean Power	P_{mean}	[kW]	215	183	153	150	88	88	225
Mean Cut	Cut_{mean}	[mm]	134	152	138	142	143	134	152
Sump in Depth	SD	[mm]	750	630	650	650	650	630	750
Mean Slewing Speed	v_s	[m/s]	0,2	0,2	0,2	0,2	0,2	0,2	0,2

Table 5.1: Overview of the rock and rock mass parameters and geometrical parameters for the roadheader sites

For all underground mines and tunnel sites the roadway drifting was done with the ALPINE MINER ATM 105 manufactured by VOEST- ALPINE Bergtechnik in Zeltweg.

The ALPINE MINER ATM 105 is an extremely powerful boom-type roadheader of the 100 tons class and has proven its unique transverse cutting technology in hard rock applications worldwide. This machine has an extended field of operation for mechanised tunnelling in hard and abrasive rock formations. The corresponding data sheet can be found in Appendix 6.

Figure 5.1: Roadheader ATM 105 ICUTROC

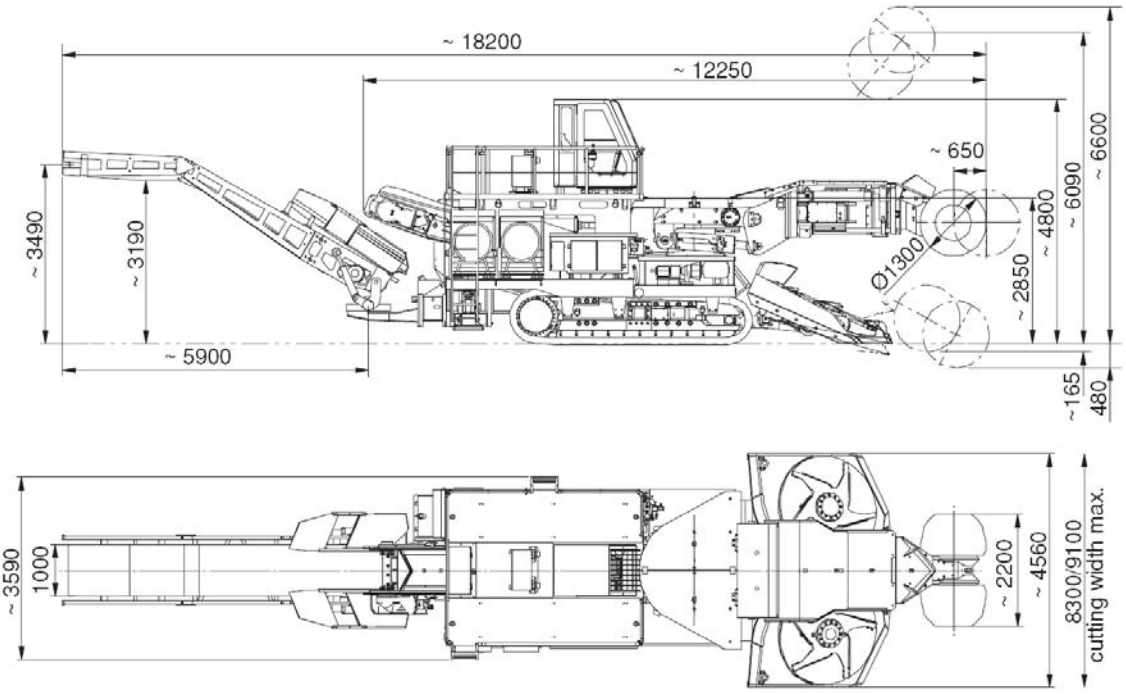

Figure 5.2: Plan view and cross section of the roadheader ATM 105 ICUTROC

5.1 Pozzano Road Tunnel in Sorrent (Italy)

Ground vibration measurements were performed during an operation of roadheader ATM 105 at Pozzano Road Tunnel. The measurements were taken by DI Christian Reichl / Department of Mining Engineering at the University of Leoben. To obtain information about the ground vibrations attributable to the roadheader operation and to keep them below 1,8 mm/s in an adjacent tunnel of the Transvesuvian railway was the main purpose of this measuring application. [18]

5.1.1 General information about the site

The tunnel site was located in Sorrent near Naples (Italy). The entire section of the tunnel was split into a roof section of approximately 42m² and a bench section. Figure 5.3 shows the existing pilot tunnel with a diameter of 3,6m (TBM-bored) and the roof section.

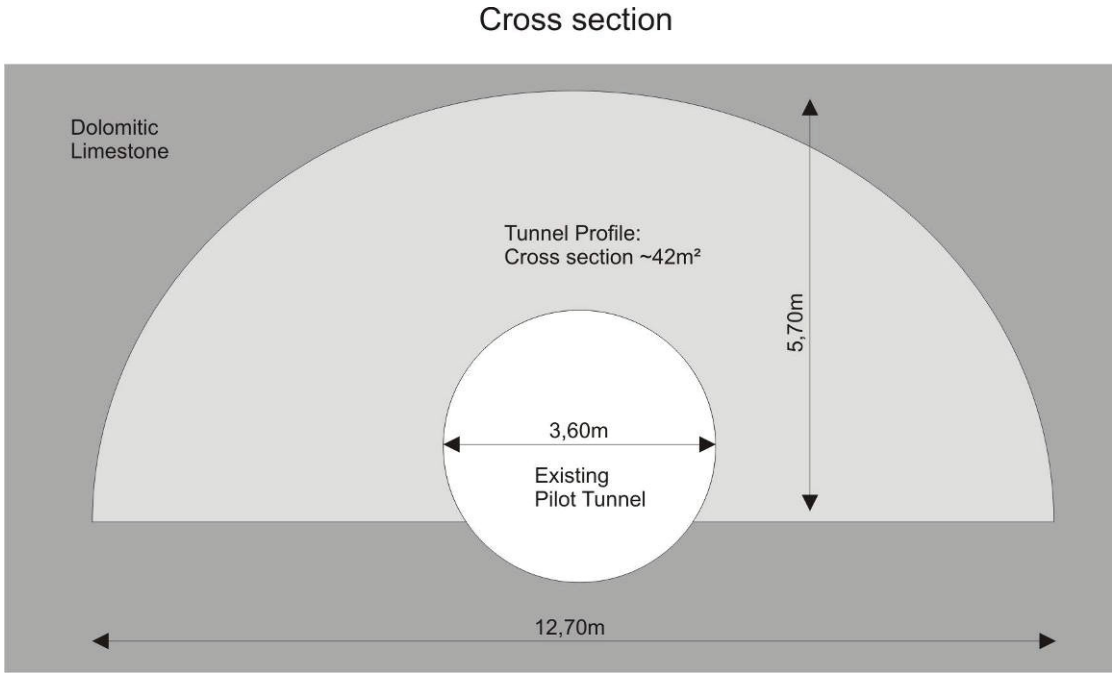

Figure 5.3: Cross section of the Pozzano Road Tunnel

5.1.2 Geological situation, rock and rock mass conditions at the tunnel site

The tunnel is located in a sequence of thickly bedded dolomitic limestone. The average thickness of the layers amounts to about 0,5m. Due to its location in a tectonically active zone the rock was fissured with varying intensity of parting. The evidence of the face was highly variable ranging from massive to destabilized within a short distance.

From every individual layer a representative sample was taken for testing at VOEST-ALPINE Bergtechnik rock testing facilities. All rock types were dolomitic limestones to limestones. The uniaxial compressive strength with an average of 180 MPa was found highly variable within the formation and also between individual samples. [6]

5.1.3 Operation sequence of the measurements

The measurements were taken on 1998/07/29. A total of six measurements was carried out using the VIBRAS 3004 measuring system with four geophones. Figure 5.4 shows the arrangement of the geophones in the tunnel.

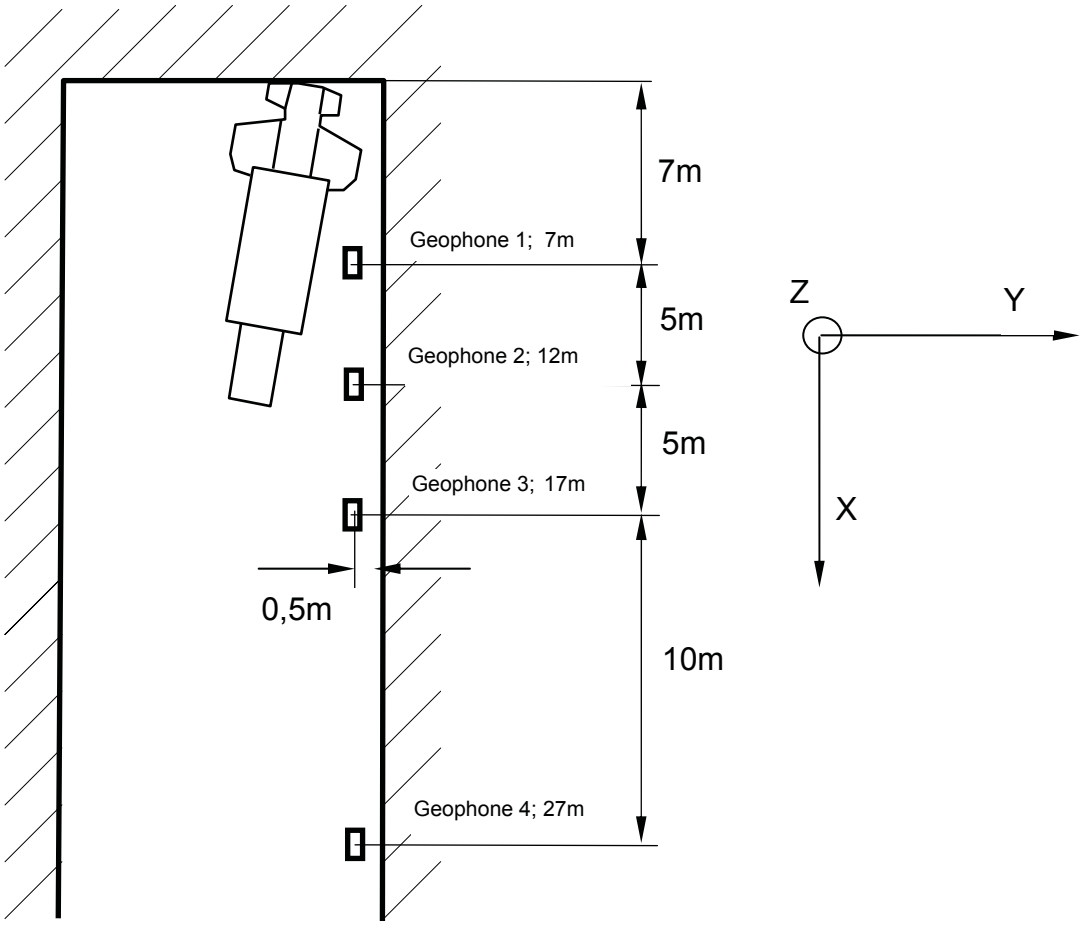

Figure 5.4: Position of the geophones during the measurements

In both cases the positions of the geophones were almost identical: The first geophone was placed close to the roadheader (1m), the remaining 3 geophones were placed 5m, 10m and 20m behind the roadheader along the tunnel axis. To get comparable results all geophones had the same orientation (x-direction outwards). The geophones were placed in a distance of 0,5m close to the sidewall. The horizontal positioning was made by means of a level on each geophone.

5.1.4 Results of the ground vibration measurements

The highest resulting ground vibration of all test measurements close to the roadheader was 3,36 mm/s. 5, 10 and 20 meters behind the roadheader the peak particle velocity decreased abruptly below 1 mm/s to a minimum of 0,32 mm/s.

Figure 5.5 shows the maximum resulting ground vibrations versus distance from source.

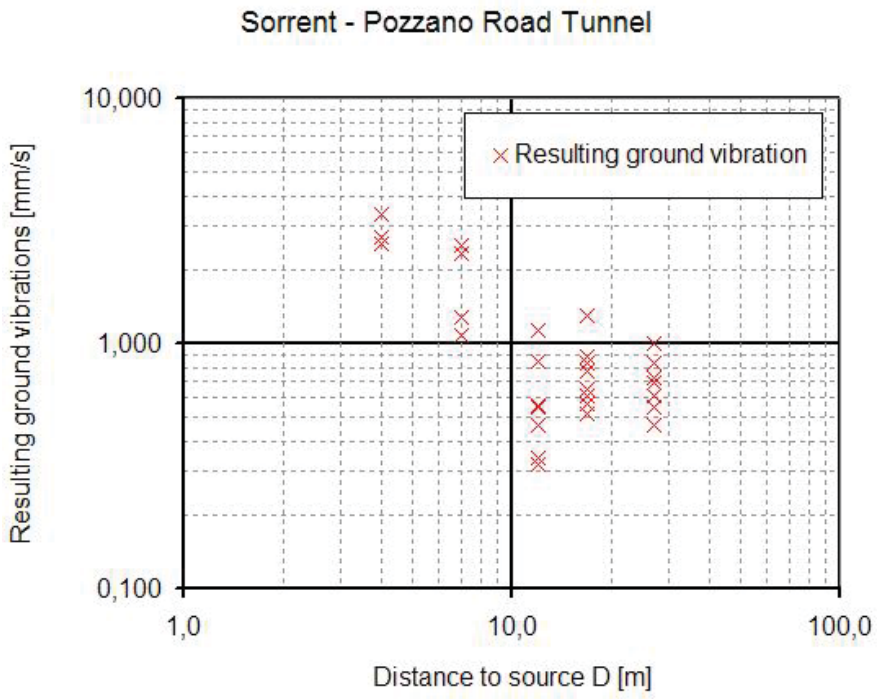

Figure 5.5: Resulting ground vibration – distance diagram, Pozzano Road Tunnel (Italy)

5.2 Iron ore mine Erzberg (Austria)

In 1998 ground vibration measurements were taken at the test site at the Iron ore mine Erzberg (Austria) during the cutting phase of the EU-Project ICACUTROC. The rock hardness was especially high in order to demonstrate the possibility for roadheaders to achieve economically significant performances in hard rock conditions. [22]

5.2.1 General information about the site

The test site was located in an old drift which was used to serve the Erzberg iron deposits. The test site was situated about 60m away from the open air in a breakaway of the main gallery. The roof support was ensured by bolting and jet grouting. [23]

5.2.2 Geological situation, rock and rock mass conditions in the mine

The predominating rock was porphyrite with the following constitution:

26% quartz
14% feldspath
50% silicate
9% carbonate and clay minerals
1% other minerals

Geological conditions were summarized by a VOEST-ALPINE Bergtechnik intern face classification. Due to the face classification the rock mass rating after Bieniawski was 46.
The rock parameters of the porphyroid rock were determined by the Department of Mining und Tunneling at the University of Leoben and at the rock testing facilities at VOEST-ALPINE Bergtechnik in Zeltweg.

At the Erzberg mine the drifting was done by blasting before the cutting test phase commenced. Hence the footwall was in a bad condition. The rock mass of the footwall was highly jointed and fractured, so that the contact of the geophones to the footwall was poor.

5.2.3 Operation sequence of the measurements

The measurements were performed at the test site Erzberg. Six individual vibration measurements were carried out. The duration of the measurements was 1 to 1,6 seconds per measurement. [7]

The positions of the triaxial-geophones of the VIBRAS 3004 are shown in Figure 5.6.

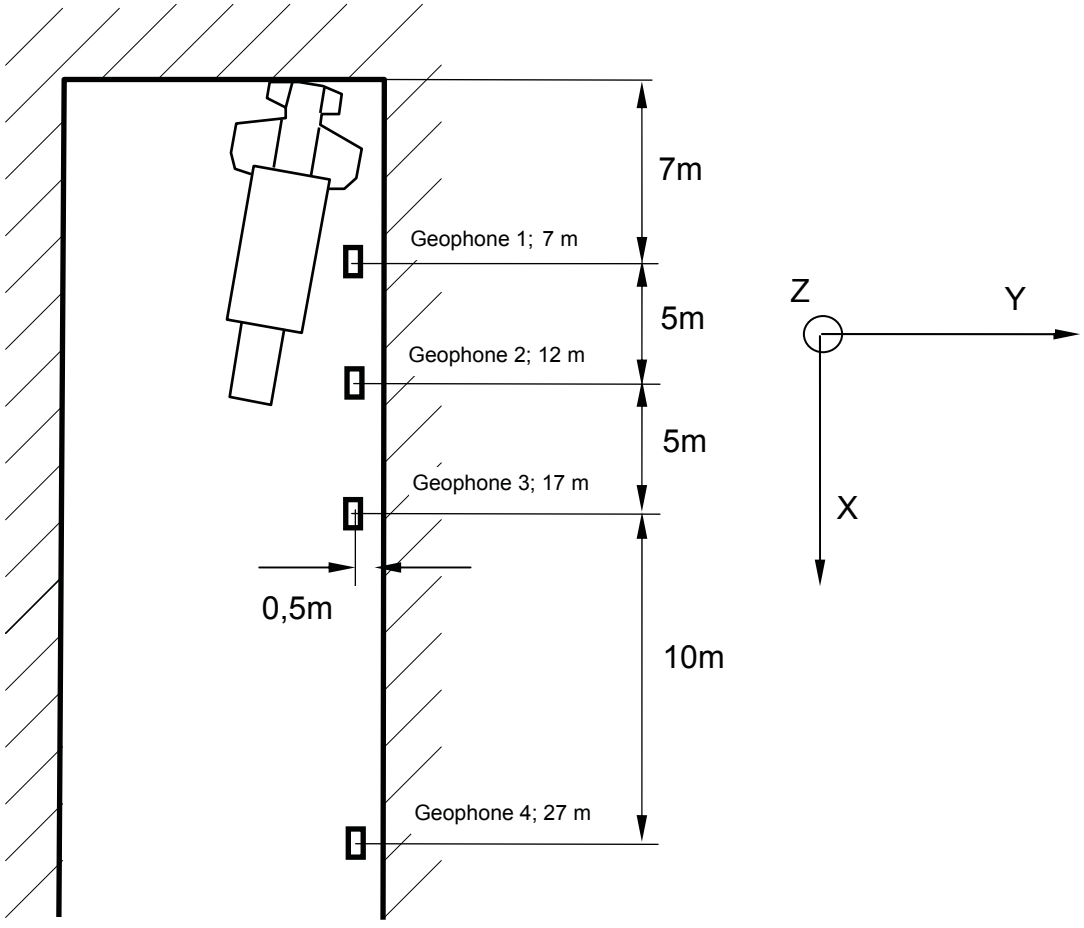

Figure 5.6: Position of the geophones during the ground vibration measurements

The first geophone was placed close to the roadheader (1m), the other 3 geophones were placed 5m, 10m and 20m behind the roadheader. All geophones had the same orientation (x-direction outwards) to get comparable results. The geophones were placed 0,5m close to the sidewall. Horizontal positioning was made by means of a level on each geophone.

5.2.4 Results of the ground vibration measurements

The values of ground vibrations during cutting process were very low. The maximum resulting ground vibration of all test measurements close to the roadheader was 0,93 mm/s. 5m, 10m and 20m behind the roadheader there was an abrupt decrease of the resulting ground vibrations to less than 0,1 mm/s.

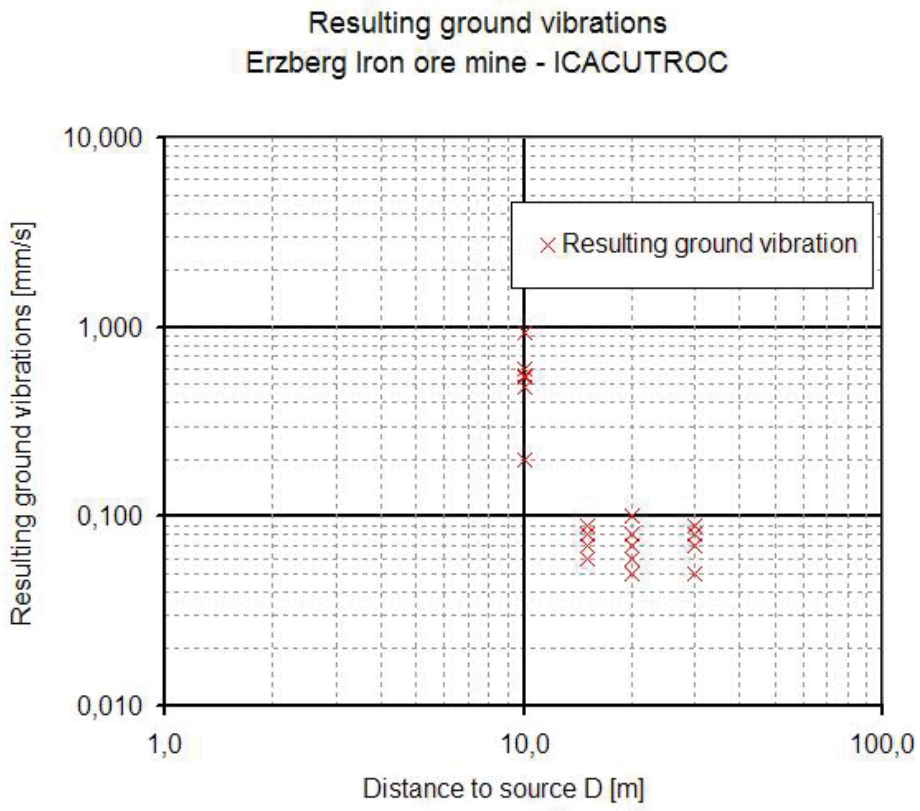

Figure 5.7: Resulting ground vibration – distance diagram, Erzberg (Austria)

5.3 Montreal Metro Tunnel (Canada)

The VOEST-ALPINE Bergtechnik commissioned vibration measurements as a part of a tunnel driving project in Montreal/ Canada.

These measurements were part of the diploma thesis of Sabine Leitgeb with the title “Ground Vibrations Resulting from Roadheader Operations” in collaboration with the Department of Mining and Tunneling at the University of Leoben and the Institute of Engineering Geology and Applied Mineralogy at Graz University of Technology [9].

The measuring stage was from 2003/04/28 and 2003/04/30. The measurements were accomplished by Sabine Leitgeb and Mag. Uwe Restner (VOEST ALPINE Bergtechnik). The main task of this thesis was to record the magnitude of the peak particle velocities and to present it in relation to the distance of the cutting face.

A total of 87 measurements using triaxial-geophones fixed in boreholes and 6 measurements using the VIBRAS geophones were taken.

The entire raw data from the ground vibration measurements was analyzed again in order to determine the statistical parameters, as explained in Chapter 4.1. All determined parameters for the measurements can be found on the enclosed Data-DVD.

5.3.1 General information about the site

The extension of Montreal Metro started in July 2002 and was scheduled to be finished in January 2006. In the fourth of five phases of construction the area between the stations Cartier and De La Concorde was worked on and offered the possibility to carry out the measurements. The tunnel should be excavated over a length of 1200m with a cross section of 46m² by means of a roadheader. After cutting free a ramp at the Parc Saint-Claude the excavation was carried out on both sides. On one day excavation work was done in direction Montmorency (West) and on the other day, following the place change of the machine, in direction Cartier (East).

5.3.2 Geological situation, rock and rock mass conditions at the tunnel site

An engineering geological documentation in the area of the measurements was carried out. On the basis of this documentation and the existing core-log the following longitudinal section (Figure 5.8*)* could be provided:

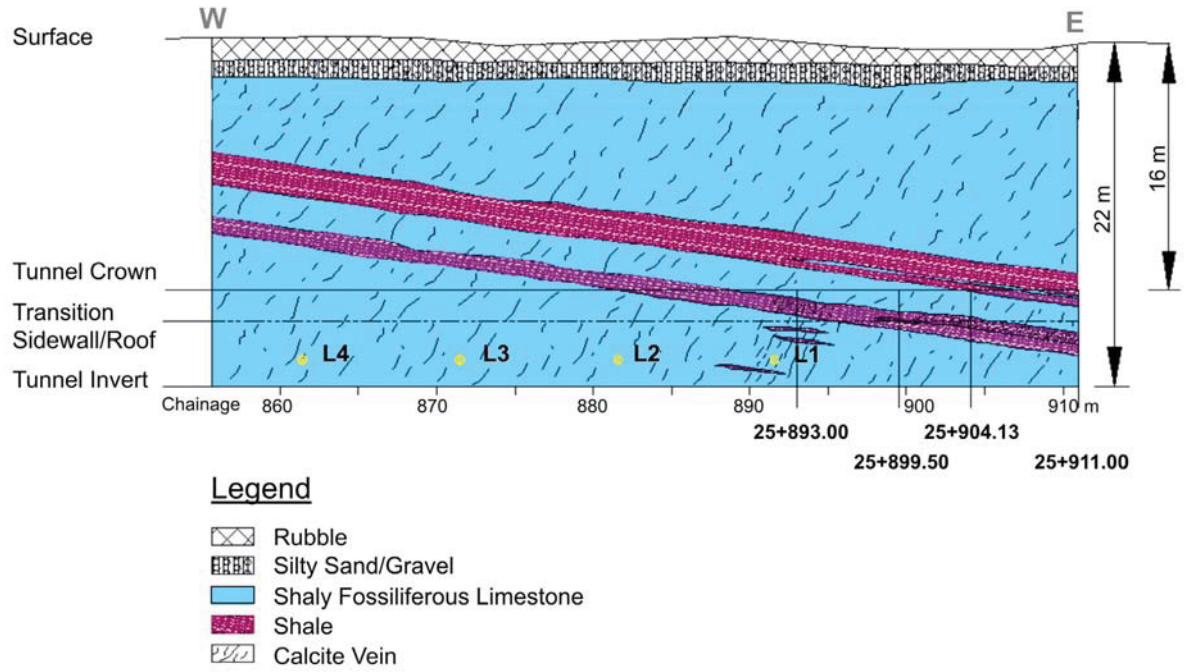

Figure 5.8: Longitudinal section of the measurement area

The main rock type in the study area is a shaly fossiliferous limestone with numerous calcite veins in it. The persistence of these veins is in the range between a few millimeters and a few meters. Layers of shale are intercalated, with a thickness between 30 and 155 centimeters. The bedding gently dips about 8° towards east. That means that the rock mass strikes perpendicular to the tunnel axis.

In order to be able to determine the important parameters for VOEST-ALPINE Bergtechnik two employees of the company had inspected representative rock samples during a site visit. From numerous drill cores three typical rock samples were selected and tested in the laboratory with different rock tests, like UCS and BTS. The results of the different methods are evident in Table 5.2.

The samples came from a sequence of sedimentary rocks and consist of

- shale
- shaly fossiliferous limestone
- slightly shaly crystalline limestone

Special attention was given to mechanical testing of the shaly fossiliferous limestone, which represents the main rock type within the tunnel alignment as the longitudinal section shows. The fracture Energy E_f in Table 5.2 was noted with W_f.

Sample-number	Rock Type	ρ [g/cm³]	UCS [MPa]			BTS [MPa]			W_f [Nm]			UCS:BTS	w_f:UCS [Nm/MPa]	CAI		
			from	*to*	*mean*	*from*	*to*	*mean*	*from*	*to*	*mean*			*from*	*to*	*mean*
1	*Shale*	**2.60**	45.43	71.01	**63.18**	3.35	6.75	**4.92**	11.01	27.04	**18.48**	**13**	**0.29**	0.36	0.94	**0.65**
2	*Shaly fossiliferous limestone*	**2.65**	63.55	134.78	**102.26**	4.81	10.89	**6.81**	9.20	37.19	**24.93**	**15**	**0.24**	0.55	1.15	**0.82**
3	*Slightly shaly crystalline limestone*	**2.64**	88.09	117.05	**105.87**	5.11	9.81	**7.50**	21.52	34.99	**27.09**	**14**	**0.26**	0.29	0.84	**0.62**

ρ	Density [g/cm³]	W_f	Fracture Energy [Nm] (equals E_f)
UCS	Uniaxial Compressive Strength [MPa]	w_f	Specific or demanded fracture energy, derived from the ratio of E_f to UCS [Nm/MPa]
BTS	Brazilian Tensile Strength [MPa]		
CAI	Abrasively Index [-]		

Table 5.2: Summary of rock tests

5.3.3 Operation sequence of the measurements

1,43m behind the cutting face, at a height of 1,70m, the first geophone (L1) was positioned on the left sidewall. Three more geophones (L2 to L4) were positioned at the same height and 10 meters apart from each other. Opposite L1 and L2, at the same height, the geophones R1 and R2 were inserted into the right sidewall. The geophones L1 to L4, R1 and R2 were positioned in a depth of 2,3 m in the borehole. Figure 5.9 shows the arrangement of the triaxial-geophones in the tunnel.

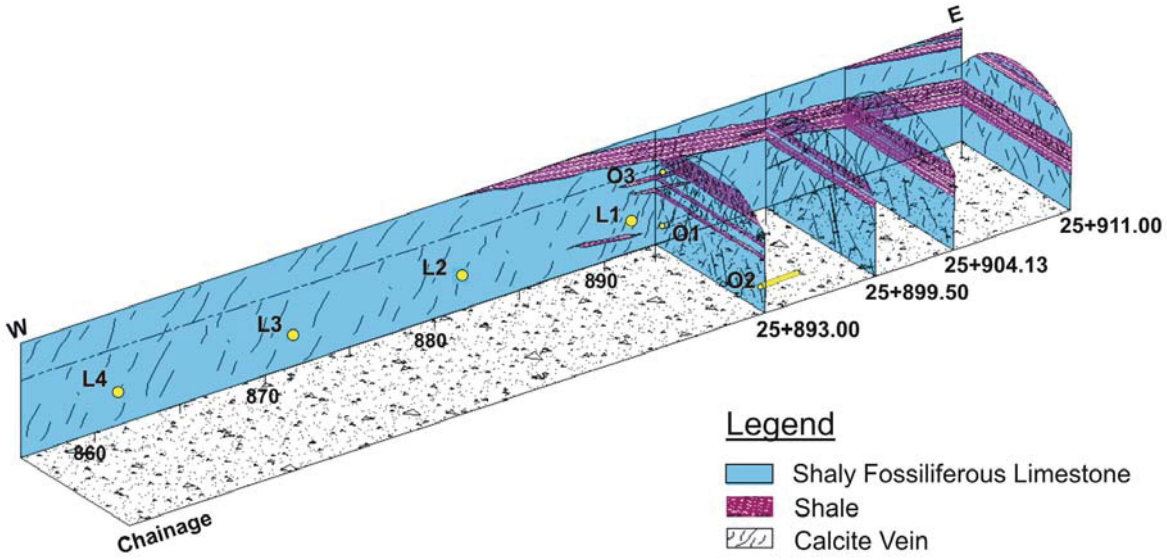

Figure 5.9: Arrangement of the geophones in measurement area, Montreal Metro Tunnel

5.3.4 Results of the measurements

5.3.4.1 Results of the measurements of the background noise

The measurements to estimate the background noise showed an average resulting ground velocity of the maximum values for the background noise of 0,041mm/s.

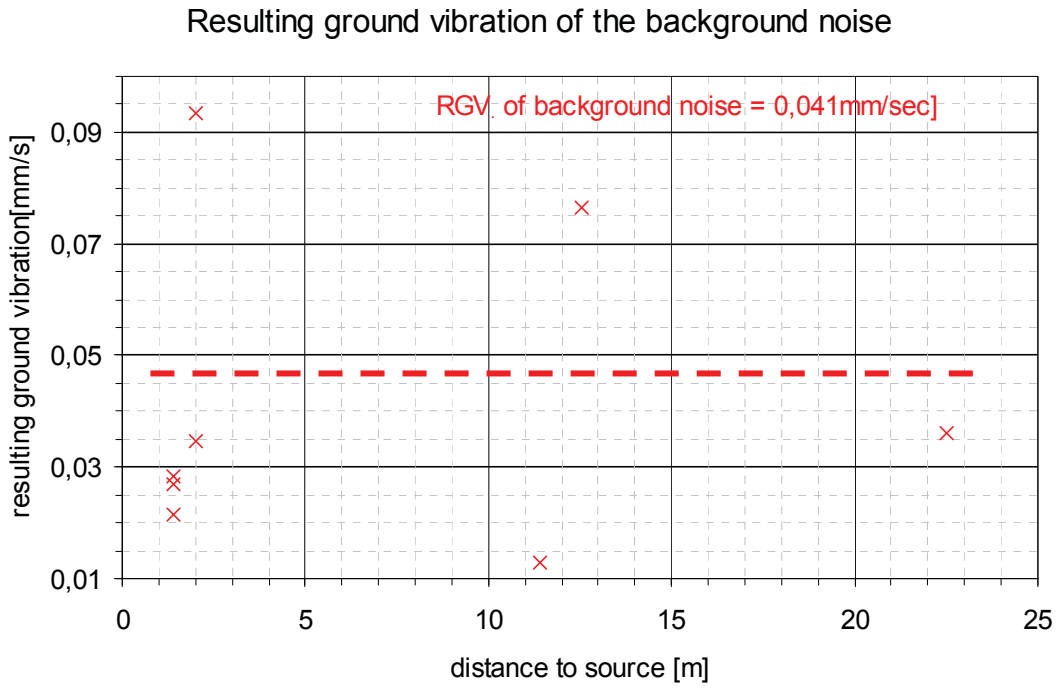

Figure 5.10: Resulting ground vibration of the background noise, Montreal Metro Tunnel

5.3.4.2 Results of the ground vibration measurements

The resulting ground vibrations showed maximum values of 1,6mm/s at a distance of 2,7m. The measuring range was from 2,7m to 50m from the source of impact.

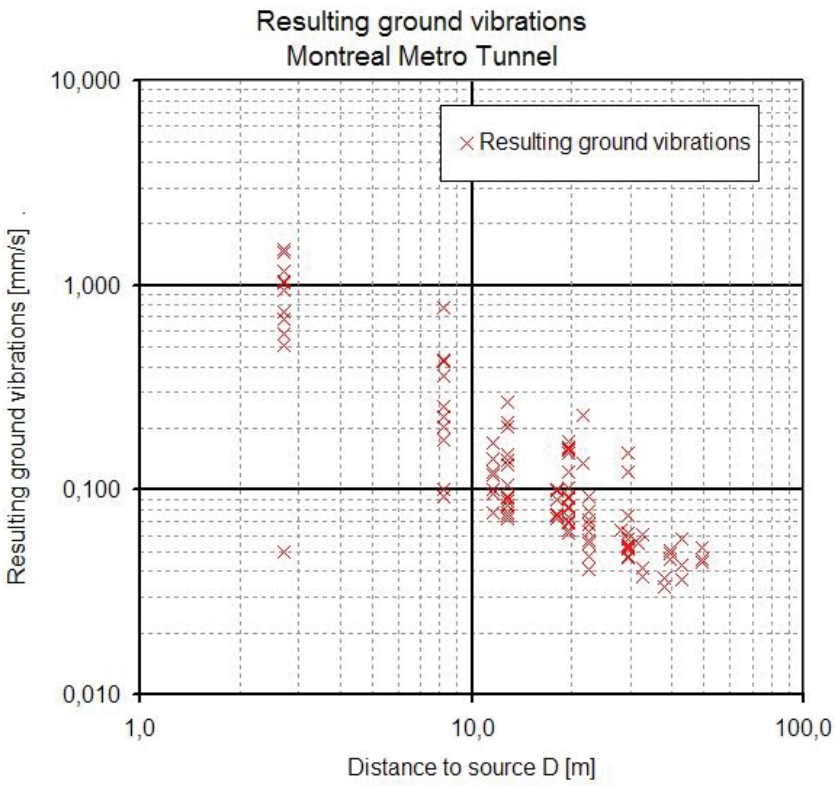

Figure 5.11: Resulting ground vibration – distance diagram, Montreal Metro Tunnel

5.4 Cullinan Diamond Mine (South Africa)

In the course of a stability project at Cullinan Diamond Mine, the Department of Mining and Tunneling at the University of Leoben carried out seismic measurements to determine the degree of ground disturbance caused by the cutting action of the roadheader [4], [16]. These measurements were done by Florian Egger and Miroslav Nagy (Department of Mining and Tunneling at the University of Leoben) in collaboration with the De Beers Group. The measuring stage was from 2004/11/24 to 2004/12/17.

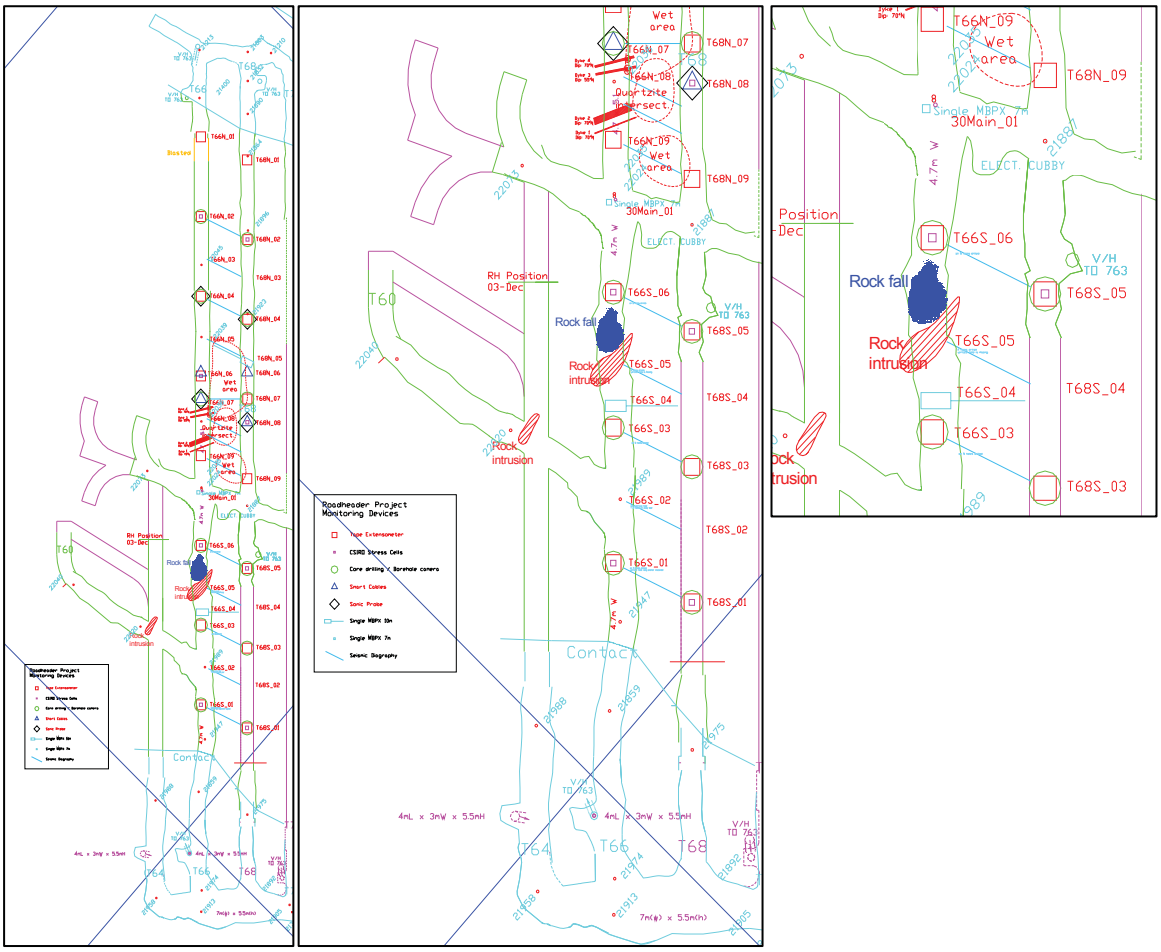

Figure 5.12: General arrangement drawing, level 717

A total of 24 measurements using triaxial-geophones were taken in Tunnel T66 South to determine ground vibrations caused by roadheader action.

5.4.1 Geological situation, rock and rock mass conditions in the mine

The rock in the project area at level 717 was Kimberlite Type I Grey TKB (tuffistic kimberlite breccia). According to the data of the Geotechnical Department of De Beers at Cullinan Diamond Mine the rock mass rating according to Bieniawski was 55. As the uniaxial compressive strength was only 79MPa, a good cutting performance was to be expected for roadheader drifting.

Rock specimens were tested at VOEST-ALPINE Bergtechnik – rock testing facilities (Appendix 9).

5.4.2 Operation sequence of the measurements

Ground vibration measurements were made while the roadheader was cutting in T64 south from South towards North. The geophones were installed in the boreholes T66 South 3, 3a, 5 and 6 West. The following Table gives an overview of the position of the geophones. A total of 14 measurements were taken on 2004/12/01 between 11:39 am and 12:43 pm and further 5 measurements on 2004/12/04 between 01:05 am and 01:16 am. On 2004/12/01 also 3 measurements were made of the background noise caused by the ventilation system and heavy machinery traffic. The background noise was of course also part of the records of the ground vibration measurements.

Geophone No.	Borehole	Installation depths	Height above level	Distance to cutting head on 2004/12/01	Distance to the cutting head on 2004/12/02
[#]		[m]	[m]	[m]	[m]
1	T 66 S 03 A W	0,9	2,5	21,9	25,3
2	T 66 South 03 W	1,2	2,2	18,6	21,8
3	T 66 South 05 W	1,3	1,4	9,4	12,1
4	T 66 South 06 W	1,2	1,7	8	7,1
5	T 66 South 06 W	3,1	1,7	7,2	5

Table 5.3: Overview of the positioning of the geophones.

A problem, which encountered, was the general poor condition of the boreholes which were not very straight and full of drill cuttings. As a result it was not possible to install geophones at borehole depths greater than 3,1m.

Measurement [#]	Date [yyyy-mm-dd]	Time [hh:mm:ss]	Geophone [#]					Scan rate	Number of acquired scans	Duration of measurement [s]	Trigger channel [##]	Deleted parts (peak number of channel)	Comment
			1	2	3	4	5						
1	01.12.2004	11:39:00	X	X	X	X	X	15000	300000	6,7	x- G2	0-10000	background noise
2	01.12.2004	11:41:00		X	X	X	X	15000	300000	15	x- G2	0-20000	
3	01.12.2004	11:43:00	X	X	X	X	X	15000	300000	20	x- G2	0-20000	
4	01.12.2004	11:52:00	X	X	X	X	X	15000	200000	13,3	x- G2	0-20000	
5	01.12.2004	11:55:00	X	X	X	X	X	15000	200000	13,3	x- G2	0-20000; 57000-77000	background noise
6	01.12.2004	12:02:00	X	X	X	X	X	15000	200000	13,3	x- G2	0-25000	
7	01.12.2004	12:04:00	X	X	X	X	X	30000	200000	6,7	x- G2	0-30000	
8	01.12.2004	12:08:00	X	X	X	X	X	20000	200000	10	x- G2	0-10000; 105000-135000	
9	01.12.2004	12:14:00	X	X	X	X	X	20000	200000	10	x- G2	0-24000	
10	01.12.2004	12:16:00						20000	200000	10	x- G2	0-25000	
11	01.12.2004	12:18:00	X	X	X	X	X	20000	200000	10	x- G2	0-23000	
12	01.12.2004	12:20:00	X	X	X	X	X	20000	150000	7,5	x- G2	0-30000	background noise
13	01.12.2004	12:22:30	X	X	X	X	X	30000	150000	5	x- G2	0-4000; 86000-110000	
14	01.12.2004	12:25:30	X	X	X	X	X	30000	150000	5	x- G2	0-25000	
15	01.12.2004	12:34:20	X	X	X	X	X	30000	150000	5	x- G2	110000-150000	
16	01.12.2004	12:35:40	X	X	X	X	X	30000	150000	5	x- G2	-	
17	01.12.2004	12:36:40	X	X	X	X	X	15000	300000	20	x- G2	-	
18	01.12.2004	12:38:00	X	X	X	X	X	15000	300000	20	x- G2	-	
19	01.12.2004	12:42:00	X	X	X	X	X	15000	300000	20	x- G2	-	
20	02.12.2004	01:05:00	X	X	X	X	X	15000	300000	20	z-G5	-	hard rock intrusion
21	02.12.2004	01:10:20	X	X	X	X	X	15000	300000	20	z-G5	-	hard rock intrusion
22	02.12.2004	01:13:15	X	X	X	X	X	15000	300000	20	z-G5	-	hard rock intrusion
23	02.12.2004	01:15:00	X	X	X	X	X	15000	300000	20	z-G5	-	hard rock intrusion
24	02.12.2004	01:19:00	X	X	X	X	X	15000	300000	20	z-G5	-	hard rock intrusion

Table 5.4: Overview of all measurements

Parts of the measurements that were influenced by the impact of the trigger (measurements 1-15) were deleted for the calculation of the resulting ground vibrations and for the frequency analysis.

As shown in Table 5.4 the results of the vibration measurements No. 20 to No. 24 were most likely influenced by a quartzite intrusion which ultimately resulted in the stoppage of cutting two hours after completion of measurement No. 24.

According to Table 5.4, 118 individual measurements were made with the triaxial-geophones. Geophone 1 was installed in a core drilled borehole, geophone 2, 3, 4 and 5 in percussion drilled holes. In some instances the signals were too weak to be recorded by all geophones. These are marked by an “X” in Table 5.4.

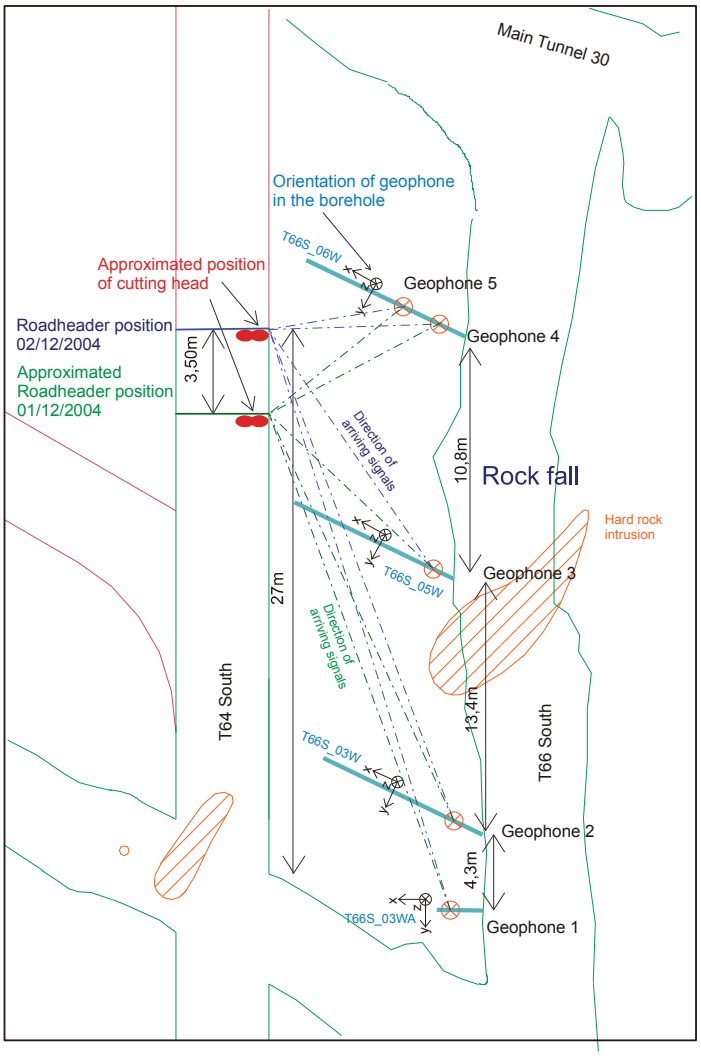

Figure 5.13: Overview of the position of the geophones at level 717

The position of the tunnel face in T64 south was measured on 2004/12/03 soon after the roadheader stopped cutting. The position marked “Roadheader position 2004/12/01” was used for the analysis of the measurements No. 20 to No. 24. The respective roadheader position for measurements No.1 to No. 19 is marked in Figure 5.13 as “Roadheader position 2004/12/01”.

5.4.3 Results of the measurements

In total 118 resultant ground vibrations for the maximum peak value were calculated. All measurements were taken between 5,0 m and 25,3m distance to the roadheader boom. The exact distance between the geophone and the boom is not known as the

cutting head position is permanently changing during the cut. In general the uncertainty decreases with the distance of geophone from the tunnel face.

For analysis of the results it has to be noted that the orientations of the geophones were determined by the borehole directions, whereas the direction of the arriving signal was determined by the cutting head relative to the position of the geophone.

Since the cutting head position relative to the independent geophone varies, care has to be taken at the interpretation of the magnitude of the components of the ground vibrations measured by individual geophones.

5.4.3.1 Results of the measurements of the background noise

In order to determine the ground vibration caused by heavy machinery traffic, the ventilation system and other activities in the mine, 3 measurements (number 1, 5, 12) were taken in periods without cutting activity of the roadheader. In this analysis, an average resulting ground vibration, independent of the distance to the roadheader, was calculated. The results of these resulting ground vibrations of the background noise are shown in Figure 5.14

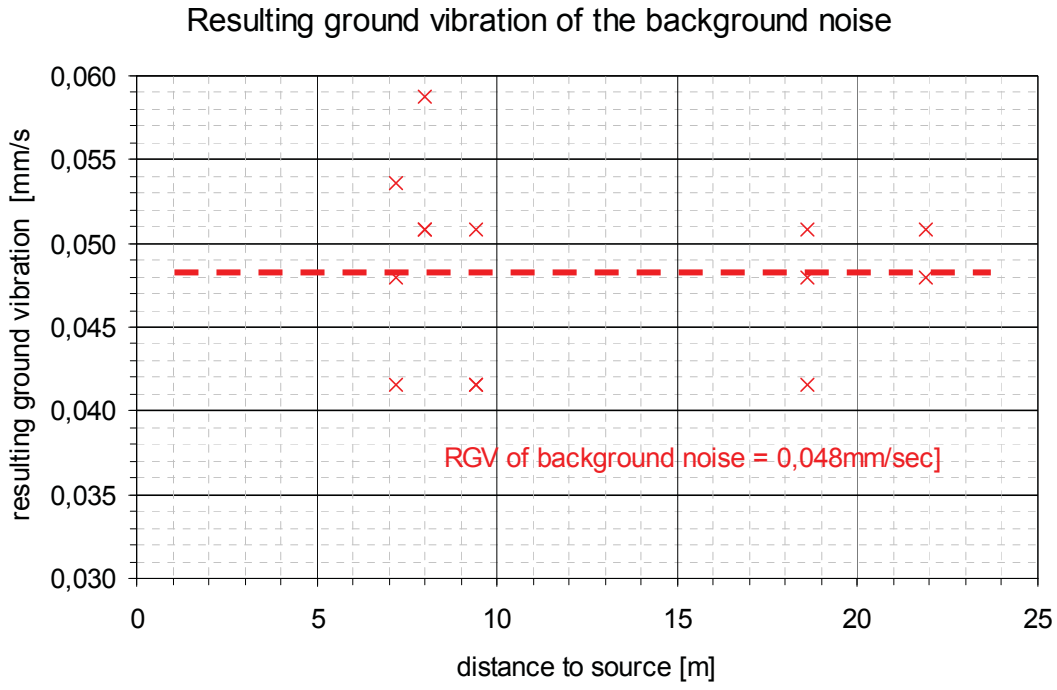

Figure 5.14: Resulting ground vibration of the background noise, measurements No. 1, 5, 12

5.4.3.2 Results of the ground vibration measurements

In total 19 measurements were taken. As shown in Table 5.7 the results of the vibration measurements No. 20 to No. 24 were influenced by a quartzite intrusion, which ultimately resulted in the stoppage of cutting soon after completion of measurement No. 24.

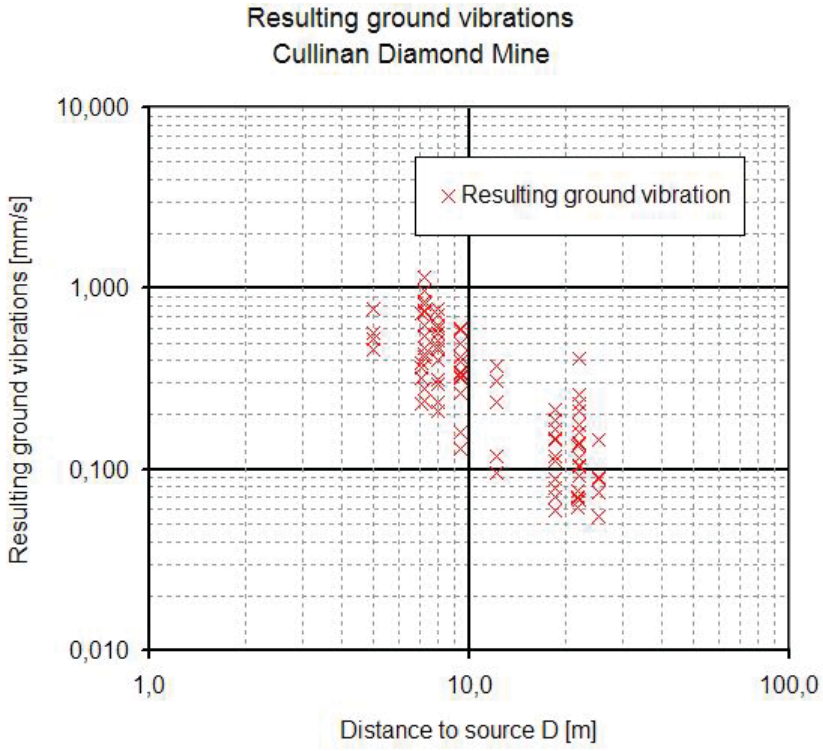

Figure 5.15: Resulting ground vibration – distance diagram, Cullinan Diamond Mine/ South Africa

5.5 Trial site at VOEST-ALPINE Bergtechnik in Zeltweg (Austria)

Ground vibration measurements were performed during an operation of roadheader ATM 105 at a concrete block at the test rig at VOEST-ALPINE Bergtechnik in Zeltweg. The concrete block was built on a foundation slab and was made in the quality C50. The side walls and the roof of the block were built of reinforced concrete.

A total of 54 ground vibration measurements were taken with borehole geophones. The measuring stage was on the 2005/11/24 and on the 2005/11/29. On the second day of measuring also the cutter current of the roadheader was recorded.

5.5.1 General information about the site

The concrete block was set up on a reinforced concrete basement in soil. The concrete block was 11m by 11m with a height of 8m. Figure 5.16 shows a sketch of the test rig and the measurement set up. The concrete was tested at VOEST-ALPINE Bergtechnik- rock testing facilities (Appendix 10).

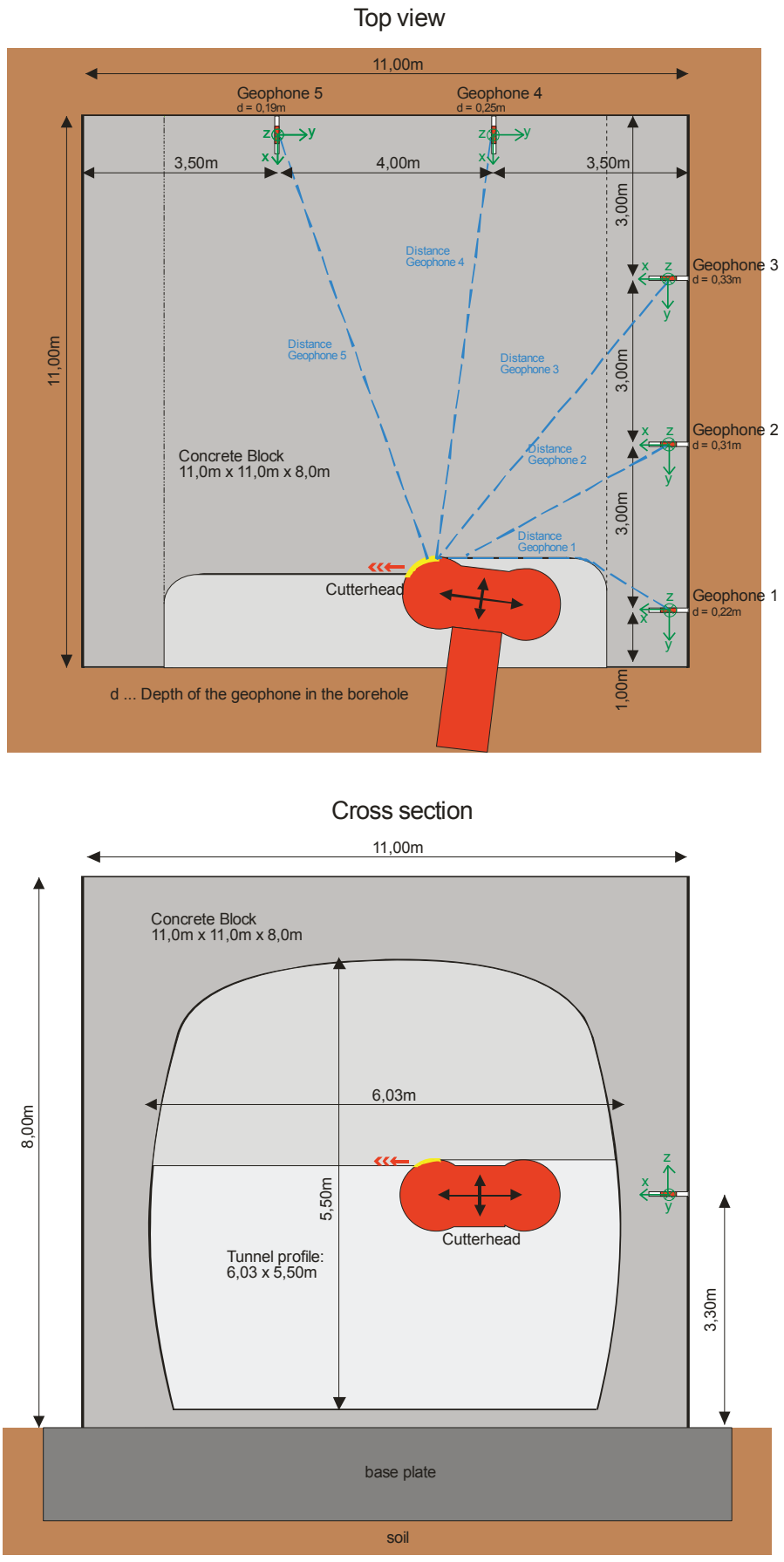

Figure 5.16: Test rig at VOEST-ALPINE Bergtechnik in Zeltweg

5.5.2 Results of the ground vibration measurements

The highest resulting ground vibration of all test measurements was 16,1 mm/s. The results show a broad spectrum of different ground vibrations. The arithmetic means of all maximum resulting ground vibrations is 3,65 mm/s. The measurements showed that the ground vibrations were highly depending on the cutting mode as well as on the position of the cutting head. For further analysis only measurements at the cutting mode “horizontal slewing” were taken. During this measurements also the exact position of the cutting head was recorded by sensors on the roadheader. As the position of the cutting head was changing during a measurement of 10 seconds, always the smallest distance between a geophone and cutting head was taken for the analysis.

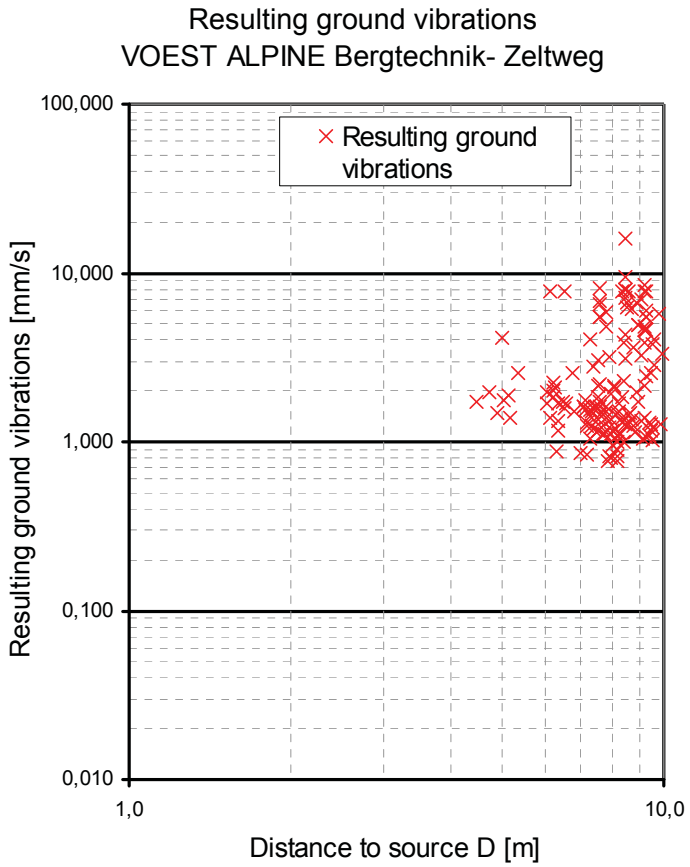

Figure 5.17: Resulting ground vibration – distance diagram, VOEST-ALPINE Bergtechnik in Zeltweg

Figure 5.16 shows the maximum resulting ground vibrations along the distance to the source.

6 Vibration measurements in tunnels developed by means of drilling and blasting

Measurements were taken at two different underground mines for full rounds of shots and at one mine for blasting tests:

- Wolfram Mine Mittersill:
  - Austrogel G1, Wandex
  - 65 boreholes, 3,8m advance per round
- Magnesite Mine Breitenau RHI
  - Gelatin Donarit 1, Emulgit LWC AI
  - 54 boreholes, 4,2m advance per round
- Erzberg Iron Ore Mine – test rig of the University of Leoben
  - Rockracker, Hanal 1U, Polyadin
  - Single shots

The main objective to perform measurements was to obtain data from different rock and impact conditions for an analysis to improve the function for the propagation of ground vibrations determined by the measurements at roadheader development and to determine the impact of energy for drill and blast development.

Parameter	Index	Unit	Location		
			Mittersill	Breitenau	Erzberg
Overburden	OV	[m]	775	800	60
Depth Geophone	DG	[m]	2,6-3,0	1,9-2,1	0,35-0,55
Mean Distance of the geophones	D_{mean}	[m]	60,2	30,1	14,3
Cross Section	CS	[m²]	22,0	24,0	12,0
Density	ρ	[kg/m³]	2958	2700	2703
Uniaxial Compressive Strength	UCS	[Mpa]	91,2	136,0	35,0
Brazilian Tensile Strength	BTS	[Mpa]	10,9	8,7	7,6
Young's Modulus	Y_M	[Mpa]	19361	102000	18136
Fracture Energy	E_f	[J]	29,5	7,3	4,2
Rock Mass Rating (Bieniawski)	RMR	[-]	55	41	55

Table 6.1: Overview of the rock and rock mass parameters and geometrical parameters for the drill and blast sites

6.1 Magnesite Mine Breitenau (Austria)

Ground vibration measurements were carried out during a drill and blast development in Revier III Süd at Horizont 12 at Magnesite Mine Breitenau. The measurements were taken from 2005/12/28 to 2006/01/03 with geophones fixed in boreholes. Only two measurements could be taken because of hardware problems of the measuring computer. The roadway had a cross section of 23,4m² and an overburden of about 800m.

6.1.1 Geological situation, rock and rock mass conditions in the mine

The Magnesite Mine Breitenau is in the eastern part of the Austrian Alps and the massive deposit dips with approximately 25° degrees opposite that of the mountain slope. The overburden varies between 0m and 1000m, where the overburden in the test area was approximately 800m.

During the investigation of rock and rock mass conditions of pillars of Dipl.-Ing. Matthias Sieffert a number of parameters for different areas in the mine were determined. It was decided that the test area in Revier III Süd was mainly similar to the test areas No. 1.1 in Revier III Nord [20].

6.1.2 Operation sequence of the measurement

The measurements were taken one level above the drill and blast excavation. The geophones were installed in percussion drilled boreholes in about 1,5m height above the floor. The distances from the geophones to the blast were determined by knowing the location of the geophones relative to a surveyed point at the level and the height above level as well as the height of the intermediate level. The location of the front faces of the blasts was known as the distance to the next surveyed point at the level was known.

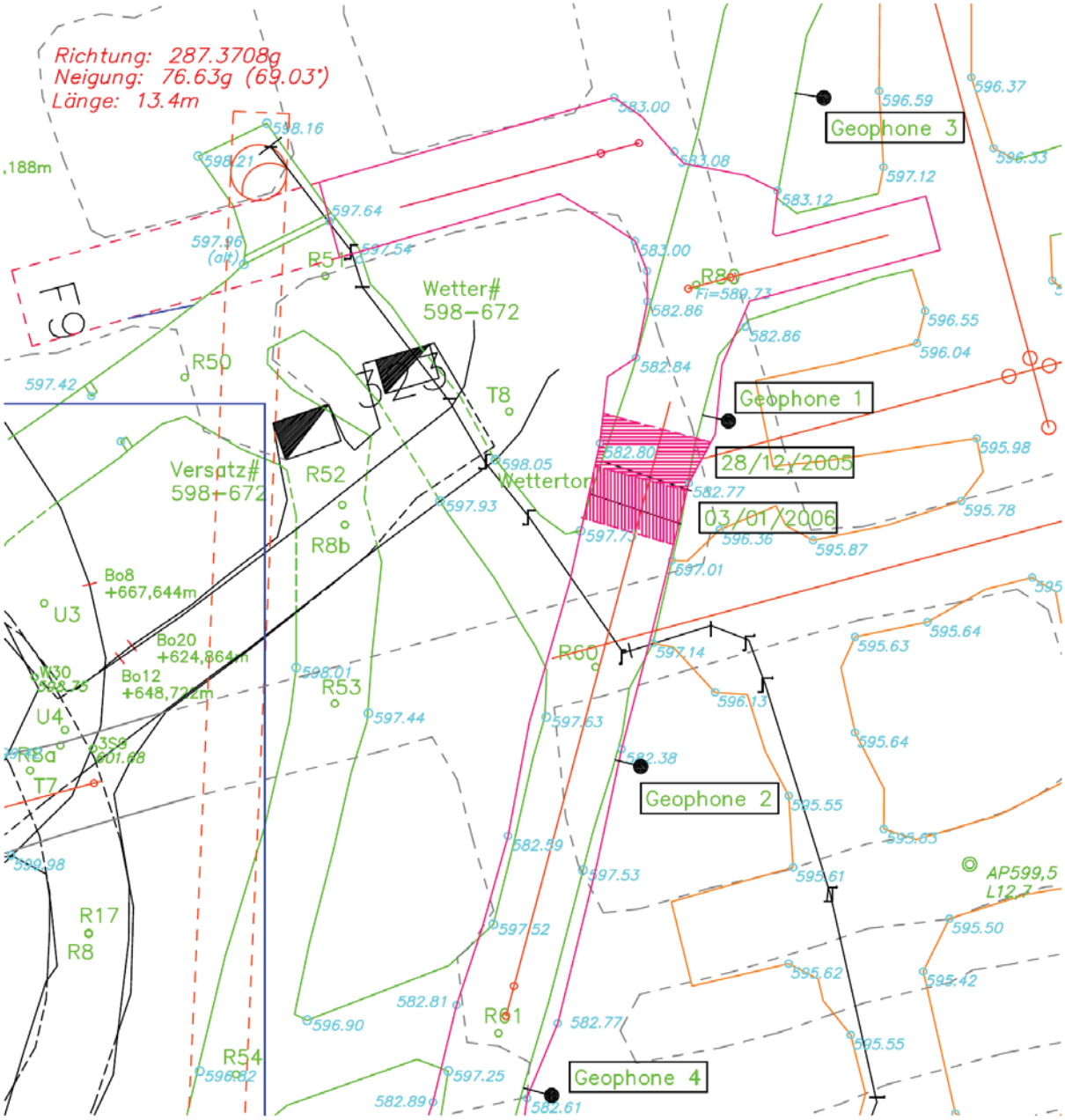

Figure 6.1: Geophone arrangement at Magnesite Mine Breitenau

Figure 6.1 shows the geophone arrangement at Horizont 12 Revier III Süd at Magnesite Mine Breitenau.

6.1.3 Drill pattern

A total of 54 boreholes were drilled for each round of shots. Parameters and constants of drilling and blasting are shown in Table 6.2

Parameter		Unit	Location
			Breitenau
Cross section		[m²]	23,4
Number of boreholes		[#]	54
Diameter of boreholes		[mm]	45
Advance per round		[m]	4,2
Name of igniter	Type I	[-]	MS
Number of igniters	Type I	[#]	8
Delay time	Type I	[ms]	25
Delay stages	Type I	[#]	8
Name of igniter	Type II	[-]	LP
Number of igniters	Type II	[#]	46
Delay time	Type II	[ms]	40
Delay stages	Type II	[#]	6
Name of igniter	Type III	[-]	-
Number of igniters	Type III	[#]	-
Delay time	Type III	[ms]	-
Delay stages	Type III	[#]	-
Name of explosive	Type I	[-]	Gelatin Donarit 1
Mass of explosive	Type I	[kg]	50
Specific energy of explosive	Type I	[kJ/kg]	900
Detonation speed of explosive	Type I	[m/s]	6000
Name of explosive	Type II	[-]	Emulgit LWC Al
Mass of explosive	Type II	[kg]	210
Specific energy of explosive	Type II	[kJ/kg]	920
Detonation speed of explosive	Type II	[m/s]	3600
Name of explosive	Type III	[-]	-
Mass of explosive	Type III	[kg]	-
Specific energy of explosive	Type III	[kJ/kg]	-
Detonation speed of explosive	Type III	[m/s]	-

Table 6.2: Drill and blast parameter, Magnesite Mine Breitenau

Figure 6.3 shows the drill pattern and igniter arrangement for a round of shots.

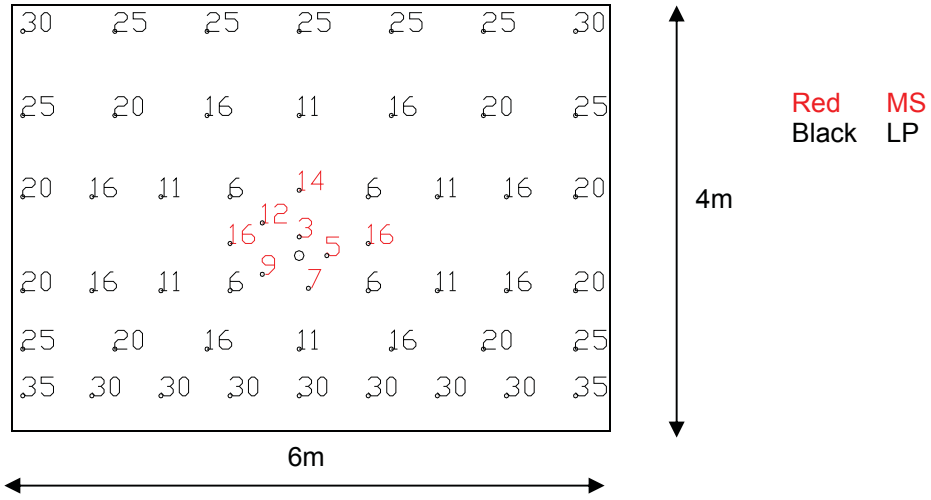

Figure 6.2: Drill pattern, Magnesite Mine Breitenau

6.1.4 Results of the ground vibration measurements

The maximum resulting ground vibrations were 90 mm/s at a distance of 15,6m from the source.

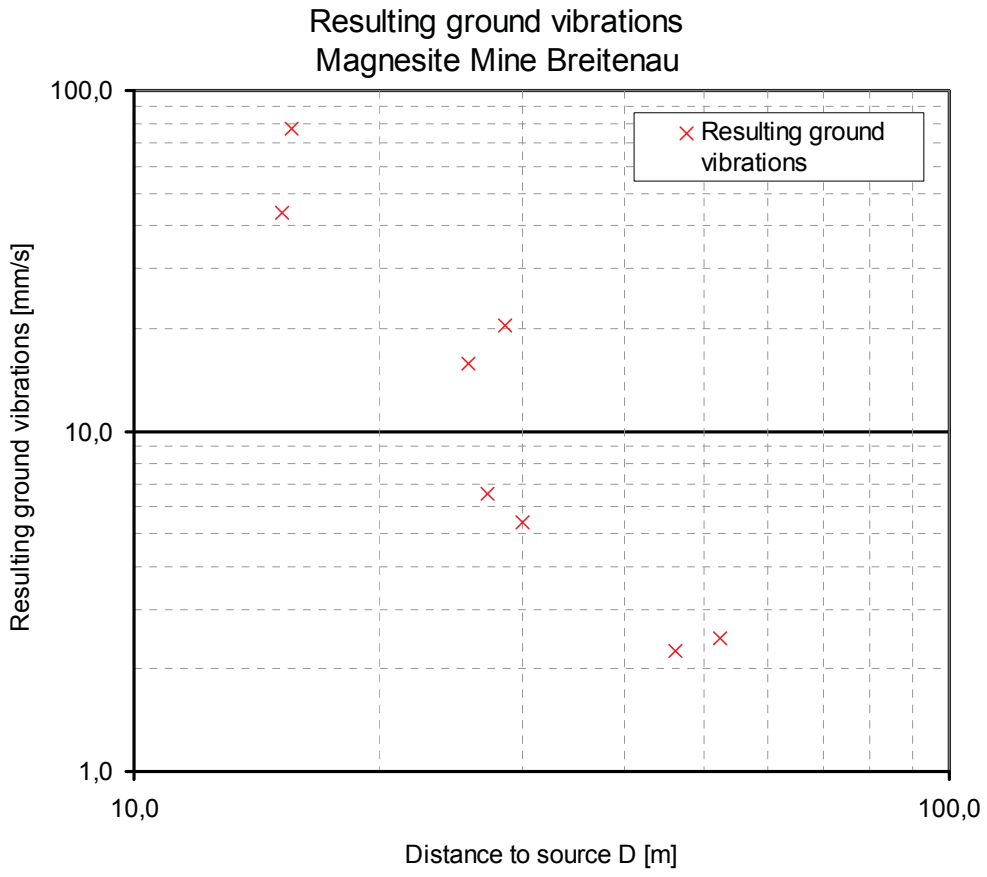

Figure 6.3: Resulting ground vibration – distance diagram, Magnesite Mine Breitenau

6.2 Wolfram Mine Mittersill (Austria)

Ground vibration measurements were performed during a drill and blast development at level TS775 at Wolfram Mine Mittersill. The measurements were taken from 2005/10/11 to 2005/10/13 with geophones fixed in boreholes and VIBRAS 3004 measurement system. The roadway had a cross section of 22,5m² and the overburden was about 775m.

6.2.1 Geological situation, rock and rock mass conditions in the mine

Rock specimens from level TS775 were taken and analyzed at VOEST-ALPINE Bergtechnik rock testing facilities. Data sheets of the rock testing can be found in Appendix 7.

Care has to be taken at the interpretation of the results of the rock testing as the specimens were taken from the excavated rock of the blasting. For that reason results show smaller values, as the rock was pre-fractured.

6.2.2 Operation sequence of the measurements

An overview of level 775 and the arrangement of the geophones is illustrated in Figure 6.5 and Figure 6.6.

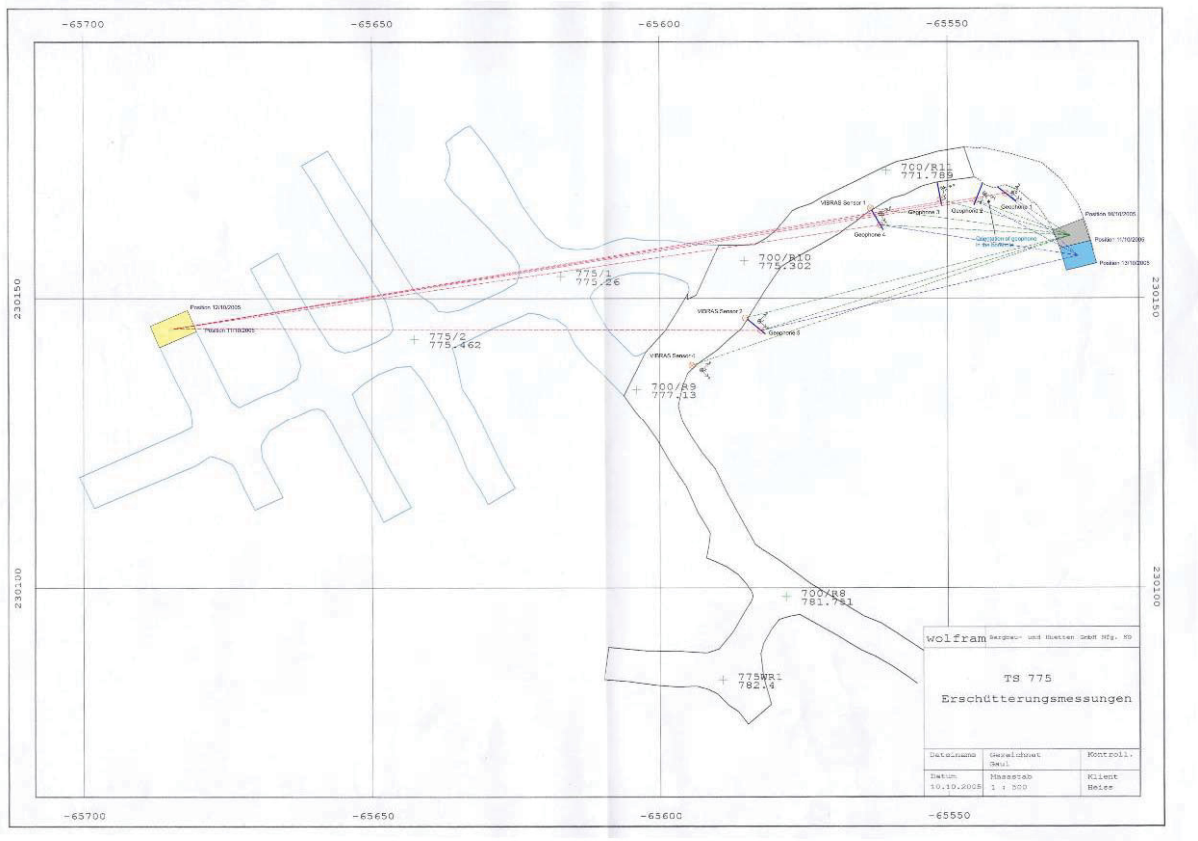

Figure 6.4: Overview, Level TS 775, geophone arrangement, Wolfram Mine Mittersill

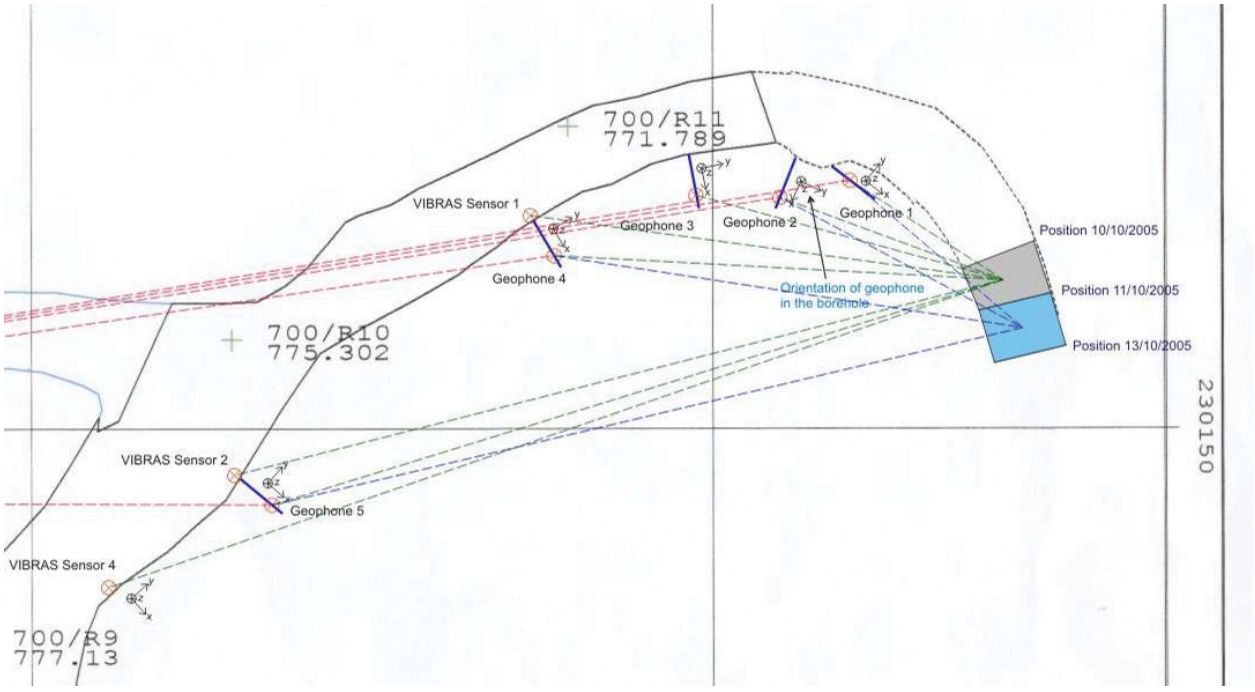

Figure 6.5: Level TS 775, geophone arrangement, Wolfram Mine Mittersill

6.2.3 Drill pattern

A total of 65 boreholes were drilled for each round of shots. Parameters and constants of drilling and blasting are shown in Table 6.4

Parameter		Unit	Location
			Mittersill
Cross section		[m²]	22
Number of boreholes		[#]	65
Diameter of boreholes		[mm]	52
Advance per round		[m]	3,8
Name of igniter	Type I	[-]	O-HU
Number of igniters	Type I	[#]	1
Delay time	Type I	[ms]	0
Delay stages	Type I	[#]	1
Name of igniter	Type II	[-]	DEM-P-HU
Number of igniters	Type II	[#]	17
Delay time	Type II	[ms]	80
Delay stages	Type II	[#]	7
Name of igniter	Type III	[-]	DEP-HU
Number of igniters	Type III	[#]	47
Delay time	Type III	[ms]	500
Delay stages	Type III	[#]	7
Name of explosive	Type I	[-]	Austrogel G1
Mass of explosive	Type I	[kg]	90
Specific energy of explosive	Type I	[kJ/kg]	1020
Detonation speed of explosive	Type I	[m/s]	6000
Name of explosive	Type II	[-]	Wandex
Mass of explosive	Type II	[kg]	165
Specific energy of explosive	Type II	[kJ/kg]	1000
Detonation speed of explosive	Type II	[m/s]	2750
Name of explosive	Type III	[-]	Wandex
Mass of explosive	Type III	[kg]	165
Specific energy of explosive	Type III	[kJ/kg]	1000
Detonation speed of explosive	Type III	[m/s]	2750

Table 6.3: Drill and blast parameter, Wolfram Mine Mittersill

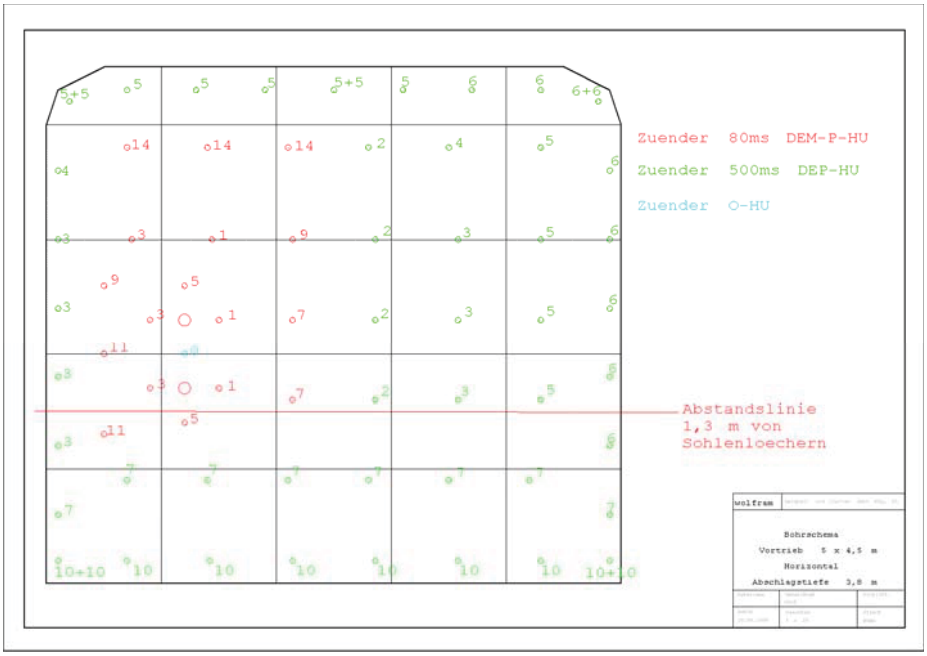

Figure 6.6: Drill pattern and igniter arrangement, Wolfram Mine Mittersill

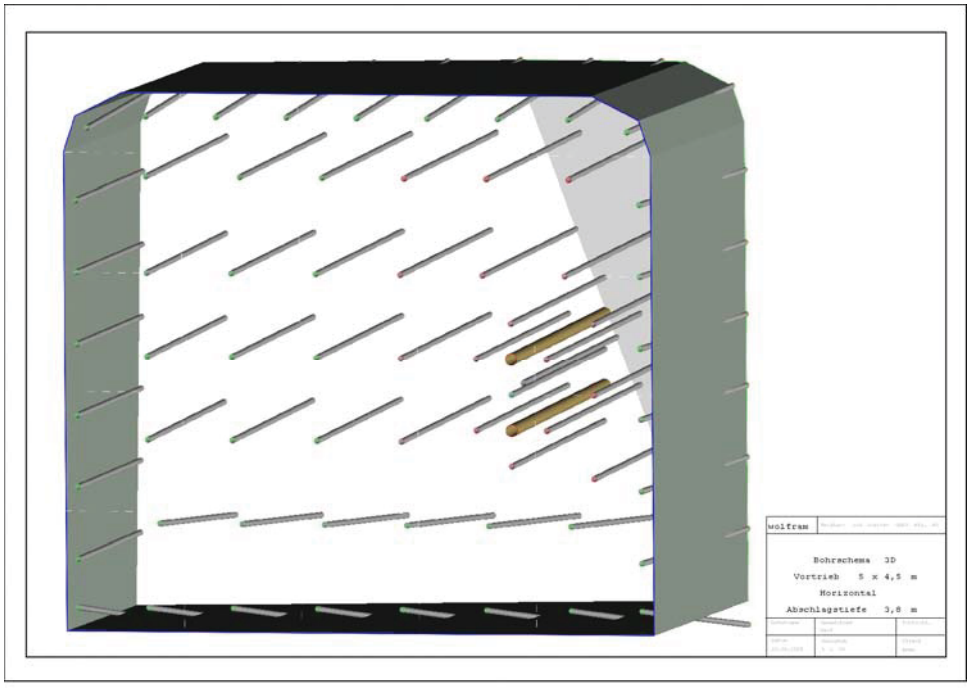

Figure 6.7: Drill pattern, 3D, Wolfram Mine Mittersill

Figure 6.7 and Figure 6.8 show the drill pattern and igniter arrangement for a round of shots.

6.2.4 Results of the ground vibration measurements

The maximum resulting ground vibration was 124mm/s at a distance of 14,5m from the source.

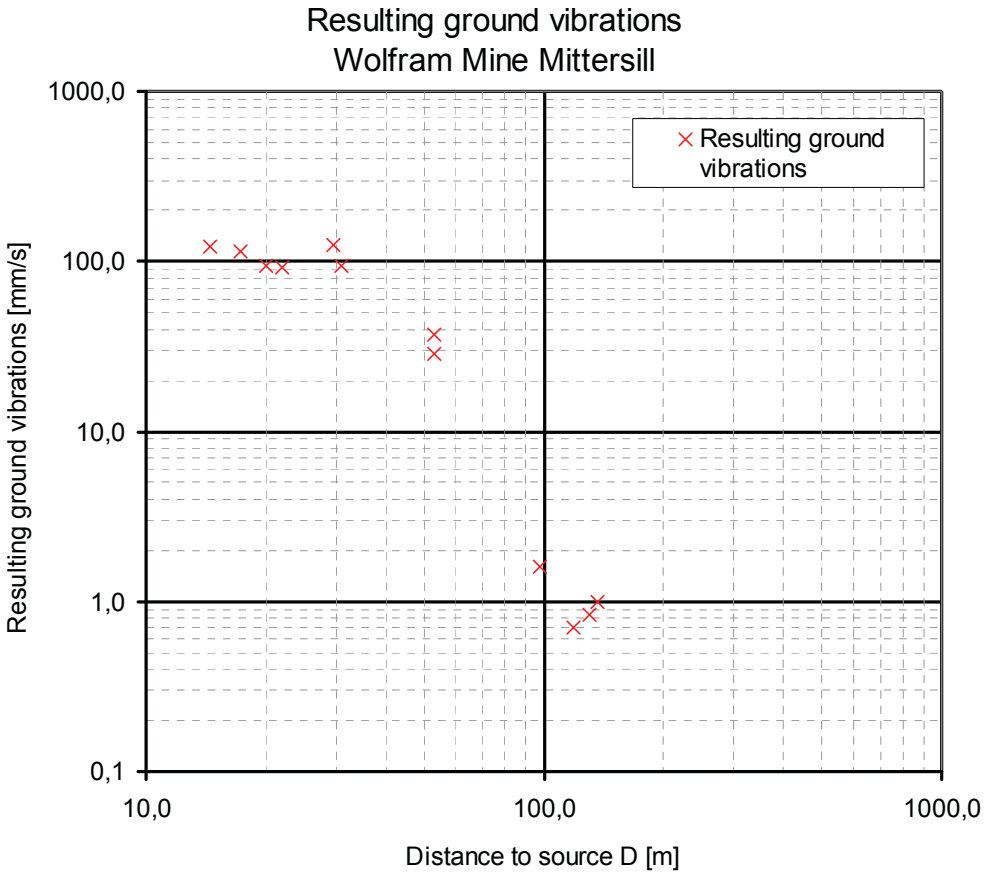

Figure 6.8: Resulting ground vibration – distance diagram, Wolfram Mine Mittersill

6.3 Erzberg Iron Ore Mine (Austria)

The test site was located in the test area of the Department of Mining and Tunneling of the University of Leoben at the Erzberg Iron Ore Mine. The ground vibration measurements were performed by Dipl.-Ing. Christian Heiss and Florian Egger during blast experiments with Rockrackers accomplished by Dipl.-Ing. Julia Vargek from the Department of Mining and Tunneling during [24].

6.3.1 Geological situation at the test site

Rock specimens from the excavated rock of the shot in borehole 5 were taken and analyzed at VOEST-ALPINE Bergtechnik rock testing facilities. Data sheets of the rock testing can be found in Appendix 8.

Care has to be taken at the interpretation of the results of the rock testing as the specimens were taken from the excavated rock of the blasting. For that reason results show smaller values, as the rock was pre-fractured.

6.3.2 Operation sequence of the measurements

During this experiments the depth of the borehole and the mass of the explosives was varied. Table 6.4 shows the blasting parameters for the five single shots.

	Borehole-diameter	Length of the borehole	Side distance	Borehole distance	Blasted Volume	Rock-kracker	Hanal 1U	Polyadin
	[mm]	[m]	[m]	[m]	[m³]	[g]	[g]	[g]
Borehole 1	38	1,40	0,50	0,40	0,28	30,00	13,60	-
Borehole 2	38	1,00	0,50	0,40	0,20	20,00	27,20	-
Borehole 3	38	1,20	0,50	0,40	0,24	50,00	113,60	-
Borehole 4	38	1,40	0,50	0,40	0,36	-	-	500
Borehole 5	38	1,40	0,50	0,40	0,28	180,00	81,60	-

Table 6.4: Blasting parameters for the five single shots, test area of the University of Leoben at the Erzberg Iron Ore Mine

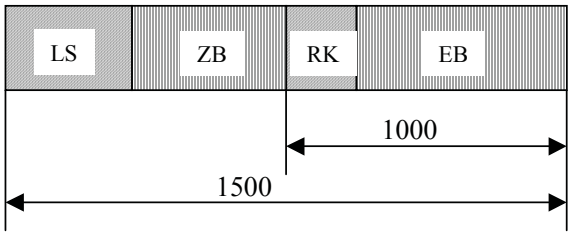

LS: Rockracker and Hanal 1U
ZB: Intermediate tamping
RK: Rockracker
EB: Final tamping

Figure 6.9: Arrangement of the column load, test area University of Leoben at the Erzberg Iron Ore Mine

Figure 6.10 shows the arrangement of the column load in the borehole and Figure 6.8 shows the arrangement of the boreholes in the sidewall.

Figure 6.10: Arrangement of the boreholes in the sidewall, test area University of Leoben at the Erzberg Iron Ore Mine

6.3.3 Results of the ground vibration measurements

In Figure 6.12 the diagram on the left side shows the resulting ground vibrations along the distance to the source for the different shots. The diagram on the right side shows the resulting ground vibrations along the scaled distance to the source for the different shots. The scaling of the distance by dividing the distance with the square root of the mass of the explosives leads to a very good normalization of the results of the single shots with different charge. [14], [15]

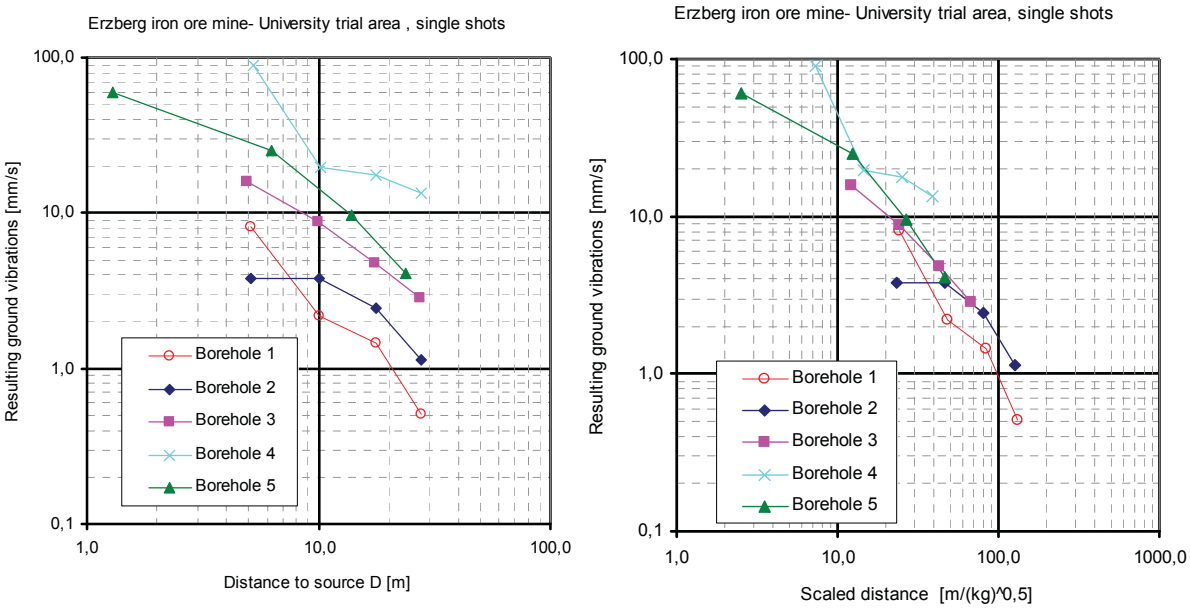

Figure 6.11: Resulting ground vibration – distance diagram and scaled distance, test area University of Leoben at the Erzberg Iron Ore Mine

7 Analysis and modelling

More than four hundred measurements to determine the resulting ground vibrations were used for the analysis and modelling. The measurements were taken at four different underground mines and one test site on the surface for roadheader development and three different underground mines for drill and blast development.

One main objective of the study was to quantify the impact of energy of the heading method along the sidewall of a roadway. Therefore the function for the propagation of ground vibrations of different conditions had to be determined and then using this function, the impact of energy for a unit element in the sidewall during 1m of roadway excavation was modeled.

The analysis and modeling were performed by using measurement data from four underground mines with roadheader development. The results of this process were tested for the trial site on the surface and then used to perform a suitable analysis for drill and blast development, as only a view data for drill and blast excavation was accessible.

An overview of assumptions and simplifications is given in Chapter 7.3.

7.1 Model for the propagation of ground vibrations caused by roadheader development

The development of rock mechanics depends substantially on experimental results. Solutions to most problems in rock mechanics involve a combination of analysis and experimental information. Most of the work on propagation of ground vibrations is based on either specific local experiments or empirical formulas. No generally acceptable method exists for predicting the ground vibrations along the sidewall in tunnels, based only on rock mass properties, rock properties, geometrical parameters and parameters for the excavation method.

7.1.1 Introduction to the function for the propagation of ground vibrations

In geophysics the following equation for the propagation of ground motions is used:

(9) $$V_D = V_0 \cdot \left(\frac{D_0}{D}\right)^n \cdot e^{\alpha \cdot (D_0 - D)}$$

D Distance [m]

D_0 Distance, where V_0 is known [m]

V_D Vibration in the distance D [mm/s]

V_0 Vibration in the distance D_0 [mm/s]

α Absorption coefficient [1/m]

n Exponent depending on the wave type [-]:

n=0 for plate waves

n=1 for spherical waves

The function is composed by a power function and an exponential function.

For a material with an absorption coefficient α=0 the function would be:

(10) $$V_D = V_0 \cdot \left(\frac{D_0}{D}\right)^n$$

which is a power function with the exponent n.
For plate waves (n=0) the vibration in the distance D would be the same like the vibration in the distance D_0.[12]

For a plate wave in a material with an absorption coefficient α>0 the function would be:

(11) $$V_D = V_0 \cdot e^{\alpha \cdot (D_0 - D)}$$

which is an exponential function.

In the equation used in geophysics it was assumed that the same wave type arrives at the distance D and at the distance D_0. In the equation in this paper it was assumed that at the distance D and at the distance D_0 from the source of impact different wave types arrive depending on geometrical parameters, which means that D and D_0 have different exponents.

In the equation used in geophysics V_0 can be the vibration at any distance D_0. In the equation in this paper it was assumed that V_0 was always the maximum vibration at the distance from the impact (e.g. borehole with explosive or chisel of roadheader) to the rapture zone (e.g. the depth of the cut of the cutting head).

The absorption coefficient was depending on the rock mass properties, the rock properties, the compressive stress (overburden) and the frequency (low-pass filter effect of rock).

According to this assumptions a function for the propagation of ground vibrations for roadheader development is:

(12) $$RGV_D = RGV_{Cut} \cdot \frac{D_{Cut}^{n_{Cut}}}{D^{n_D}} \cdot e^{\alpha \cdot (D_{Cut} - D)}$$

Parameter	Index	Unit
Resulting ground vibration at the distance D_{Cut}	RGV_{Cut}	[m/s]
Resulting ground vibration at the distance D	RGV_D	[m/s]
Spherical Cut Distance	D_{Cut}	[m]
Distance	D	[m]
Wave form factor for the distance D_{cut} and Overburden OV	n_{Cut}	[-]
Wave form factor for the distance D and Overburden OV	n_D	[-]
Absorption coefficient	α	[1/m]

Table 7.1: Parameters of the function for the propagation of ground vibrations.

In the following Chapters the determination of the resulting ground vibration at the source of impact, the wave form factor and the absorption coefficient are explained.

7.1.2 Spherical Cut Distance

Figure 7.1 shows the movement of the cutting head for horizontal slewing.

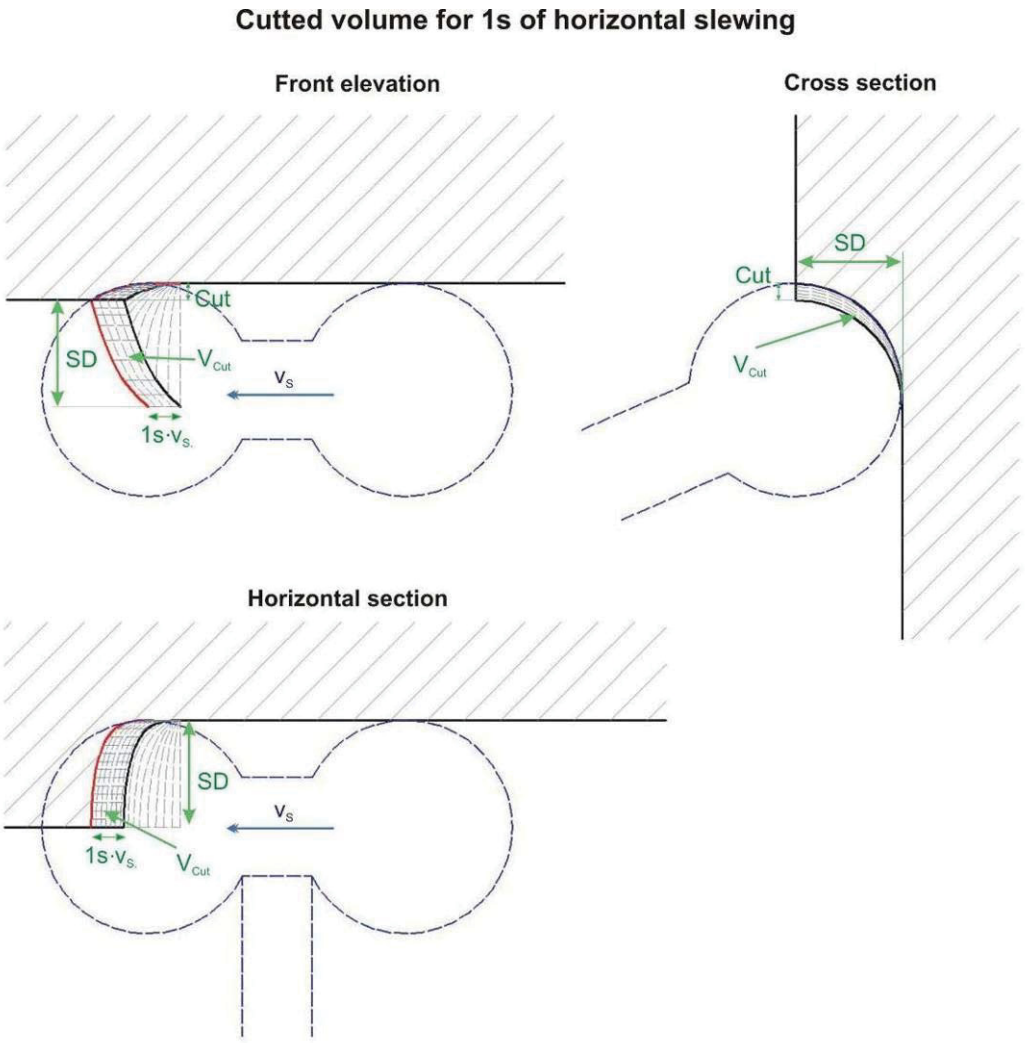

Figure 7.1: Horizontal slewing of the cutting head

The spherical cut distance D_{Cut} is the radius of a sphere with the volume VO_{Sphere} that equals the cut volume for horizontal slewing of the cutting head for a time period t of 1 second.

(13) $$SD \cdot Cut \cdot v_s \cdot t = VO_{Cut} = VO_{Sphere} = \frac{4 \cdot \pi \cdot D_{Cut}^{\ 3}}{3}$$

where SD is the sump in depth of the cutting head and v_s is the slewing speed of the cutting head.

(14) $$D_{Cut} = \sqrt[3]{\frac{3 \cdot SD \cdot Cut \cdot v_s \cdot t}{4 \cdot \pi}}$$

7.1.3 Resulting ground vibrations at the source of impact for a roadheader development

The resulting ground vibrations at the source of impact RGV_{Cut} are the vector sum of the vibrations in the three axis x, y and z.

It was assumed that the principal part of the seismic energy that is induced into the rock mass arrives as a series of n equal sinusoidal waves with the length λ, the amplitude $A_{max,}$ the period T_0, the instantaneous particle velocity V_{in} and the mass M of the particle. The kinetic energy for an instantaneous particle velocity V_{in} is:

(15) $$E_{Kin}=0{,}5\cdot M\cdot V_{in}{}^{2}.$$

The velocity of the particle V_{in} at any time of the wave is:

(16) $$V_{in}=V_{max}\cdot\sin\frac{2\cdot\pi\cdot t}{T_0}$$

and therefore the instantaneous kinetic energy is:

(17) $$E_{Kin,in}=0{,}5\cdot M\cdot V_{max}{}^{2}\cdot\sin^{2}\frac{2\cdot\pi\cdot t}{T_0}$$

The average kinetic energy for a unit volume element of the density ρ in a single period is then determined by integral calculus:

(18) $$E_{av}=\frac{\rho\cdot V_{max}{}^{2}}{4}=\frac{\pi^{2}\cdot\rho\cdot A_{max}{}^{2}}{T_0{}^{2}}$$

where

(19) $$V_{max}=RGV=2\cdot\pi\cdot\frac{A_{max}}{T_0}$$

The surface area of a spherical shell AR_{Shell} of the thickness $q\cdot\lambda$ with the focus as a center, where q is the number of periods and D the distance from the source was:

(20) $$AR_{Shell}=4\cdot\pi\cdot D^{2}$$

The kinetic energy E_T within that spherical shell was:

(21) $$E_T=4\cdot\pi\cdot D^{2}\cdot q\cdot\lambda\cdot E_{av}$$

For a propagation velocity v of the energy the wave length was:

(22) $$\lambda = T_0 \cdot v = \frac{v}{\varphi}$$

and the kinetic energy was:

(23) $$E_T = 4 \cdot \pi \cdot D^2 \cdot q \cdot T_0 \cdot v \cdot \frac{\pi^2 \cdot \rho \cdot A_{max}{}^2}{T_0{}^2} = \pi \cdot D^2 \cdot q \cdot T_0 \cdot v \cdot V_{max}{}^2$$

Within a thickness of the shell of D_W there are q waves of the wave length λ:

(24) $$q = \frac{D_W}{\lambda} = \frac{D_W \cdot \varphi}{v}$$

and the kinetic energy was:

(25) $$E_T = \pi \cdot D^2 \cdot \frac{D_W \cdot \varphi}{v} \cdot \frac{v}{\varphi} \cdot V_{max}{}^2 \cdot \rho = \pi \cdot D^2 \cdot D_W \cdot V_{max}{}^2 \cdot \rho$$

For a time t of 1 second where the number of oscillations r is:

(26) $$r = \frac{t}{T_0} = t \cdot \varphi$$

the kinetic energy was:

(27) $$E_T = \pi \cdot D^2 \cdot D_W \cdot \rho \cdot RGV^2 \cdot r = \pi \cdot D^2 \cdot D_W \cdot \rho \cdot RGV^2 \cdot t \cdot \varphi$$

As the spherical cut distance D_{Cut} is given by:

(14) $$D_{Cut} = \sqrt[3]{\frac{3 \cdot SD \cdot Cut \cdot v_s \cdot t}{4 \cdot \pi}}$$ (see 7.1.2),

the resulting ground vibration at the distance D_{Cut} is:

(28) $$RGV_{Cut} = \sqrt{\frac{E_{T,Cut}}{\frac{1}{4} \cdot \frac{4 \cdot \pi \cdot D_{Cut}{}^3}{3} \cdot \rho \cdot t \cdot \varphi}} = \sqrt{\frac{4 \cdot E_{T,Cut}}{SD \cdot Cut \cdot v_s \cdot \rho \cdot t^2 \cdot \varphi}}$$

by implementing equation (14).

The consumed energy of the cutting head of the roadheader E_{RH} in a period t depends on a number of parameters. Apart from the parameters which are constrained by the construction of the roadheader that were equal as always the same roadheader was used for drifting, a rock parameter with easy access is the

fracture energy E_f,. The fracture energy is defined by the area under the load-compression curve by laboratory testing. A parameter that reflects the relationship between fracturing/crushing and energy consumption more adequate is the “Rittinger Koeffizient”, but this parameter was not available for the rock at the test sites. The fracture energy used in this analysis was always related to the specimen dimensions used in the rock testing laboratory at VOEST ALPINE Bergtechnik. Data sheets with detailed information can be found from Appendix 7 to Appendix 10.

The cutting head efficiency factor was defined as:

(29) $$\eta_{RH} = (\kappa \cdot E_f)$$

where κ is the cutting head efficiency rate and constrained by the roadheader and cutting head properties.

(30) $$E_{T,Cut} = E_{RH} \cdot (\kappa \cdot E_f)$$

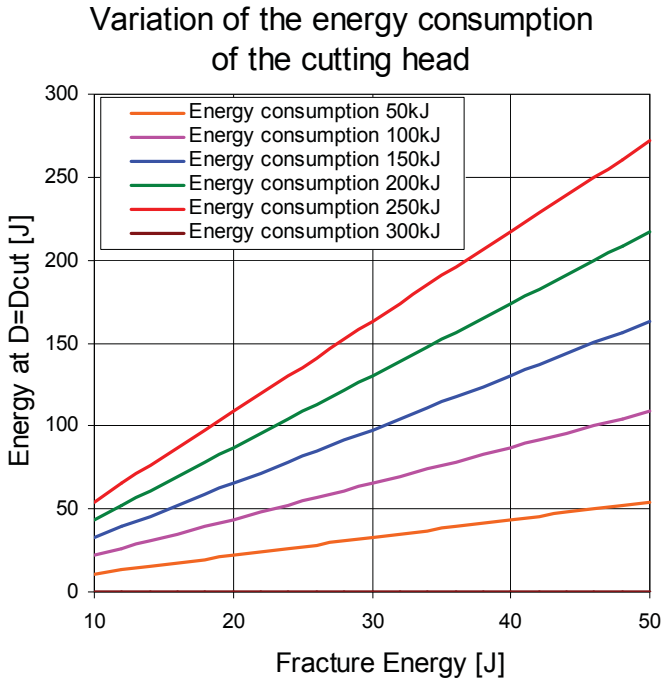

Figure 7.2: Variation of the fracture energy E_f and the energy consumption of the roadheader E_{RH}

Figure 7.2 shows the radiated energy at $D=D_{Cut}$ as a function of the fracture energy and the energy consumption of the roadheader.

This relation leads to the equation for the resulting ground vibration at the distance D_{Cut}:

(31) $$RGV_{Cut} = \sqrt{\frac{4 \cdot E_{RH} \cdot (\kappa \cdot E_f)}{SD \cdot Cut \cdot v_s \cdot \rho \cdot t^2 \cdot \varphi}}$$

7.1.4 Wave form factor

In a solid bar (with a thickness much smaller than the wavelength) the wave form factor n is 0, but in a solid with lateral dimensions much larger than the wavelength, the wave form factor n is unlike 0 and can reach the maximum of 1 for spherical waves, which means that n is within the boundaries:
$0 < n < 1$

The ratio of lateral dimensions to the wavelength plays a major role in determining the wave form factor, which can be seen in the comparison above. When ground vibrations are propagated through a solid (e.g. rock mass) of certain lateral dimensions, the shortest distance to the surface of this solid plays a major role for the wave type.
That means that the wave form factor is a function of the shortest distance to the next surface. This was, for measurements by means of borehole-geophones, the perpendicular distance of the geophone's position to the sidewall.

(32) $$n = f(DG)$$

It was decided that the most suitable function for the relationship of wave form factor and distance was a tangential function, whose argument was the root of the geophone depths multiplied with an empirical determined coefficient, namely the wave form factor coefficient m. After calculating the arctangent of the function, it was normalized by the multiplication with $2/\pi$ to a maximum value of 1.
The final equation for the wave form factor was:

(33) $$n_D = \frac{2 \cdot \arctan\left(h \cdot \sqrt{DG}\right)}{\pi}$$

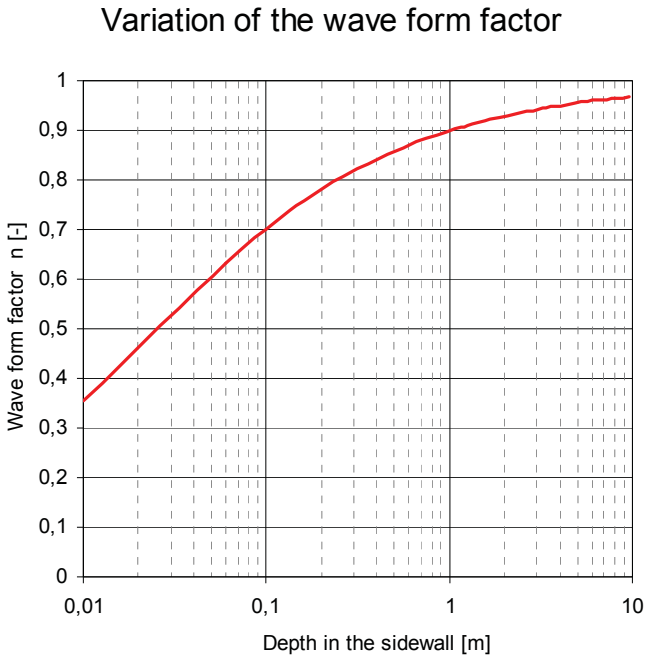

Figure 7.3: Variation of the wave form factor

Figure 7.3 shows the variation of the wave form factor depending on the depth in the sidewall. The smaller the depth in the sidewall, the smaller is the wave form factor.

The wave form factor at the source of impact for roadheader development was:

(34) $$n_{Cut} = \frac{2 \cdot \arctan\left(h \cdot \sqrt{D_{Cut}}\right)}{\pi}$$

7.1.5 Absorption coefficient

The absorption coefficient is a property of a material. It defines the extent to which a material absorbs waves. When elastic waves are passing a solid, a loss of energy occurs, mainly because of internal friction, when vibration energy is partly transformed into heat energy. The absorption is the "missing piece", when comparing the total reflected and transmitted energy with the incident energy. It is the property of a material that changes seismic energy into usually heat energy. A material or surface that absorbs sound waves does not reflect them. [13]

For the absorption of ground vibrations with certain frequencies in a rock mass, the absorption coefficient is depending on the rock mass properties, the rock properties, the compressive stress (overburden) and the frequency of the vibration (low-pass filter effect of rock).

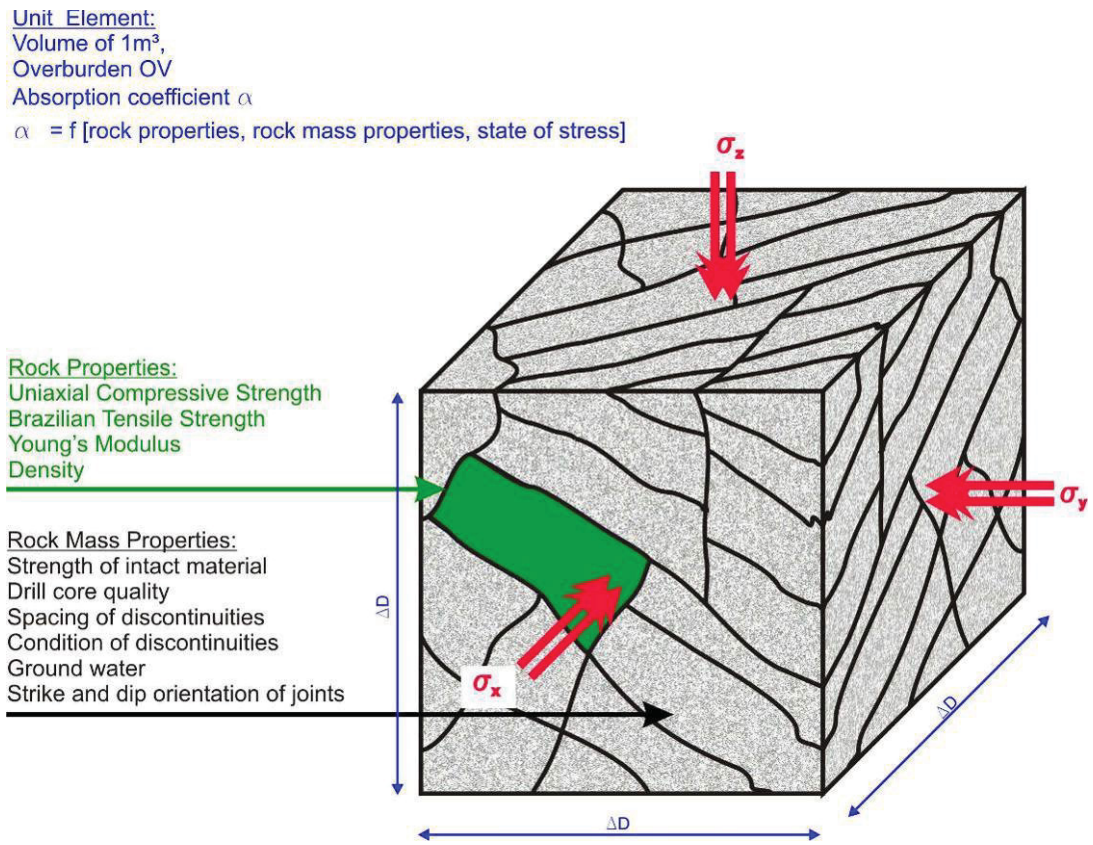

Figure 7.4: Parameters of the absorption coefficient considering as example a unit element

The accessible parameters to determine the absorption coefficient were:

- Rock mass rating
- Uniaxial compressive strength
- Brazilian tensile strength
- Young's modulus
- Overburden
- Density of the rock
- Frequency of the vibration φ

(35) $$\alpha = f\{\rho, RMR, UCS, BTS, Y_M, OV, \varphi\}$$

It was decided to determine α by using dimensional analysis, which was assumed to be the most suitable way to find out a relationship between α to seven more parameters. In the next Chapter the determination of the absorption coefficient is explained in greater detail.

7.1.6 Dimensional analysis

Dimensional analysis has been used to solve a wide range of engineering problems. It is a mighty tool that can help engineers and researchers to maximize information by analyzing just a small number of tests and hence to develop predictive models and scaling correlations using small-scale experimental prototypes. The following explanation of the dimensional analysis is taken in large part from the technical note "An application of linearised dimensional analysis to rock cutting" by H. Alehossein and M. Hood. [1]

7.1.6.1 Introduction

Dimensional analysis is a tool based on the observations that:

- physical quantities have dimensions (usually mass, length and time) and
- physical laws must remain unaltered when the fundamental units for measuring dimensions are changed.

Dimensional analysis alone does not give an exact form of an equation, but can lead to a significant reduction of the number of variables and thereby provide some non-trivial information. It also provides the means of "normalization" to final results for a range of test conditions. A normalized (non-dimensional) set of results for one test condition can be used to predict the performance at different rock or excavation conditions.

In the optimization procedure initially seven dependent and three independent parameters were defined. Then dimensional analysis was used to reduce these to one dependent and six independent group variables. Six unknown exponents were

assigned to these six independent variables for a least-squares regression process. Together with the regression line parameter, seven unknown parameters need to be optimized to produce the best fit in a linear function. This produces seven simultaneous nonlinear equations which are solved by the *Microsoft Excel*® Solver tool, which uses the Generalized Reduced Gradient (GRG2) nonlinear optimization code developed by Leon Lasdon, University of Texas at Austin, and Allan Waren, Cleveland State University. The output is a linear arrangement of the experimental data with a good correlation coefficient.

7.1.6.2 Dimensions, dimensional homogeneity and independent dimensions

Dimensional quantities are those whose numerical values depend upon the system of units used, i.e. on the system of the units of measurement, and quantities are dimensionless if their values are independent of the system of units. Typical dimensional quantities are mass, length, time, force and speed. Angles, the ratio of two angles, the ratio of the square of a length to an area, the ratio of energy to moment, etc. are examples of dimensionless quantities. Dimension of all quantities can be expressed in terms of the primary or fundamental dimensions: length, mass, time, etc.

7.1.6.3 The Buckingham Pi Theorem

The Buckingham Pi Theorem has been widely used to reduce the total number of parameters or variables involved in a problem. Assuming w as the minimum number of required primary dimensions of a problem, the theorem states that the total number of dimensional parameters, u, can be reduced implicitly to $u-w$ dimensionless variables.

In this process:

1. a mathematical relation is set up between each dimensionless variable Π and a selected set of dimensional parameters PD.
2. a functional relation is formed among all group variables Π to identify new dependent and independent variables.

The mathematical form of the reduced functional relation among the independent, dimensionless variables Π is the primary unknown and must be determined experimentally. The formal statement of the Buckingham Pi Theorem is as follows.

Given a relation among u parameters, or more specifically between a dependent parameter PD_1 and $u-1$ independent parameters PD_a, of the form $P_1=g(PD_2, PD_3, \ldots, PD_a, \ldots, PD_u)$, the u parameters may then be regrouped into $u-w$ independent ratios or dimensionless variables (Π_b) expressible in functional form by $\Pi_1=y(\Pi_2, \Pi_3, \ldots, \Pi_b, \ldots, \Pi_{u-w})$. The number w is usually, but not always, equal to the minimum number of independent dimensions required to specify the dimensions of all the parameters PD_1, PD_2, … PD_a, … PD_u. As mentioned earlier, the mathematical functional form of y needs to be determined experimentally. The procedure involved in reducing the original functional equation (g) to one containing the dimensionless variables (y) can be described as follows.

- Step I: given the total number of parameters u, determine the w fundamental dimensions and thus the number of Π terms given by $u-w$.
- Step II: select a product set of repeating parameters (PD_2, …, PD_c) so that they include among them all of the w fundamental dimensions and exclude the dependent dimensional parameter (PD_1).
- Step III: assign (multiply) to each value of Π a different P term ($PD=PD_{u-c}$), which is not equal to those selected as repeating parameters (i.e. $P\neq P_c$).
- Step IV: find the exponents in each Π term by solving simultaneous equations for the unknown exponents of the repeating parameters (PD_c) where the nonrepeating parameters (PD_{u-c}) have a unit exponent.
- Step V: write the equation $\Pi_1=y(\Pi_2, \ldots, \Pi_b, \ldots, \Pi_{u-w})$ in terms of the Π terms and rearrange the terms as necessary.

In the next section this technique was applied to the analysis of the propagation of ground vibrations to determine a suitable relation for the absorption coefficient with the intention of deriving a set of dimensionless groups which could thereafter be used to correlate the experimental data and develop appropriate mathematical functional relationships.

Parameter	Index	Unit
Independent Parameters		
Density	ρ	[kg/m³]
Length segment	ΔD	[m]
Time segment	t	[s]
Dependent Parameters		
Absorption coefficient	α	**[1/m]**
Rock Mass Rating	RMR	[-]
Uniaxial Compressive Strength	UCS	[MPa]
Brazilian Tensile Strength	BTS	[MPa]
Young's modulus	Y_M	[MPa]
Overburden	OV	[m]
Frequency	φ	[1/s]

Table 7.3: Independent and dependent parameters used in the dimensional analysis

Table 7.3 shows the independent and dependent parameters used in the dimensional analysis.

The tests for the propagation of ground vibration measurements were conducted to study the effects of variations of these parameters on the determined absorption coefficient. Therefore the absorption coefficient was chosen as the dependent parameter and the physical equation defining the variation of the absorption coefficient in the following functional form:

(36) $$\alpha = f\{\rho, \Delta D, t, RMR, UCS, BTS, Y_M, OV, \varphi\}$$

This means that the total number of parameters *u*=10. We choose mass [kg], length [m] and time [s] as the required fundamental dimensions and the density, the length segment and the time segment as the repeating parameters. Thus knowing that *w*=3 the function f was reduced to one including *u*−*w*=7 dimensionless variables. To ensure these variables were dimensionless it was needed to assign six sets of unknown exponents to the three repeating parameters:

$$\Pi_1 = y = \alpha \cdot \Delta D$$
$$\Pi_2 = \frac{RMR}{100}$$
$$\Pi_3 = \frac{UCS \cdot t^2}{\rho \cdot \Delta D}$$
(37) $$\Pi_4 = \frac{BTS \cdot t^2}{\rho \cdot \Delta D}$$
$$\Pi_5 = \frac{Y_M \cdot t^2}{\rho \cdot \Delta D}$$
$$\Pi_6 = \frac{OV}{\Delta D}$$
$$\Pi_7 = \varphi \cdot t$$

Solving for the unknown exponents in each *Π* term leads to the following functional relation containing seven dimensionless groups:

(38) $$\Pi_1 = \alpha \cdot \Delta D = y\left[\left(\frac{RMR}{100}\right),\left(\frac{UCS \cdot t^2}{\rho \cdot \Delta D}\right),\left(\frac{BTS \cdot t^2}{\rho \cdot \Delta D}\right),\left(\frac{Y_M \cdot t^2}{\rho \cdot \Delta D}\right),\left(\frac{OV}{\Delta D}\right),(\varphi \cdot t)\right]$$

7.1.6.4 Least squares regression

The challenging task in any dimensional analysis is the systematic determination and formulation of the analytical form of the implicit function *y* from the experimental data. Although data curve fitting is the basis of all methods, there is no unique or standard method of determining mathematical form of the function *y*, particularly when there is limited experimental data. A potentially generic approach for finding *y* was proposed, which is simple in mathematical form, sensitive to every data point and appropriate for nonlinear correlations. In this method a multiple exponential function of all independent variables, i.e. $x=\Pi_2^{\alpha 2}\Pi_3^{\alpha 3}\ldots\Pi_z^{\alpha z}$, is formulated initially for each data point. Then the function *y* is obtained from a linear regression: $y=\omega x$, so that the constant *a* together with the exponents α_z all have optimum values for the best fit which is equivalent to producing the maximum correlation coefficient.

Consider a total of *J* data sets or experiments where at each data sets *j* the error is simply:

(39) $$e_j = \left[\ln\left(RGV_{Measured,j}\right) - \ln\left(RGV_{Calculated,j}\right)\right]^2$$

The $RGV_{Calculated}$ at data point j can be determined by using the same parameters like $RGV_{Measured}$ in the following equation:

(12) $$RGV_D = RGV_{Cut} \cdot \frac{D_{Cut}^{n_{Cut}}}{D^{n_D}} \cdot e^{\alpha \cdot (D_{Cut} - D)}$$

In the method of least squares regression of a function the sum of the error squares (e_{tot}) were minimized:

(40) $$e_{tot}^2 = \sum_{j=1}^{J} e_j^2$$

by using *Microsoft Excel*® Solver tool, which uses the Generalized Reduced Gradient (GRG2) nonlinear optimization code. In *Microsoft Excel*® Solver iterates values for all α_z and for the wave form factor coefficient *h*, which was explained in Chapter 7.1.4. The iteration process can stop whenever the computed roots converge to a set of fixed values, i.e. when there is no significant change in root values with further iterations. In general convergence and uniqueness of solutions depend on the selected initial values. The general rule of convergence and uniqueness is to estimate the initial values of the unknown parameters close to the exact solutions. This may be achieved after several computing trials and incremental analyses of reduced data.

For given α_z and Π_z x can be determined:

(41) $$x = \Pi_2^{\alpha_2} \cdot \Pi_3^{\alpha_3} \cdot \Pi_4^{\alpha_4} \cdot \Pi_5^{\alpha_5} \cdot \Pi_6^{\alpha_6} \cdot \Pi_7^{\alpha_7}$$

For given x-Values the constant a can be determined by using the Microsoft Excel trend line function which is optimizing the constants to best fit in a linear trend line of the form:

(42) $$y = \omega \cdot x$$

The solution for the constant ω and for the exponents $\alpha_{2,..,}\alpha_z$ were at the minimum of the sum of the error squares.

The successful result is a simple model, which is shown in Figure 7.5 and at which y is the dependent variable and x includes all the dimensionless variables.

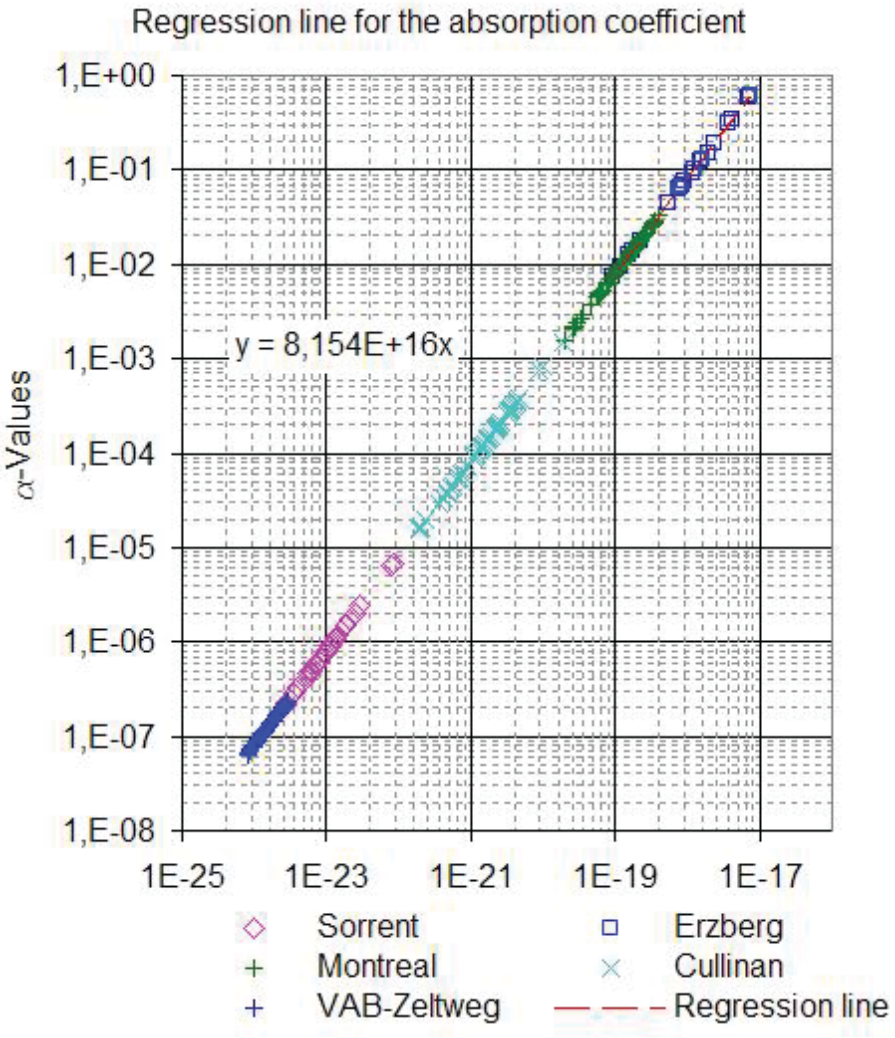

Figure 7.5: Function of the absorption coefficient

7.1.7 Modified function for the propagation of ground vibrations

The modified function for the propagation of ground vibrations takes a number of different parameters into account:

- Parameters of the excavation method
  - Roadheader parameters:
    + *Cut*
    + *Sump in depth*
    + *Slewing speed*
    + *Energy consumption of the cutting head*

- Parameters to consider the wave
  - Depth of the geophone (alternatively depth in the sidewall)
  - Frequency of the wave

- Parameters of the rock and the rock mass
  - Rock mass rating
  - Uniaxial compressive strength
  - Brazilian tensile strength
  - Young's Modulus
  - Fracture Energy
  - Overburden

During the regression analysis the following parameters where approximated:

Global exponents and coefficients			
Parameter	Index	Unit	
Cutting head efficiency rate	κ	[1/J]	0,0000217
Rock mass rating factor exponent	$\alpha 2$	[-]	-27,41
Uniaxial Compressive strength factor exponent	$\alpha 3$	[-]	-0,011
Brazilian tensile strength factor exponent	$\alpha 4$	[-]	0
Young's modulus factor exponent	$\alpha 5$	[-]	-3,86
Overburden factor exponent	$\alpha 6$	[-]	-2,12
Frequency factor exponent	$\alpha 7$	[-]	1,64
Absorption coefficient factor	ω	[-]	8,15 E16
Wave form coefficient factor	h	[-]	6,24

Table 7.4: Approximated exponents and coefficients

The final form of the approximation equation for the absorption coefficient is:

(43) $$\alpha = 8{,}15 \cdot 10^{16} \cdot \left(\frac{RMR}{100}\right)^{-27{,}41} \cdot UCS^{-0{,}011} \cdot Y_M{}^{-3{,}86} \cdot OV^{-2{,}12} \cdot \rho^{31{,}281} \cdot \varphi^{1{,}64}$$

assuming that ΔD is 1m and t is 1second. SI- Units must be used for the parameters, when calculating the absorption coefficient.

The simple form of the modified function for the propagation of ground vibrations caused by horizontal slewing of a roadheader development is:

(12) $$RGV_D = RGV_{Cut} \cdot \frac{D_{Cut}^{n_{Cut}}}{D^{n_D}} \cdot e^{\alpha \cdot (D_{Cut} - D)}$$

The variables of the equation above were explained from Chapter 7.1.1 to Chapter 7.1.6.

7.1.8 Results for the propagation of ground vibrations for tunnel drifting by means of a roadheader

The propagation of ground vibrations depends highly on the wave form (plate wave – spherical wave), but also on the absorption coefficient.

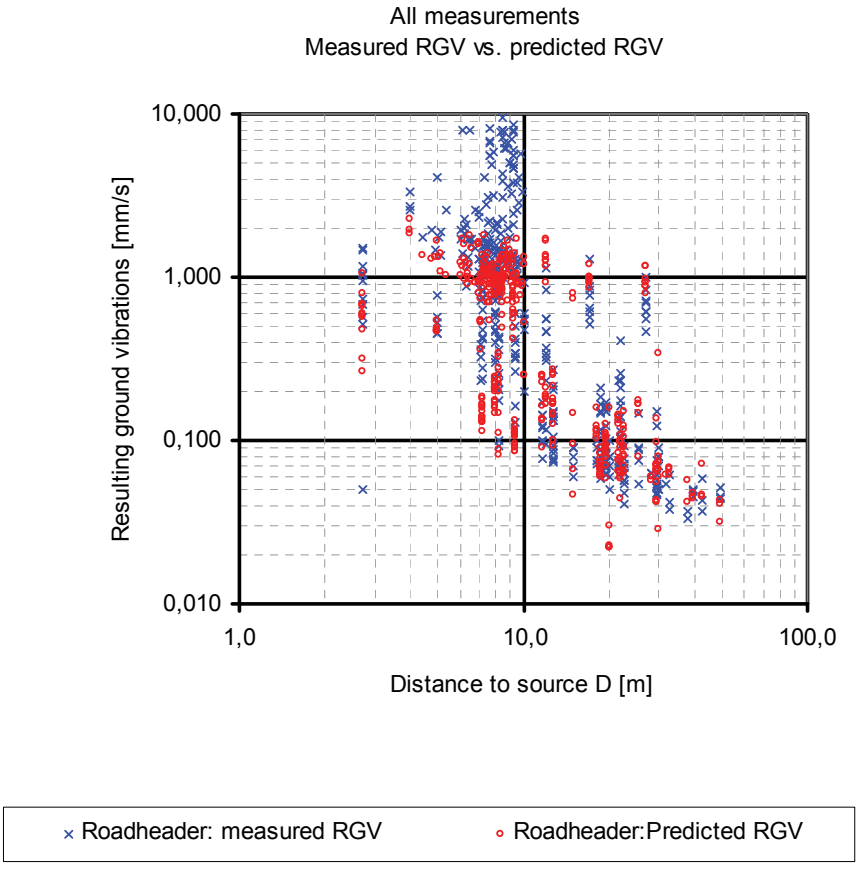

Figure 7.6: Overview of the results of the dimensional analysis and the regression analysis

In Figure 7.6 the measured resulting ground vibrations are compared with the predicted resulting ground vibrations. To predict the resulting ground vibrations all boundary parameters, the global exponents and coefficients had to be known:

Parameter	Index	Unit	Location					Boundaries	
			Sorrent	Erzberg	Montreal	Cullinan	VAB	min	max
Overburden	OV	[m]	250	50	20	717	2,5	2,5	717
Depth Geophone	DG	[m]	0,1	0,1	2	0,9-3,5	0,2	0,1	2
Mean Distance of the geophones	D_{mean}	[m]	14,0	17,3	15,6	11,8	7,8	7,8	17,3
Cross Section	CS	[m²]	42,0	28,8	46,0	25,0	33,1	25,0	46,0
Density	ρ	[kg/m³]	2720	2630	2640	2698	2250	2250	2720
Uniaxial Compressive Strength	UCS	[Mpa]	188,0	152,0	94,4	79,4	32,3	32,3	188
Brazilian Tensile Strength	BTS	[Mpa]	7,7	11,0	6,4	6,6	3,1	3,1	11,0
Young's modulus	Y_M	[Mpa]	47083	22550	10374	13704	10047	10047	47083
Fracture Energy	E_f	[J]	41	25	24	7,5	12	7,5	41
Mean Frequency	φ	[1/s]	48	74	236	299	7	7	299
Rock Mass Rating (Bieniawski)	RMR	[-]	54	46	64	55	89	44	89
Mean Power	P_{mean}	[kW]	215	183	153	150	88	88	225
Mean Cut	Cut_{mean}	[mm]	134	152	138	142	143	134	152
Sump in Depth	SD	[mm]	750	630	650	650	650	630	750
Mean Slewing speed	v_s	[m/s]	0,2	0,2	0,2	0,2	0,2	0,2	0,2

Table 7.5: Parameters of the measurement sites

Table 7.5 shows the parameters which are necessary to estimate the predicted resulting ground vibrations. The procedure to estimate the resulting ground vibrations is described in the following eight steps:

1) (31) $$RGV_{Cut} = \sqrt{\frac{4 \cdot E_{RH} \cdot (\kappa \cdot E_f)}{SD \cdot Cut \cdot v_s \cdot \rho \cdot t^2 \cdot \varphi}}$$

2) (34) $$n_{Cut} = \frac{2 \cdot \arctan\left(h \cdot \sqrt{D_{Cut}}\right)}{\pi}$$

3) (33) $$n_D = \frac{2 \cdot \arctan\left(h \cdot \sqrt{DG}\right)}{\pi}$$

4) (41) $$x = \Pi_2^{\alpha_2} \cdot \Pi_3^{\alpha_3} \cdot \Pi_4^{\alpha_4} \cdot \Pi_5^{\alpha_5} \cdot \Pi_6^{\alpha_6} \cdot \Pi_7^{\alpha_7}$$

5) (42) $$y = \omega \cdot x$$

6) (37) $$\alpha = \frac{y}{\Delta D}$$

7) (12) $$RGV_D = RGV_{Cut} \cdot \frac{D_{Cut}^{n_{Cut}}}{D^{n_D}} \cdot e^{\alpha \cdot (D_{Cut} - D)}$$

Local exponents and coefficients

Parameter	Index	Unit	Location				
			Sorrent	Erzberg	Montreal	Cullinan	VAB
Wave form factor	n_{Cut}	[-]	0,74	0,74	0,74	0,74	0,74
Wave form factor	n_D	[-]	0,60	0,60	0,93	0,91	0,80
Absorption coefficient	α	[1/m]	1,26E-06	2,99E-04	1,37E-02	1,86E-04	1,25E-07
Background noise	RGV_{BN}	[mm/s]	0,022				

Table 7.6: Local exponents and coefficients

Table 7.6 shows the results of the local exponents and coefficients for the different measuring sites for roadheader development.

The determined absorption coefficients for Sorrent, Erzberg, Montreal and Cullinan show good correlation with the absorption coefficients in Figure 7.7. The absorption coefficient for the measurements at VOEST-ALPINE Bergtechnik at the concrete block did not correlate very well. The general setup of that test site was different to the others:

- Concrete is not directly comparable with rock
- The concrete block was on the surface and not located underground
- Reflexion on the sidewalls of the concrete block leads to different resulting ground vibrations
- Reflexion also had high influence on the measured frequencies
- Reinforcement in the sidewall of the measurement leads to less absorption

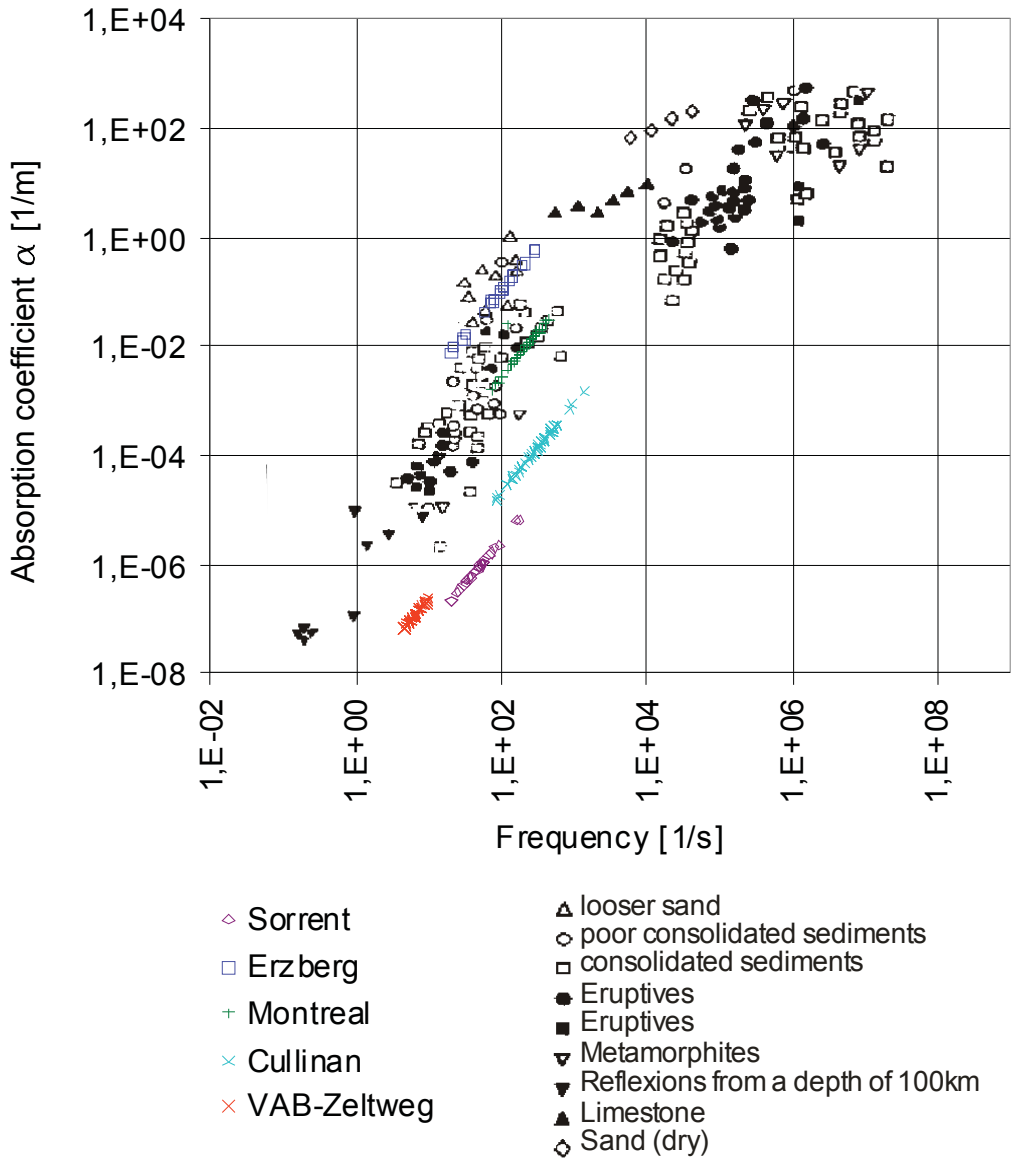

Figure 7.7: Absorption coefficient – frequency diagram [13]

The coefficient of correlation C compares predicted and measured resulting ground vibrations and ranges in value from 0 to 1. If it is 1, there is a perfect correlation in the sample — there is no difference between the predicted and measured resulting ground vibrations. At the other extreme, if the coefficient of correlation is 0, the regression equation is not helpful in predicting a resulting ground vibration. The coefficient of correlation C for the data of the least squares analysis was C=0,698.

The following diagrams show the measured and the predicted resulting ground vibrations for the different measuring sites for roadheader development.

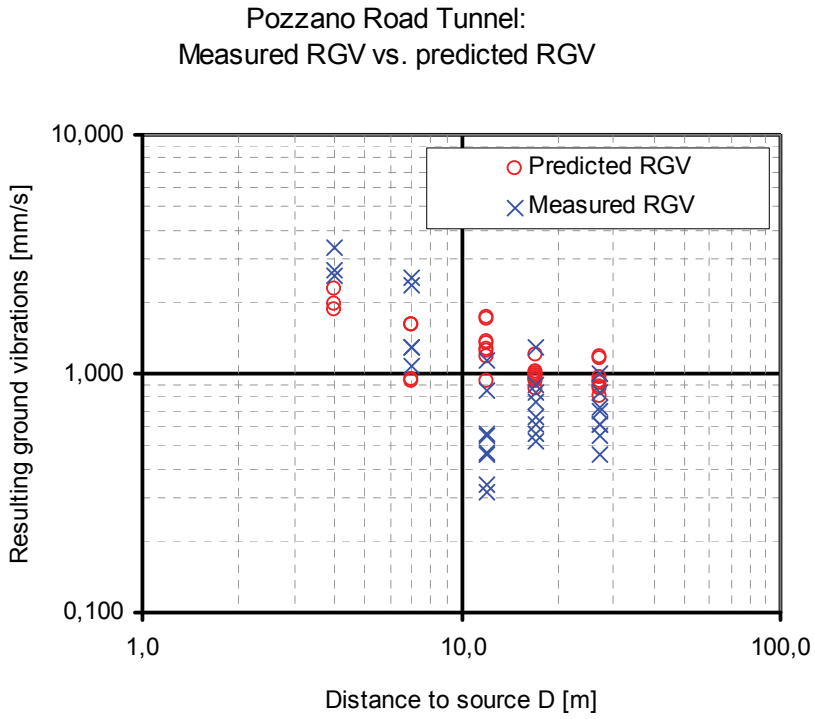

Figure 7.8: Measured and predicted resulting ground vibrations, Pozzano Road Tunnel

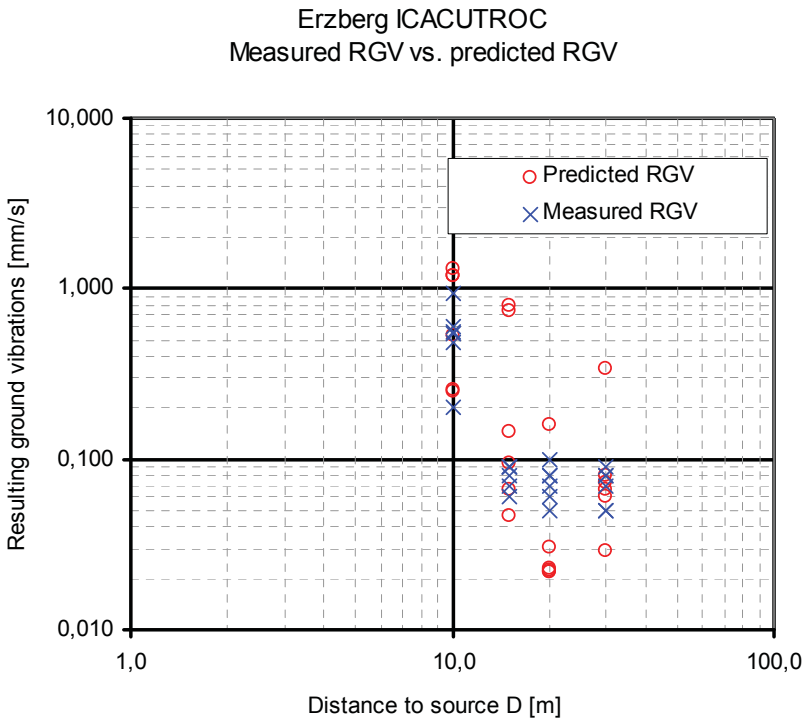

Figure 7.9: Measured and predicted resulting ground vibrations, Erzberg ICACUTROC

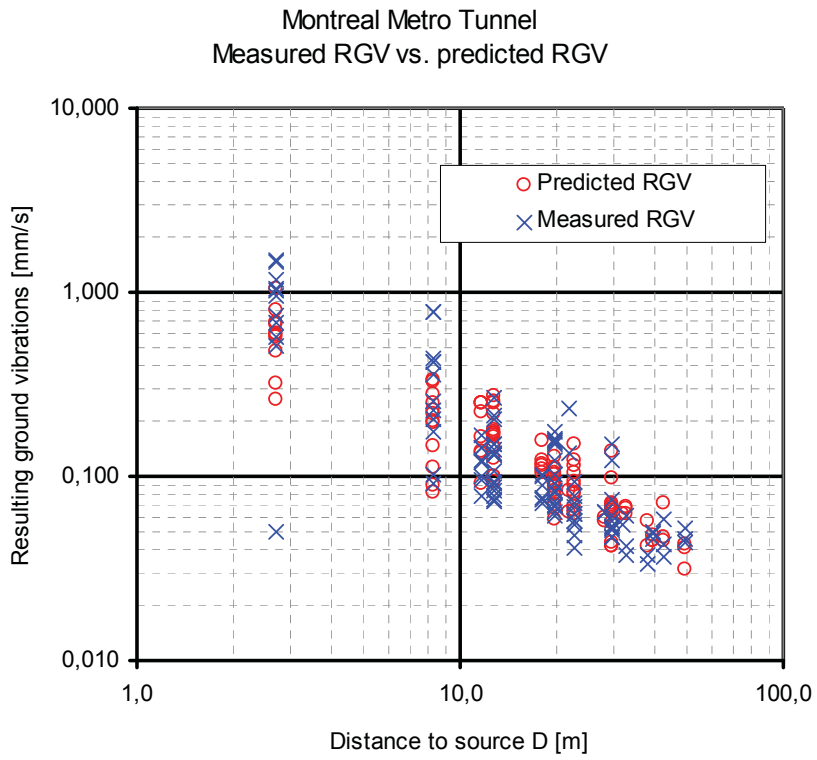

Figure 7.10: Measured and predicted resulting ground vibrations, Montreal Metro Tunnel

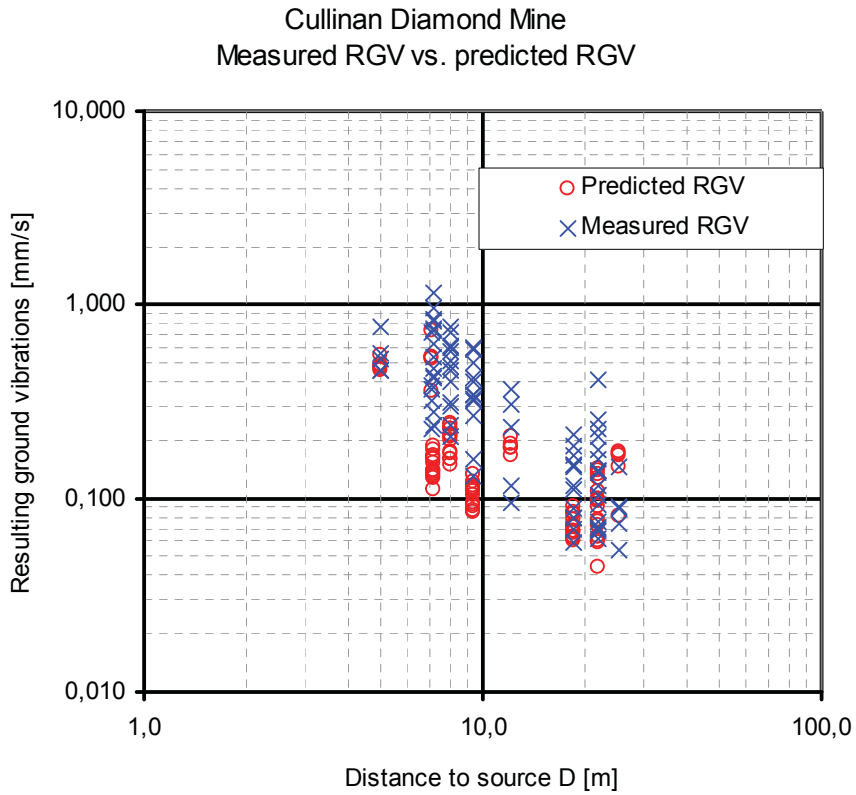

Figure 7.11: Measured and predicted resulting ground vibrations, Cullinan Diamond Mine

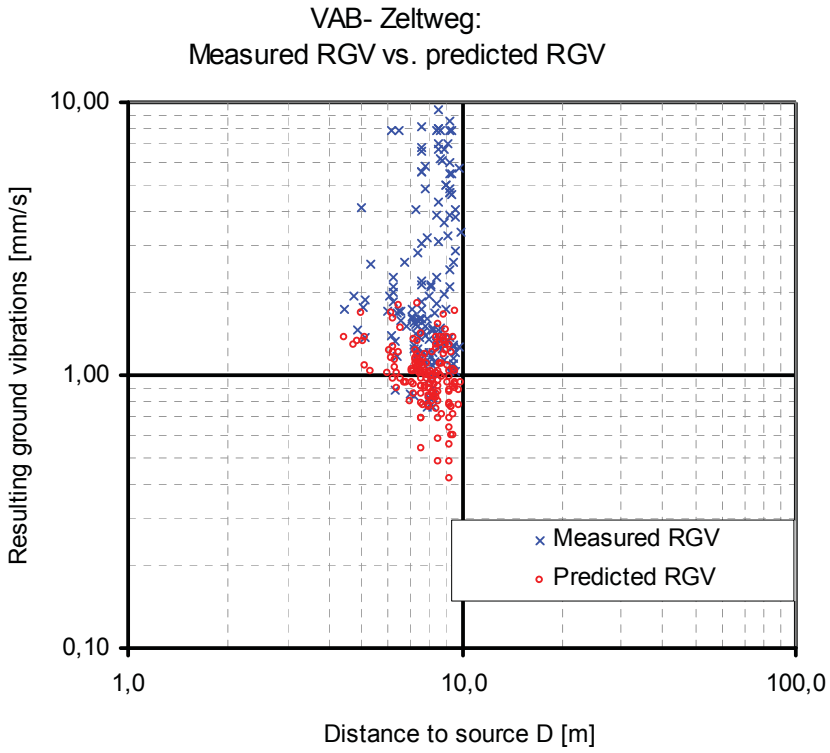

Figure 7.12: Measured and predicted resulting ground vibrations, VOEST-ALPINE Bergtechnik trial site

7.2 Model for the quantification of the impact energy for roadheader development

As mentioned in Chapter 7.1.3 the kinetic energy in a spherical shell, with a width of D_W, which is exposed for a time t (defined to be 1 second) was:

(27) $$E_T = \pi \cdot D^2 \cdot D_W \cdot \rho \cdot RGV^2 \cdot \varphi \cdot t$$

As shown in the equation above, the propagation function RGV_D had to be known first and was already determined in Chapter 7.1.7.

According to the equation above the radiated seismic energy of a unit element with a certain distance to the source of impact and located in a certain depth in the sidewall could be estimated. Therefore the overburden, the rock mass and rock parameters as well as the impact specific parameters have to be taken into account.

As the source of impact was no static location, but depending on the location of the cutting head on the front face and on the location of the front face along the roadway axis itself, it was decided to determine five characteristics to describe the impact of energy along the sidewall of a roadway while the excavation was passing the unit element with a certain excavation speed:

- the specific energy consumption of the roadheader ($E_{spec,RH}$)
- the radiated seismic energy ($E_{spec,rad}$) caused for a unit element [19]
- the cumulated seismic energy (E_{rad})[5]
- the seismic efficiency factor (η_{SE})
- the impact quantification number (IQN)

The five characteristics are normalized either to 1m of axial roadway development or to 1m³ of excavated rock.

7.2.1 Characteristics to quantify the impact of energy

To determine characteristics which quantify the impact of energy analytically, the function of the propagation of ground vibrations has to be integrated. The area under the function of the propagation of ground vibrations is proportional to the total radiated vibrations, whereas the total radiated vibrations are proportional to the radiated seismic energy [10]. As it is not possible to determine this area analytically with integral calculus, it was decided to create an approximation calculation.

In this process:

- predefinitions for the approximation calculation and the division into certain segments were specified
- direct distances from the source of impact to the unit element were substituted with distances along the roadway axis
- within nine calculation steps the characteristics could be determined

7.2.1.1 Predefinitions for the approximation calculation

During this calculation the area could be approximated by the following predefinitions:

- the total area is the sum of all segments k of the total area
- the total area is defined as the product of the maximum distance and the average resulting ground vibration
- the area of a segment is the product of width of a segment and the average resulting ground vibration of the segment
- the distance is divided in segments in a logarithmic scale
- every segment k has a certain lower limit distance D_k and an upper limit distance D_{k+1}.
- the width of the segment is the difference between the upper limit distance D_k and the lower limit distance D_{k+1}.

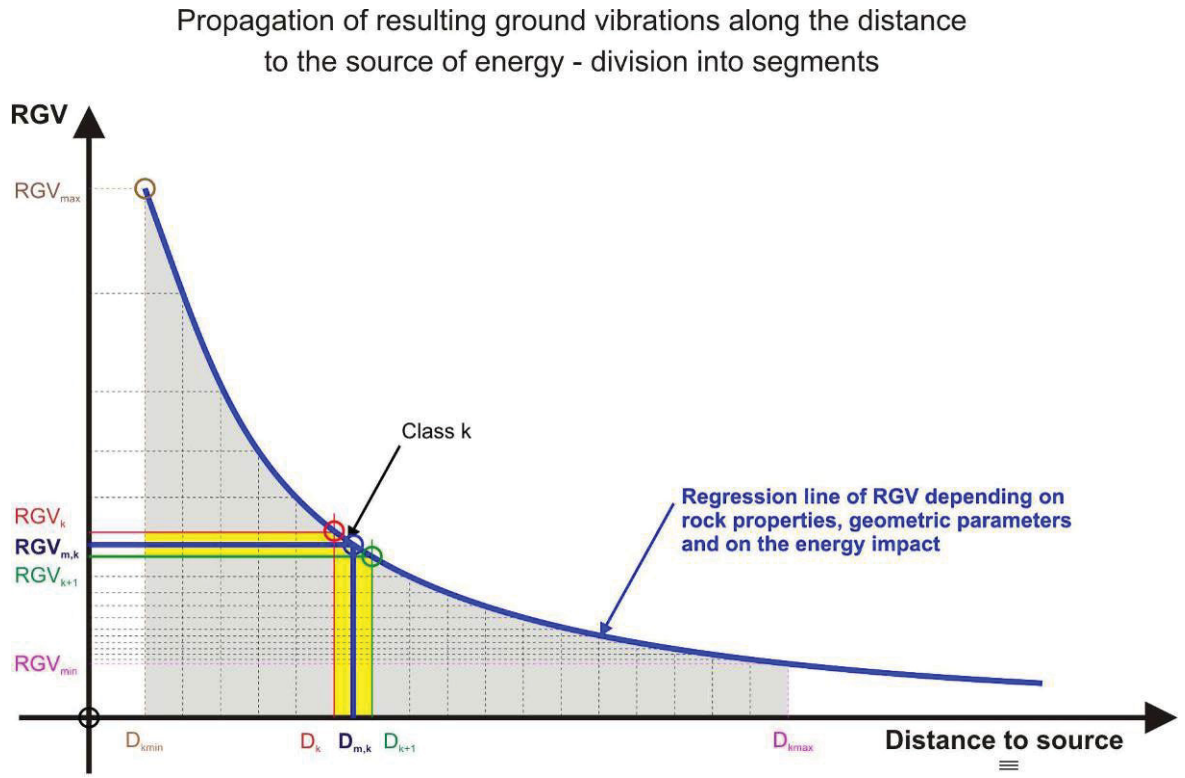

Figure 7.13: Regression line – division into segments

7.2.1.2 Substitution of average distances to distances along the tunnel axis

As the distance from the average position of the source on the front face to the segment k is not equal to the distance along the tunnel axis, the distances D_k had to be substituted by the distance along the roadway for an energy balance.

Two different cases for the substitution were defined:

- the distance along the tunnel axis before the excavation has passed
- the distance along the tunnel axis after the excavation has passed

- Distance along the tunnel axis before the excavation passed

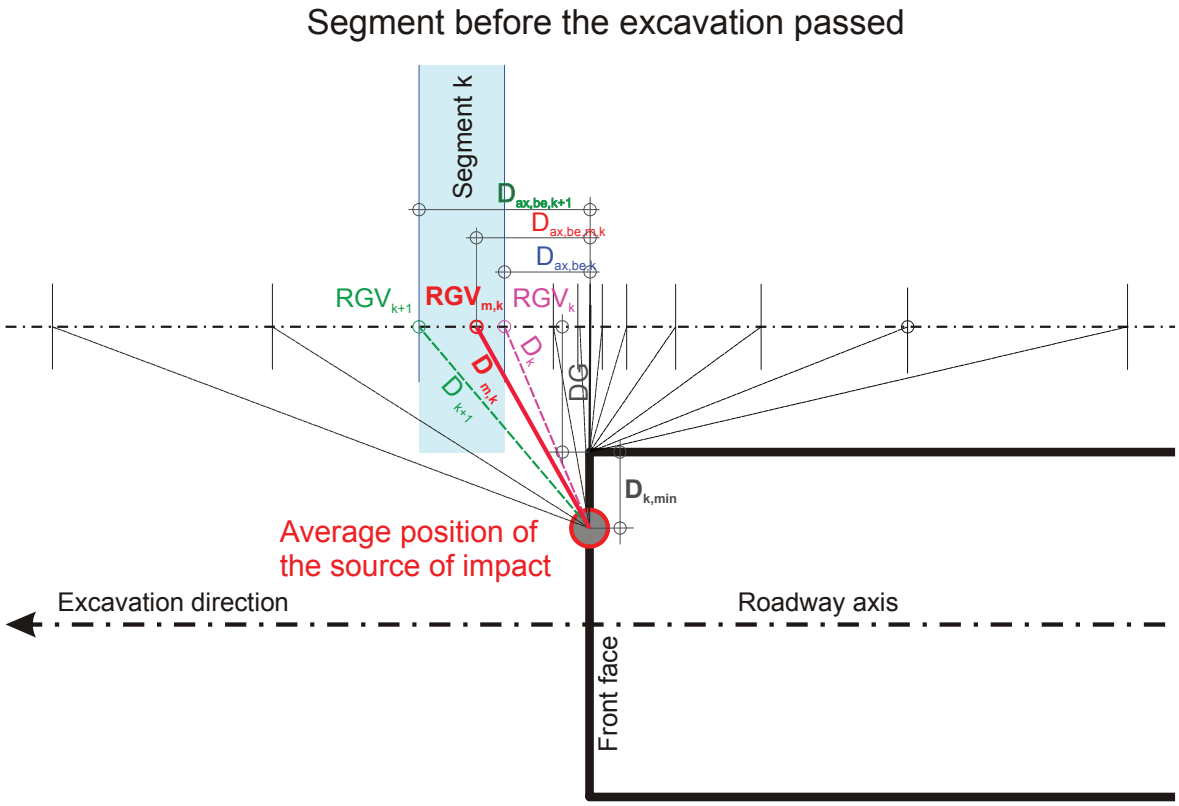

Figure 7.14: Segment k before the excavation has passed

For that case the distance along the tunnel axis could be calculated by the following equation:

(44) $$D_{ax,be,m,k} = \sqrt{D_{m,k}{}^2 - \left(D_{m,k_{min}} + DG\right)^2}$$

- Distance along the tunnel axis after the excavation passed:

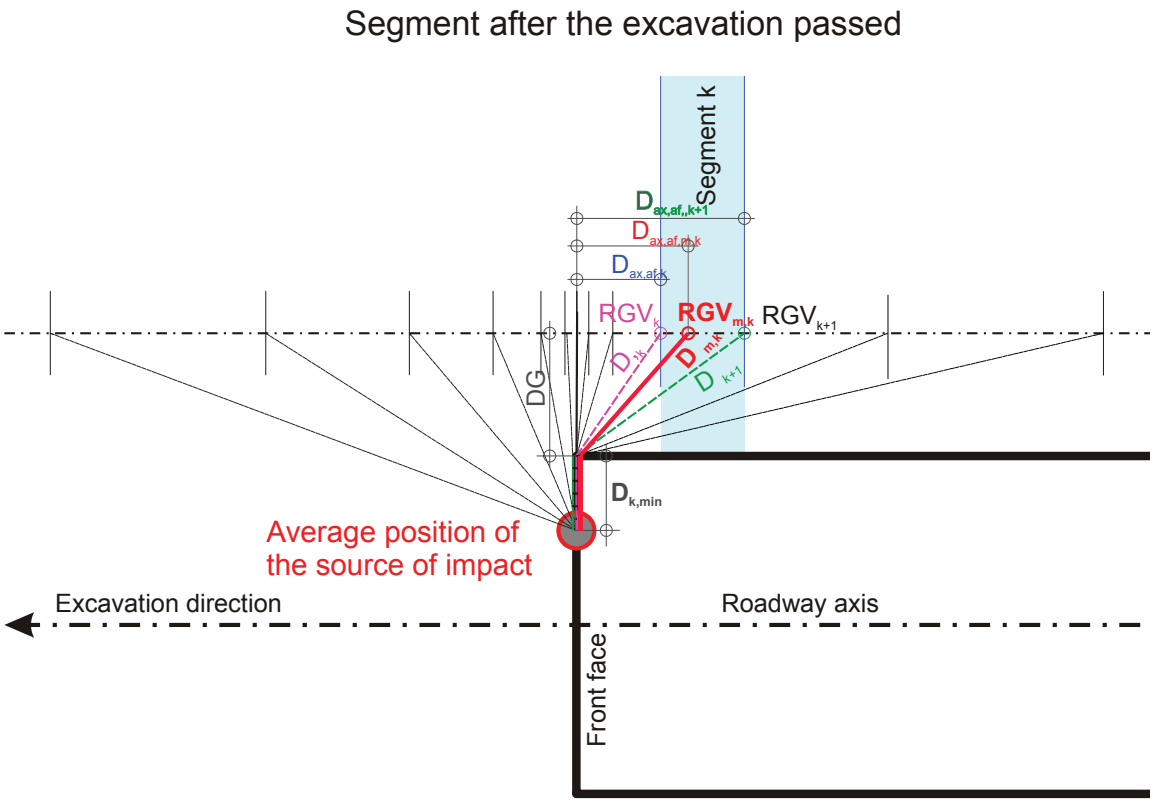

Figure 7.15: Segment k after the excavation passed

In that case the distance along the tunnel axis could be calculated by the following equation:

(45) $$D_{ax,af,m,k} = \sqrt{\left(D_{m,k} - D_{m,k_{min}}\right)^2 - DG^2}$$

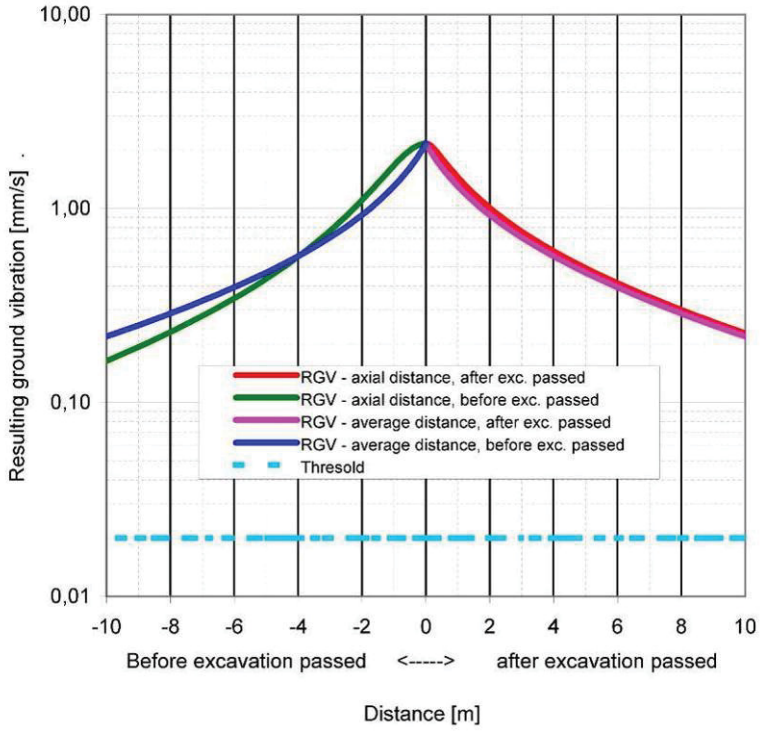

Figure 7.16: Comparison: axial distance – average distance for the propagation function

Figure 7.16 shows that using the average distance to the source leads to a higher regression of the line of RGV along the sidewall.
For shallow depths in the sidewall the regression of the average distance and the axial distance is equal, but the deeper the unit element is located in the sidewall, the bigger is the difference in the regression of the functions.

7.2.1.3 Determination of the characteristics with the approximation calculation

Taking the predefinitions and the substitution into account the five characteristics could be determined by the following steps:

1. Calculation of the cutted volume VO_{Cut}:

   (13) $$VO_{Cut} = SD \cdot Cut \cdot v_s \cdot t$$

2. Calculation of the excavation speed $v_{ex,RH}$ for horizontal slewing along the tunnel axis:

   (46) $$v_{ex,RH} = \frac{VO_{Cut}}{CS}$$

3. Division of the distance in a logarithmic scale (10 segments per decimal power)

4. Calculation of the average distance of a class $D_{m,k}$ in logarithmic scale:

(47) $$D_{m,k} = e^{\frac{\ln(D_k)+\ln(D_{k+1})}{2}}$$

5. Calculation of the average resulting ground velocity RGV_k of the segment k:
   - Position of the segment before the excavation has passed:

(48) $$RGV_{k,be} = RGV_{Cut} \cdot \frac{D_{Cut}^{n_{Cut}}}{D_{m,k}^{n_{D,be,k}}} \cdot e^{\alpha \cdot (D_{Cut} - D_{m,k})}$$

   where the wave form factor had to be calculated separately for every segment as the distance to the next free surface DG changed for every segment:

(49) $$n_{D,be,k} = \frac{2 \cdot \arctan\left(m \cdot \sqrt{\sqrt{DG^2 + D_{ax,be,m,k}^{\ 2}}} \right)}{\pi}$$

   - Position of the segment after the excavation has passed:

(12) $$RGV_{k,af} = RGV_{Cut} \cdot \frac{D_{Cut}^{n_{Cut}}}{D_{m,k}^{n_D}} \cdot e^{\alpha \cdot (D_{Cut} - D_{m,k})}$$

   where the wave form factor was constant for all the segments.

6. Calculation of the minimum average distance $D_{m,kmin}$ to the average location of the source of impact in logarithmic scale:

(50) $$D_{m,k_{min}} = e^{\frac{\ln(TW)+\ln(TH)+2 \cdot \ln(D_{Cut})}{4}}$$

where TW is the width and TH is the height of the roadway. As the function of the propagation of ground vibrations refers to certain positions of the source impact, but this source was moving during the excavation process (cutting head), an average distance of the average position of the impact source to the sidewall had to be approximated.

7. Substitution of the average distance depending on the position of the segment:
    - Position of the segment before the excavation has passed:

    (51) $$D_{ax,be,m,k} = \sqrt{D_{m,k}{}^2 - \left(D_{m,k_{min}} + DG\right)^2}$$

    - Position of the segment after the excavation has passed:

    (52) $$D_{ax,af,m,k} = \sqrt{\left(D_{m,k} - D_{m,k_{min}}\right)^2 - DG^2}$$

8. Definition of the maximum average distance

    (53) $$D_{m,k_{max}} = D_{m,k_{max}} \left\{ D_{m,k} \left| \left[\left(RGV_k > RGV_{BN}\right) \wedge \left(RGV_{k+1} < RGV_{BN}\right) \right] \right. \right\}$$

    The maximum average distance was defined as the average distance of segment k, at which the related resulting ground vibration RGV_k was higher than the background noise, but the resulting ground vibration RGV_{k+1} of segment k+1 was smaller than the background noise.

9. Calculation of the exposed time T_k of the segment k during the excavation process

    (54) $$T_k = \frac{v_{ex}}{D_{ax,k} - D_{ax,k+1}}$$

The five characteristics could then be determined using the parameters defined above:

- **Specific energy consumption** of the roadheader $E_{spec,RH}$ per meter roadway development

    (55) $$E_{spec,RH} = \frac{E_{RH} \cdot CS}{VO_{Cut}}$$

- Radiated seismic energy $E_{spec,rad}$ caused per meter roadway development for the segment k was:
    - Position of the segment before the excavation has passed:

    (56) $$E_{spec,rad,be,k} = 0,25 \cdot \rho \cdot \left(D_{m,be,k+1} - D_{m,be,k}\right) \cdot RGV_{k,be}{}^2 \cdot \varphi$$

    - Position of the segment after the excavation has passed:

- (57) $$E_{spec,rad,af,k} = 0,25 \cdot \rho \cdot \left(D_{m,af,k+1} - D_{m,af,k}\right) \cdot RGV_{k,af}{}^2 \cdot \varphi$$

- **Radiated seismic energy $E_{spec,rad}$** caused per meter roadway development for a unit element of density ρ and a volume of 1m³ was:

(58) $$E_{spec,rad} = \sum_{k=1}^{K} E_{spec,rad,af,k} + \sum_{k=1}^{K} E_{spec,rad,be,k}$$

- Cumulated radiated seismic energy $E_{rad,k}$ caused per meter roadway development for the segment k was:

(59) $$E_{rad,k} = \pi \cdot \rho \cdot D_{m,k}{}^{2} \cdot \left(D_{m,k+1} - D_{m,k}\right) \cdot RGV_{k}{}^{2} \cdot \varphi$$

- **Cumulated seismic energy E_{rad}** caused per meter roadway development was:

(60) $$E_{rad} = \sum_{k=1}^{K} E_{rad,k}$$

- **Seismic efficiency factor η_{SE}:**

(61) $$\eta_{SE} = \frac{Output}{Input} = \frac{E_{rad}}{E_{spec,RH}}$$

- **Impact quantification number**

(62) $$IQN = \left(\sum_{k=1}^{K} T_{k,af} \cdot RGV_{k,af} \cdot \frac{1}{2 \cdot \pi}\right) + \left(\sum_{k=1}^{K} T_{k,be} \cdot RGV_{k,be} \cdot \frac{1}{2 \cdot \pi}\right)$$

The impact quantification number IQN does not depend on the frequency φ as the IQN is a qualitative parameter for the cumulated movement of a particle. As the amplitude for a sinusoidal wave can be described as:

(63) $$A_{max} = \frac{RGV}{2 \cdot \pi \cdot \varphi}$$

the cumulative movement $A_{Cum,k}$ is not depending on the frequency:

$r = T_k \cdot \varphi$ ... Number of periods r during time T_k

(64) $$A_{Cum,k} = \frac{RGV}{2 \cdot \pi \cdot \varphi} \cdot r = \frac{RGV}{2 \cdot \pi \cdot \varphi} \cdot T_k \cdot \varphi = \frac{RGV}{2 \cdot \pi} \cdot T_k$$

$$A_{Cum,k} = IQN_k$$

The total movement of a particle was expected to be qualitatively equal to the cumulative movement A_{Cum}, which is equal to the sum of the impact quantification numbers of the segments.

7.2.2 Results of the impact quantification for the test sites

For the development of 1m roadway or for the excavation of 1m³ of rock the results of the quantification of the impact's energy, which are shown from Figure 7.19 to Figure 7.24, were related to 1m roadway development to a unit element of 1m³ in a depth of 0,30m in the sidewall. For the simulation of the impact quantification a background noise of 0,022mm/s was supposed.

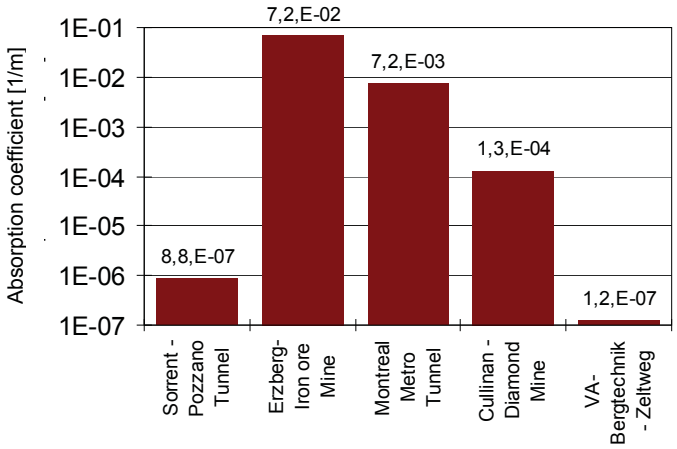

Figure 7.17: Absorption coefficients for the test sites

The different absorption coefficients as well as the different wave form factors and specific energy consumptions of the cutting head lead to different distances, at which the resulting ground vibration reached the background noise of 0,022 mm/s.

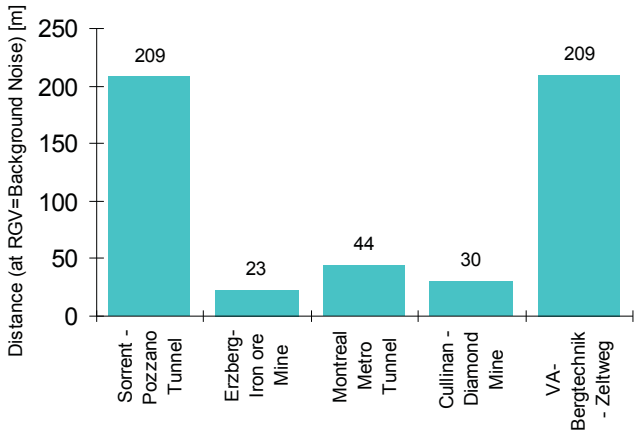

Figure 7.18: Distances, where resulting ground vibration approaches the background noise

Figure 7.19 and Figure 7.20 show the influence on the radiated seismic energy of segments in different distances. Thereby the radiated seismic energy was cumulated for a roadway development of 1m before the roadheader passed the segment. The sum of the radiated seismic energies is the total amount of energy induced into the segment for a roadway development of 1m.

The main part of the total energy before the roadheader has passed comes from excavation activities within a distance of about 0,5m to 5m, whereas the main part of the total energy after the roadheader has passed the segment comes from excavation activities within a distance of about 0,7m to 7m.

The radiated seismic energy of close segments after the roadheader has passed appear with higher influence than close segments before the roadheader has passed the segment. The total amount of energy for the unit element is the sum of the energies of the segments before and after the roadheader has passed. The fraction of the total amount of radiated seismic energy for a unit element after the roadheader had passed the segment was higher than the fraction attenuation before the roadheader had passed. This effect lead from the different attenuation of ground vibrations along the distance before and after the roadheader had passed.

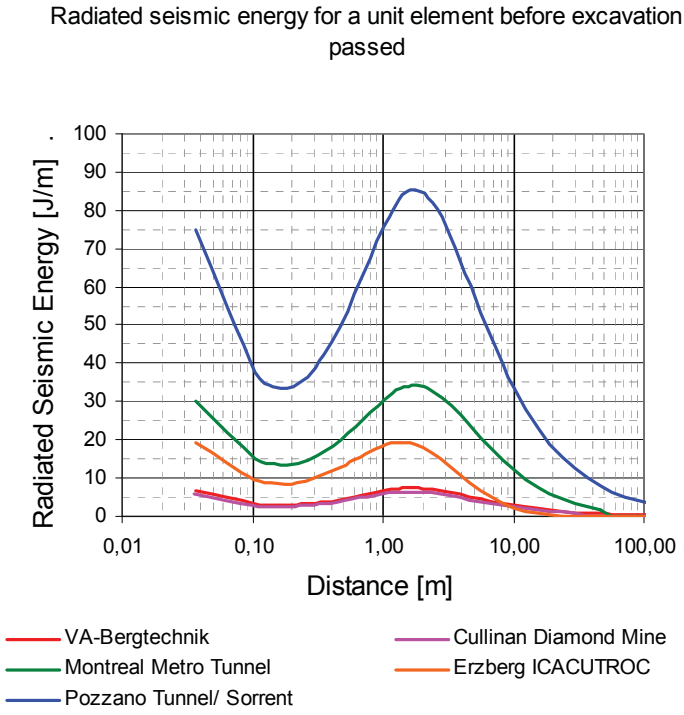

Figure 7.19: Influence of different distances on the radiated seismic energy

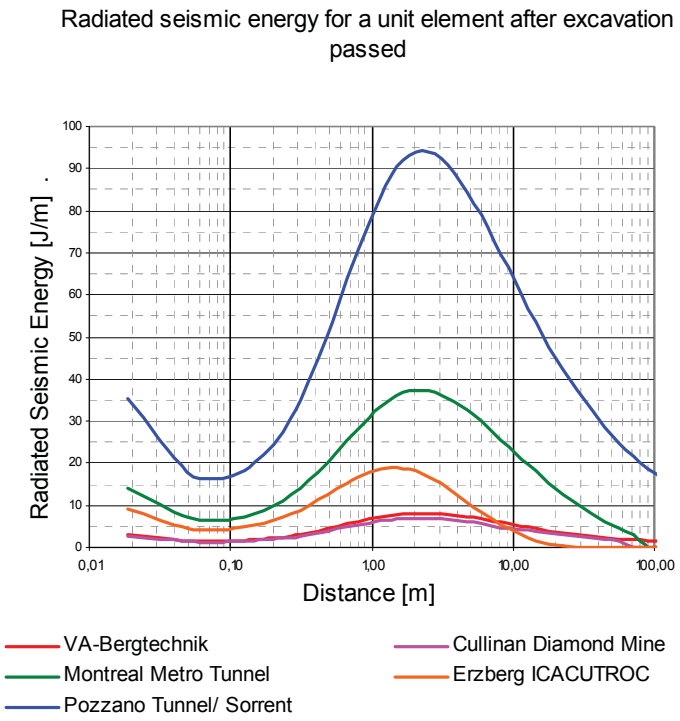

Figure 7.20: Influence of different distances on the radiated seismic energy

Figure 7.21 shows the contribution of the radiated seismic energy for a unit element for Pozzano Road Tunnel (Sorrent). 90 % of the seismic energy was radiated from excavation activities within a distance of about 12m (after the roadheader had passed) and about 7m (before the roadheader had passed).

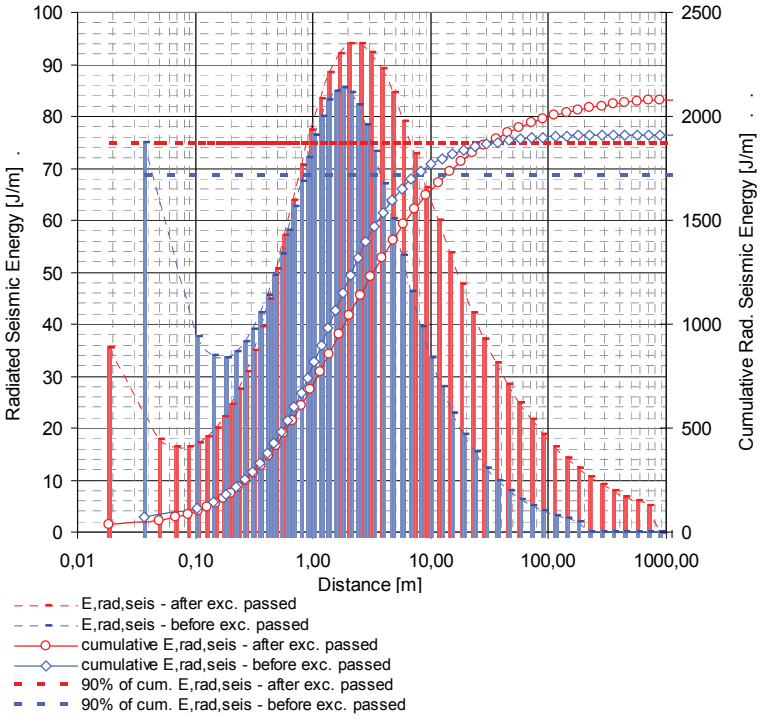

Figure 7.21: Radiated seismic energy for a unit element

Figure 7.22 and Figure 7.23 show the influence of segments in different distances on the impact quantification number cumulated for a roadway development of 1m before the roadheader has passed. The sum of the impact quantification numbers is qualitatively the total amount of oscillation induced into the unit element for a roadway development of 1m. The distances on which the main part of the total oscillation is based highly depend on the absorption coefficient as well as on the background noise. E.g. Erzberg (ICACUTROC), where high absorption was approximated, the maximum was reached at a distance of about 6m, whereas the maximum for Pozzano Road Tunnel would only be reached at distances higher than 200m.

The impact quantification numbers of close segments before the roadheader has passed appear with a higher influence than close segments after the roadheader has passed.

The fraction of the total amount of the impact quantification number of a unit element before the roadheader has passed is higher than the fraction after the roadheader has passed.

In comparison to the radiated seismic energy, the impact quantification number leads to smaller differences between the sites, as the energy is calculated of the square of the resulting ground vibration.

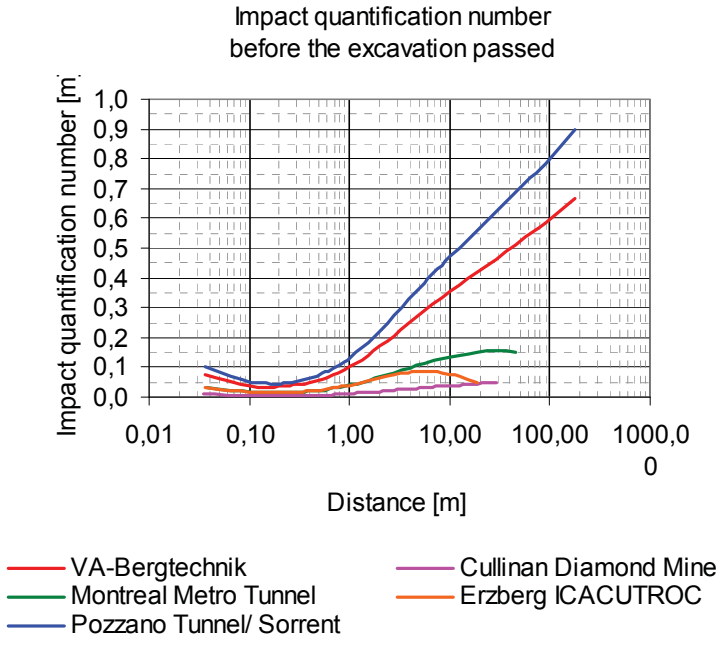

Figure 7.22: Influence of different distances on the impact quantification number

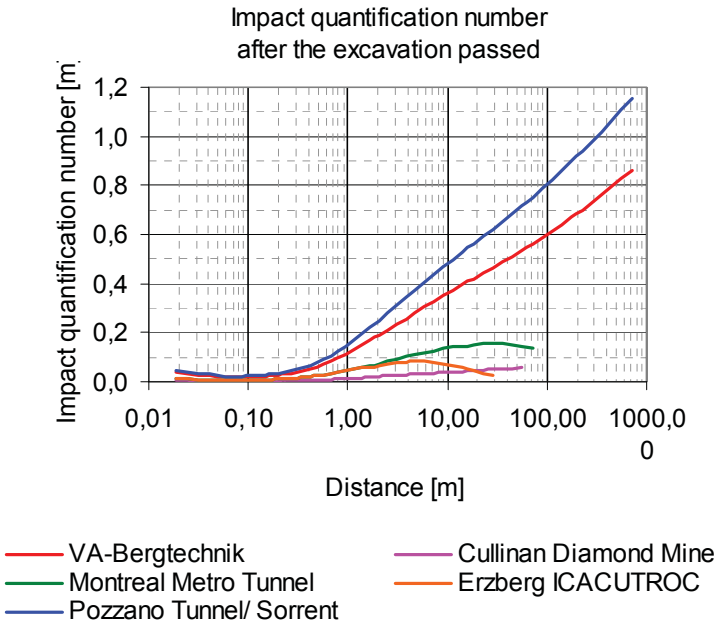

Figure 7.23: Influence of different distances on the impact quantification number

Figure 7.24 shows the contribution of the impact quantification number of Erzberg ICACUTROC project. 90 % of the impact quantification number are based on excavation activities within a distance of about 10,5m (after the roadheader has passed) and about 10m (before the roadheader has passed).

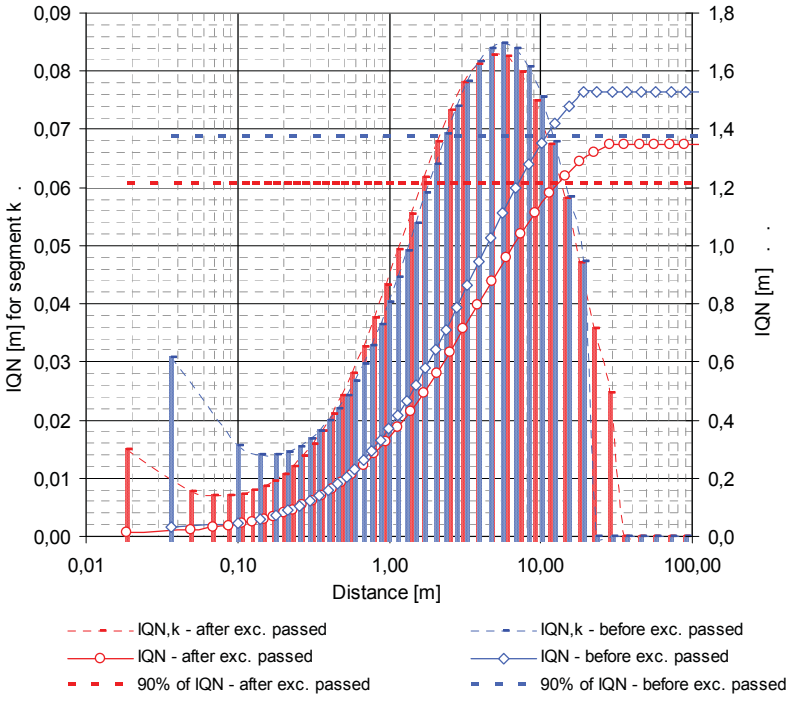

Figure 7.24: Impact quantification number, Erzberg ICACUTROC

The final results of the impact of energy quantification of the five characteristics are summarized in Figure 7.25 to Figure 7.29

The characteristic “energy consumption of the roadheader” per m³ excavated rock for horizontal slewing was in the range of 7,0 to 10,7 MJ/m³ for the four underground test sites. Only for the concrete block the energy consumption was about 4 MJ/m³.

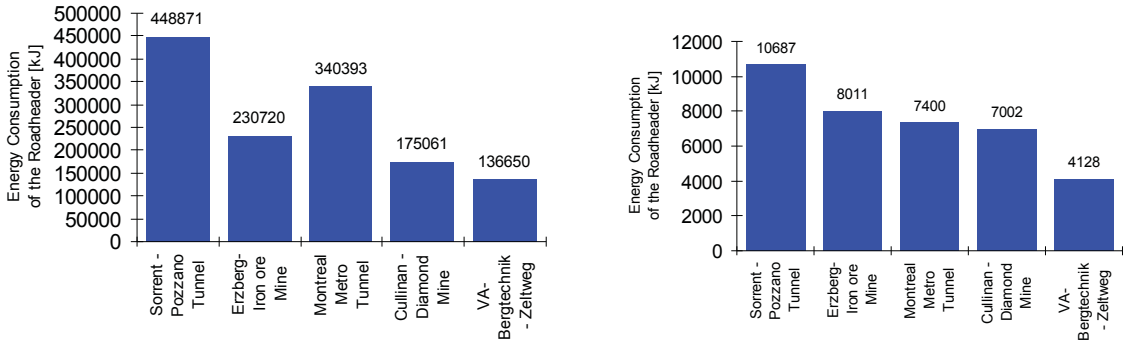

Figure 7.25: Energy consumption of the roadheader for 1m roadway development (left) and per m³ excavation (right)

The cumulated radiated seismic energy (apart from the concrete block) was the highest for Pozzano Road Tunnel as the fracture energy and the uniaxial compressive strength of 188MPa, a Young’s Modulus of 47GPa and a RMR of 54 (fair rock) as well as low frequencies lead to low absorption and high maximum resulting ground vibrations. The lowest cumulated seismic energy was observed at Erzberg Iron Ore Mine.

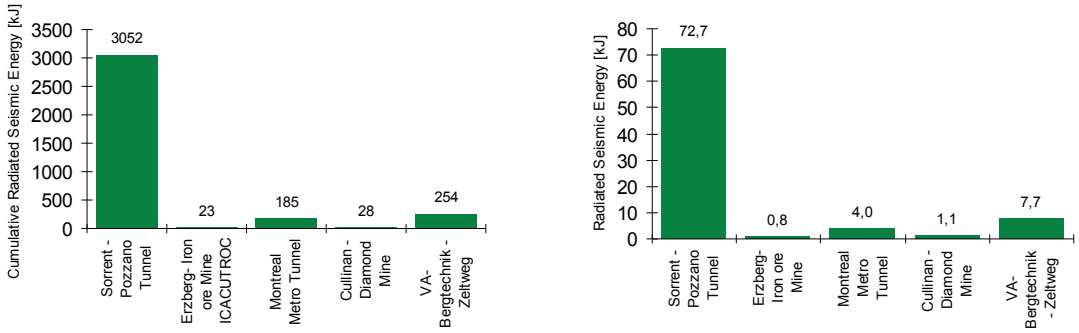

Figure 7.26: Radiated seismic energy for 1m roadway development (left) and per m³ excavation (right)

The radiated seismic energy for a unit element in a depth of 0,3m was again the highest for Pozzano Road Tunnel, and the lowest for Cullinan Diamond Mine.

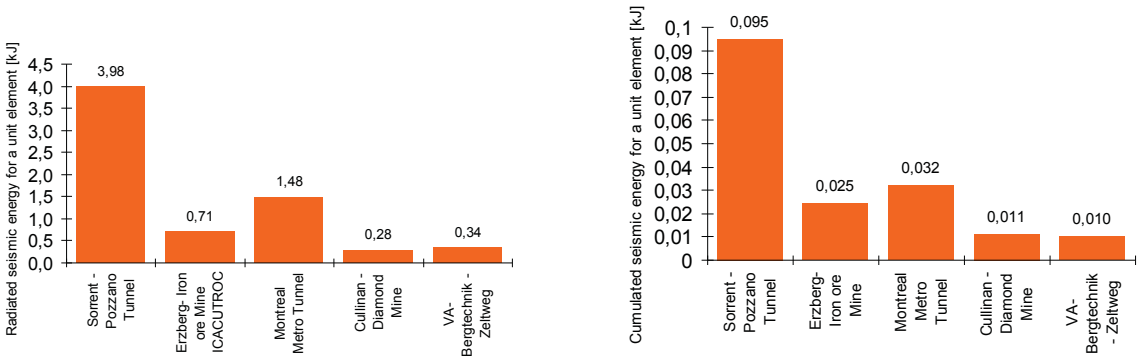

Figure 7.27: Radiated seismic energy for a unit element in a depth of 0,3m in the sidewall for 1m of roadway development (left) and per m³ excavation (right)

The seismic efficiency factor was the highest at Pozzano Road Tunnel. In general the seismic efficiency was very low.

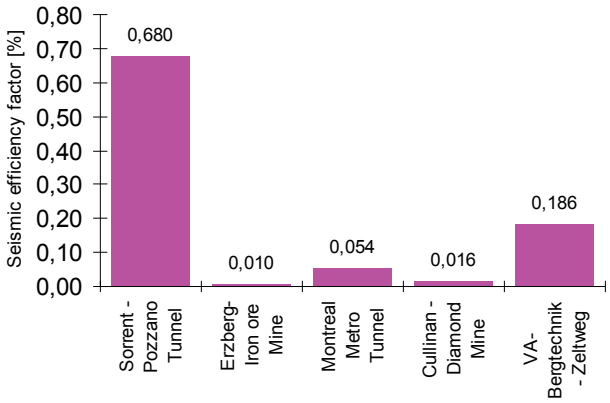

Figure 7.28: Seismic efficiency

The impact quantification number in general shows smaller differences for the test sites than the radiated seismic energy, but here also Pozzano Road Tunnel shows the highest value.

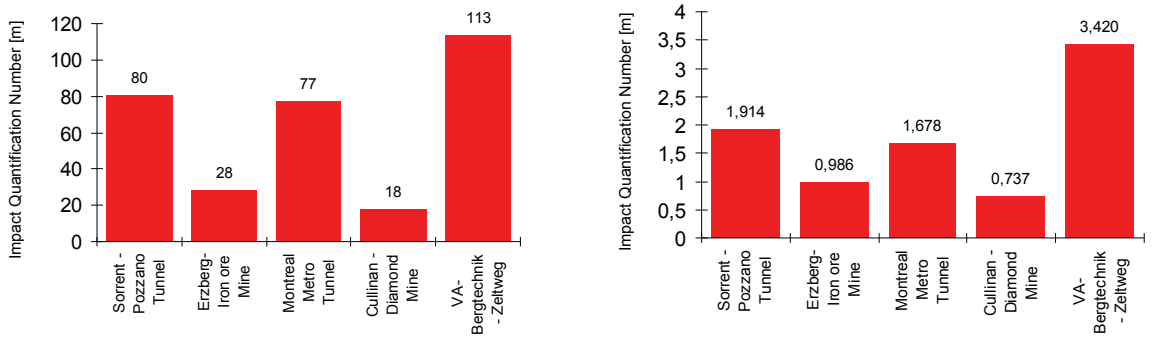

Figure 7.29: Impact quantification number for 1m of roadway development (left) and per m³ excavation (right)

Depending on the emphasis of the characteristics it was deduced that the highest impact of energy was at Pozzano Road Tunnel and the second highest at the test site of VOEST-ALPINE Bergtechnik.

1. Sorrent – Pozzano Road Tunnel — high impact of energy
2. VOEST-ALPINE Bergtechnik –trial site
3. Montreal Metro Tunnel
4. Erzberg Iron Ore Mine and Cullinan Diamond Mine — low impact of energy

7.3 Substitutions for drill and blast development

When the function of the propagation of ground vibrations and the model of the impact quantification for roadheader drifting were determined, several substitutions had to be performed for a drill and blast development.

First the impact parameters of the function of the propagation of ground vibrations had to be adopted. Based on this adopted function the five characteristics which describe the impact of energy caused by drill and blast development were calculated for the test sites.

7.3.1 Function for the propagation of ground vibrations

The modified function for the propagation of ground vibrations from roadheader drifting was:

(12) $$RGV_D = RGV_{Cut} \cdot \frac{D_{Cut}^{n_{Cut}}}{D^{n_D}} \cdot e^{\alpha \cdot (D_{Cut} - D)}$$

Parameter	Index	Unit
Resulting ground vibration at the distance D_{Cut}	**RGV_{Cut}**	[m/s]
Resulting ground vibration at the distance D	RGV_D	[m/s]
Spherical Cut Distance	**D_{Cut}**	[m]
Distance	D	[m]
Wave form factor for the distance D_{cut} and Overburden OV	**n_{Cut}**	[-]
Wave form factor for the distance D and Overburden OV	n_D	[-]
Absorption coefficient	α	[1/m]

Table 7.7: Parameters of the function for the propagation of ground vibrations due to roadheader development

The parameters which are bold in Table 7.10 had to be substituted. The equation for the ground vibrations in a certain distance to the blasting was:

(65) $$RGV_D = RGV_{DB} \cdot \frac{D_{DB}^{n_{DB}}}{D^{n_D}} \cdot e^{\alpha \cdot (D_{DB} - D)}$$

Table 7.11 shows the parameters adopted for drill and blast development. More detailed information about the determination of parameters is given in Chapter 7.3.1.1 to Chapter 7.3.1.3.

Parameter	Index	Unit
Resulting ground vibration at the distance D_{DB}	**RGV_{DB}**	[m/s]
Resulting ground vibration at the distance D	RGV_D	[m/s]
Spherical blast distance	**D_{DB}**	[m]
Distance	D	[m]
Wave form factor for the distance D_{DB} and overburden OV	**n_{DB}**	[-]
Wave form factor for the distance D and Overburden OV	n_D	[-]
Absorption coefficient	α	[1/m]

Table 7.8: Parameters of the function for the propagation of ground vibrations. Drill and blast development

7.3.1.1 Spherical blast distance

The spherical blast distance D_{DB} is the radius of a sphere with the volume VO_B which equals the average blasted volume for one delay stage of a round of shots:

(66) $$D_{DB} = \sqrt[3]{\frac{VO_{\varnothing DB} \cdot 3}{4 \cdot \pi}}$$

whereas the average blasted volume V_{ODB} was calculated from:

(67) $$VO_{\varnothing DB} = \frac{ar \cdot CS}{ds}$$

ar … advance per round [m]

CS … Cross section of the roadway [m²]

ds … Number of delay stages [#]

7.3.1.2 Resulting ground vibration at the spherical blast distance

The resulting ground vibration at the distance “spherical blast distance” was the maximum resulting ground vibration in the function and was calculated from the energy of the explosives and the blasting efficiency factor ϑ. The blasting efficiency rate depends on a number of parameters:

- ratio borehole diameter vs. diameter of the cartridge
- type of tamping
- detonation speed varies depending on the diameter of the cartridge
- accuracy of the igniters, as the superposition of blast waves is very complex

The parameters which are influenced by human activities are more for drill and blast development than the highly automated process of rock cutting.
To acquire all these parameters is a very time-consuming process and in some cases their measurement is very difficult.

Hence it was decided that in contrast to excavation by means of the ALPINE Miner AM105 for drill and blast development the blasting efficiency factor was no constant value. Since all other parameters in the function of the propagation of ground vibrations were known for each site, the blasting efficiency factor was approximated by a least squares analysis.

After approximating the blasting efficiency factor, the blasting efficiency factor was calculated:

(68) $$\eta_{DB} = \left(\vartheta \cdot E_f\right)$$

where ϑ was the blasting efficiency rate and the corresponding energy E_T equals:

(69) $$E_{T,Blast} = E_{DB} \cdot \left(\vartheta \cdot E_f\right)$$

E_{DB} was the average energy per delay stage:

(70) $$E_{DB} = \frac{\sum_{et=1}^{ET} E_{spec,et} \cdot M_{et}}{ds}$$

For further calculation also the average detonation time per delay stage was approximated by calculating a weighted mean value of the detonation speeds of the different explosives:

$$t_{\varnothing Det} = \frac{\sum_{et=1}^{ET} v_{det,et} \cdot ar \cdot M_{et}}{\sum_{et=1}^{ET} M_{et}} \quad (71)$$

Every type of explosive had a different index *et* for the calculations as they had different detonation speeds and different specific energies.

From this relation the equation for the resulting ground velocity at the distance D_{DB} is:

$$RGV_{DB} = \sqrt{\frac{4 \cdot E_{DB} \cdot (\vartheta \cdot E_f)}{VO_{\varnothing DB} \cdot \rho \cdot t_{\varnothing DB} \cdot \varphi}} \quad (72)$$

7.3.2 Results for the propagation of ground vibrations for tunnel drifting by means of D&B

The propagation function of drill and blast development is basically the same as that of roadheader development.

$$RGV_D = RGV_{DB} \cdot \frac{D_{DB}^{n_{DB}}}{D^{n_D}} \cdot e^{\alpha \cdot (D_{DB} - D)} \quad (65)$$

At Wolfram Mine Mittersill and Magnesite Mine Breitenau full rounds of shots, and at Erzberg Iron Ore Mine single shots were recorded. At Erzberg Iron Ore Mine the explosive “Rockracker” was used. As the blasting efficiency rate for single shots vs. full rounds of shots and Rockracker [24] vs. standard explosives is different, a separate blasting efficiency rate for Erzberg Iron Ore Mine was approximated.

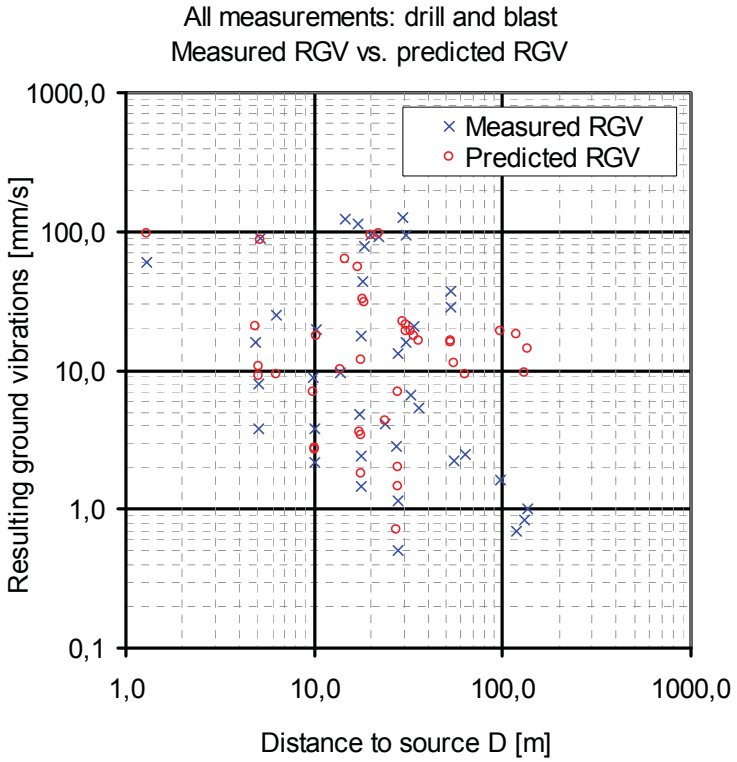

Figure 7.30: Measured and predicted resulting ground vibrations, drill and blast development

In Figure 7.30 the measured resulting ground vibrations are compared to the predicted resulting ground vibrations. To predict the resulting ground vibrations all the boundary parameters, the global exponents and coefficients had to be known.

Parameter		Unit	Location		
			Mittersill	Breitenau	Erzberg
Overburden	OV	[m]	775	800	60
Depth Geophone	DG	[m]	2,6-3,0	1,9-2,1	0,35-0,55
Mean Distance of the geophones	D_{mean}	[m]	60,2	36,0	14,3
Cross Section	CS	[m²]	22,0	24,0	14,0
Density	δ	[kg/m³]	2958	2700	2703
Uniaxial Compressive Strength	UCS	[Mpa]	140,0	136,0	35,0
Brazilian Tensile Strength	BTS	[Mpa]	10,9		7,6
Young´s modulus	Y_M	[Mpa]	19361	102000	18136
Fracture Energy	E_f	[J]	29	7,3	4
Rock Mass Rating (Bieniawski)	RMR	[-]	55	41	41
Number of boreholes		[#]	65	54	1
Diameter of boreholes		[mm]	52	45	38
Advance per round		[m]	3,8	4,2	single shots
Name of igniter	Type I	[-]	O-HU	MS	
Number of igniters	Type I	[#]	1	8	1
Delay time	Type I	[ms]	0	25	
Delay stages	Type I	[#]	1	8	1
Name of igniter	Type II	[-]	DEM-P-HU	LP	-
Number of igniters	Type II	[#]	17	46	-
Delay time	Type II	[ms]	80	40	-
Delay stages	Type II	[#]	7	6	-
Name of igniter	Type III	[-]	DEP-HU	-	-
Number of igniters	Type III	[#]	47	-	-
Delay time	Type III	[ms]	500	-	-
Delay stages	Type III	[#]	7	-	-
Name of explosive	Type I	[-]	Austrogel G1	Gelatin Donarit 1	Rockracker
Mass of explosive	Type I	[kg]	90	50	0,02-0,18
Specific energy of explosive	Type I	[kJ/kg]	1020	900	1036
Detonation speed of explosive	Type I	[m/s]	6000	6000	400
Name of explosive	Type II	[-]	Wandex	Emulgit LWC Al	Hanal 1U
Mass of explosive	Type II	[kg]	165	210	0,014-0,114
Specific energy of explosive	Type II	[kJ/kg]	1000	920	1010
Detonation speed of explosive	Type II	[m/s]	2750	3600	3200
Name of explosive	Type III	[-]	Wandex	-	Polyadin
Mass of explosive	Type III	[kg]	165	-	0,5
Specific energy of explosive	Type III	[kJ/kg]	1000	-	1100
Detonation speed of explosive	Type III	[m/s]	2750	-	5140

Table 7.9: Parameters of the measurement sites

Table 7.9 shows the parameters which are necessary to estimate the predicted resulting ground vibrations.

Local exponents and coefficients

Parameter	Index	Unit	Location		
			Mittersill	Breitenau	Erzberg
Wave form factor	n_{DB}	[-]	0,903	0,907	0,834
Wave form factor	n_D	[-]	0,940	0,960	0,851
Absorption coefficient	α	[1/m]	5,39E-05	5,00E-05	1,63E-02
Blasting efficiency rate	ϑ	[1/J]	0,0237	0,0036	0,0237

Table 7.10: Local exponents and coefficients

The results of the local exponents and coefficients of the different measuring sites for drill and blast development are shown in Table 7.10.

The determined absorption coefficients for Mittersill, Breitenau and Erzberg versus frequency are shown in Figure 7.31.

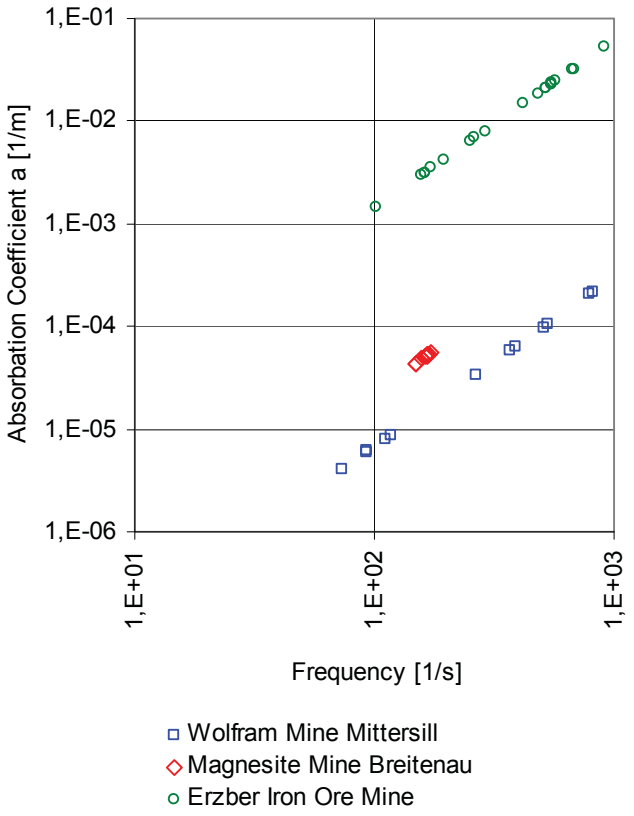

Figure 7.31: Absorption coefficient – frequency diagram

For drill and blast development the following diagrams show the measured and the predicted resulting ground vibrations of the different measuring sites.

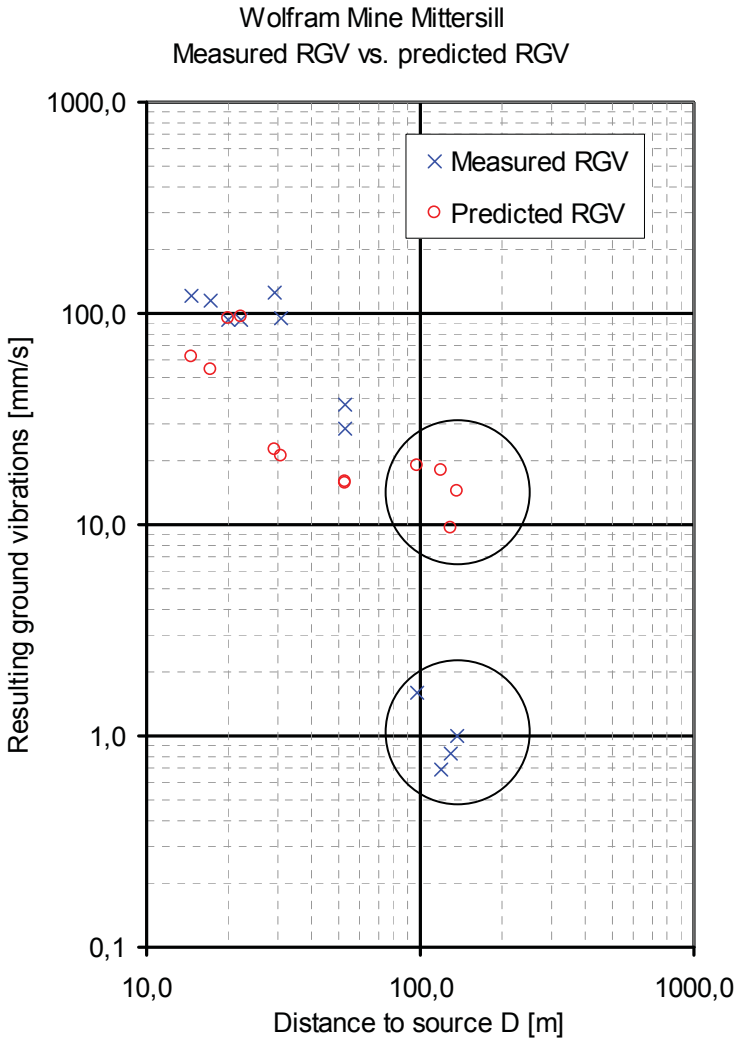

Figure 7.32: Measured and predicted resulting ground vibrations, Wolfram Mine Mittersill

The low measuring results at about 100m distance were influenced by a fault zone of about 2m width close to the round of shots. As this fault zone was not considered in the approximation, the predicted resulting ground vibrations for this round of shots are too high.

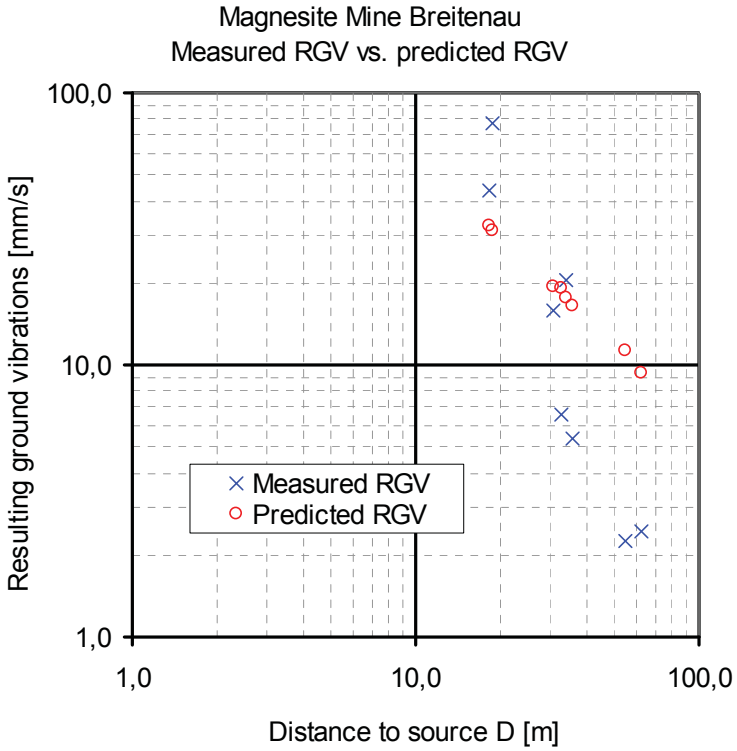

Figure 7.33: Measured and predicted resulting ground vibrations, Magnesite Mine Breitenau

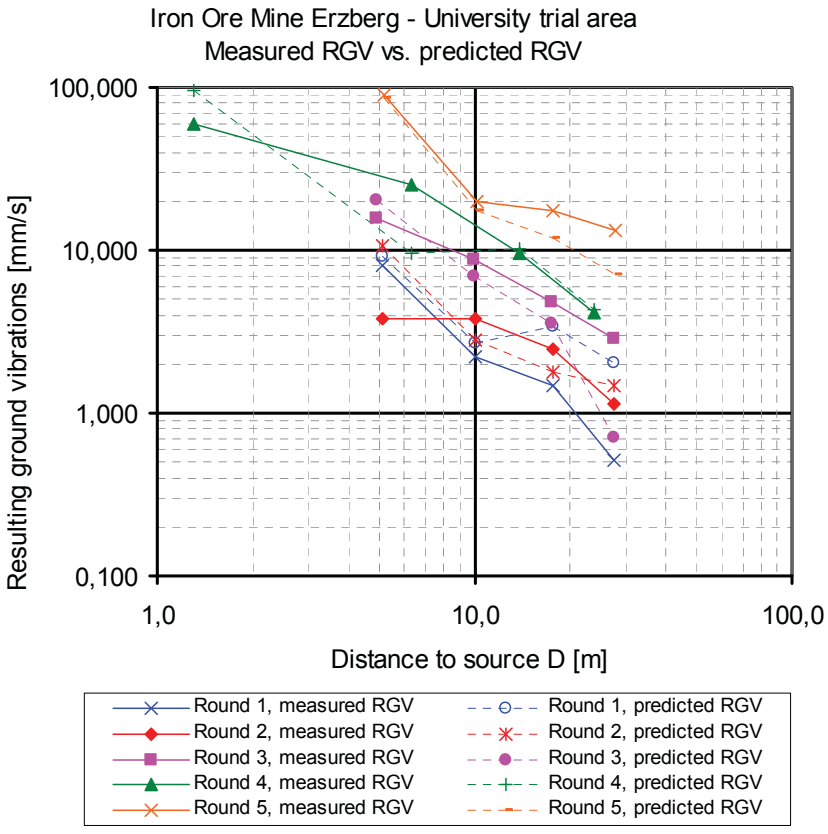

Figure 7.34: Measured and predicted resulting ground vibrations, Erzberg/ University test site

7.3.3 Model of the quantification of the impact of energy

Taking the predefinitions and the substitutions of Chapter 7.2.1.2 and Chapter 7.3.1 into account, the five characteristics could be determined by the following steps which are similar to the steps of Chapter 7.2.1, in which the determination of the characteristics to quantify the impact of energy for roadheader drifting is described:

1. Calculation of the blasted volume VO_{oDB}:

   (67) $$VO_{\varnothing DB} = \frac{ar \cdot CS}{ds}$$

2. Calculation of the excavation speed $v_{ex,DB}$ along the tunnel axis:

   (72) $$v_{ex,DB} = \frac{VO_{\varnothing DB}}{CS \cdot t_{\varnothing Det}}$$

3. Division of the distance in a logarithmic scale (10 segments per decimal power)

4. Calculation of the average distance of a class $D_{m,k}$ in logarithmic scale:

   (47) $$D_{m,k} = e^{\frac{\ln(D_k)+\ln(D_{k+1})}{2}}$$

5. Calculation of the average resulting ground velocity RGV_k of the segment k:
   - Position of the segment before the excavation passed:

     (73) $$RGV_{k,be} = RGV_{DB} \cdot \frac{D_{DB}{}^{n_{DB}}}{D_{m,k}{}^{n_{D,be,k}}} \cdot e^{\alpha \cdot (D_{DB} - D_{m,k})}$$

     where the wave form factor had to be calculated separately for every segment:

     (49) $$n_{D,be,k} = \frac{2 \cdot \arctan\left(h \cdot \sqrt{\sqrt{DG^2 + D_{ax,be,m,k}{}^2}}\right)}{\pi}$$

   - Position of the segment after the excavation had passed:

     (65) $$RGV_{k,af} = RGV_{DB} \cdot \frac{D_{DB}{}^{n_{DB}}}{D_{m,k}{}^{n_D}} \cdot e^{\alpha \cdot (D_{DB} - D_{m,k})}$$

     where the wave form factor was constant for all the segments.

6. Calculation of the minimum average distance $D_{m,kmin,DB}$ to the average location of the source of impact in logarithmic scale:

(74) $$D_{m,k_{min},DB} = e^{\frac{\ln(TW)+\ln(TH)+2\cdot\ln(D_{DB})}{4}}$$

where TW is the width and TH is the height of the roadway. As the function of the propagation of ground vibrations revered to certain positions of the source impact, but this source was moving during the excavation process (different boreholes), an average distance of the average position of the impact source to the sidewall had to be approximated.

7. Substitution of the average distance depending on the position of the segment:
   - Position of the segment before the excavation has passed:

(44) $$D_{ax,be,m,k} = \sqrt{D_{m,k}{}^2 - \left(D_{m,k_{min}} + DG\right)^2}$$

   - Position of the segment after the excavation has passed:

(45) $$D_{ax,af,m,k} = \sqrt{\left(D_{m,k} - D_{m,k_{min}}\right)^2 - DG^2}$$

8. Definition of the maximum average distance

(53) $$D_{m,k_{max}} = D_{m,k_{max}}\left\{D_{m,k}\left|\left[\left(RGV_k > BN\right) \wedge \left(RGV_{k+1} < BN\right)\right]\right.\right\}$$

The maximum average distance was defined as the average distance of the segment k at which the related resulting ground vibration RGV_k was higher than the background noise, but at which the resulting ground vibration RGV_{k+1} of the segment k+1 was smaller than the background noise.

9. Calculation of the exposed time T_k of the segment k during the excavation process

(75) $$T_k = \frac{v_{ex,DB}}{D_{ax,k} - D_{ax,k+1}}$$

Then the five characteristics could be determined using the parameters defined above:

- **Specific energy** of the explosives per meter roadway development:

$$E_{spec,DB} = \frac{E_{DB} \cdot CS}{VO_{\varnothing DB}}$$

- Radiated seismic energy $E_{spec,rad}$ caused per meter roadway development [11] for the segment k was:
  - Position of the segment before the excavation has passed:

$$E_{spec,rad,be,k} = 0,25 \cdot \rho \cdot \left(D_{m,be,k+1} - D_{m,be,k} \right) \cdot RGV_{k,be}{}^2 \cdot \varphi$$

  - Position of the segment after the excavation has passed:

- $$E_{spec,rad,af,k} = 0,25 \cdot \rho \cdot \left(D_{m,af,k+1} - D_{m,af,k} \right) \cdot RGV_{k,af}{}^2 \cdot \varphi$$

- **Radiated seismic energy $E_{spec,rad,k}$** caused per meter roadway development for a unit element of density ρ and volume of 1m³ was:

$$E_{spec,rad} = \sum_{k=1}^{K} E_{spec,rad,af,k} + \sum_{k=1}^{K} E_{spec,rad,be,k}$$

- Cumulated seismic energy $E_{rad,k}$ caused per meter roadway development for the segment k was:

$$E_{rad,k} = \pi \cdot \rho \cdot D_{m,k}{}^2 \cdot \left(D_{m,k+1} - D_{m,k} \right) \cdot RGV_k{}^2 \cdot \varphi$$

- **Cumulated seismic energy $E_{spec,cum}$** caused per meter roadway development was:

$$E_{rad} = \sum_{k=1}^{K} E_{rad,k}$$

- **Seismic efficiency factor η_{SE}:**

$$\eta_{SE} = \frac{Output}{Input} = \frac{E_{rad}}{E_{spec,DB}}$$

- **Impact quantification number**

$$IQN = \left(\sum_{k=1}^{K} T_{k,DB,af} \cdot RGV_{k,af} \cdot \frac{1}{2 \cdot \pi} \right) + \left(\sum_{k=1}^{K} T_{k,DB,be} \cdot RGV_{k,be} \cdot \frac{1}{2 \cdot \pi} \right)$$

7.3.4 Results of the impact quantification for the test sites

Related either to the development of 1m roadway or to the excavation of 1m³ of rock the results of the quantification of the impact of energy in this Chapter were related to a depth of 0,30m in the sidewall of a unit element of 1m³.

In this Chapter the impacts of energy of three test sites are compared. As “Round 3” of the single shots showed high correlation for the prediction of ground vibrations, it was taken as example of the impact quantification of the blasting tests at Erzberg Iron Ore Mine.

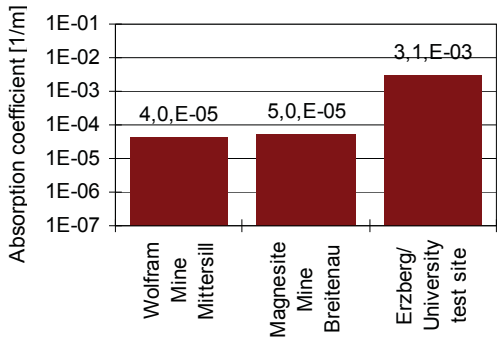

Figure 7.35: Absorption coefficients for the test sites

The different absorption coefficients as well as the different wave form factors and specific energies of the explosives lead to different distances, at which the resulting ground vibration reaches the background noise. As this distance is in the range of more than 1000m, it was decided to use the maximum threshold distance from the roadheader test sites, which was 209m.

Figure 7.36 and Figure 7.37 show the influence on the radiated seismic energy of segments in different distances. Thereby the radiated seismic energy was cumulated for a roadway development of 1m before the excavation passed the segment. The sum of the radiated seismic energies is the total amount of energy induced into the segment for a roadway development of 1m.

The main part of the total radiated seismic energy before the excavation has passed, comes from excavation activities within a distance of about 2m to 8m, whereas the main part of the total radiated seismic energy after the excavation has passed, comes from excavation activities within a distance of about 3m to 10m.

The radiated seismic energy of close segments before the excavation has passed appear with higher influence than close segments after the excavation has passed the segment. The total amount of energy for the unit element is the sum of the energies of the segments before and after the excavation has passed. The fraction of the total amount of radiated seismic energy for a unit element after the excavation had passed the segment was higher than the fraction before the excavation passed.

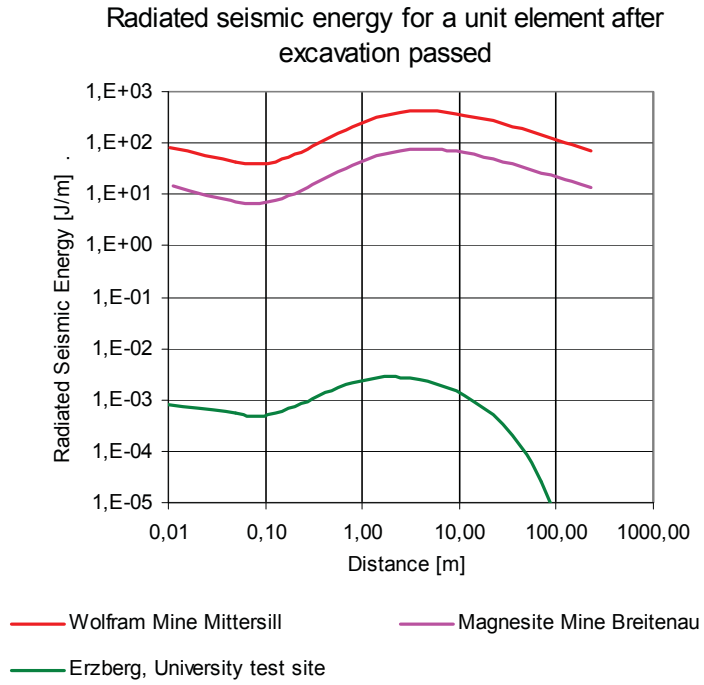

Figure 7.36: Influence of different distances on the radiated seismic energy

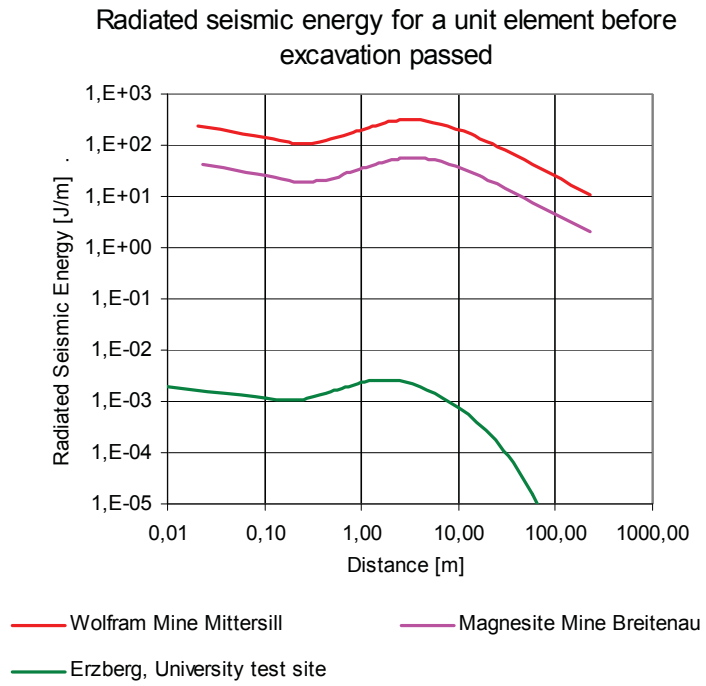

Figure 7.37: Influence of different distances on the radiated seismic energy

Figure 7.38 shows the contribution of the radiated seismic energy to a unit element for the Wolfram Mine Mittersill caused by 1m roadway development. 90 % of the seismic energy was radiated from excavation activities within a distance of about 70m (after the excavation had passed) and about 0,5m (before the excavation passed).

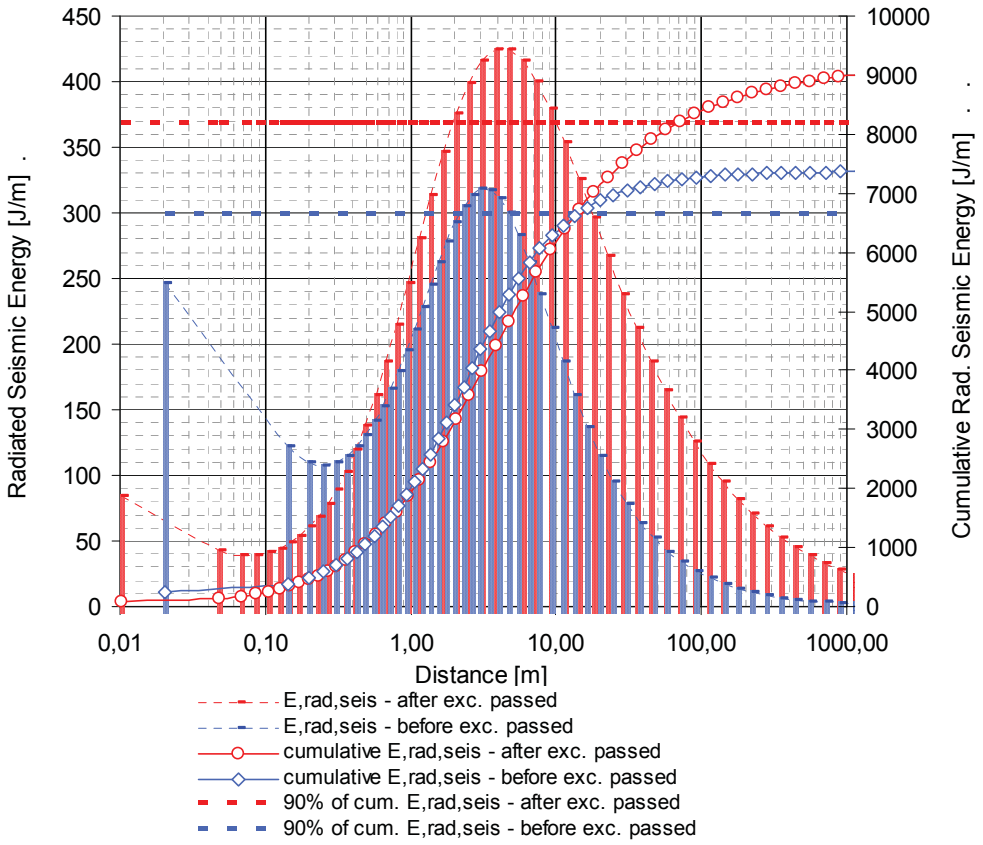

Figure 7.38: Radiated seismic energy for a unit element, Wolfram Mine Mittersill

Figure 7.39 and Figure 7.40 show the influence of segments in different distances on the impact quantification number cumulated for a roadway development of 1m before the excavation has passed. The sum of the impact quantification numbers is qualitatively the total amount of oscillation induced into the segment for a roadway development of 1m. The distances on which the main part of the total oscillation is based highly depend on the absorption coefficient as well as on the background noise and the impact energy. E.g. for Erzberg/ University test site, where 0,5kg of explosives were used, the maximum was reached at a distance of about 11m, whereas the maximum for Wolfram Mine Mittersill and Magnesite Mine Breitenau would only be reached at distances higher than 200m.

The impact quantification numbers of close segments before the excavation has passed appear with higher influence than close segments after the excavation has passed.

The fraction of the total amount of energy of a unit element before the excavation has passed is higher than the fraction after the excavation has passed.

In comparison to the radiated seismic energy, the impact quantification number leads to smaller differences between the sites, as the energy is calculated of the square of the resulting ground vibration.

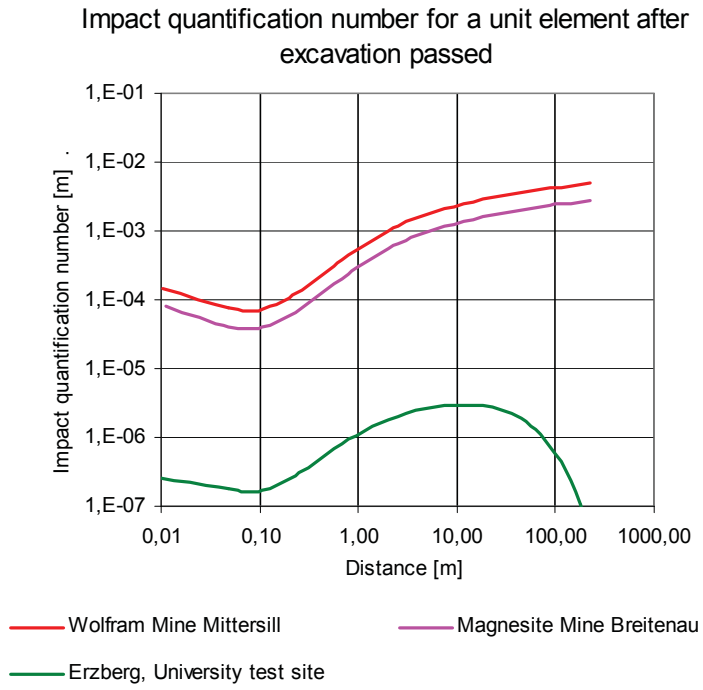

Figure 7.39: Influence of different distances on the impact quantification number

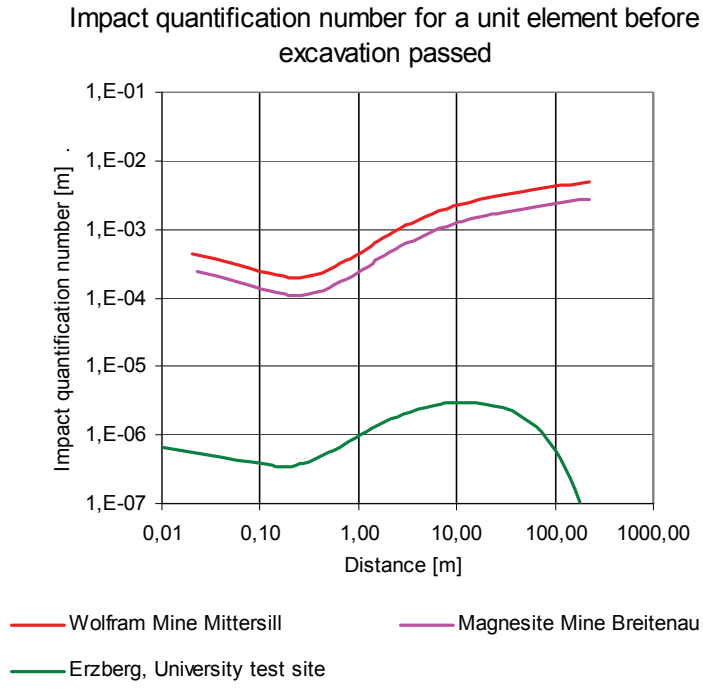

Figure 7.40: Influence of different distances on the impact quantification number

Figure 7.41 shows the contribution of the impact quantification number of “Round 3” of Erzberg/ University test site. 90 % of the impact quantification number are based on excavation activities within a distance of about 25m (after the excavation has passed) and about 27m (before the excavation has passed).

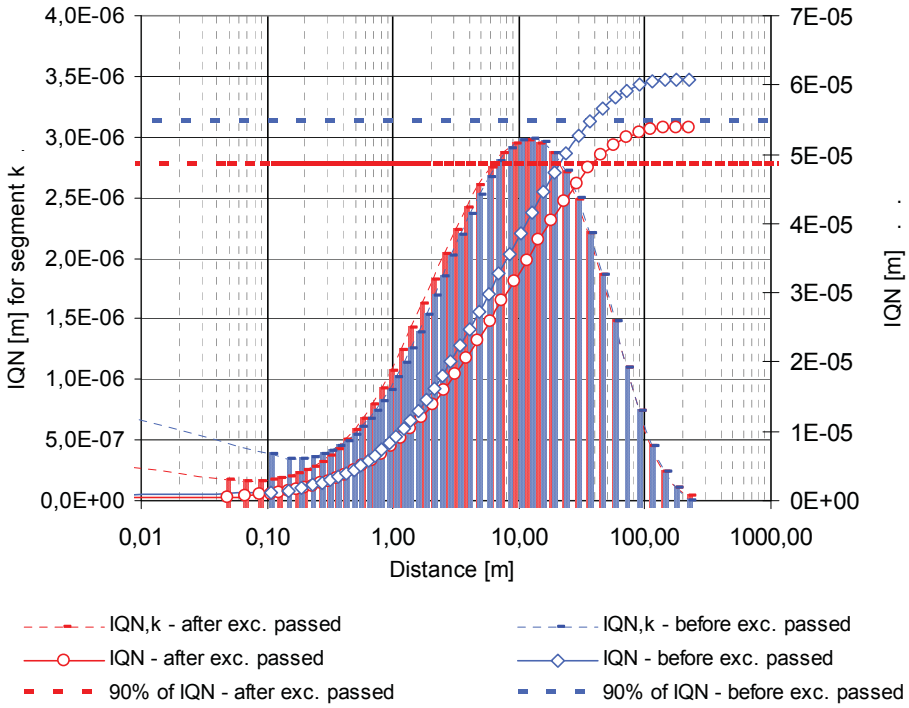

Figure 7.41: Impact quantification number, Erzberg/ University test site

The final results of the impact of energy quantification of the five characteristics are summarized in Figure 7.42 to Figure 7.44

The characteristic “specific energy of the explosives” per m³ excavated rock was in the range of 2,3 to 3,15 MJ/m³ for the full round of shots.

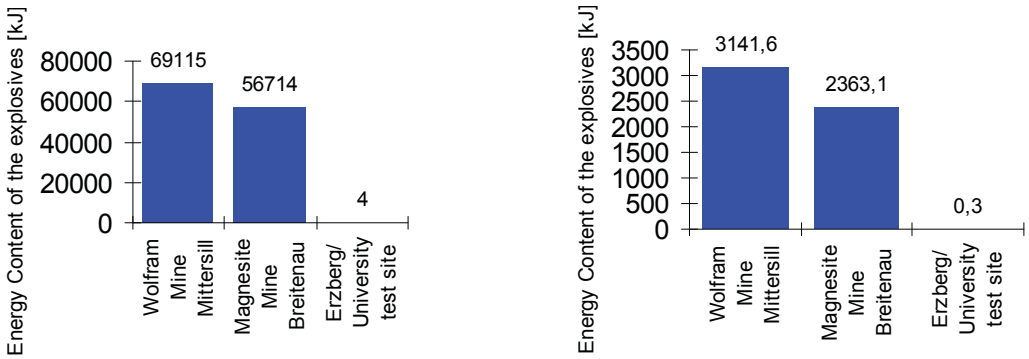

Figure 7.42: Energy content of the explosives for 1m roadway development (left) and per m³ excavation (right)

Low absorption and a high maximum resulting ground vibration lead to a high cumulated seismic energy at Wolfram Mine Mittersill.

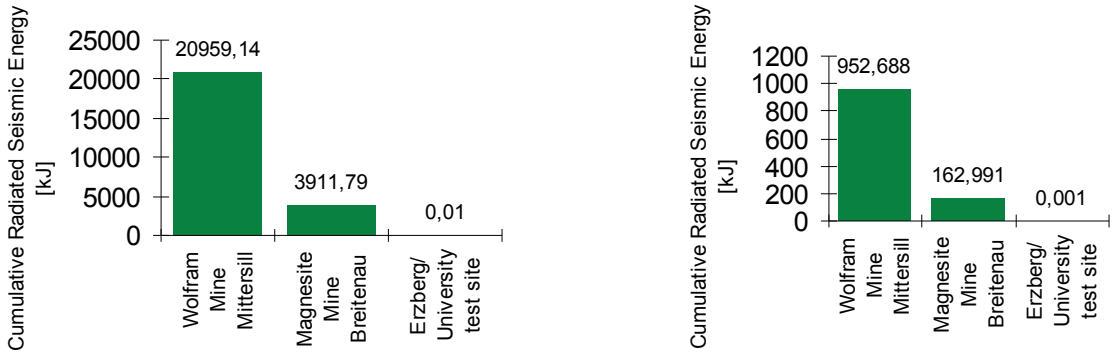

Figure 7.43: Radiated seismic energy for 1m roadway development (left) and per m³ excavation (right)

The radiated seismic energy for a unit element in a depth of 0,3m showed the highest values for Wolfram Mine Mittersill.

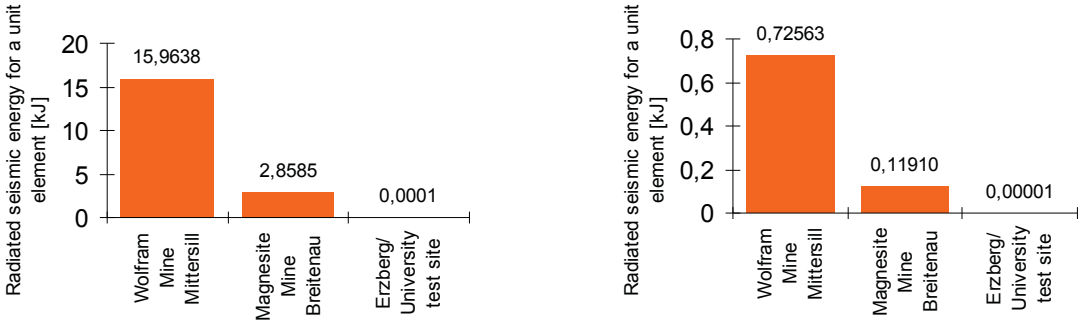

Figure 7.44: Cumulative seismic energy for a unit element in a depth of 0,3m in the sidewall for 1m of roadway development (left) and per m³ excavation (right)

The seismic efficiency factor was the highest at Wolfram Mine Mittersill. A very low seismic efficiency at Erzberg/ University test site was approximated as Rockrackers were used.

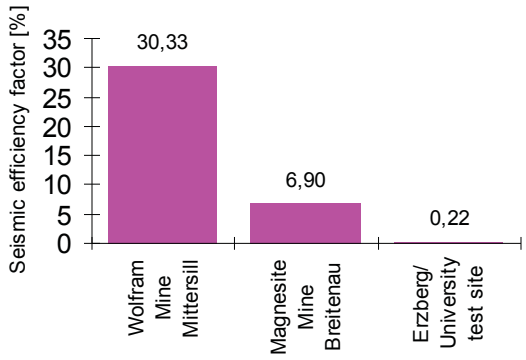

Figure 7.45: Seismic efficiency

The impact quantification number in general shows smaller differences for the test sites than the radiated seismic energy.

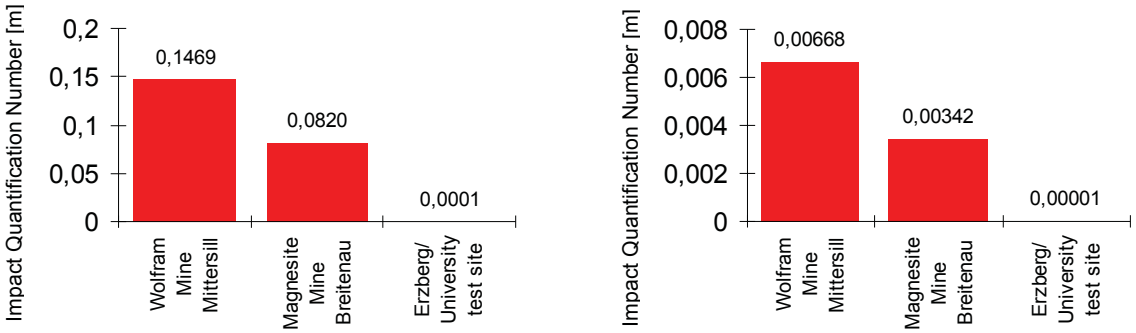

Figure 7.46: Impact quantification number for 1m of roadway development (left) and per m³ excavation (right)

Depending on the emphasis of the characteristics the following ranking was deduced for the three test sites:

1. Wolfram Mine Mittersill — high impact of energy
2. Magnesite Mine Breitenau
3. Erzberg/ University trial site — low impact of energy

7.4 Assumptions made for analysis and modeling

Several assumptions had to be made to simulate the complex process of drifting and the complex function of the propagation of seismic waves in a rock mass for the analysis. It remains crucial to keep in mind that in spite of an extensive scale of data, reality can never be strictly described. Hence the approximated data must be considered with caution.

The following listing gives an overview of the assumptions which are divided in:

- general assumptions
- assumptions during data analysis
- assumptions for the propagation function
- assumptions to quantify the impact of energy:

1. General assumptions:

- Elastic material behavior: When a material is not stressed in tension or compression beyond its elastic limit, its individual particles perform elastic oscillations. When the particles of a medium are displaced from their equilibrium positions, internal restoration forces arise. It is these elastic restoring forces between particles, combined with inertia of the particles, that leads to oscillatory motions of the medium.
- In solids, molecules can support vibrations in different directions, hence, a number of different types (modes) of sound waves are possible. However, at surfaces and interfaces, various types of elliptical or complex vibrations of the particles make different wave types possible. In this investigation plate waves and spherical waves were considered.
- The typical elastic constants of materials include:
    - the Young's modulus, Y_M: a proportionality constant between uniaxial stress and strain
    - the Poisson's Ratio, ν: the ratio of radial strain to axial strain
    - the Shear Modulus, G: also called rigidity, a degree of substance's resistance to shear

As only the Young's modulus was known for the test sites, the other constants could not be taken into account.

- In isotropic materials, the elastic constants are the same for all directions within the material. However, rock is anisotropic and the elastic constants differ with each direction.

2. Assumptions during data analysis:

- The exact distance between the geophones and the place of impact energy was not known, since the cutting head position was permanently changing during the cutting process. Variations of +/- 2m can be estimated for the distances. In general the (relative) uncertainty decreases when the distance of geophone from the tunnel face increases.
- The maximum peak value of the resulting ground vibration of every measurement was taken for further analysis. This does not reflect the average exposure of ground vibration.
- Frequencies were determined by FFT Transformation from the raw data of each axes. In the analysis an arithmetic mean of the frequencies with highest occurrence of the three axes for every individual measurement was assumed.
- The low pass filter effect for frequencies of the rock mass was not taken into account.
- Determined frequencies depend on the used measurement system, as the construction can filter certain frequencies
- Superposition, reflexion and refraction were not considered as the structure of the rock mass was not known exactly

3. Assumptions for the propagation function

- The energy of the excavation method:
    - The energy consumption of the cutting head of the roadheader does not reflect exactly the energy used for the chisels to cut rock. For some test sites the energy consumption was not measured while taking ground vibration measurements. For this cases the energy consumption of the cutting head was approximated of average values of each test site provided by VOEST-ALPINE Bergtechnik.

  - The energy consumption per delay stage of drill and blast development was determined by the mass of the explosives, the specific energy of the explosives and the number of delay stages. As the used mass of the explosives varies per round of shots, only average values provided by the mine offices could be used.
- The wave form factor depends also on the wave length, which influences the penetration depth of the surface waves.
- The rock mass ratings, which were provided by the mine offices and the VOEST-ALPINE Bergtechnik, have to be considered with caution, because they were not determined exactly at the locations where ground vibration measurements were carried out, and, for some cases, were recalculated by the $RMR_{Cutting}$ of VOEST-ALPINE Bergtechnik.
- Rock specific parameters, like the uniaxial compressive strength and the Young's modulus, have high variation and depend highly on the origin of the specimen.
- As in the propagation function a sphere source for the impact was assumed, a spherical cut/blast distance/radius had to be calculated from the real form of the excavated volume.
- The degree of rock disintegration in different depths in the sidewall was not considered as the size of the Excavation Damaged Zone (EDZ) was not known.
- The excavated volume per time period/ delay stage:
  - The excavated volume of roadheader development was calculated only for horizontal slewing of the sump in depth, the cut, a time period of 1 second and the slewing speed. As these parameters were not measured while measuring the ground vibration, only average values of each test site provided by VOEST-ALPINE Bergtechnik were taken.
  - The excavated volume for drill and blast development was determined by the blasted volume of the full round of shots and the number of delay stages. The duration of one single delay stage was determined by detonation speed of the explosives and the length of the charge. Both values were not constant and depended on a number of other parameters, e.g. the borehole diameter, which were not taken into account.

4. Assumptions to quantify the impact of energy:

- It was assumed that the principal part of the seismic energy that is induced into the rock arrived as a series of n equal sinusoidal waves with the length λ, the amplitude A_0, the period T_0, the instantaneous particle velocity v_0 and the mass m of the particle.
- As the source of impact was no static location, but depending on the position of the cutting head/ borehole on the front face, an average location of the impact on the front face was approximated.
- To determine characteristics for an analytical quantification of the impact of energy, the function of the propagation of ground vibrations had to be integrated. The area under function of the propagation of ground vibrations was proportional to the total radiated vibrations, whereas the total radiated vibrations were proportional to the radiated seismic energy. Because it was not possible to determine this area analytically with integral calculus, an approximation calculation was performed.
- Direct distances of the source of impact to a unit element were substituted by distances along the roadway axis.

8 Conclusions and discussion

The large number of field tests provided a large range of data which was estimated regarding resulting ground vibrations of different drifting methods in different conditions. They offered the opportunity to carry out deep investigations and to furnish worthy information about the impact of energy. The results showed that the impact of energy depends on a number of parameters, mainly the energy input of the excavation method, its seismic efficiency, the absorption coefficient and the location of the subject matter .
However, it remains crucial to keep in mind that in spite of an extensive scale of data, reality can never be strictly described. Hence approximated data must be considered with caution.

One main objective of the diploma thesis was to determine a suitable function of the propagation of ground vibrations caused by heading along the sidewall of a roadway considering different geometrical, rock and rock mass conditions. Based on this propagation function a model which describes the impact of energy was set up to quantify the cumulative impact during 1m of axial roadway development or during the excavation of 1m³ of rock.

To determine a suitable function measurement, results of roadheader drifting sites were used in this investigation. Some basic equations were defined to approximate the resulting ground vibrations at the source of impact and at any distance to the source of impact and to set up a relationship between impact and vibrations.

Several assumptions had to be made to simulate the complex process of drifting and the complex function of the propagation of seismic waves in the rock mass.

The developed function of seismic wave propagation in hard rock is composed of a power function - to consider the wave type (depending on geometrical parameters) - and an exponential function - to consider absorption (mainly depending on internal friction, when a loss of energy occurs and vibration energy is partly transformed into heat energy).

The absorption was determined by performing a dimensional analysis and a regression analysis using the measurement results of four drifts developed by means of roadheader. There the correlation coefficient which was reached in the least squares analysis was 0,69.

The parameters with the highest influence on the value of the absorption coefficient α were the:

- Rock mass rating RMR
- Density ρ
- Young's modulus Y_M
- Overburden OV
- Frequency φ.

The uniaxial compressive strength UCS and the Brazilian tensile strength BTS had little influence on the absorption coefficient. The uniaxial compressive strength is already considered in the Rock Mass Rating.

The absorption coefficients for rock varied from 10^{-7} m^{-1} to 10^{-1} m^{-1}.

$$\alpha = 8{,}15 \cdot 10^{16} \cdot \left(\frac{\mathrm{RMR}}{100}\right)^{-27{,}41} \cdot \mathrm{UCS}^{-0{,}011} \cdot \mathrm{Y_M}^{-3{,}86} \cdot \mathrm{OV}^{-2{,}12} \cdot \rho^{31{,}281} \cdot \varphi^{1{,}64}$$

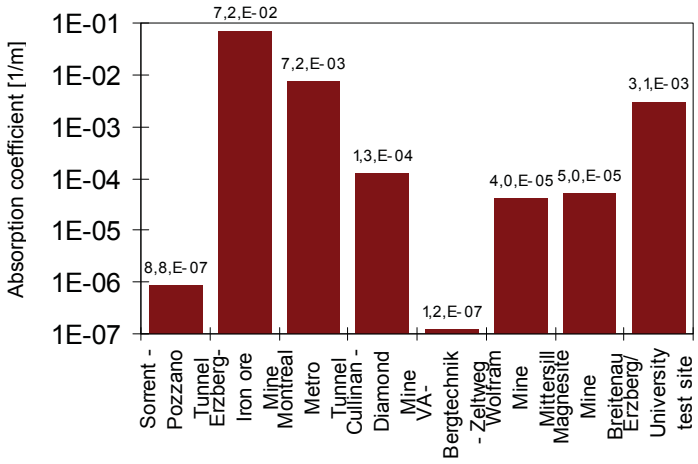

Figure 8.1: Determined absorption coefficients for the test sites

The wave form factor for the test sites was in the range of 0,6 to 1,0. The parameters which determined the wave form factor were the

- Depth in the sidewall
- Wave form factor coefficient

Figure 8.2 shows the propagation functions for ground vibrations for the different test sites before and after the excavation passed the drift face. The propagation functions are related to depth of 0,3m in the sidewall of the roadways.

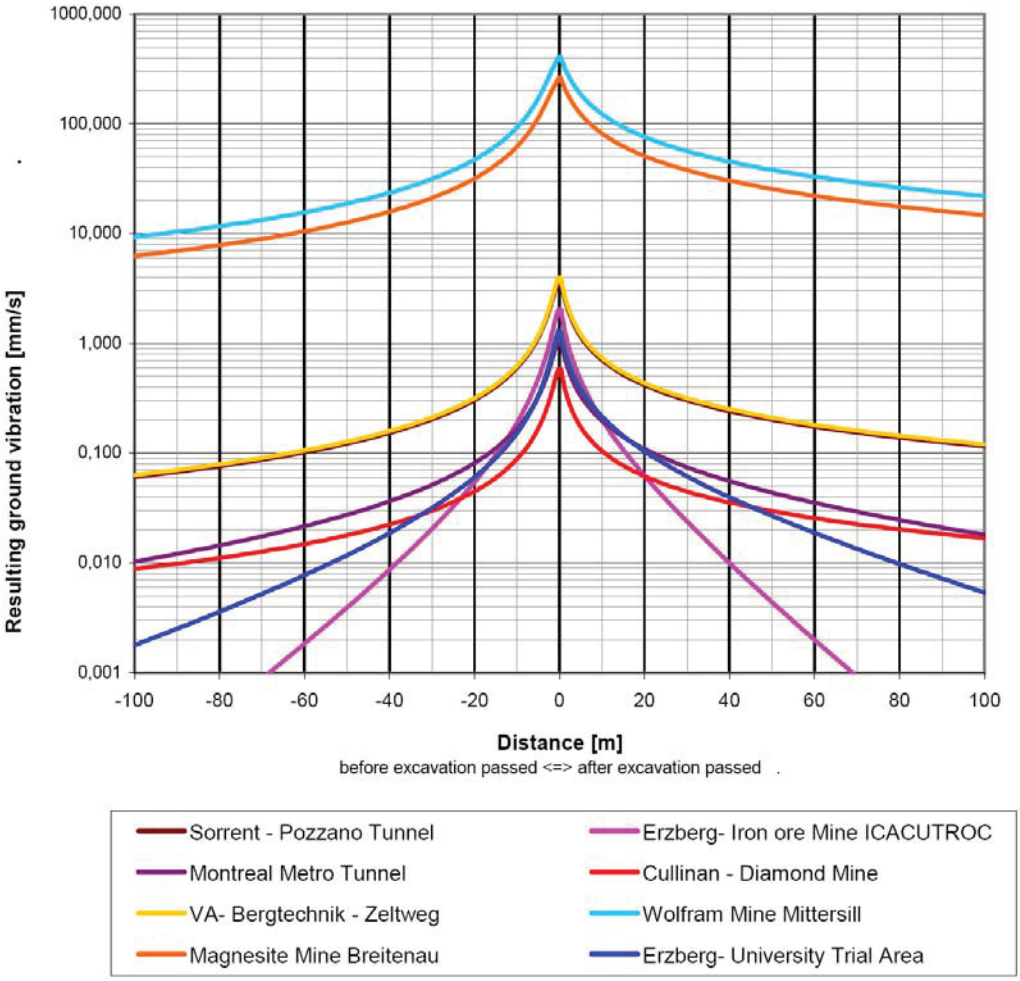

Figure 8.2: Propagation functions for the drifting sites

The third main objective of this thesis was the quantification of the impact of energy. As a consequence of the complex form of the propagation function an approximation calculation was performed to quantify the impact of energy in five characteristics related either to 1m roadway development or to 1m³ of excavate rock:

- **the energy consumption of the excavation method** E_{spec} (energy consumption of the cutting head, energy of the explosives)
- **the radiated seismic energy** $E_{spec,rad}$ for an unit element at certain distances in the sidewall
- **the cumulated seismic energy** E_{rad}

- **seismic efficiency factor** η_{SE} (quotient of the cumulated radiated seismic energy and the energy consumption of the excavation method)
- **Impact quantification number** IQN, which is related to the cumulated movement of the unit element

On a *Microsoft Excel*® interface different geometrical, rock and rock mass conditions as well as drifting specific parameters were be used to estimate the resulting ground vibrations at certain distances and to estimate the impact of energy for a unit element in a certain depth of the sidewall of the roadway.

A critical parameter for this estimation was the threshold value of the resulting ground vibrations, which was assumed to be equal to the background noise. Resulting ground vibrations lower than the threshold value have not been taken into account for the quantification of the impact energy. For a more precise estimation the threshold value has to be the resulting ground vibration, where it starts to cause damage in the rock and in the rock mass. This threshold value can be higher or lower than the background noise. As this threshold value was not further investigated in this paper, care has to be taken by the interpretation of the results.

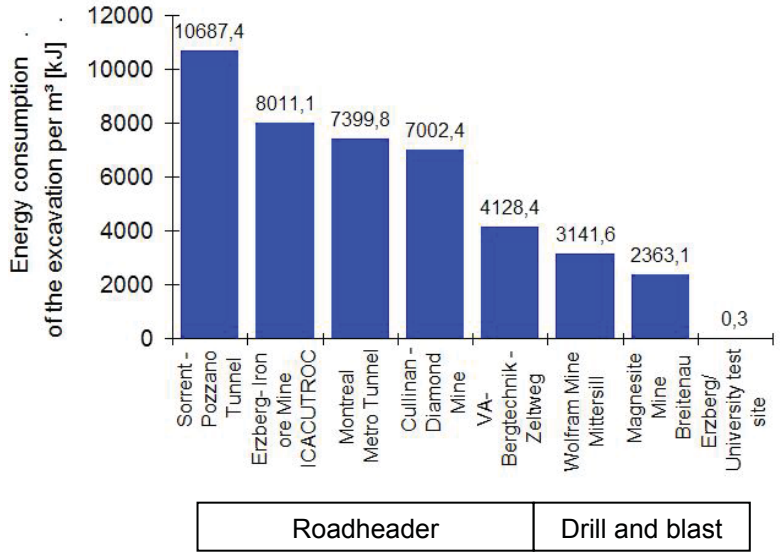

Figure 8.3: Specific energy consumptions of the test sites

The highest specific energy was determined at the Pozzano Road Tunnel site. All determined specific energies were higher for roadheader development than for drill and blast development.

The simulation of the roadheader drifting sites showed that the main part of the seismic energy of a unit element close to the sidewall of the roadway (< ~2m) was radiated within the first meters (2m - 10m). The main part of the impact quantification number was based on segments within an average distance from the front face of about 10 to 100m for roadheader drifting. For drill and blast development these distances were generally higher, but mainly depending on the absorption coefficient and the wave form factor.

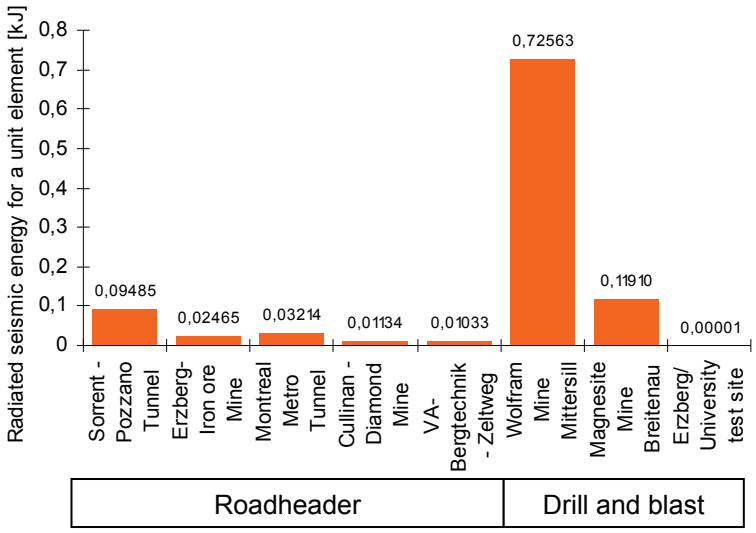

Figure 8.4: Radiated seismic energy for a unit element per m³ excavated rock

The radiated seismic energy for a unit element in a depth of 0,3m in the sidewall was lower for roadheader drifting, whereas for Pozzano and Breitenau, the energy differed less than 20%. The lowest radiated seismic energy was determined for the single shots using Rockracker, as it is a very gentle explosive.

The seismic efficiency shows the portion of the input energy which is transformed into seismic energy. The seismic efficiencies for full round of shots were much higher than for roadheader development. The seismic efficiency for the single shot of “Round 3” using Rockracker was very low compared to full round of shots.

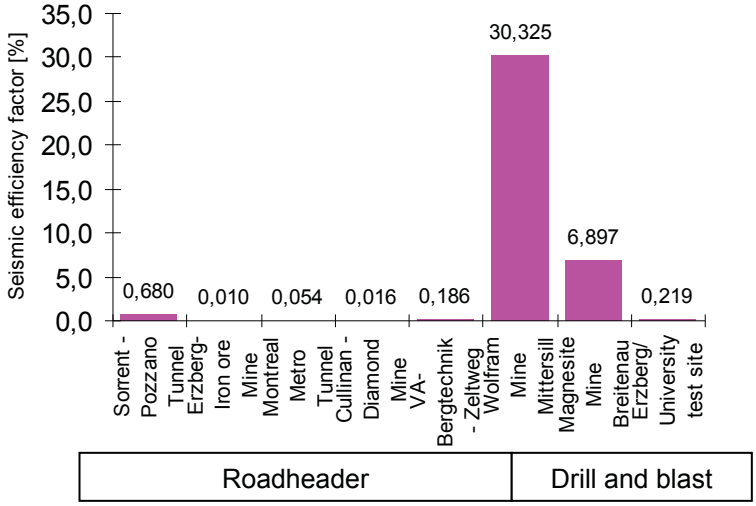

Figure 8.5: Seismic efficiency for the test sites

The impact quantification number gives an indication of the cumulative oscillation movement of a unit element of rock for the whole excavation process, e.g. initially the element is ahead of the excavation, then the element is in the vicinity of the excavation and ultimately it is distance from the excavation face. The impact quantification number was 10 to 200 times higher (but at low amplitudes) for roadheader development than for D&B development, because in the case of a roadheader the unit element is continuous subjected to oscillations as a result of the roadheading drum, whereas in D&B the unit element is only subjected to ground vibrations during blasting time. This means that in the case of a roadheader development the duration of excitation is about 10^5 times higher than that of D&B development.

The highest impact quantification number for roadheader development was determined at Pozzano Road Tunnel and the VOEST-ALPINE Bergtechnik- test rig, where the absorption coefficients were the lowest.

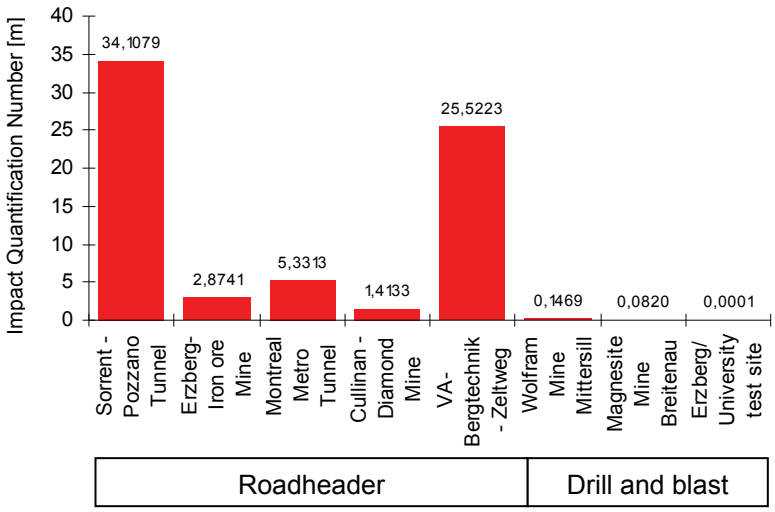

Figure 8.6: Impact quantification number for the test sites per m³ excavated rock

As the impact of the excavation method into the surrounding rock mass may be one of the major influences on the development of the excavation damaged zone, it could help substantially for a better understanding and approximation of the degree of rock disintegration around roadways caused by excavation.

References

[1] ALEHOSSEIN, H., HOOD, M., 1999, An application of linearised dimensional analysis to rock cutting, International Journal of Rock Mechanics and Mining Sciences, Volume 36, Issue 5 , pp 701-709

[2] BENDER, F., 1985, Methoden der angewandten Geophysik und mathematische Verfahren in den Geowissenschaften, Ferdinand Enke Verlag Stuttgart, 1985, pp.156-164

[3] EGGER F., 2004, Bergmännische Meldearbeit: Untersuchung zum Einsatz von Geophonen für begleitende Messungen während eines Streckenvortriebes, Department Mining and Tunneling at the University of Leoben.

[4] EGGER F., 2005, Seismic measurements with geophones as a part of the geotechnical monitoring programme for the Roadheader Project, Department Mining and Tunneling at the University of Leoben.

[5] EMSLEY, S., OLSSON, O., 1997, ZEDEX- A study of damage and disturbance from tunnel excavation by blasting and tunnel boring, SKB intern paper

[6] GEHRING, H., 1999, Geologie und Leistungsmessungen- Pozzano Tunnel/ Italien AM 105 Icacutroc, VOEST-ALPINE Bergtechnik, Confidential Paper.

[7] HINTERPLATTNER, B., TOCKNER, J., 1998, Projekt Icacutroc, Messungen der Gebirgserschütterungen während des Schneidens von Hartgestein mit einer AM105 am Erzberg, Contribution of the Department of Mining Engineering and Mineral Economics at the University of Leoben

[8] KARGL, H., 2003, Messeinsatz ATM 105 039 Montreal: technische Berechnung und Simulation, VOEST-ALPINE Bergtechnik, Confidential Paper.

[9] LEITGEB, S., 2004, Ground Vibrations Resulting from Roadheader Operations, Institute of Engineering Geology and Applied Mineralogy at Graz University of Technology.

[10] Mc GARR, A., GAY, N.C., WAINWRIGHT, E.H., 1982, Some Applications of seismic source mechanism studies to assessing underground hazard, Proceedings of the 1st international congress of Rockbursts and Seismicity in Mines, The South African Institute of Mining and Metallurgy Symposium Series No. 6.

[11] HOWELL, B., F., 1959, Introduction to geophysics, pp 124-128

[12] MILLITZER, H., SCHÖN, J., STÖTZNER, U., 1986, Angewandte Geophysik im Ingenieur- und Bergbau

[13] MILITZER, H. & WEBER, F., 1987, Angewandte Geophysik Band 3 Seismik.

[14] MOSER, P., 2004, Universitätskurs „Sprengingeneurwesen“, Department Mining and Tunneling at the University of Leoben.

[15] MOSER, P., REICHL, C., 1998, Messungen von Sprengerschütterungen am Steirischen Erzberg, Etage Elias, Department Mining and Tunneling at the University of Leoben.

[16] NAGY, M., EGGER, F., MOSER, P., 2005, Seismic measurements to determine the degree of rock disintegration in roadways by a roadheader ATM 105 in comparison to roadways developed by drilling and blasting, Department Mining and Tunneling at the University of Leoben.

[17] NEIL, D., M., ROSTAMI, J., OZDEMIR, L., GERTSCH, R., 1994, Production estimating techniques for underground mining using roadheaders, Earth Mechanics Institute at the Colorado School of Mines

[18] REICHL, C., TOCKNER J., 1999, Erschütterungsmessungen beim Tunnelvortrieb mit einer AM 105 im Pozzano- Tunnel (Italien), Department Mining and Tunneling at the University of Leoben.

[19] SAFAK, E., 2000, Characterization of seismic hazard and structural response by energy flux, Soil Dynamics and Earthquake Engineering, Volume 20, Issues 1-4, pp 39-43

[20] SIEFERT, M., 2004, Development of a methodology for the evaluation of pillar conditions, Department Mining and Tunneling at the University of Leoben.

[21] TANG, C., A., KAISER, P., K., 1998, Numerical Simulation of Cumulative Damage and Seismic Energy Release During Brittle Rock Failure—Part I: Fundamentals, International Journal of Rock Mechanics and Mining Sciences, Volume 35, Issue 2, pp 113-121

[22] TOCKNER, J., HINTERPLATTNER, B., WAGNER, H., 1998, Projekt Icacutroc, Task 8, Evaluation and optimization of the performance of the total cutting system in „close to reality“ conditions, Contribution of the Department of Mining Engineering and Mineral Economics at the University of Leoben

[23] VALICOURT, H., 1998, Erzberg test evaluation- methodological report, VOEST-ALPINE Bergtechnik, Confidential Paper.

[24] VARGEK-IPSA, J., 2005, Zusammenfassung der Versuche mit Rockrackern unter Tage am Steirischen Erzberg, Department Mining and Tunneling at the University of Leoben, Intern Report.

[25] WAGNER, H., GAY, N.C., WAINWRIGHT, E.H., 1982, Support requirements for rockburst conditions, Proceedings of the 1st international congress of Rockbursts and Seismicity in Mines, The South African Institute of Mining and Metallurgy Symposium Series No. 6.

[26] WAGNER, H. 2004, Universitätskurs „Sprengingeneurwesen“, Department Mining and Tunneling at the University of Leoben.

[27] YONG, L., 2005, Underground blast induced ground shock and its modelling using artificial neural network, Computers and Geotechnics, Volume 32, Issue 3, pp 164-178

[28] Non Destructive Testing-Research Center, Introduction to ultrasonic testing, http://www.ndtd.org/EducationResources/CommunityCollege/Ultrasonics/cc_ut_index.htm, Iowa State University

Data DVD

- Photo documentation
- Raw data
- Ground vibration measurement protocols
- Microsoft Excel Data Sheets
- Diadem Files for automated data analysis

Appendices

1. SM6- Geophone
2. Data sheet plug-in signal conditioner DAQP-V
3. Data sheet analogue input card AI-16E-4
4. Script file from Diadem 8.1 Software for signal analysis from roadheader development
5. Script file from Diadem 8.1 Software for signal analysis from drill and blast development
6. Roadheader ATM 105, data sheet
7. Rock testing results: Wolfram Mine Mittersill
8. Rock testing results: Erzberg Iron Ore Mine/ University test area
9. Rock testing results: Cullinan Diamond Mine, Kimberlite
10. Rock testing results: Concrete Block VOEST-ALPINE Bergtechnik

APPENDIX 1

SM6- Geophone

INPUT/OUTPUT, INC.

SENSOR Nederland bv

SM-6 Geophone

- Long travel version of the SM-4 (8-Hz, 10-Hz, & 14-Hz) geophone; also available in 4.5-Hz natural frequency
- Special orientations upon request beyond the normal vertical and horizontal options
- Widely used in industrial vibration-monitoring systems
- Rugged construction with precious-metal, rotating-coil contacts
- 2-year limited warranty

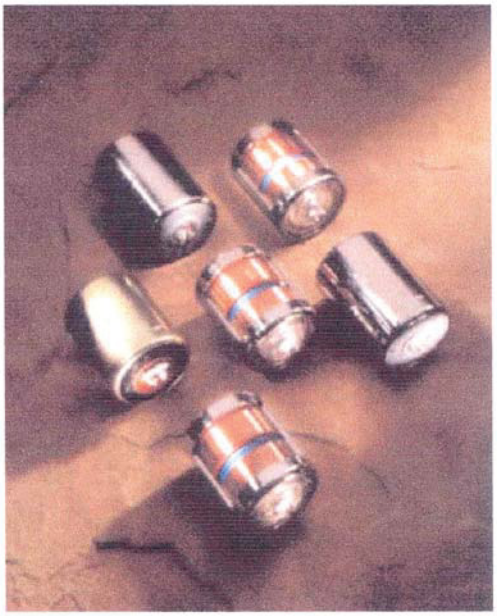

The SM-6 geophone is a long coil travel version of the time-proven SM-4 geophone. The extra coil travel offers an advantage for higher tilt requirements and where larger amplitude signals may be encountered, for example, in industrial vibration monitoring. A range of natural frequencies is available from 4.5 Hz to 14 Hz, providing choice of the correct geophone for a wide variety of applications.

The SM-6 can be supplied for vertical and horizontal orientation. Other specialized versions are available upon request, for example, Galperin (54.7°), 45°.

The SM-6 is an ideal choice for the shear-wave horizontal elements, partnering an SM-4 vertical geophone in a 3-component package.

A variety of I/O Sensor land cases can accommodate the SM-6 geophone elements, making them suitable for an extensive range of field applications.

Specifications (cont.)

SM-6 LOW FREQUENCY GEOPHONE	A-Coil	B-Coil
Frequency		
Natural frequency (f_n)	4.5 Hz	4.5 Hz
Tolerance	±0.5 Hz	±0.5 Hz
Maximum tilt angle for specified f_n	0°	0°
Typical spurious frequency	140 Hz	140 Hz
Distortion		
Distortion with 0.7 ips p.p. coil-to-case velocity	<0.3%	<0.3%
Distortion measurement frequency	12 Hz	12 Hz
Maximum tilt angle for distortion specification	0°	0°
Damping		
Open-circuit damping	0.265	0.56
Open-circuit damping tolerance	±5%	±5%
Resistance		
Standard coil resistance	375 Ω	375 Ω
Tolerance	±5%	±5%
Sensitivity		
Open-circuit sensitivity	28.0 V/m/s (0.71 V/in/s)	28.8 V/m/s (0.73 V/in/s)
Tolerance	±5%	±5%
$R_tB_cf_n$	3,875 ΩHz	6,000 ΩHz
Moving mass	16.1 g (0.57 oz)	11.1 g (0.39 oz)
Maximum coil excursion p.p.	4 mm (0.16 in)	4mm (0.16 in)
Physical		
Diameter	25.4 mm (1 in)	25.4 mm (1 in)
Height	36 mm (1.42 in)	36 mm (1.42 in)
Weight	81 g (2.85 oz)	81 g (2.85 oz)
Operating temperature range	–40°C to +100°C (–40°F to +212°F)	–40°C to +100°C (–40°F to +212°F)
Limited Warranty Period*	1 year	1 year

* Warranty excludes damage caused by high-voltage and physical damage to the element case.

All parameters are specified at +20°C in the vertical position unless otherwise stated.

Ordering Information

SM-6 4.5 Hz	
SM-6/U-A 4.5 Hz 375 Ω (upright A-coil)	P/N 1006050
SM-6/H-A 4.5 Hz 375 Ω (horizontal A-coil)	P/N 1006090
SM-6/U-B 4.5 Hz 375 Ω (upright B-coil)	P/N 1006060
SM-6/H-B 4.5 Hz 375 Ω (horizontal B-coil)	P/N 1006100
SM-6 8 Hz	
SM-6/U-B 8 Hz 375 Ω (upright)	P/N 1006280
SM-6/H-B 8 Hz 375 Ω (horizontal)	P/N 1006300
SM-6 10 Hz	
SM-6/U-B 10 Hz 375 Ω (upright)	P/N 1006330
SM-6/H-B 10 Hz 375 Ω (horizontal)	P/N 1006350
SM-6 14 Hz	
SM-6/U-B 14 Hz 375 Ω (upright)	P/N 1006400
SM-6/H-B 14 Hz 375 Ω (horizontal)	P/N 1006420

Geophone Response Curve and Phase Lag

INPUT/OUTPUT, INC.

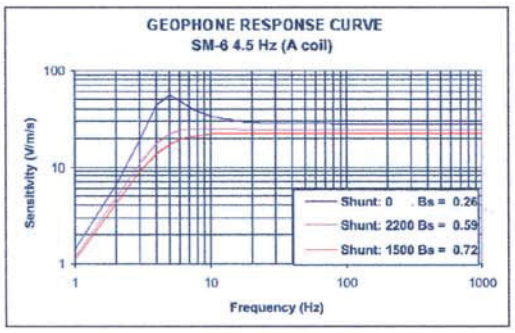

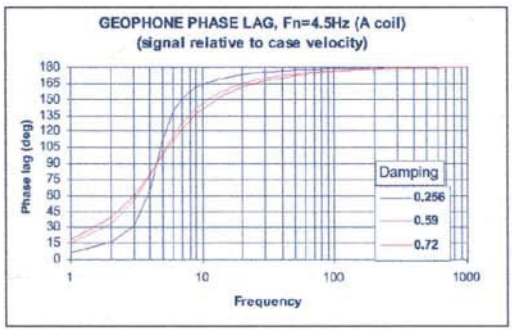

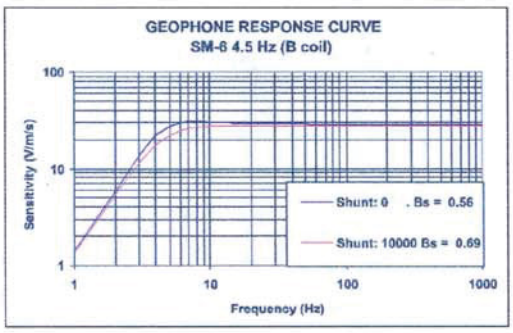

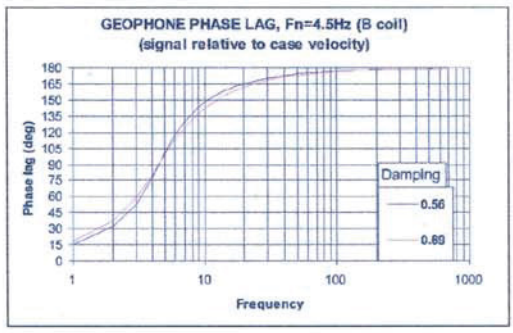

United States – Stafford, TX
Input/Output, Inc.
Fax 281.879.3500
Phone 281.933.3339

Russia
Input/Output, Inc.
Fax 7.095.2322240
Phone 7.095.2322254

England
Input/Output, Inc.
Fax 44.1603.411403
Phone 44.1603.411400

Web Site
www.i-o.com

121026B
01/01

APPENDIX 2

Data sheet plug-in signal conditioner DAQP-V

Eingangsbereiche:	+/-10 mV, +/-100 mV, +/-1V +/-5 V, +/-10 V und +/-50 V
Bereichsauswahl:	Drucktasten oder über Software
Genauigkeit:	+/-0.05 %
Bandbreite:	DC bis 50 kHz (-3 dB)
Tiefpaßfilter:	10 Hz, 100 Hz, 1 kHz, 10 kHz
Filtersteilheit:	40 dB/Dekade (12 dB/Oktave)
Charakteristik:	Bessel oder Butterworth
Filterauswahl:	Drucktasten oder über Software
Isolationsspannung:	1 kVrms
Eingangsschutz:	300 Vrms
Anschlußtechnik:	Sicherheitsbananenbuchsen, BNC oder 9 pol. SUB-D Buchse
Ausgangssignal:	+/-5 V

APPENDIX 3

Data sheet analogue input card AI-16E-4

Analog Input Accuracy Specifications	
Bus:	PCMCIA
Analog Inputs	16 SE/8 DI
Resolution	12 bits
Sampling Rate	500/250' kS/s
Input Range	+/-0.05 to +/-10 V
Digital I/O	8
Counter/Timers	2,24-bit
Triggers	Analog and Digital

Input Signal Ranges	
Range (Software Selectable)	10 V
	5 V
Input Range Bipolar	+/- 5 V
	+/- 2.5 V
Input Range Unipolar	0 to 10 V
	0 to 5 V

Relative Accuracy	
Typical Dithered	+/-0.5 LSB
Maximum Undithered	+/-1.5 LSB

Input Impedance	
Normal Powered On	100 GOhm in parallel with 100 pF
Powered Off	1 kOhm
Overload	1 kOhm

CMRR, DC to 60 Hz	
Range	10 to 20 V
CMRR	85 dB

Bandwidth	
Small Signal (-3 dB)	800 kHz
Large Signal (1% THD)	400 kHz

APPENDIX 4

Script file from Diadem 8.1 Software for signal analysis from roadheader development

```
' ------------------------------------------------------------------------------------------
' Name:             Roadheader_Power.vbs
'
' Ersteller:        Egger Florian
'
' Zweck:            Ground vibration measurements
'
' Beschreibung:     Eliminierung des Background noise und Berechnung von
'                   Kennwerten.
' ------------------------------------------------------------------------------------------
Option Explicit


' Script initialisieren.
' Anzeige des aktuell in Bearbeitung befindlichen Befehls unterdrücken.
AutoEcho = "No"

' Keine akustischen Signale ausgeben.
SoundActive = "No"


' ------------------------------------------------------------------------------------------
' HAUPTTEIL
' ------------------------------------------------------------------------------------------
' Informations-Dialog anzeigen.
Call Info_Message

' Falls 'Weiter' gewählt wurde, Script weiter ausführen.
If MsgState = "IDOk" Then


  ' Daten laden.
  Call DataDelAll(1)
  Call DATAFILEIMPORT("C:\Dokumente und Einstellungen\Egger\Eigene Dateien\Daten\Diploma Thesis\VAB\Rohdaten\65.dat","",0) '...
DATAFILENAME,FILEIMPORTFILTER,PARTIALMODE
  Call DATAFILEIMPORT("C:\Dokumente und Einstellungen\Egger\Eigene Dateien\Daten\Diploma
Thesis\VAB\Diademfiles\blast_cutting.TDM","",0) '... DATAFILENAME,FILEIMPORTFILTER,PARTIALMODE


T2 = "29/11/2005, No. 65"
T3 = "Roadheader"
T4 = "VAB-Zeltweg"
T5 = "Trial Site"
T6 = "Austria"

' Vorbereitetes Grafik-Layout laden.,
Call PICLOAD("C:\Dokumente und Einstellungen\Egger\Eigene Dateien\Daten\Diploma Thesis\VAB\Diademfiles\RGV_FFT_RH_Power.TDR")
'... PICFILE

Call CHNDELETE("31,32") '... CLPSOURCE

Call CHNRENUMBER()

'Call DATABLDEL("1-40",1,12000)       '... CHNNOSTR,CHNROW,VALNO
'Call DATABLDEL("41",138001,150000)       '... CHNNOSTR,CHNROW,VALNO

Call CHNDELETE("1,3,5,7,9,11,13,15,17,19,21,23,25,27,29,31,33,35,37,39") '... CLPSOURCE


      Call CHNRENUMBER()

  Call FormulaCalc("ch(1)            :=  ch(1)/0.0288")
  Call FormulaCalc("ch(2)            :=  ch(2)/0.0288")
  Call FormulaCalc("ch(3)            :=  ch(3)/0.0288")
  Call FormulaCalc("ch(4)            :=  ch(4)/0.0288")
  Call FormulaCalc("ch(5)           :=  ch(5)/0.0288")
  Call FormulaCalc("ch(6)           :=  ch(6)/0.0288")
  Call FormulaCalc("ch(7)           :=  ch(7)/0.0288")
  Call FormulaCalc("ch(8)           :=  ch(8)/0.0288")
  Call FormulaCalc("ch(9)           :=  ch(9)/0.0288")
  Call FormulaCalc("ch(10)           :=  ch(10)/0.0288")
  Call FormulaCalc("ch(11)           :=  ch(11)/0.0288")
  Call FormulaCalc("ch(12)           :=  ch(12)/0.0288")
  Call FormulaCalc("ch(13)           :=  ch(13)/0.0288")
  Call FormulaCalc("ch(14)           :=  ch(14)/0.0288")
  Call FormulaCalc("ch(15)           :=  ch(15)/0.0288")

ChnName(1) = "G1 x-axis"
ChnName(2) = "G1 y-axis"
ChnName(3) = "G1 z-axis"
ChnName(4) = "G2 x-axis"
ChnName(5) = "G2 y-axis"
ChnName(6) = "G2 z-axis"
ChnName(7) = "G3 x-axis"
ChnName(8) = "G3 y-axis"
ChnName(9) = "G3 z-axis"
ChnName(10) = "G4 x-axis"
ChnName(11) = "G4 y-axis"
ChnName(12) = "G4 z-axis"
ChnName(13) = "G5 x-axis"
```

```
ChnName(14) = "G5 y-axis"
ChnName(15) = "G5 z-axis"


  Call FormulaCalc("ch(16)          :=  ((ch(1)^2 + ch(2)^2 + ch(3)^2)^0.5)")
  Call FormulaCalc("ch(17)          :=  ((ch(4)^2 + ch(5)^2 + ch(6)^2)^0.5)")
  Call FormulaCalc("ch(18)          :=  ((ch(7)^2 + ch(8)^2 + ch(9)^2)^0.5)")
  Call FormulaCalc("ch(19)          :=  ((ch(10)^2 + ch(11)^2 + ch(12)^2)^0.5)")
  Call FormulaCalc("ch(20)          :=  ((ch(13)^2 + ch(14)^2 + ch(15)^2)^0.5)")



FFTINTERVUSER    ="NumberStartOverl"
FFTINTERVPARA(1) =1
FFTINTERVPARA(2) =131072
FFTINTERVPARA(3) =1
FFTINTERVOVERL   =0
FFTWNDFCT        ="Hanning"
FFTWNDPARA       =10
FFTWNDCHN        ="Time"
FFTWNDCORRECTTYP ="No"
FFTAVERAGETYPE   ="No"
FFTAMPLFIRST     ="Amplitude"
FFTAMPL          =1
FFTAMPLTYPE      ="Ampl.Peak"
FFTCALC          =0
FFTAMPLEXT       ="No"
FFTPHASE         =0
FFTCEPSTRUM      =0
Call CHNFFT1("Timek","1-15") '... X,CHNNOSTR



'Alte Berechnung von Frequenzen und Hüllkurven.
Call DATABLDEL("24-39",1,10)           '... CHNNOSTR,CHNROW,VALNO

Call CHNNORMALIZE("Ampl_Peak","FFT G1 x-axis ") '... Y,E
Call CHNNORMALIZE("Ampl_Peak1","FFT G1 y-axis") '... Y,E
Call CHNNORMALIZE("Ampl_Peak2","FFT G1 z-axis") '... Y,E
Call CHNNORMALIZE("Ampl_Peak3","FFT G2 x-axis") '... Y,E
Call CHNNORMALIZE("Ampl_Peak4","FFT G2 y-axis") '... Y,E
Call CHNNORMALIZE("Ampl_Peak5","FFT G2 z-axis") '... Y,E
Call CHNNORMALIZE("Ampl_Peak6","FFT G3 x-axis") '... Y,E
Call CHNNORMALIZE("Ampl_Peak7","FFT G3 y-axis") '... Y,E
Call CHNNORMALIZE("Ampl_Peak8","FFT G3 z-axis") '... Y,E
Call CHNNORMALIZE("Ampl_Peak9","FFT G4 x-axis") '... Y,E
Call CHNNORMALIZE("Ampl_Peak10","FFT G4 y-axis") '... Y,E
Call CHNNORMALIZE("Ampl_Peak11","FFT G4 z-axis") '... Y,E
Call CHNNORMALIZE("Ampl_Peak12","FFT G5 x-axis") '... Y,E
Call CHNNORMALIZE("Ampl_Peak13","FFT G5 y-axis") '... Y,E
Call CHNNORMALIZE("Ampl_Peak14","FFT G5 z-axis") '... Y,E

ChnName(16) = "G1-Vector"
ChnName(17) = "G2-Vector"
ChnName(18) = "G3-Vector"
ChnName(19) = "G4-Vector"
ChnName(20) = "G5-Vector"

Call CHNSMOOTH("G1-Vector","G1-Mean-Smooth",400,"maxNumber") '... Y,E,SMOOTHWIDTH,SMOOTHTYPE
Call CHNSMOOTH("G2-Vector","G2-Mean-Smooth",400,"maxNumber") '... Y,E,SMOOTHWIDTH,SMOOTHTYPE
Call CHNSMOOTH("G3-Vector","G3-Mean-Smooth",400,"maxNumber") '... Y,E,SMOOTHWIDTH,SMOOTHTYPE
Call CHNSMOOTH("G4-Vector","G4-Mean-Smooth",400,"maxNumber") '... Y,E,SMOOTHWIDTH,SMOOTHTYPE
Call CHNSMOOTH("G5-Vector","G5-Mean-Smooth",400,"maxNumber") '... Y,E,SMOOTHWIDTH,SMOOTHTYPE

Call CHNENVELOPES("Timek","G1-Vector","G1 Time Envelope","G1 Envelope","X_HüllMin","Y_HüllMin",0.7) '... X,Y,E,E,E,E,DXPEAK
Call CHNENVELOPES("Timek","G2-Vector","G2 Time Envelope","G2 Envelope","X_HüllMin1","Y_HüllMin1",0.7) '... X,Y,E,E,E,E,DXPEAK
Call CHNENVELOPES("Timek","G3-Vector","G3 Time Envelope","G3 Envelope","X_HüllMin2","Y_HüllMin2",0.7) '... X,Y,E,E,E,E,DXPEAK
Call CHNENVELOPES("Timek","G4-Vector","G4 Time Envelope","G4 Envelope","X_HüllMin3","Y_HüllMin3",0.7) '... X,Y,E,E,E,E,DXPEAK
Call CHNENVELOPES("Timek","G5-Vector","G5 Time Envelope","G5 Envelope","X_HüllMin4","Y_HüllMin4",0.7) '... X,Y,E,E,E,E,DXPEAK

Call CHNNORMALIZE("G1 Envelope","G1 Envelope Normalized") '... Y,E
Call CHNNORMALIZE("G2 Envelope","G2 Envelope Normalized") '... Y,E
Call CHNNORMALIZE("G3 Envelope","G3 Envelope Normalized") '... Y,E
Call CHNNORMALIZE("G4 Envelope","G4 Envelope Normalized") '... Y,E
Call CHNNORMALIZE("G5 Envelope","G5 Envelope Normalized") '... Y,E

     Call CHNRENUMBER()


Call CHNDELETE("25-39,62,63,66,67,70,71,74,75,78,79") '... CLPSOURCE

Call CHNMOVE(40,2,2)                  '... SOURCECHNINDEX,TARGETGROUPINDEX,TARGETCHNINDEX
Call CHNMOVE(41,2,4)                  '... SOURCECHNINDEX,TARGETGROUPINDEX,TARGETCHNINDEX
Call CHNMOVE(42,2,6)                  '... SOURCECHNINDEX,TARGETGROUPINDEX,TARGETCHNINDEX
Call CHNMOVE(43,2,8)                  '... SOURCECHNINDEX,TARGETGROUPINDEX,TARGETCHNINDEX
Call CHNMOVE(44,2,10)                 '... SOURCECHNINDEX,TARGETGROUPINDEX,TARGETCHNINDEX
Call CHNMOVE(45,2,3)                  '... SOURCECHNINDEX,TARGETGROUPINDEX,TARGETCHNINDEX
Call CHNMOVE(46,2,4)                  '... SOURCECHNINDEX,TARGETGROUPINDEX,TARGETCHNINDEX
Call CHNMOVE(47,2,7)                  '... SOURCECHNINDEX,TARGETGROUPINDEX,TARGETCHNINDEX
Call CHNMOVE(48,2,8)                  '... SOURCECHNINDEX,TARGETGROUPINDEX,TARGETCHNINDEX
Call CHNMOVE(49,2,11)                 '... SOURCECHNINDEX,TARGETGROUPINDEX,TARGETCHNINDEX
Call CHNMOVE(50,2,12)                 '... SOURCECHNINDEX,TARGETGROUPINDEX,TARGETCHNINDEX
Call CHNMOVE(51,2,15)                 '... SOURCECHNINDEX,TARGETGROUPINDEX,TARGETCHNINDEX
Call CHNMOVE(52,2,16)                 '... SOURCECHNINDEX,TARGETGROUPINDEX,TARGETCHNINDEX
Call CHNMOVE(53,2,19)                 '... SOURCECHNINDEX,TARGETGROUPINDEX,TARGETCHNINDEX
Call CHNMOVE(54,2,20)                 '... SOURCECHNINDEX,TARGETGROUPINDEX,TARGETCHNINDEX
Call CHNMOVE(55,2,5)                  '... SOURCECHNINDEX,TARGETGROUPINDEX,TARGETCHNINDEX
Call CHNMOVE(56,2,10)                 '... SOURCECHNINDEX,TARGETGROUPINDEX,TARGETCHNINDEX
Call CHNMOVE(57,2,11)                 '... SOURCECHNINDEX,TARGETGROUPINDEX,TARGETCHNINDEX
Call CHNMOVE(58,2,20)                 '... SOURCECHNINDEX,TARGETGROUPINDEX,TARGETCHNINDEX
Call CHNMOVE(57,2,15)                 '... SOURCECHNINDEX,TARGETGROUPINDEX,TARGETCHNINDEX
```

```
Call CHNMOVE(59,2,25)                   '... SOURCECHNINDEX,TARGETGROUPINDEX,TARGETCHNINDEX
Call CHNRENUMBER()



     Call CHNRENUMBER()

call ChnPeakFind("Frequenz","FFT G1 x-axis", 60, 61, 1, "Max.Peaks", "Amplitude")

call ChnPeakFind("Frequenz","FFT G1 y-axis", 62, 63, 1, "Max.Peaks", "Amplitude")
Call DATABLCLPCOPY("62,63",1,1)         '... CHNNOSTR,CHNROW,VALNO
Call DATABLCLPPASTE("60,61",2,0)        '... CHNNOSTR,CHNROW,VALNO
Call CHNDELETE("62,63")                 '... CLPSOURCE

call ChnPeakFind("Frequenz","FFT G1 z-axis", 62, 63, 1, "Max.Peaks", "Amplitude")
Call DATABLCLPCOPY("62,63",1,1)         '... CHNNOSTR,CHNROW,VALNO
Call DATABLCLPPASTE("60,61",3,0)        '... CHNNOSTR,CHNROW,VALNO
Call CHNDELETE("62,63")                 '... CLPSOURCE

call ChnPeakFind("Frequenz","FFT G2 x-axis", 62, 63, 1, "Max.Peaks", "Amplitude")
Call DATABLCLPCOPY("62,63",1,1)         '... CHNNOSTR,CHNROW,VALNO
Call DATABLCLPPASTE("60,61",4,0)        '... CHNNOSTR,CHNROW,VALNO
Call CHNDELETE("62,63")                 '... CLPSOURCE

call ChnPeakFind("Frequenz","FFT G2 y-axis", 62, 63, 1, "Max.Peaks", "Amplitude")
Call DATABLCLPCOPY("62,63",1,1)         '... CHNNOSTR,CHNROW,VALNO
Call DATABLCLPPASTE("60,61",5,0)        '... CHNNOSTR,CHNROW,VALNO
Call CHNDELETE("62,63")                 '... CLPSOURCE

call ChnPeakFind("Frequenz","FFT G2 z-axis", 62, 63, 1, "Max.Peaks", "Amplitude")
Call DATABLCLPCOPY("62,63",1,1)         '... CHNNOSTR,CHNROW,VALNO
Call DATABLCLPPASTE("60,61",6,0)        '... CHNNOSTR,CHNROW,VALNO
Call CHNDELETE("62,63")                 '... CLPSOURCE

call ChnPeakFind("Frequenz","FFT G3 x-axis", 62, 63, 1, "Max.Peaks", "Amplitude")
Call DATABLCLPCOPY("62,63",1,1)         '... CHNNOSTR,CHNROW,VALNO
Call DATABLCLPPASTE("60,61",7,0)        '... CHNNOSTR,CHNROW,VALNO
Call CHNDELETE("62,63")                 '... CLPSOURCE

call ChnPeakFind("Frequenz","FFT G3 y-axis", 62, 63, 1, "Max.Peaks", "Amplitude")
Call DATABLCLPCOPY("62,63",1,1)         '... CHNNOSTR,CHNROW,VALNO
Call DATABLCLPPASTE("60,61",8,0)        '... CHNNOSTR,CHNROW,VALNO
Call CHNDELETE("62,63")                 '... CLPSOURCE

call ChnPeakFind("Frequenz","FFT G3 z-axis", 62, 63, 1, "Max.Peaks", "Amplitude")
Call DATABLCLPCOPY("62,63",1,1)         '... CHNNOSTR,CHNROW,VALNO
Call DATABLCLPPASTE("60,61",9,0)        '... CHNNOSTR,CHNROW,VALNO
Call CHNDELETE("62,63")                 '... CLPSOURCE

call ChnPeakFind("Frequenz","FFT G4 x-axis", 62, 63, 1, "Max.Peaks", "Amplitude")
Call DATABLCLPCOPY("62,63",1,1)         '... CHNNOSTR,CHNROW,VALNO
Call DATABLCLPPASTE("60,61",10,0)        '... CHNNOSTR,CHNROW,VALNO
Call CHNDELETE("62,63")                 '... CLPSOURCE

call ChnPeakFind("Frequenz","FFT G4 y-axis", 62, 63, 1, "Max.Peaks", "Amplitude")
Call DATABLCLPCOPY("62,63",1,1)         '... CHNNOSTR,CHNROW,VALNO
Call DATABLCLPPASTE("60,61",11,0)        '... CHNNOSTR,CHNROW,VALNO
Call CHNDELETE("62,63")                 '... CLPSOURCE

call ChnPeakFind("Frequenz","FFT G4 z-axis", 62, 63, 1, "Max.Peaks", "Amplitude")
Call DATABLCLPCOPY("62,63",1,1)         '... CHNNOSTR,CHNROW,VALNO
Call DATABLCLPPASTE("60,61",12,0)        '... CHNNOSTR,CHNROW,VALNO
Call CHNDELETE("62,63")                 '... CLPSOURCE

call ChnPeakFind("Frequenz","FFT G5 x-axis", 62, 63, 1, "Max.Peaks", "Amplitude")
Call DATABLCLPCOPY("62,63",1,1)         '... CHNNOSTR,CHNROW,VALNO
Call DATABLCLPPASTE("60,61",13,0)        '... CHNNOSTR,CHNROW,VALNO
Call CHNDELETE("62,63")                 '... CLPSOURCE

call ChnPeakFind("Frequenz","FFT G5 y-axis", 62, 63, 1, "Max.Peaks", "Amplitude")
Call DATABLCLPCOPY("62,63",1,1)         '... CHNNOSTR,CHNROW,VALNO
Call DATABLCLPPASTE("60,61",14,0)        '... CHNNOSTR,CHNROW,VALNO
Call CHNDELETE("62,63")                 '... CLPSOURCE

call ChnPeakFind("Frequenz","FFT G5 z-axis", 62, 63, 1, "Max.Peaks", "Amplitude")
Call DATABLCLPCOPY("62,63",1,1)         '... CHNNOSTR,CHNROW,VALNO
Call DATABLCLPPASTE("60,61",15,0)        '... CHNNOSTR,CHNROW,VALNO
Call CHNDELETE("62,63")                 '... CLPSOURCE

Call CHNDELETE("61")                     '... CLPSOURCE


STATSEL(1)       ="No"
STATSEL(2)       ="No"
STATSEL(3)       ="No"
STATSEL(4)       ="Yes"
STATSEL(5)       ="Yes"
STATSEL(6)       ="Yes"
STATSEL(7)       ="Yes"
STATSEL(8)       ="No"
STATSEL(9)       ="No"
STATSEL(10)      ="No"
STATSEL(11)      ="No"
STATSEL(12)      ="No"
STATSEL(13)      ="No"
STATSEL(14)      ="Yes"
STATSEL(15)      ="Yes"
STATSEL(16)      ="No"
STATSEL(17)      ="No"
STATSEL(18)      ="No"
STATSEL(19)      ="No"
STATSEL(20)      ="No"
STATSEL(21)      ="No"
```

```
STATSEL(22)      ="No"
STATCLIPCOPY     =0
STATCLIPVALUE    =0
STATFORMAT       =""
Call STATBLOCKCALC("Channel","1-","1-16,21,26,31,36") '... STATDIREC,ROWNOSTR,CHNNOSTR
Call CHNMOVE(60,2,51)                  '... SOURCECHNINDEX,TARGETGROUPINDEX,TARGETCHNINDEX
Call CHNRENUMBER()
Call DATABLCLPCOPY("60-66",1,20)       '... CHNNOSTR,CHNROW,VALNO


  Call DATAFILEIMPORT("C:\Dokumente und Einstellungen\Egger\Eigene Dateien\Daten\Diploma Thesis\VAB\Rohdaten\65.dat","",0) '...
DATAFILENAME,FILEIMPORTFILTER,PARTIALMODE


Call CHNDELETE("67-97") '... CLPSOURCE

Call CHNRENUMBER()

  Call FormulaCalc("ch(67)           :=  (((ch(67)-0.2)/0.8)*300)")


ChnName(67) = "Power-RH"


Call CHNNORMALIZE("Power-RH","Power-Normalized") '... Y,E

Call CHNSMOOTH("Power-RH","Power-Mean-Smooth",400,"maxNumber") '... Y,E,SMOOTHWIDTH,SMOOTHTYPE

Call CHNENVELOPES("Timek","Power-RH","Power Time Envelope","Power Envelope","X_HüllMin","Y_HüllMin",0.7) '... X,Y,E,E,E,E,DXPEAK

Call CHNNORMALIZE("Power Envelope","Power Envelope Normalized") '... Y,E

Call CHNDELETE("72,73") '... CLPSOURCE

Call CHNRENUMBER()


STATSEL(1)       ="No"
STATSEL(2)       ="No"
STATSEL(3)       ="No"
STATSEL(4)       ="No"
STATSEL(5)       ="Yes"
STATSEL(6)       ="Yes"
STATSEL(7)       ="Yes"
STATSEL(8)       ="No"
STATSEL(9)       ="No"
STATSEL(10)      ="No"
STATSEL(11)      ="No"
STATSEL(12)      ="No"
STATSEL(13)      ="No"
STATSEL(14)      ="Yes"
STATSEL(15)      ="Yes"
STATSEL(16)      ="No"
STATSEL(17)      ="No"
STATSEL(18)      ="No"
STATSEL(19)      ="No"
STATSEL(20)      ="No"
STATSEL(21)      ="No"
STATSEL(22)      ="No"
STATCLIPCOPY     =0
STATCLIPVALUE    =0
STATFORMAT       =""
Call STATBLOCKCALC("Channel","1-","67") '... STATDIREC,ROWNOSTR,CHNNOSTR

Call DATABLCLPCOPY("73-77",1,1)       '... CHNNOSTR,CHNROW,VALNO
Call DATABLCLPPASTE("61-65",21,0)      '... CHNNOSTR,CHNROW,VALNO
Call CHNDELETE("73-77")               '... CLPSOURCE

Call DATABLCLPCOPY("60-66",1,21)       '... CHNNOSTR,CHNROW,VALNO


PRINTLEFTMARG    =1.5
PRINTTOPMARG     =1.5
PRINTWIDTH       =38.5
PRINTORIENT      ="landscape"
Call PICPRINT("WinPrint")              '... PRINTDEVICE



  ' Grafik anzeigen.
  Call PicUpdate

  ' Endmeldung anzeigen.
  Call MsgBoxDisp("Die Berechnung ist beendet.")

' Wenn Dialog abgebrochen wurde.
Else

  ' Meldung ausgeben.                                                    ' Wenn Abbruch
  Call MsgBoxDisp("Es wurde <Abbruch> ausgewählt! Das Script wird beendet.")
End If                                                  ' Meldung ausgeben.


' ------------------------------------------------------------------------------------
' PROZEDUREN
' ------------------------------------------------------------------------------------
' ------------------------------------------------------------------------------------
' Name:      UserDlg_Info
'
' Zweck:     Informationsdialog anzeigen.
```

```
'
' Parameter: Keine
' ------------------------------------------------------------------------------------------
Sub Info_Message
  T1 = "In folgendem Script werden die xyz Kanäle von 5 Geophonen  " & vbCRLF & _
       "analysiert. Schwinggeschwindigkeiten die geringer als das " & vbCRLF & _
       "Background noise sind identifiziert, zunächst durch NOVALUE ersetzt, " & vbCRLF & _
       "danach gelöscht und zusätzlich wird das Signal geglättet und eine  " & vbCRLF & _
       "Hüllkurve berechnet. Es werden weiters die resultierenden " & vbCRLF & _
       "Schwinggeschwindigkeiten berechnet, eine Frequenzanalyse wird" & vbCRLF & _
       "durchgeführt und statistische Kennwerte werden berechnet. "  & vbCRLF & vbCRLF & _
       "Achtung! Daten und Grafiklayout werden gelöscht!Wenn Sie Sichern möchten, betätigen Sie bitte <Abbruch>."
  Call MsgboxDisp(T1,"MB_OKCancel")
End Sub
```

APPENDIX 5

Script file from Diadem 8.1 Software for signal analysis from drill and blast development

```
' ------------------------------------------------------------------------------------------
' Name:             Blast_cutting1.vbs
'
' Ersteller:        Egger Florian
'
' Zweck:            Ground vibration measurements
'
' Beschreibung:     Eliminierung des Background noise und Berechnung von
'                   Kennwerten.
' ------------------------------------------------------------------------------------------
Option Explicit


' Script initialisieren.
' Anzeige des aktuell in Bearbeitung befindlichen Befehls unterdrücken.
AutoEcho = "No"

' Keine akustischen Signale ausgeben.
SoundActive = "No"


' ------------------------------------------------------------------------------------------
' HAUPTTEIL
' ------------------------------------------------------------------------------------------
' Informations-Dialog anzeigen.
Call Info_Message

' Falls 'Weiter' gewählt wurde, Script weiter ausführen.
If MsgState = "IDOk" Then

  ' Daten laden.
  Call DataDelAll(1)
  Call DATAFILEIMPORT("C:\Dokumente und Einstellungen\Egger\Eigene Dateien\Daten\Diploma Thesis\Erzberg2005\Sprengung6.dat","",0)
'... DATAFILENAME,FILEIMPORTFILTER,PARTIALMODE
  Call            DATAFILEIMPORT("C:\Dokumente           und           Einstellungen\Egger\Eigene           Dateien\Daten\Diploma
Thesis\VAB\Diademfiles\blast_cutting.TDM","",0) '... DATAFILENAME,FILEIMPORTFILTER,PARTIALMODE

T2 = "15/11/2005, No.6"
T3 = "Drill & Blast, Single Shot"
T4 = "Erzberg Mine"
T5 = "Research Area, MUL"
T6 = "Austria"

' Vorbereitetes Grafik-Layout laden.,
Call PICLOAD("C:\Dokumente und Einstellungen\Egger\Eigene Dateien\Daten\Diploma Thesis\VAB\Diademfiles\RGV_FFT_blast1.TDR") '...
PICFILE

Call DATABLDEL("1-40",1,12000)       '... CHNNOSTR,CHNROW,VALNO
Call DATABLDEL("41",138001,150000)       '... CHNNOSTR,CHNROW,VALNO


      Call CHNRENUMBER()

  Call FormulaCalc("ch(2)            :=  ch(2)/0.0288")
  Call FormulaCalc("ch(4)            :=  ch(4)/0.0288")
  Call FormulaCalc("ch(6)            :=  ch(6)/0.0288")
  Call FormulaCalc("ch(8)            :=  ch(8)/0.0288")
  Call FormulaCalc("ch(10)           :=  ch(10)/0.0288")
  Call FormulaCalc("ch(12)           :=  ch(12)/0.0288")
  Call FormulaCalc("ch(14)           :=  ch(14)/0.0288")
  Call FormulaCalc("ch(16)           :=  ch(16)/0.0288")
  Call FormulaCalc("ch(18)           :=  ch(18)/0.0288")
  Call FormulaCalc("ch(20)           :=  ch(20)/0.0288")
  Call FormulaCalc("ch(22)           :=  ch(22)/0.0288")
  Call FormulaCalc("ch(24)           :=  ch(24)/0.0288")
  Call FormulaCalc("ch(26)           :=  ch(26)/0.0288")
  Call FormulaCalc("ch(28)           :=  ch(28)/0.0288")
  Call FormulaCalc("ch(30)           :=  ch(30)/0.0288")

ChnName(2) = "G1 x-axis"
ChnName(4) = "G1 y-axis"
ChnName(6) = "G1 z-axis"
ChnName(8) = "G2 x-axis"
ChnName(10) = "G2 y-axis"
ChnName(12) = "G2 z-axis"
ChnName(14) = "G3 x-axis"
ChnName(16) = "G3 y-axis"
ChnName(18) = "G3 z-axis"
ChnName(20) = "G4 x-axis"
ChnName(22) = "G4 y-axis"
ChnName(24) = "G4 z-axis"
ChnName(26) = "G5 x-axis"
ChnName(28) = "G5 y-axis"
ChnName(30) = "G5 z-axis"


  Call FormulaCalc("ch(32)           :=  ((ch(2)^2 + ch(4)^2 + ch(6)^2)^0.5)")
  Call FormulaCalc("ch(34)           :=  ((ch(8)^2 + ch(10)^2 + ch(12)^2)^0.5)")
  Call FormulaCalc("ch(36)           :=  ((ch(14)^2 + ch(16)^2 + ch(18)^2)^0.5)")
```

```
  Call FormulaCalc("ch(38)          :=  ((ch(20)^2 + ch(22)^2 + ch(24)^2)^0.5)")
  Call FormulaCalc("ch(40)          :=  ((ch(26)^2 + ch(28)^2 + ch(30)^2)^0.5)")


STATSEL(1)       ="No"
STATSEL(2)       ="No"
STATSEL(3)       ="No"
STATSEL(4)       ="Yes"
STATSEL(5)       ="Yes"
STATSEL(6)       ="No"
STATSEL(7)       ="No"
STATSEL(8)       ="No"
STATSEL(9)       ="No"
STATSEL(10)      ="No"
STATSEL(11)      ="No"
STATSEL(12)      ="No"
STATSEL(13)      ="No"
STATSEL(14)      ="No"
STATSEL(15)      ="No"
STATSEL(16)      ="No"
STATSEL(17)      ="No"
STATSEL(18)      ="No"
STATSEL(19)      ="No"
STATSEL(20)      ="No"
STATSEL(21)      ="No"
STATSEL(22)      ="No"
STATCLIPCOPY     =0
STATCLIPVALUE    =0
STATFORMAT       =""

Call STATBLOCKCALC("Channel","1-3000","2,4,6,8,10,12,14,16,18,20,22,24,26,28,30,32,34,36,38,40") '... STATDIREC,ROWNOSTR,CHNNOSTR


  Call FormulaCalc("Ch('G1 x-axis Filtered') := Ch(2)+(Ch(2) >= Chd(1,44) and ch(2) <= Chd(1,45))*NoValue")
  Call FormulaCalc("Ch('G1 y-axis Filtered') := Ch(4)+(Ch(4) >= Chd(2,44) and ch(4) <= Chd(2,45))*NoValue")
  Call FormulaCalc("Ch('G1 z-axis Filtered') := Ch(6)+(Ch(6) >= Chd(3,44) and ch(6) <= Chd(3,45))*NoValue")
  Call FormulaCalc("Ch('G2 x-axis Filtered') := Ch(8)+(Ch(8) >= Chd(4,44) and ch(8) <= Chd(4,45))*NoValue")
  Call FormulaCalc("Ch('G2 y-axis Filtered') := Ch(10)+(Ch(10) >= Chd(5,44) and ch(10) <= Chd(5,45))*NoValue")
  Call FormulaCalc("Ch('G2 z-axis Filtered') := Ch(12)+(Ch(12) >= Chd(6,44) and ch(12) <= Chd(6,45))*NoValue")
  Call FormulaCalc("Ch('G3 x-axis Filtered') := Ch(14)+(Ch(14) >= Chd(7,44) and ch(14) <= Chd(7,45))*NoValue")
  Call FormulaCalc("Ch('G3 y-axis Filtered') := Ch(16)+(Ch(16) >= Chd(8,44) and ch(16) <= Chd(8,45))*NoValue")
  Call FormulaCalc("Ch('G3 z-axis Filtered') := Ch(18)+(Ch(18) >= Chd(9,44) and ch(18) <= Chd(9,45))*NoValue")
  Call FormulaCalc("Ch('G4 x-axis Filtered') := Ch(20)+(Ch(20) >= Chd(10,44) and ch(20) <= Chd(10,45))*NoValue")
  Call FormulaCalc("Ch('G4 y-axis Filtered') := Ch(22)+(Ch(22) >= Chd(11,44) and ch(22) <= Chd(11,45))*NoValue")
  Call FormulaCalc("Ch('G4 z-axis Filtered') := Ch(24)+(Ch(24) >= Chd(12,44) and ch(24) <= Chd(12,45))*NoValue")
  Call FormulaCalc("Ch('G5 x-axis Filtered') := Ch(26)+(Ch(26) >= Chd(13,44) and ch(26) <= Chd(13,45))*NoValue")
  Call FormulaCalc("Ch('G5 y-axis Filtered') := Ch(28)+(Ch(28) >= Chd(14,44) and ch(28) <= Chd(14,45))*NoValue")
  Call FormulaCalc("Ch('G5 z-axis Filtered') := Ch(30)+(Ch(30) >= Chd(15,44) and ch(30) <= Chd(15,45))*NoValue")
  Call FormulaCalc("Ch('G1 Filtered') := Ch(32)+(Ch(32) <= Chd(16,45))*NoValue")
  Call FormulaCalc("Ch('G2 Filtered') := Ch(34)+(Ch(34) <= Chd(17,45))*NoValue")
  Call FormulaCalc("Ch('G3 Filtered') := Ch(36)+(Ch(36) <= Chd(18,45))*NoValue")
  Call FormulaCalc("Ch('G4 Filtered') := Ch(38)+(Ch(38) <= Chd(19,45))*NoValue")
  Call FormulaCalc("Ch('G5 Filtered') := Ch(40)+(Ch(40) <= Chd(20,45))*NoValue")


' Funktion: NOVALUE-Interpolation

  Call ChnNovHandle(46,1, "Delete", "X", 1)
  Call ChnNovHandle(47,3, "Delete", "X", 1)
  Call ChnNovHandle(48,5, "Delete", "X", 1)
  Call ChnNovHandle(49,7, "Delete", "X", 1)
  Call ChnNovHandle(50,9, "Delete", "X", 1)
  Call ChnNovHandle(51,11, "Delete", "X", 1)
  Call ChnNovHandle(52,13, "Delete", "X", 1)
  Call ChnNovHandle(53,15, "Delete", "X", 1)
  Call ChnNovHandle(54,17, "Delete", "X", 1)
  Call ChnNovHandle(55,19, "Delete", "X", 1)
  Call ChnNovHandle(56,21, "Delete", "X", 1)
  Call ChnNovHandle(57,23, "Delete", "X", 1)
  Call ChnNovHandle(58,25, "Delete", "X", 1)
  Call ChnNovHandle(59,27, "Delete", "X", 1)
  Call ChnNovHandle(60,29, "Delete", "X", 1)
  Call ChnNovHandle(61,31, "Delete", "X", 1)
  Call ChnNovHandle(62,33, "Delete", "X", 1)
  Call ChnNovHandle(63,35, "Delete", "X", 1)
  Call ChnNovHandle(64,37, "Delete", "X", 1)
  Call ChnNovHandle(65,39, "Delete", "X", 1)

FFTINTERVUSER    ="NumberStartOverl"
FFTINTERVPARA(1) =1
FFTINTERVPARA(2) =131072
FFTINTERVPARA(3) =1
FFTINTERVOVERL   =0
FFTWNDFCT        ="Hanning"
FFTWNDPARA       =10
FFTWNDCHN        ="Time"
FFTWNDCORRECTTYP ="No"
FFTAVERAGETYPE   ="No"
FFTAMPLFIRST     ="Amplitude"
FFTAMPL          =1
FFTAMPLTYPE      ="Ampl.Peak"
FFTCALC          =0
FFTAMPLEXT       ="No"
FFTPHASE         =0
FFTCEPSTRUM      =0
Call CHNFFT1("Timek","2,4,6,8,10,12,14,16,18,20,22,24,26,28,30") '... X,CHNNOSTR


  Call FormulaCalc("ch(1) := ch('timek')")
  Call FormulaCalc("ch(3) := ch('timek')")
  Call FormulaCalc("ch(5) := ch('timek')")
  Call FormulaCalc("ch(7) := ch('timek')")
```

```
  Call FormulaCalc("ch(9) := ch('timek')")
  Call FormulaCalc("ch(11) := ch('timek')")
  Call FormulaCalc("ch(13) := ch('timek')")
  Call FormulaCalc("ch(15) := ch('timek')")
  Call FormulaCalc("ch(17) := ch('timek')")
  Call FormulaCalc("ch(19) := ch('timek')")
  Call FormulaCalc("ch(21) := ch('timek')")
  Call FormulaCalc("ch(23) := ch('timek')")
  Call FormulaCalc("ch(25) := ch('timek')")
  Call FormulaCalc("ch(27) := ch('timek')")
  Call FormulaCalc("ch(29) := ch('timek')")
  Call FormulaCalc("ch(31) := ch('timek')")
  Call FormulaCalc("ch(33) := ch('timek')")
  Call FormulaCalc("ch(35) := ch('timek')")
  Call FormulaCalc("ch(37) := ch('timek')")
  Call FormulaCalc("ch(39) := ch('timek')")

  ChnLength(1)=ChnLength(46)
  ChnLength(3)=ChnLength(47)
  ChnLength(5)=ChnLength(48)
  ChnLength(7)=ChnLength(49)
  ChnLength(9)=ChnLength(50)
  ChnLength(11)=ChnLength(51)
  ChnLength(13)=ChnLength(52)
  ChnLength(15)=ChnLength(53)
  ChnLength(17)=ChnLength(54)
  ChnLength(19)=ChnLength(55)
  ChnLength(21)=ChnLength(56)
  ChnLength(23)=ChnLength(57)
  ChnLength(25)=ChnLength(58)
  ChnLength(27)=ChnLength(59)
  ChnLength(29)=ChnLength(60)
  ChnLength(31)=ChnLength(61)
  ChnLength(33)=ChnLength(62)
  ChnLength(35)=ChnLength(63)
  ChnLength(37)=ChnLength(64)
  ChnLength(39)=ChnLength(65)

Call CHNMOVE(1,2,16)                    '... SOURCECHNINDEX,TARGETGROUPINDEX,TARGETCHNINDEX
Call CHNMOVE(3,2,18)                    '... SOURCECHNINDEX,TARGETGROUPINDEX,TARGETCHNINDEX
Call CHNMOVE(5,2,20)                    '... SOURCECHNINDEX,TARGETGROUPINDEX,TARGETCHNINDEX
Call CHNMOVE(7,2,22)                    '... SOURCECHNINDEX,TARGETGROUPINDEX,TARGETCHNINDEX
Call CHNMOVE(9,2,24)                    '... SOURCECHNINDEX,TARGETGROUPINDEX,TARGETCHNINDEX
Call CHNMOVE(11,2,26)                   '... SOURCECHNINDEX,TARGETGROUPINDEX,TARGETCHNINDEX
Call CHNMOVE(13,2,28)                   '... SOURCECHNINDEX,TARGETGROUPINDEX,TARGETCHNINDEX
Call CHNMOVE(15,2,30)                   '... SOURCECHNINDEX,TARGETGROUPINDEX,TARGETCHNINDEX
Call CHNMOVE(17,2,32)                   '... SOURCECHNINDEX,TARGETGROUPINDEX,TARGETCHNINDEX
Call CHNMOVE(19,2,34)                   '... SOURCECHNINDEX,TARGETGROUPINDEX,TARGETCHNINDEX
Call CHNMOVE(21,2,36)                   '... SOURCECHNINDEX,TARGETGROUPINDEX,TARGETCHNINDEX
Call CHNMOVE(23,2,38)                   '... SOURCECHNINDEX,TARGETGROUPINDEX,TARGETCHNINDEX
Call CHNMOVE(25,2,40)                   '... SOURCECHNINDEX,TARGETGROUPINDEX,TARGETCHNINDEX
Call CHNMOVE(27,2,42)                   '... SOURCECHNINDEX,TARGETGROUPINDEX,TARGETCHNINDEX
Call CHNMOVE(29,2,44)                   '... SOURCECHNINDEX,TARGETGROUPINDEX,TARGETCHNINDEX

Call CHNMOVE(32,1,16)                   '... SOURCECHNINDEX,TARGETGROUPINDEX,TARGETCHNINDEX
Call CHNMOVE(34,1,17)                   '... SOURCECHNINDEX,TARGETGROUPINDEX,TARGETCHNINDEX
Call CHNMOVE(36,1,18)                   '... SOURCECHNINDEX,TARGETGROUPINDEX,TARGETCHNINDEX
Call CHNMOVE(38,1,19)                   '... SOURCECHNINDEX,TARGETGROUPINDEX,TARGETCHNINDEX
Call CHNMOVE(40,1,20)                   '... SOURCECHNINDEX,TARGETGROUPINDEX,TARGETCHNINDEX
Call CHNMOVE(41,1,21)                   '... SOURCECHNINDEX,TARGETGROUPINDEX,TARGETCHNINDEX
Call CHNMOVE(31,2,40)                   '... SOURCECHNINDEX,TARGETGROUPINDEX,TARGETCHNINDEX
Call CHNMOVE(33,2,40)                   '... SOURCECHNINDEX,TARGETGROUPINDEX,TARGETCHNINDEX
Call CHNMOVE(31,2,38)                   '... SOURCECHNINDEX,TARGETGROUPINDEX,TARGETCHNINDEX
Call CHNMOVE(35,2,41)                   '... SOURCECHNINDEX,TARGETGROUPINDEX,TARGETCHNINDEX
Call CHNMOVE(37,2,42)                   '... SOURCECHNINDEX,TARGETGROUPINDEX,TARGETCHNINDEX
Call CHNMOVE(39,2,43)                   '... SOURCECHNINDEX,TARGETGROUPINDEX,TARGETCHNINDEX
Call CHNMOVE(42,1,22)                   '... SOURCECHNINDEX,TARGETGROUPINDEX,TARGETCHNINDEX
Call CHNMOVE(43,1,23)                   '... SOURCECHNINDEX,TARGETGROUPINDEX,TARGETCHNINDEX
Call CHNMOVE(44,1,24)                   '... SOURCECHNINDEX,TARGETGROUPINDEX,TARGETCHNINDEX
Call CHNMOVE(45,1,25)                   '... SOURCECHNINDEX,TARGETGROUPINDEX,TARGETCHNINDEX
Call GROUPMOVE(2,1)                     '... SOURCEGROUPINDEX,TARGETGROUPINDEX


Call CHNRENUMBER()

'Alte Berechnung von Frequenzen und Hüllkurven.

STATSEL(1)       ="No"
STATSEL(2)       ="No"
STATSEL(3)       ="No"
STATSEL(4)       ="Yes"
STATSEL(5)       ="Yes"
STATSEL(6)       ="Yes"
STATSEL(7)       ="Yes"
STATSEL(8)       ="No"
STATSEL(9)       ="No"
STATSEL(10)      ="No"
STATSEL(11)      ="No"
STATSEL(12)      ="No"
STATSEL(13)      ="No"
STATSEL(14)      ="Yes"
STATSEL(15)      ="Yes"
STATSEL(16)      ="No"
STATSEL(17)      ="No"
STATSEL(18)      ="No"
STATSEL(19)      ="No"
STATSEL(20)      ="No"
STATSEL(21)      ="No"
STATSEL(22)      ="No"
STATCLIPCOPY     =0
STATCLIPVALUE    =0
STATFORMAT       =""
Call STATBLOCKCALC("Channel","1-","2") '... STATDIREC,ROWNOSTR,CHNNOSTR
```

```
STATSEL(1)       ="No"
STATSEL(2)       ="No"
STATSEL(3)       ="No"
STATSEL(4)       ="Yes"
STATSEL(5)       ="Yes"
STATSEL(6)       ="Yes"
STATSEL(7)       ="Yes"
STATSEL(8)       ="No"
STATSEL(9)       ="No"
STATSEL(10)      ="No"
STATSEL(11)      ="No"
STATSEL(12)      ="No"
STATSEL(13)      ="No"
STATSEL(14)      ="Yes"
STATSEL(15)      ="Yes"
STATSEL(16)      ="No"
STATSEL(17)      ="No"
STATSEL(18)      ="No"
STATSEL(19)      ="No"
STATSEL(20)      ="No"
STATSEL(21)      ="No"
STATSEL(22)      ="No"
STATCLIPCOPY     =0
STATCLIPVALUE    =0
STATFORMAT       =""
Call STATBLOCKCALC("Channel","1-","4")  '... STATDIREC,ROWNOSTR,CHNNOSTR
Call DATABLCLPCOPY("88-93",1,1)         '... CHNNOSTR,CHNROW,VALNO
Call DATABLCLPPASTE("82-87",2,0)        '... CHNNOSTR,CHNROW,VALNO
Call CHNDELETE("88-93")                 '... CLPSOURCE

STATSEL(1)       ="No"
STATSEL(2)       ="No"
STATSEL(3)       ="No"
STATSEL(4)       ="Yes"
STATSEL(5)       ="Yes"
STATSEL(6)       ="Yes"
STATSEL(7)       ="Yes"
STATSEL(8)       ="No"
STATSEL(9)       ="No"
STATSEL(10)      ="No"
STATSEL(11)      ="No"
STATSEL(12)      ="No"
STATSEL(13)      ="No"
STATSEL(14)      ="Yes"
STATSEL(15)      ="Yes"
STATSEL(16)      ="No"
STATSEL(17)      ="No"
STATSEL(18)      ="No"
STATSEL(19)      ="No"
STATSEL(20)      ="No"
STATSEL(21)      ="No"
STATSEL(22)      ="No"
STATCLIPCOPY     =0
STATCLIPVALUE    =0
STATFORMAT       =""
Call STATBLOCKCALC("Channel","1-","6")  '... STATDIREC,ROWNOSTR,CHNNOSTR
Call DATABLCLPCOPY("88-93",1,1)         '... CHNNOSTR,CHNROW,VALNO
Call DATABLCLPPASTE("82-87",3,0)        '... CHNNOSTR,CHNROW,VALNO
Call CHNDELETE("88-93")                 '... CLPSOURCE

STATSEL(1)       ="No"
STATSEL(2)       ="No"
STATSEL(3)       ="No"
STATSEL(4)       ="Yes"
STATSEL(5)       ="Yes"
STATSEL(6)       ="Yes"
STATSEL(7)       ="Yes"
STATSEL(8)       ="No"
STATSEL(9)       ="No"
STATSEL(10)      ="No"
STATSEL(11)      ="No"
STATSEL(12)      ="No"
STATSEL(13)      ="No"
STATSEL(14)      ="Yes"
STATSEL(15)      ="Yes"
STATSEL(16)      ="No"
STATSEL(17)      ="No"
STATSEL(18)      ="No"
STATSEL(19)      ="No"
STATSEL(20)      ="No"
STATSEL(21)      ="No"
STATSEL(22)      ="No"
STATCLIPCOPY     =0
STATCLIPVALUE    =0
STATFORMAT       =""
Call STATBLOCKCALC("Channel","1-","8")  '... STATDIREC,ROWNOSTR,CHNNOSTR
Call DATABLCLPCOPY("88-93",1,1)         '... CHNNOSTR,CHNROW,VALNO
Call DATABLCLPPASTE("82-87",4,0)        '... CHNNOSTR,CHNROW,VALNO
Call CHNDELETE("88-93")                 '... CLPSOURCE

STATSEL(1)       ="No"
STATSEL(2)       ="No"
STATSEL(3)       ="No"
STATSEL(4)       ="Yes"
STATSEL(5)       ="Yes"
STATSEL(6)       ="Yes"
STATSEL(7)       ="Yes"
STATSEL(8)       ="No"
STATSEL(9)       ="No"
STATSEL(10)      ="No"
STATSEL(11)      ="No"
STATSEL(12)      ="No"
```

```
STATSEL(13)      ="No"
STATSEL(14)      ="Yes"
STATSEL(15)      ="Yes"
STATSEL(16)      ="No"
STATSEL(17)      ="No"
STATSEL(18)      ="No"
STATSEL(19)      ="No"
STATSEL(20)      ="No"
STATSEL(21)      ="No"
STATSEL(22)      ="No"
STATCLIPCOPY     =0
STATCLIPVALUE    =0
STATFORMAT       =""
Call STATBLOCKCALC("Channel","1-","10")  '... STATDIREC,ROWNOSTR,CHNNOSTR
Call DATABLCLPCOPY("88-93",1,1)          '... CHNNOSTR,CHNROW,VALNO
Call DATABLCLPPASTE("82-87",5,0)         '... CHNNOSTR,CHNROW,VALNO
Call CHNDELETE("88-93")                  '... CLPSOURCE

STATSEL(1)       ="No"
STATSEL(2)       ="No"
STATSEL(3)       ="No"
STATSEL(4)       ="Yes"
STATSEL(5)       ="Yes"
STATSEL(6)       ="Yes"
STATSEL(7)       ="Yes"
STATSEL(8)       ="No"
STATSEL(9)       ="No"
STATSEL(10)      ="No"
STATSEL(11)      ="No"
STATSEL(12)      ="No"
STATSEL(13)      ="No"
STATSEL(14)      ="Yes"
STATSEL(15)      ="Yes"
STATSEL(16)      ="No"
STATSEL(17)      ="No"
STATSEL(18)      ="No"
STATSEL(19)      ="No"
STATSEL(20)      ="No"
STATSEL(21)      ="No"
STATSEL(22)      ="No"
STATCLIPCOPY     =0
STATCLIPVALUE    =0
STATFORMAT       =""
Call STATBLOCKCALC("Channel","1-","12")  '... STATDIREC,ROWNOSTR,CHNNOSTR
Call DATABLCLPCOPY("88-93",1,1)          '... CHNNOSTR,CHNROW,VALNO
Call DATABLCLPPASTE("82-87",6,0)         '... CHNNOSTR,CHNROW,VALNO
Call CHNDELETE("88-93")                  '... CLPSOURCE


STATSEL(1)       ="No"
STATSEL(2)       ="No"
STATSEL(3)       ="No"
STATSEL(4)       ="Yes"
STATSEL(5)       ="Yes"
STATSEL(6)       ="Yes"
STATSEL(7)       ="Yes"
STATSEL(8)       ="No"
STATSEL(9)       ="No"
STATSEL(10)      ="No"
STATSEL(11)      ="No"
STATSEL(12)      ="No"
STATSEL(13)      ="No"
STATSEL(14)      ="Yes"
STATSEL(15)      ="Yes"
STATSEL(16)      ="No"
STATSEL(17)      ="No"
STATSEL(18)      ="No"
STATSEL(19)      ="No"
STATSEL(20)      ="No"
STATSEL(21)      ="No"
STATSEL(22)      ="No"
STATCLIPCOPY     =0
STATCLIPVALUE    =0
STATFORMAT       =""
Call STATBLOCKCALC("Channel","1-","14")  '... STATDIREC,ROWNOSTR,CHNNOSTR
Call DATABLCLPCOPY("88-93",1,1)          '... CHNNOSTR,CHNROW,VALNO
Call DATABLCLPPASTE("82-87",7,0)         '... CHNNOSTR,CHNROW,VALNO
Call CHNDELETE("88-93")                  '... CLPSOURCE

STATSEL(1)       ="No"
STATSEL(2)       ="No"
STATSEL(3)       ="No"
STATSEL(4)       ="Yes"
STATSEL(5)       ="Yes"
STATSEL(6)       ="Yes"
STATSEL(7)       ="Yes"
STATSEL(8)       ="No"
STATSEL(9)       ="No"
STATSEL(10)      ="No"
STATSEL(11)      ="No"
STATSEL(12)      ="No"
STATSEL(13)      ="No"
STATSEL(14)      ="Yes"
STATSEL(15)      ="Yes"
STATSEL(16)      ="No"
STATSEL(17)      ="No"
STATSEL(18)      ="No"
STATSEL(19)      ="No"
STATSEL(20)      ="No"
STATSEL(21)      ="No"
STATSEL(22)      ="No"
STATCLIPCOPY     =0
STATCLIPVALUE    =0
```

```
STATFORMAT       =""
Call STATBLOCKCALC("Channel","1-","16")  '... STATDIREC,ROWNOSTR,CHNNOSTR
Call DATABLCLPCOPY("88-93",1,1)          '... CHNNOSTR,CHNROW,VALNO
Call DATABLCLPPASTE("82-87",8,0)         '... CHNNOSTR,CHNROW,VALNO
Call CHNDELETE("88-93")                  '... CLPSOURCE

STATSEL(1)       ="No"
STATSEL(2)       ="No"
STATSEL(3)       ="No"
STATSEL(4)       ="Yes"
STATSEL(5)       ="Yes"
STATSEL(6)       ="Yes"
STATSEL(7)       ="Yes"
STATSEL(8)       ="No"
STATSEL(9)       ="No"
STATSEL(10)      ="No"
STATSEL(11)      ="No"
STATSEL(12)      ="No"
STATSEL(13)      ="No"
STATSEL(14)      ="Yes"
STATSEL(15)      ="Yes"
STATSEL(16)      ="No"
STATSEL(17)      ="No"
STATSEL(18)      ="No"
STATSEL(19)      ="No"
STATSEL(20)      ="No"
STATSEL(21)      ="No"
STATSEL(22)      ="No"
STATCLIPCOPY     =0
STATCLIPVALUE    =0
STATFORMAT       =""
Call STATBLOCKCALC("Channel","1-","18")  '... STATDIREC,ROWNOSTR,CHNNOSTR
Call DATABLCLPCOPY("88-93",1,1)          '... CHNNOSTR,CHNROW,VALNO
Call DATABLCLPPASTE("82-87",9,0)         '... CHNNOSTR,CHNROW,VALNO
Call CHNDELETE("88-93")                  '... CLPSOURCE

STATSEL(1)       ="No"
STATSEL(2)       ="No"
STATSEL(3)       ="No"
STATSEL(4)       ="Yes"
STATSEL(5)       ="Yes"
STATSEL(6)       ="Yes"
STATSEL(7)       ="Yes"
STATSEL(8)       ="No"
STATSEL(9)       ="No"
STATSEL(10)      ="No"
STATSEL(11)      ="No"
STATSEL(12)      ="No"
STATSEL(13)      ="No"
STATSEL(14)      ="Yes"
STATSEL(15)      ="Yes"
STATSEL(16)      ="No"
STATSEL(17)      ="No"
STATSEL(18)      ="No"
STATSEL(19)      ="No"
STATSEL(20)      ="No"
STATSEL(21)      ="No"
STATSEL(22)      ="No"
STATCLIPCOPY     =0
STATCLIPVALUE    =0
STATFORMAT       =""
Call STATBLOCKCALC("Channel","1-","20")  '... STATDIREC,ROWNOSTR,CHNNOSTR
Call DATABLCLPCOPY("88-93",1,1)          '... CHNNOSTR,CHNROW,VALNO
Call DATABLCLPPASTE("82-87",10,0)         '... CHNNOSTR,CHNROW,VALNO
Call CHNDELETE("88-93")                  '... CLPSOURCE


STATSEL(1)       ="No"
STATSEL(2)       ="No"
STATSEL(3)       ="No"
STATSEL(4)       ="Yes"
STATSEL(5)       ="Yes"
STATSEL(6)       ="Yes"
STATSEL(7)       ="Yes"
STATSEL(8)       ="No"
STATSEL(9)       ="No"
STATSEL(10)      ="No"
STATSEL(11)      ="No"
STATSEL(12)      ="No"
STATSEL(13)      ="No"
STATSEL(14)      ="Yes"
STATSEL(15)      ="Yes"
STATSEL(16)      ="No"
STATSEL(17)      ="No"
STATSEL(18)      ="No"
STATSEL(19)      ="No"
STATSEL(20)      ="No"
STATSEL(21)      ="No"
STATSEL(22)      ="No"
STATCLIPCOPY     =0
STATCLIPVALUE    =0
STATFORMAT       =""
Call STATBLOCKCALC("Channel","1-","22")  '... STATDIREC,ROWNOSTR,CHNNOSTR
Call DATABLCLPCOPY("88-93",1,1)          '... CHNNOSTR,CHNROW,VALNO
Call DATABLCLPPASTE("82-87",11,0)         '... CHNNOSTR,CHNROW,VALNO
Call CHNDELETE("88-93")                  '... CLPSOURCE


STATSEL(1)       ="No"
STATSEL(2)       ="No"
STATSEL(3)       ="No"
STATSEL(4)       ="Yes"
STATSEL(5)       ="Yes"
```

```
STATSEL(6)       ="Yes"
STATSEL(7)       ="Yes"
STATSEL(8)       ="No"
STATSEL(9)       ="No"
STATSEL(10)      ="No"
STATSEL(11)      ="No"
STATSEL(12)      ="No"
STATSEL(13)      ="No"
STATSEL(14)      ="Yes"
STATSEL(15)      ="Yes"
STATSEL(16)      ="No"
STATSEL(17)      ="No"
STATSEL(18)      ="No"
STATSEL(19)      ="No"
STATSEL(20)      ="No"
STATSEL(21)      ="No"
STATSEL(22)      ="No"
STATCLIPCOPY     =0
STATCLIPVALUE    =0
STATFORMAT       =""
Call STATBLOCKCALC("Channel","1-","24")  '... STATDIREC,ROWNOSTR,CHNNOSTR
Call DATABLCLPCOPY("88-93",1,1)          '... CHNNOSTR,CHNROW,VALNO
Call DATABLCLPPASTE("82-87",12,0)         '... CHNNOSTR,CHNROW,VALNO
Call CHNDELETE("88-93")                  '... CLPSOURCE

STATSEL(1)       ="No"
STATSEL(2)       ="No"
STATSEL(3)       ="No"
STATSEL(4)       ="Yes"
STATSEL(5)       ="Yes"
STATSEL(6)       ="Yes"
STATSEL(7)       ="Yes"
STATSEL(8)       ="No"
STATSEL(9)       ="No"
STATSEL(10)      ="No"
STATSEL(11)      ="No"
STATSEL(12)      ="No"
STATSEL(13)      ="No"
STATSEL(14)      ="Yes"
STATSEL(15)      ="Yes"
STATSEL(16)      ="No"
STATSEL(17)      ="No"
STATSEL(18)      ="No"
STATSEL(19)      ="No"
STATSEL(20)      ="No"
STATSEL(21)      ="No"
STATSEL(22)      ="No"
STATCLIPCOPY     =0
STATCLIPVALUE    =0
STATFORMAT       =""
Call STATBLOCKCALC("Channel","1-","26")  '... STATDIREC,ROWNOSTR,CHNNOSTR
Call DATABLCLPCOPY("88-93",1,1)          '... CHNNOSTR,CHNROW,VALNO
Call DATABLCLPPASTE("82-87",13,0)         '... CHNNOSTR,CHNROW,VALNO
Call CHNDELETE("88-93")                  '... CLPSOURCE

STATSEL(1)       ="No"
STATSEL(2)       ="No"
STATSEL(3)       ="No"
STATSEL(4)       ="Yes"
STATSEL(5)       ="Yes"
STATSEL(6)       ="Yes"
STATSEL(7)       ="Yes"
STATSEL(8)       ="No"
STATSEL(9)       ="No"
STATSEL(10)      ="No"
STATSEL(11)      ="No"
STATSEL(12)      ="No"
STATSEL(13)      ="No"
STATSEL(14)      ="Yes"
STATSEL(15)      ="Yes"
STATSEL(16)      ="No"
STATSEL(17)      ="No"
STATSEL(18)      ="No"
STATSEL(19)      ="No"
STATSEL(20)      ="No"
STATSEL(21)      ="No"
STATSEL(22)      ="No"
STATCLIPCOPY     =0
STATCLIPVALUE    =0
STATFORMAT       =""
Call STATBLOCKCALC("Channel","1-","28")  '... STATDIREC,ROWNOSTR,CHNNOSTR
Call DATABLCLPCOPY("88-93",1,1)          '... CHNNOSTR,CHNROW,VALNO
Call DATABLCLPPASTE("82-87",14,0)         '... CHNNOSTR,CHNROW,VALNO
Call CHNDELETE("88-93")                  '... CLPSOURCE

STATSEL(1)       ="No"
STATSEL(2)       ="No"
STATSEL(3)       ="No"
STATSEL(4)       ="Yes"
STATSEL(5)       ="Yes"
STATSEL(6)       ="Yes"
STATSEL(7)       ="Yes"
STATSEL(8)       ="No"
STATSEL(9)       ="No"
STATSEL(10)      ="No"
STATSEL(11)      ="No"
STATSEL(12)      ="No"
STATSEL(13)      ="No"
STATSEL(14)      ="Yes"
STATSEL(15)      ="Yes"
STATSEL(16)      ="No"
STATSEL(17)      ="No"
STATSEL(18)      ="No"
```

```
STATSEL(19)      ="No"
STATSEL(20)      ="No"
STATSEL(21)      ="No"
STATSEL(22)      ="No"
STATCLIPCOPY     =0
STATCLIPVALUE    =0
STATFORMAT       =""
Call STATBLOCKCALC("Channel","1-","30")  '... STATDIREC,ROWNOSTR,CHNNOSTR
Call DATABLCLPCOPY("88-93",1,1)          '... CHNNOSTR,CHNROW,VALNO
Call DATABLCLPPASTE("82-87",15,0)        '... CHNNOSTR,CHNROW,VALNO
Call CHNDELETE("88-93")                  '... CLPSOURCE

STATSEL(1)       ="No"
STATSEL(2)       ="No"
STATSEL(3)       ="No"
STATSEL(4)       ="Yes"
STATSEL(5)       ="Yes"
STATSEL(6)       ="Yes"
STATSEL(7)       ="Yes"
STATSEL(8)       ="No"
STATSEL(9)       ="No"
STATSEL(10)      ="No"
STATSEL(11)      ="No"
STATSEL(12)      ="No"
STATSEL(13)      ="No"
STATSEL(14)      ="Yes"
STATSEL(15)      ="Yes"
STATSEL(16)      ="No"
STATSEL(17)      ="No"
STATSEL(18)      ="No"
STATSEL(19)      ="No"
STATSEL(20)      ="No"
STATSEL(21)      ="No"
STATSEL(22)      ="No"
STATCLIPCOPY     =0
STATCLIPVALUE    =0
STATFORMAT       =""
Call STATBLOCKCALC("Channel","1-","32")  '... STATDIREC,ROWNOSTR,CHNNOSTR
Call DATABLCLPCOPY("88-93",1,1)          '... CHNNOSTR,CHNROW,VALNO
Call DATABLCLPPASTE("82-87",16,0)        '... CHNNOSTR,CHNROW,VALNO
Call CHNDELETE("88-93")                  '... CLPSOURCE

STATSEL(1)       ="No"
STATSEL(2)       ="No"
STATSEL(3)       ="No"
STATSEL(4)       ="Yes"
STATSEL(5)       ="Yes"
STATSEL(6)       ="Yes"
STATSEL(7)       ="Yes"
STATSEL(8)       ="No"
STATSEL(9)       ="No"
STATSEL(10)      ="No"
STATSEL(11)      ="No"
STATSEL(12)      ="No"
STATSEL(13)      ="No"
STATSEL(14)      ="Yes"
STATSEL(15)      ="Yes"
STATSEL(16)      ="No"
STATSEL(17)      ="No"
STATSEL(18)      ="No"
STATSEL(19)      ="No"
STATSEL(20)      ="No"
STATSEL(21)      ="No"
STATSEL(22)      ="No"
STATCLIPCOPY     =0
STATCLIPVALUE    =0
STATFORMAT       =""
Call STATBLOCKCALC("Channel","1-","34")  '... STATDIREC,ROWNOSTR,CHNNOSTR
Call DATABLCLPCOPY("88-93",1,1)          '... CHNNOSTR,CHNROW,VALNO
Call DATABLCLPPASTE("82-87",17,0)        '... CHNNOSTR,CHNROW,VALNO
Call CHNDELETE("88-93")                  '... CLPSOURCE

STATSEL(1)       ="No"
STATSEL(2)       ="No"
STATSEL(3)       ="No"
STATSEL(4)       ="Yes"
STATSEL(5)       ="Yes"
STATSEL(6)       ="Yes"
STATSEL(7)       ="Yes"
STATSEL(8)       ="No"
STATSEL(9)       ="No"
STATSEL(10)      ="No"
STATSEL(11)      ="No"
STATSEL(12)      ="No"
STATSEL(13)      ="No"
STATSEL(14)      ="Yes"
STATSEL(15)      ="Yes"
STATSEL(16)      ="No"
STATSEL(17)      ="No"
STATSEL(18)      ="No"
STATSEL(19)      ="No"
STATSEL(20)      ="No"
STATSEL(21)      ="No"
STATSEL(22)      ="No"
STATCLIPCOPY     =0
STATCLIPVALUE    =0
STATFORMAT       =""
Call STATBLOCKCALC("Channel","1-","36")  '... STATDIREC,ROWNOSTR,CHNNOSTR
Call DATABLCLPCOPY("88-93",1,1)          '... CHNNOSTR,CHNROW,VALNO
Call DATABLCLPPASTE("82-87",18,0)        '... CHNNOSTR,CHNROW,VALNO
Call CHNDELETE("88-93")                  '... CLPSOURCE
```

```
STATSEL(1)       ="No"
STATSEL(2)       ="No"
STATSEL(3)       ="No"
STATSEL(4)       ="Yes"
STATSEL(5)       ="Yes"
STATSEL(6)       ="Yes"
STATSEL(7)       ="Yes"
STATSEL(8)       ="No"
STATSEL(9)       ="No"
STATSEL(10)      ="No"
STATSEL(11)      ="No"
STATSEL(12)      ="No"
STATSEL(13)      ="No"
STATSEL(14)      ="Yes"
STATSEL(15)      ="Yes"
STATSEL(16)      ="No"
STATSEL(17)      ="No"
STATSEL(18)      ="No"
STATSEL(19)      ="No"
STATSEL(20)      ="No"
STATSEL(21)      ="No"
STATSEL(22)      ="No"
STATCLIPCOPY     =0
STATCLIPVALUE    =0
STATFORMAT       =""
Call STATBLOCKCALC("Channel","1-","38")  '... STATDIREC,ROWNOSTR,CHNNOSTR
Call DATABLCLPCOPY("88-93",1,1)         '... CHNNOSTR,CHNROW,VALNO
Call DATABLCLPPASTE("82-87",19,0)        '... CHNNOSTR,CHNROW,VALNO
Call CHNDELETE("88-93")                 '... CLPSOURCE

STATSEL(1)       ="No"
STATSEL(2)       ="No"
STATSEL(3)       ="No"
STATSEL(4)       ="Yes"
STATSEL(5)       ="Yes"
STATSEL(6)       ="Yes"
STATSEL(7)       ="Yes"
STATSEL(8)       ="No"
STATSEL(9)       ="No"
STATSEL(10)      ="No"
STATSEL(11)      ="No"
STATSEL(12)      ="No"
STATSEL(13)      ="No"
STATSEL(14)      ="Yes"
STATSEL(15)      ="Yes"
STATSEL(16)      ="No"
STATSEL(17)      ="No"
STATSEL(18)      ="No"
STATSEL(19)      ="No"
STATSEL(20)      ="No"
STATSEL(21)      ="No"
STATSEL(22)      ="No"
STATCLIPCOPY     =0
STATCLIPVALUE    =0
STATFORMAT       =""
Call STATBLOCKCALC("Channel","1-","40")  '... STATDIREC,ROWNOSTR,CHNNOSTR
Call DATABLCLPCOPY("88-93",1,1)         '... CHNNOSTR,CHNROW,VALNO
Call DATABLCLPPASTE("82-87",20,0)        '... CHNNOSTR,CHNROW,VALNO
Call CHNDELETE("88-93")                 '... CLPSOURCE


Call CHNNORMALIZE("Ampl_Peak","FFT G1 x-axis ") '... Y,E
Call CHNNORMALIZE("Ampl_Peak1","FFT G1 y-axis") '... Y,E
Call CHNNORMALIZE("Ampl_Peak2","FFT G1 z-axis") '... Y,E
Call CHNNORMALIZE("Ampl_Peak3","FFT G2 x-axis") '... Y,E
Call CHNNORMALIZE("Ampl_Peak4","FFT G2 y-axis") '... Y,E
Call CHNNORMALIZE("Ampl_Peak5","FFT G2 z-axis") '... Y,E
Call CHNNORMALIZE("Ampl_Peak6","FFT G3 x-axis") '... Y,E
Call CHNNORMALIZE("Ampl_Peak7","FFT G3 y-axis") '... Y,E
Call CHNNORMALIZE("Ampl_Peak8","FFT G3 z-axis") '... Y,E
Call CHNNORMALIZE("Ampl_Peak9","FFT G4 x-axis") '... Y,E
Call CHNNORMALIZE("Ampl_Peak10","FFT G4 y-axis") '... Y,E
Call CHNNORMALIZE("Ampl_Peak11","FFT G4 z-axis") '... Y,E
Call CHNNORMALIZE("Ampl_Peak12","FFT G5 x-axis") '... Y,E
Call CHNNORMALIZE("Ampl_Peak13","FFT G5 y-axis") '... Y,E
Call CHNNORMALIZE("Ampl_Peak14","FFT G5 z-axis") '... Y,E


Call CHNSMOOTH("G1 Filtered","G1 Filtered Mean",24,"maxNumber") '... Y,E,SMOOTHWIDTH,SMOOTHTYPE
Call CHNSMOOTH("G2 Filtered","G2 Filtered Mean",24,"maxNumber") '... Y,E,SMOOTHWIDTH,SMOOTHTYPE
Call CHNSMOOTH("G3 Filtered","G3 Filtered Mean",24,"maxNumber") '... Y,E,SMOOTHWIDTH,SMOOTHTYPE
Call CHNSMOOTH("G4 Filtered","G4 Filtered Mean",24,"maxNumber") '... Y,E,SMOOTHWIDTH,SMOOTHTYPE
Call CHNSMOOTH("G5 Filtered","G5 Filtered Mean",24,"maxNumber") '... Y,E,SMOOTHWIDTH,SMOOTHTYPE

Call CHNENVELOPES("Time15","G1 Filtered","G1 Time Envelope","G1 Envelope","X_HüllMin","Y_HüllMin",0.25) '... X,Y,E,E,E,E,DXPEAK
Call CHNENVELOPES("Time16","G2 Filtered","G2 Time Envelope","G2 Envelope","X_HüllMin1","Y_HüllMin1",0.25) '... X,Y,E,E,E,E,DXPEAK
Call CHNENVELOPES("Time17","G3 Filtered","G3 Time Envelope","G3 Envelope","X_HüllMin2","Y_HüllMin2",0.25) '... X,Y,E,E,E,E,DXPEAK
Call CHNENVELOPES("Time18","G4 Filtered","G4 Time Envelope","G4 Envelope","X_HüllMin3","Y_HüllMin3",0.25) '... X,Y,E,E,E,E,DXPEAK
Call CHNENVELOPES("Time19","G5 Filtered","G5 Time Envelope","G5 Envelope","X_HüllMin4","Y_HüllMin4",0.25) '... X,Y,E,E,E,E,DXPEAK

Call CHNNORMALIZE("G1 Envelope","G1 Envelope Normalized") '... Y,E
Call CHNNORMALIZE("G2 Envelope","G2 Envelope Normalized") '... Y,E
Call CHNNORMALIZE("G3 Envelope","G3 Envelope Normalized") '... Y,E
Call CHNNORMALIZE("G4 Envelope","G4 Envelope Normalized") '... Y,E
Call CHNNORMALIZE("G5 Envelope","G5 Envelope Normalized") '... Y,E


     Call CHNRENUMBER()

Call CHNDELETE("80,81,84,85,88,89,92,93,96,97") '... CLPSOURCE
Call CHNMOVE(93,1,2)                    '... SOURCECHNINDEX,TARGETGROUPINDEX,TARGETCHNINDEX
Call CHNMOVE(94,1,5)                    '... SOURCECHNINDEX,TARGETGROUPINDEX,TARGETCHNINDEX
Call CHNMOVE(95,1,8)                    '... SOURCECHNINDEX,TARGETGROUPINDEX,TARGETCHNINDEX
```

```
Call CHNMOVE(96,1,11)                  '... SOURCECHNINDEX,TARGETGROUPINDEX,TARGETCHNINDEX
Call CHNMOVE(97,1,14)                  '... SOURCECHNINDEX,TARGETGROUPINDEX,TARGETCHNINDEX
Call CHNMOVE(98,1,17)                  '... SOURCECHNINDEX,TARGETGROUPINDEX,TARGETCHNINDEX
Call CHNMOVE(99,1,20)                  '... SOURCECHNINDEX,TARGETGROUPINDEX,TARGETCHNINDEX
Call CHNMOVE(100,1,23)                 '... SOURCECHNINDEX,TARGETGROUPINDEX,TARGETCHNINDEX
Call CHNMOVE(101,1,26)                 '... SOURCECHNINDEX,TARGETGROUPINDEX,TARGETCHNINDEX
Call CHNMOVE(102,1,29)                 '... SOURCECHNINDEX,TARGETGROUPINDEX,TARGETCHNINDEX
Call CHNMOVE(103,1,32)                 '... SOURCECHNINDEX,TARGETGROUPINDEX,TARGETCHNINDEX
Call CHNMOVE(104,1,35)                 '... SOURCECHNINDEX,TARGETGROUPINDEX,TARGETCHNINDEX
Call CHNMOVE(105,1,38)                 '... SOURCECHNINDEX,TARGETGROUPINDEX,TARGETCHNINDEX
Call CHNMOVE(106,1,41)                 '... SOURCECHNINDEX,TARGETGROUPINDEX,TARGETCHNINDEX
Call CHNMOVE(107,1,44)                 '... SOURCECHNINDEX,TARGETGROUPINDEX,TARGETCHNINDEX
Call CHNDELETE("42-56")                '... CLPSOURCE
Call CHNMOVE(41,1,62)                  '... SOURCECHNINDEX,TARGETGROUPINDEX,TARGETCHNINDEX
Call CHNMOVE(63,1,48)                  '... SOURCECHNINDEX,TARGETGROUPINDEX,TARGETCHNINDEX
Call CHNMOVE(64,1,49)                  '... SOURCECHNINDEX,TARGETGROUPINDEX,TARGETCHNINDEX
Call CHNMOVE(65,1,52)                  '... SOURCECHNINDEX,TARGETGROUPINDEX,TARGETCHNINDEX
Call CHNMOVE(66,1,53)                  '... SOURCECHNINDEX,TARGETGROUPINDEX,TARGETCHNINDEX
Call CHNMOVE(67,1,56)                  '... SOURCECHNINDEX,TARGETGROUPINDEX,TARGETCHNINDEX
Call CHNMOVE(68,1,57)                  '... SOURCECHNINDEX,TARGETGROUPINDEX,TARGETCHNINDEX
Call CHNMOVE(69,1,60)                  '... SOURCECHNINDEX,TARGETGROUPINDEX,TARGETCHNINDEX
Call CHNMOVE(70,1,61)                  '... SOURCECHNINDEX,TARGETGROUPINDEX,TARGETCHNINDEX
Call CHNMOVE(71,1,64)                  '... SOURCECHNINDEX,TARGETGROUPINDEX,TARGETCHNINDEX
Call CHNMOVE(72,1,65)                  '... SOURCECHNINDEX,TARGETGROUPINDEX,TARGETCHNINDEX
CHNNAME(93)="G1 Mean Smooth"
CHNNAME(94)="G2 Mean Smooth"
CHNNAME(95)="G3 Mean Smooth"
CHNNAME(96)="G4 Mean Smooth"
CHNNAME(97)="G5 Mean Smooth"
Call CHNMOVE(93,1,48)                  '... SOURCECHNINDEX,TARGETGROUPINDEX,TARGETCHNINDEX
Call CHNMOVE(94,1,52)                  '... SOURCECHNINDEX,TARGETGROUPINDEX,TARGETCHNINDEX
Call CHNMOVE(95,1,58)                  '... SOURCECHNINDEX,TARGETGROUPINDEX,TARGETCHNINDEX
Call CHNMOVE(96,1,63)                  '... SOURCECHNINDEX,TARGETGROUPINDEX,TARGETCHNINDEX
Call CHNMOVE(97,1,68)                  '... SOURCECHNINDEX,TARGETGROUPINDEX,TARGETCHNINDEX
Call CHNMOVE(42,2,6)                   '... SOURCECHNINDEX,TARGETGROUPINDEX,TARGETCHNINDEX
Call CHNMOVE(43,2,7)                   '... SOURCECHNINDEX,TARGETGROUPINDEX,TARGETCHNINDEX
Call CHNMOVE(44,2,8)                   '... SOURCECHNINDEX,TARGETGROUPINDEX,TARGETCHNINDEX
Call CHNMOVE(45,2,9)                   '... SOURCECHNINDEX,TARGETGROUPINDEX,TARGETCHNINDEX
Call CHNMOVE(46,2,10)                  '... SOURCECHNINDEX,TARGETGROUPINDEX,TARGETCHNINDEX
Call CHNMOVE(47,2,11)                  '... SOURCECHNINDEX,TARGETGROUPINDEX,TARGETCHNINDEX
Call CHNMOVE(41,2,12)                  '... SOURCECHNINDEX,TARGETGROUPINDEX,TARGETCHNINDEX
Call CHNMOVE(73,1,51)                  '... SOURCECHNINDEX,TARGETGROUPINDEX,TARGETCHNINDEX
Call CHNMOVE(74,1,57)                  '... SOURCECHNINDEX,TARGETGROUPINDEX,TARGETCHNINDEX
Call CHNMOVE(75,1,63)                  '... SOURCECHNINDEX,TARGETGROUPINDEX,TARGETCHNINDEX
Call CHNMOVE(76,1,69)                  '... SOURCECHNINDEX,TARGETGROUPINDEX,TARGETCHNINDEX
Call CHNMOVE(77,1,75)                  '... SOURCECHNINDEX,TARGETGROUPINDEX,TARGETCHNINDEX
Call CHNMOVE(41,1,76)                  '... SOURCECHNINDEX,TARGETGROUPINDEX,TARGETCHNINDEX


     Call CHNRENUMBER()

Call FormulaCalc("ch('G1 Vector')          :=  ((ch(2)^2 + ch(5)^2 + ch(8)^2)^0.5)")
Call FormulaCalc("ch('G2 Vector')          :=  ((ch(11)^2 + ch(14)^2 + ch(17)^2)^0.5)")
Call FormulaCalc("ch('G3 Vector')          :=  ((ch(20)^2 + ch(23)^2 + ch(26)^2)^0.5)")
Call FormulaCalc("ch('G4 Vector')          :=  ((ch(29)^2 + ch(32)^2 + ch(35)^2)^0.5)")
Call FormulaCalc("ch('G5 Vector')          :=  ((ch(38)^2 + ch(41)^2 + ch(44)^2)^0.5)")

Call CHNMOVE(103,1,47)                 '... SOURCECHNINDEX,TARGETGROUPINDEX,TARGETCHNINDEX
Call CHNMOVE(104,1,54)                 '... SOURCECHNINDEX,TARGETGROUPINDEX,TARGETCHNINDEX
Call CHNMOVE(105,1,61)                 '... SOURCECHNINDEX,TARGETGROUPINDEX,TARGETCHNINDEX
Call CHNMOVE(106,1,68)                 '... SOURCECHNINDEX,TARGETGROUPINDEX,TARGETCHNINDEX
Call CHNMOVE(107,1,75)                 '... SOURCECHNINDEX,TARGETGROUPINDEX,TARGETCHNINDEX

CHNNAME("Time")="Time G1 x-axis"
CHNNAME("Time1")="Time G1 y-axis"
CHNNAME("Time2")="Time G1 z-axis"
CHNNAME("Time3")="Time G2 x-axis"
CHNNAME("Time4")="Time G2 y-axis"
CHNNAME("Time5")="Time G2 z-axis"
CHNNAME("Time6")="Time G3 x-axis"
CHNNAME("Time7")="Time G3 y-axis"
CHNNAME("Time8")="Time G3 z-axis"
CHNNAME("Time9")="Time G4 x-axis"
CHNNAME("Time10")="Time G4 y-axis"
CHNNAME("Time11")="Time G4 z-axis"
CHNNAME("Time12")="Time G5 x-axis"
CHNNAME("Time13")="Time G5 y-axis"
CHNNAME("Time14")="Time G5 z-axis"
CHNNAME("Time15")="Time G1"
CHNNAME("Time16")="Time G2"
CHNNAME("Time17")="Time G3"
CHNNAME("Time18")="Time G4"
CHNNAME("Time19")="Time G5"

     Call CHNRENUMBER()

Call DATABLDEL("81-96",1,19)           '... CHNNOSTR,CHNROW,VALNO

call ChnPeakFind("Frequenz","FFT G1 x-axis", 108, 109, 1, "Max.Peaks", "Amplitude")

call ChnPeakFind("Frequenz","FFT G1 y-axis", 110, 111, 1, "Max.Peaks", "Amplitude")
Call DATABLCLPCOPY("110,111",1,1)      '... CHNNOSTR,CHNROW,VALNO
Call DATABLCLPPASTE("108,109",2,0)     '... CHNNOSTR,CHNROW,VALNO
Call CHNDELETE("110,111")              '... CLPSOURCE

call ChnPeakFind("Frequenz","FFT G1 z-axis", 110, 111, 1, "Max.Peaks", "Amplitude")
Call DATABLCLPCOPY("110,111",1,1)      '... CHNNOSTR,CHNROW,VALNO
Call DATABLCLPPASTE("108,109",3,0)     '... CHNNOSTR,CHNROW,VALNO
Call CHNDELETE("110,111")              '... CLPSOURCE



call ChnPeakFind("Frequenz","FFT G2 x-axis", 110, 111, 1, "Max.Peaks", "Amplitude")
```

```
Call DATABLCLPCOPY("110,111",1,1)       '... CHNNOSTR,CHNROW,VALNO
Call DATABLCLPPASTE("108,109",4,0)      '... CHNNOSTR,CHNROW,VALNO
Call CHNDELETE("110,111")               '... CLPSOURCE

call ChnPeakFind("Frequenz","FFT G2 y-axis", 110, 111, 1, "Max.Peaks", "Amplitude")
Call DATABLCLPCOPY("110,111",1,1)       '... CHNNOSTR,CHNROW,VALNO
Call DATABLCLPPASTE("108,109",5,0)      '... CHNNOSTR,CHNROW,VALNO
Call CHNDELETE("110,111")               '... CLPSOURCE

call ChnPeakFind("Frequenz","FFT G2 z-axis", 110, 111, 1, "Max.Peaks", "Amplitude")
Call DATABLCLPCOPY("110,111",1,1)       '... CHNNOSTR,CHNROW,VALNO
Call DATABLCLPPASTE("108,109",6,0)      '... CHNNOSTR,CHNROW,VALNO
Call CHNDELETE("110,111")               '... CLPSOURCE


call ChnPeakFind("Frequenz","FFT G3 x-axis", 110, 111, 1, "Max.Peaks", "Amplitude")
Call DATABLCLPCOPY("110,111",1,1)       '... CHNNOSTR,CHNROW,VALNO
Call DATABLCLPPASTE("108,109",7,0)      '... CHNNOSTR,CHNROW,VALNO
Call CHNDELETE("110,111")               '... CLPSOURCE

call ChnPeakFind("Frequenz","FFT G3 y-axis", 110, 111, 1, "Max.Peaks", "Amplitude")
Call DATABLCLPCOPY("110,111",1,1)       '... CHNNOSTR,CHNROW,VALNO
Call DATABLCLPPASTE("108,109",8,0)      '... CHNNOSTR,CHNROW,VALNO
Call CHNDELETE("110,111")               '... CLPSOURCE

call ChnPeakFind("Frequenz","FFT G3 z-axis", 110, 111, 1, "Max.Peaks", "Amplitude")
Call DATABLCLPCOPY("110,111",1,1)       '... CHNNOSTR,CHNROW,VALNO
Call DATABLCLPPASTE("108,109",9,0)      '... CHNNOSTR,CHNROW,VALNO
Call CHNDELETE("110,111")               '... CLPSOURCE



call ChnPeakFind("Frequenz","FFT G4 x-axis", 110, 111, 1, "Max.Peaks", "Amplitude")
Call DATABLCLPCOPY("110,111",1,1)       '... CHNNOSTR,CHNROW,VALNO
Call DATABLCLPPASTE("108,109",10,0)      '... CHNNOSTR,CHNROW,VALNO
Call CHNDELETE("110,111")               '... CLPSOURCE

call ChnPeakFind("Frequenz","FFT G4 y-axis", 110, 111, 1, "Max.Peaks", "Amplitude")
Call DATABLCLPCOPY("110,111",1,1)       '... CHNNOSTR,CHNROW,VALNO
Call DATABLCLPPASTE("108,109",11,0)      '... CHNNOSTR,CHNROW,VALNO
Call CHNDELETE("110,111")               '... CLPSOURCE

call ChnPeakFind("Frequenz","FFT G4 z-axis", 110, 111, 1, "Max.Peaks", "Amplitude")
Call DATABLCLPCOPY("110,111",1,1)       '... CHNNOSTR,CHNROW,VALNO
Call DATABLCLPPASTE("108,109",12,0)      '... CHNNOSTR,CHNROW,VALNO
Call CHNDELETE("110,111")               '... CLPSOURCE



call ChnPeakFind("Frequenz","FFT G5 x-axis", 110, 111, 1, "Max.Peaks", "Amplitude")
Call DATABLCLPCOPY("110,111",1,1)       '... CHNNOSTR,CHNROW,VALNO
Call DATABLCLPPASTE("108,109",13,0)      '... CHNNOSTR,CHNROW,VALNO
Call CHNDELETE("110,111")               '... CLPSOURCE

call ChnPeakFind("Frequenz","FFT G5 y-axis", 110, 111, 1, "Max.Peaks", "Amplitude")
Call DATABLCLPCOPY("110,111",1,1)       '... CHNNOSTR,CHNROW,VALNO
Call DATABLCLPPASTE("108,109",14,0)      '... CHNNOSTR,CHNROW,VALNO
Call CHNDELETE("110,111")               '... CLPSOURCE

call ChnPeakFind("Frequenz","FFT G5 z-axis", 110, 111, 1, "Max.Peaks", "Amplitude")
Call DATABLCLPCOPY("110,111",1,1)       '... CHNNOSTR,CHNROW,VALNO
Call DATABLCLPPASTE("108,109",15,0)      '... CHNNOSTR,CHNROW,VALNO
Call CHNDELETE("110,111")               '... CLPSOURCE



Call CHNDELETE("109")                   '... CLPSOURCE
Call CHNMOVE(108,2,12)                  '... SOURCECHNINDEX,TARGETGROUPINDEX,TARGETCHNINDEX
Call CHNRENUMBER()

Call                    CHNALLOC("Exposed                    time",1024,1,DataTypeFloat64,"Numeric",2,13)                    '...
GHDCHNNAME,GHDCHNLENGTH,CHNNO,DATATYPE,GHDDISPFORMAT,TARGETGROUPINDEX,TARGETCHNINDEX

CHD(1, 109)=(10*CHNLENGTH(1))/CHNLENGTHMAX(1)
CHD(2, 109)=(10*CHNLENGTH(4))/CHNLENGTHMAX(4)
CHD(3, 109)=(10*CHNLENGTH(7))/CHNLENGTHMAX(7)
CHD(4, 109)=(10*CHNLENGTH(10))/CHNLENGTHMAX(10)
CHD(5, 109)=(10*CHNLENGTH(13))/CHNLENGTHMAX(13)
CHD(6, 109)=(10*CHNLENGTH(16))/CHNLENGTHMAX(16)
CHD(7, 109)=(10*CHNLENGTH(19))/CHNLENGTHMAX(19)
CHD(8, 109)=(10*CHNLENGTH(22))/CHNLENGTHMAX(22)
CHD(9, 109)=(10*CHNLENGTH(25))/CHNLENGTHMAX(25)
CHD(10, 109)=(10*CHNLENGTH(28))/CHNLENGTHMAX(28)
CHD(11, 109)=(10*CHNLENGTH(31))/CHNLENGTHMAX(31)
CHD(12, 109)=(10*CHNLENGTH(34))/CHNLENGTHMAX(34)
CHD(13, 109)=(10*CHNLENGTH(37))/CHNLENGTHMAX(37)
CHD(14, 109)=(10*CHNLENGTH(40))/CHNLENGTHMAX(40)
CHD(15, 109)=(10*CHNLENGTH(43))/CHNLENGTHMAX(43)
CHD(16, 109)=(10*CHNLENGTH(46))/CHNLENGTHMAX(46)
CHD(17, 109)=(10*CHNLENGTH(53))/CHNLENGTHMAX(53)
CHD(18, 109)=(10*CHNLENGTH(60))/CHNLENGTHMAX(60)
CHD(19, 109)=(10*CHNLENGTH(67))/CHNLENGTHMAX(67)
CHD(20, 109)=(10*CHNLENGTH(74))/CHNLENGTHMAX(74)



Call DATABLCLPCOPY("98-109",1,20)       '... CHNNOSTR,CHNROW,VALNO
'PRINTLEFTMARG    =1.5
'PRINTTOPMARG     =1.5
'PRINTWIDTH       =38.5
'PRINTORIENT      ="landscape"
'Call PICPRINT("WinPrint")               '... PRINTDEVICE
```

```
  ' Grafik anzeigen.
  Call PicUpdate

  ' Endmeldung anzeigen.
  Call MsgBoxDisp("Die Berechnung ist beendet.")

' Wenn Dialog abgebrochen wurde.
Else

  ' Meldung ausgeben.                                                    ' Wenn Abbruch
  Call MsgBoxDisp("Es wurde <Abbruch> ausgewählt! Das Script wird beendet.")
End If                                                  ' Meldung ausgeben.



' ---------------------------------------------------------------------------------------
' PROZEDUREN
' ---------------------------------------------------------------------------------------
' ---------------------------------------------------------------------------------------
' Name:      UserDlg_Info
'
' Zweck:     Informationsdialog anzeigen.
'
' Parameter: Keine
' ---------------------------------------------------------------------------------------
Sub Info_Message
  T1 = "In folgendem Script werden die xyz Kanäle von 5 Geophonen  " & vbCRLF & _
       "analysiert. Schwinggeschwindigkeiten die geringer als das " & vbCRLF & _
       "Background noise sind identifiziert, zunächst durch NOVALUE ersetzt, " & vbCRLF & _
       "danach gelöscht und zusätzlich wird das Signal geglättet und eine  " & vbCRLF & _
       "Hüllkurve berechnet. Es werden weiters die resultierenden " & vbCRLF & _
       "Schwinggeschwindigkeiten berechnet, eine Frequenzanalyse wird" & vbCRLF & _
       "durchgeführt und statistische Kennwerte werden berechnet. "  & vbCRLF & vbCRLF & _
       "Achtung! Daten und Grafiklayout werden gelöscht!Wenn Sie Sichern möchten, betätigen Sie bitte <Abbruch>."
  Call MsgboxDisp(T1,"MB_OKCancel")
End Sub
```

APPENDIX 6

Roadheader ATM 105, data sheet

ROADHEADER ATM 105/028-IC		
Overall length approximately	18.0	m
Overall length without belt conveyor	12.1	m
Width (without loading table)	3600	mm
Width (with loading table)	4500	mm
Total machine height	4950	mm
Cutter boom telescope	650	mm
Ground pressure	21	N/cm^2
Total mass approximately	125000	kg
Total power installed:	537	kW
- Cutter motor	300	kW
- Pump drive motor	132	kW
- Chain conveyor and spinners	72	kW
- Auxiliary motors	33	kW
Electrical supply	1000/60	V/Hz
Tramming speed	0-15	m/min
Cutting speed	1.4	m/sec
Max. cutting profile without telescope approximately	46.2	m^2
Max. cutting profile with telescope approximately	53.8	m^2
Cutting width from one position max.	8950	mm
Cutting height max.	6500	mm

APPENDIX 7

Rock testing results: Wolfram Mine Mittersill

VOEST-ALPINE BERGTECHNIK — SANDVIK

PROTOKOLL FÜR MECHANISCHE GESTEINSPRÜFUNG

DRUCKPROBE

	Durchmesser (D)	Höhe oder Länge (H oder L)	Masse (m)	Dichte (ρ)	Axiale USW-Laufzeit (t_p)	Bruchlast (F_{max})	Bruch-verformung (ΔL_{max})	Elastische Grenze (F_{el})	Elastische Verformung (ΔL_{el})	Axiale USW-Geschwindigkeit (v_p)	Druck-festigkeit (σ_c)	Elastizitäts-modul (E_{stat})	Verformungs-modul (E_{sec})	Verformungs-maß (ε)	Bruchenergie (W_f)
	[mm]	[mm]	[g]	[g/cm³]	[µs]	[kN]	[mm]	[kN]	[mm]	[m/s]	[MPa]	[MPa]	[MPa]	[mm/mm]	[Nm]
	51,07	49,93	307,0	3,00	11,8	59,6	0,122	59,6	0,122	4231	29,10	11908	11908	0,0024	3,64
	50,88	49,93	303,0	2,98	12,6	580,0	0,463	456,4	0,351	3963	285,26	31931	30763	0,0093	138,14
	50,74	49,98	304,0	3,01	12,6	140,9	0,160	140,9	0,160	3967	69,68	21767	21767	0,0032	11,27
	50,55	49,96	314,0	3,13	11,5	49,4	0,351	43,8	0,189	4344	24,61	5769	3504	0,0070	11,69
	50,84	50,06	300,0	2,95	12,8	223,7	0,302	223,7	0,302	3911	110,20	18266	18266	0,0060	33,78
Minimum	50,55	49,93	300,0	2,95	11,5	49,4	0,122	43,8	0,122	3911	24,61	5769	3504	0,0024	3,64
Maximum	51,07	50,06	314,0	3,13	12,8	580,0	0,463	456,4	0,351	4344	285,26	31931	30763	0,0093	138,14
Mittelwert	**50,82**	**49,97**	**305,6**	**3,02**	**12,3**	**210,7**	**0,280**	**184,9**	**0,225**	**4083**	**103,77**	**17928**	**17241**	**0,0056**	**39,70**
Standardabweichung	0,19	0,05	5,3	0,07	0,6	218,1	0,140	167,9	0,097	192	107,22	9938	10266	0,0028	56,17

ZUGPROBE

	Durchmesser (D)	Höhe oder Länge (H oder L)	Masse (m)	Dichte (ρ)	Bruchlast (F_{max})	Zugfestigkeit (σ_t)	Abrasivität
	[mm]	[mm]	[g]	[g/cm³]	[kN]	[MPa]	CAI
	51,20	25,48	153,0	2,92	21,8	10,64	1,63
	51,22	24,66	153,0	3,01	22,6	11,39	3,88
	50,87	24,30	152,0	3,08	33,7	17,36	4,17
	52,69	24,33	156,0	2,94	26,9	13,36	3,09
	50,85	24,12	147,0	3,00	10,8	5,61	3,29
Minimum	50,85	24,12	147,0	2,92	10,8	5,61	1,63
Maximum	52,69	25,48	156,0	3,08	33,7	17,36	4,17
Mittelwert	**51,37**	**24,58**	**152,2**	**2,99**	**23,2**	**11,67**	**3,21**
Standardabweichung	0,76	0,54	3,3	0,06	8,4	4,27	0,99

Verhältnis-werte

$\sigma_c:\sigma_t$= 9

$E_{sec}:E_{stat}$= 0,96

$E_{stat}:\sigma_c$= 173

$W_f:\sigma_c$= 0,38

Angaben zum Untersuchungsbericht

Untersuchungsbericht Nr.:	2006 / 009
Probe Nr.:	01
Bearbeiter:	Hebenstreit
Datum:	2006-03-08
Firma:	MUL, Institut für Bergbaukunde
Staat:	A
Einsatzort:	Mittersill
Ort der Probennahme:	Haufwerk
Datum der Probennahme:	
Gesteinsbezeichnung:	Amphibolit (sehr feinkristallin, mit Biotit und Quarz)

VOEST-ALPINE BERGTECHNIK — SANDVIK

PROTOKOLL FÜR MECHANISCHE GESTEINSPRÜFUNG

DRUCKPROBE

	Durchmesser (D)	Höhe oder Länge (H oder L)	Masse (m)	Dichte (ρ)	Axiale USW-Laufzeit (t_p)	Bruchlast (F_{max})	Bruch-verformung (ΔL_{max})	Elastische Grenze (F_{el})	Elastische Verformung (ΔL_{el})	Axiale USW-Geschwindigkeit (v_p)	Druck-festigkeit (σ_c)	Elastizitäts-modul (E_{stat})	Verformungs-modul (E_{sec})	Verformungs-maß (ε)	Bruchenergie (W_f)
	[mm]	[mm]	[g]	[g/cm³]	[µs]	[kN]	[mm]	[kN]	[mm]	[m/s]	[MPa]	[MPa]	[MPa]	[mm/mm]	[Nm]
	50,81	49,86	293,0	2,90	11,8	221,3	0,266	182,6	0,204	4225	109,14	22011	20458	0,0053	31,15
	50,91	49,89	295,0	2,90	12,9	231,2	0,242	202,9	0,186	3867	113,58	26735	23415	0,0049	31,02
	51,07	49,93	306,0	2,99	12,3	211,6	0,240	185,7	0,197	4059	103,30	22977	21490	0,0048	26,83
	50,81	49,84	293,0	2,90	12,6	236,5	0,213	189,8	0,160	3956	116,64	29159	27292	0,0043	26,48
	50,98	50,12	301,0	2,94	12,3	269,7	0,230	238,0	0,191	4075	132,13	30596	28792	0,0046	32,63
Minimum	50,81	49,84	293,0	2,90	11,8	211,6	0,213	182,6	0,160	3867	103,30	22011	20458	0,0043	26,48
Maximum	51,07	50,12	306,0	2,99	12,9	269,7	0,266	238,0	0,204	4225	132,13	30596	28792	0,0053	32,63
Mittelwert	**50,92**	**49,93**	**297,6**	**2,93**	**12,4**	**234,1**	**0,238**	**199,8**	**0,188**	**4037**	**114,96**	**26295**	**24290**	**0,0048**	**29,62**
Standardabweichung	0,11	0,11	5,7	0,04	0,4	22,1	0,019	22,7	0,017	135	10,83	3750	3625	0,0004	2,78

ZUGPROBE

	Durchmesser (D)	Höhe oder Länge (H oder L)	Masse (m)	Dichte (ρ)	Bruchlast (F_{max})	Zugfestigkeit (σ_t)	Abrasivität
	[mm]	[mm]	[g]	[g/cm³]	[kN]	[MPa]	CAI
	51,05	25,16	155,0	3,01	20,5	10,16	2,25
	51,03	25,43	152,0	2,92	15,5	7,60	2,85
	50,86	25,45	152,0	2,94	17,6	8,66	1,91
	51,04	25,15	151,0	2,93	13,2	6,55	3,91
	50,72	26,96	154,0	2,83	20,0	9,31	3,34
Minimum	50,72	25,15	151,0	2,83	13,2	6,55	1,91
Maximum	51,05	26,96	155,0	3,01	20,5	10,16	3,91
Mittelwert	**50,94**	**25,63**	**152,8**	**2,93**	**17,4**	**8,46**	**2,85**
Standardabweichung	0,15	0,76	1,6	0,07	3,1	1,42	0,81

Verhältnis-werte

$\sigma_c:\sigma_t$= 14

$E_{sec}:E_{stat}$= 0,92

$E_{stat}:\sigma_c$= 229

$W_f:\sigma_c$= 0,26

Angaben zum Untersuchungsbericht

Untersuchungsbericht Nr.:	2006 / 009
Probe Nr.:	02
Bearbeiter:	Hebenstreit
Datum:	2006-03-08
Firma:	MUL, Institut für Bergbaukunde
Staat:	A
Einsatzort:	Mittersill
Ort der Probennahme:	Haufwerk
Datum der Probennahme:	
Gesteinsbezeichnung:	Amphibolit (stark pegmatitisch)

VOEST-ALPINE BERGTECHNIK

PROTOKOLL FÜR MECHANISCHE GESTEINSPRÜFUNG

SANDVIK

DRUCKPROBE

	Durchmesser (D)	Höhe oder Länge (H oder L)	Masse (m)	Dichte (ρ)	Axiale USW-Laufzeit (t_p)	Bruchlast (F_{max})	Bruch-verformung (ΔL_{max})	Elastische Grenze (F_{el})	Elastische Verformung (ΔL_{el})	Axiale USW-Geschwindigkeit (v_p)	Druck-festigkeit (σ_c)	Elastizitäts-modul (E_{stat})	Verformungs-modul (E_{sec})	Verformungs-maß (ε)	Bruchenergie (W_f)
	[mm]	[mm]	[g]	[g/cm³]	[µs]	[kN]	[mm]	[kN]	[mm]	[m/s]	[MPa]	[MPa]	[MPa]	[mm/mm]	[Nm]
	50,93	49,98	300,0	2,95	14,6	62,7	0,209	62,7	0,209	3423	30,78	7360	7360	0,0042	6,55
	50,86	49,98	298,0	2,93	12,5	162,9	0,406	139,1	0,308	3998	80,18	11110	9871	0,0081	36,22
	50,71	49,99	299,0	2,96	14,4	149,8	0,186	144,9	0,177	3472	74,17	20263	19934	0,0037	14,15
	50,86	49,92	299,0	2,95	13,9	92,7	0,495	77,6	0,344	3591	45,63	5543	4602	0,0099	26,20
	50,76	49,94	301,0	2,98	12,3	88,6	0,246	81,7	0,201	4060	43,78	10031	8888	0,0049	12,04
Minimum	50,71	49,92	298,0	2,93	12,3	62,7	0,186	62,7	0,177	3423	30,78	5543	4602	0,0037	6,55
Maximum	50,93	49,99	301,0	2,98	14,6	162,9	0,495	144,9	0,344	4060	80,18	20263	19934	0,0099	36,22
Mittelwert	**50,82**	**49,96**	**299,4**	**2,95**	**13,5**	**111,3**	**0,308**	**101,2**	**0,248**	**3709**	**54,91**	**10861**	**10131**	**0,0062**	**19,03**
Standardabweichung	0,09	0,03	1,1	0,02	1,1	42,9	0,135	38,0	0,073	300	21,23	5694	5830	0,0027	11,99

ZUGPROBE

	Durchmesser (D)	Höhe oder Länge (H oder L)	Masse (m)	Dichte (ρ)	Bruchlast (F_{max})	Zugfestigkeit (σ_t)	Abrasivität
	[mm]	[mm]	[g]	[g/cm³]	[kN]	[MPa]	CAI
	50,87	24,71	146,0	2,91	27,3	13,83	4,07
	50,82	24,30	147,0	2,98	17,6	9,07	4,93
	50,86	24,48	145,0	2,92	34,9	17,85	2,75
	50,98	24,94	147,0	2,89	14,0	7,01	2,56
	50,92	25,05	152,0	2,98	31,4	15,67	3,37
Minimum	50,82	24,30	145,0	2,89	14,0	7,01	2,56
Maximum	50,98	25,05	152,0	2,98	34,9	17,85	4,93
Mittelwert	**50,89**	**24,70**	**147,4**	**2,93**	**25,0**	**12,69**	**3,54**
Standardabweichung	0,06	0,31	2,7	0,04	8,9	4,53	0,98

Verhältnis-werte

$\sigma_c:\sigma_t$= 4

$E_{sec}:E_{stat}$= 0,93

$E_{stat}:\sigma_c$= 198

$W_f:\sigma_c$= 0,35

Angaben zum Untersuchungsbericht

Untersuchungsbericht Nr.:	2006 / 009
Probe Nr.:	03
Bearbeiter:	Hebenstreit
Datum:	2006-03-08
Firma:	MUL, Institut für Bergbaukunde
Staat:	A
Einsatzort:	Mittersill
Ort der Probennahme:	Haufwerk
Datum der Probennahme:	
Gesteinsbezeichnung:	Amphibolit (feinkristallin, mit Biotit und Quarz)

APPENDIX 8

Rock testing results: Erzberg Iron Ore Mine/ University test area

VOEST-ALPINE BERGTECHNIK — SANDVIK

PROTOKOLL FÜR MECHANISCHE GESTEINSPRÜFUNG

DRUCKPROBE

	Durchmesser (D)	Höhe oder Länge (H oder L)	Masse (m)	Dichte (ρ)	Axiale USW-Laufzeit (t_p)	Bruchlast (F_{max})	Bruch-verformung (ΔL_{max})	Elastische Grenze (F_{el})	Elastische Verformung (ΔL_{el})	Axiale USW-Geschwindigkeit (v_p)	Druck-festigkeit (σ_c)	Elastizitäts-modul (E_{stat})	Verformungs-modul (E_{sec})	Verformungs-maß (ε)	Bruchenergie (W_f)
	[mm]	[mm]	[g]	[g/cm³]	[µs]	[kN]	[mm]	[kN]	[mm]	[m/s]	[MPa]	[MPa]	[MPa]	[mm/mm]	[Nm]
	51,10	49,83	278,0	2,72	15,0	75,8	0,104	75,8	0,104	3322	36,96	17709	17709	0,0021	3,94
	51,06	49,80	278,0	2,73	10,3	87,8	0,136	87,8	0,136	4835	42,88	15701	15701	0,0027	5,97
	51,09	49,81	278,0	2,72	12,3	85,7	0,107	85,7	0,107	4050	41,80	19460	19460	0,0021	4,58
	51,02	49,84	277,0	2,72	17,2	30,1	0,326	30,1	0,326	2898	14,72	2251	2251	0,0065	4,91
	51,05	49,82	277,0	2,72	9,8	64,5	0,123	64,5	0,123	5084	31,51	12764	12764	0,0025	3,97
Minimum	51,02	49,80	277,0	2,72	9,8	30,1	0,104	30,1	0,104	2898	14,72	2251	2251	0,0021	3,94
Maximum	51,10	49,84	278,0	2,73	17,2	87,8	0,326	87,8	0,326	5084	42,88	19460	19460	0,0065	5,97
Mittelwert	**51,06**	**49,82**	**277,6**	**2,72**	**12,9**	**68,8**	**0,159**	**68,8**	**0,159**	**4038**	**33,58**	**13577**	**13577**	**0,0032**	**4,67**
Standardabweichung	0,03	0,02	0,5	0,00	3,1	23,5	0,094	23,5	0,094	941	11,46	6803	6803	0,0019	0,83

ZUGPROBE

	Durchmesser (D)	Höhe oder Länge (H oder L)	Masse (m)	Dichte (ρ)	Bruchlast (F_{max})	Zugfestigkeit (σ_t)	Abrasivität
	[mm]	[mm]	[g]	[g/cm³]	[kN]	[MPa]	CAI
	51,00	25,56	141,0	2,70	16,9	8,25	1,16
	51,09	25,25	138,0	2,67	20,1	9,92	1,07
	51,09	25,53	140,0	2,67	15,1	7,37	0,66
	51,06	25,39	140,0	2,69	13,7	6,73	0,76
	51,07	25,27	141,0	2,72	12,6	6,22	1,25
Minimum	51,00	25,25	138,0	2,67	12,6	6,22	0,66
Maximum	51,09	25,56	141,0	2,72	20,1	9,92	1,25
Mittelwert	**51,06**	**25,40**	**140,0**	**2,69**	**15,7**	**7,70**	**0,98**
Standardabweichung	0,04	0,14	1,2	0,02	2,9	1,46	0,26

Verhältnis-werte

$\sigma_c:\sigma_t$= 4

$E_{sec}:E_{stat}$= 1,00

$E_{stat}:\sigma_c$= 404

$W_f:\sigma_c$= 0,14

Angaben zum Untersuchungsbericht

Untersuchungsbericht Nr.:	2006 / 008
Probe Nr.:	01
Bearbeiter:	Hebenstreit
Datum:	2006-03-08
Firma:	MUL, Institut für Bergbaukunde
Staat:	A
Einsatzort:	Erzberg
Ort der Probennahme:	Haufwerk
Datum der Probennahme:	
Gesteinsbezeichnung:	Kalkstein (leicht kristallin, laminiert)

VOEST-ALPINE BERGTECHNIK — SANDVIK

PROTOKOLL FÜR MECHANISCHE GESTEINSPRÜFUNG

DRUCKPROBE

	Durchmesser (D)	Höhe oder Länge (H oder L)	Masse (m)	Dichte (ρ)	Axiale USW-Laufzeit (t_p)	Bruchlast (F_{max})	Bruch-verformung (ΔL_{max})	Elastische Grenze (F_{el})	Elastische Verformung (ΔL_{el})	Axiale USW-Geschwindigkeit (v_p)	Druck-festigkeit (σ_c)	Elastizitäts-modul (E_{stat})	Verformungs-modul (E_{sec})	Verformungs-maß (ε)	Bruchenergie (W_f)
	[mm]	[mm]	[g]	[g/cm³]	[µs]	[kN]	[mm]	[kN]	[mm]	[m/s]	[MPa]	[MPa]	[MPa]	[mm/mm]	[Nm]
	50,65	50,00	276,0	2,74	8,6	53,0	0,118	53,0	0,118	5814	26,30	11146	11146	0,0024	3,13
	50,94	49,82	275,0	2,71	8,8	85,8	0,115	85,8	0,115	5661	42,10	18238	18238	0,0023	4,93
	50,98	49,80	275,0	2,71	8,8	83,0	0,120	83,0	0,120	5659	40,66	16875	16875	0,0024	4,98
	50,99	49,83	277,0	2,72	9,8	74,8	0,041	74,8	0,041	5085	36,63	44519	44519	0,0008	1,53
Minimum	50,65	49,80	275,0	2,71	8,6	53,0	0,041	53,0	0,041	5085	26,30	11146	11146	0,0008	1,53
Maximum	50,99	50,00	277,0	2,74	9,8	85,8	0,120	85,8	0,120	5814	42,10	44519	44519	0,0024	4,98
Mittelwert	**50,89**	**49,86**	**275,8**	**2,72**	**9,0**	**74,2**	**0,099**	**74,2**	**0,099**	**5555**	**36,42**	**22695**	**22695**	**0,0020**	**3,64**
Standardabweichung	0,16	0,09	1,0	0,02	0,5	14,9	0,038	14,9	0,038	322	7,13	14871	14871	0,0008	1,65

ZUGPROBE

	Durchmesser (D)	Höhe oder Länge (H oder L)	Masse (m)	Dichte (ρ)	Bruchlast (F_{max})	Zugfestigkeit (σ_t)	Abrasivität
	[mm]	[mm]	[g]	[g/cm³]	[kN]	[MPa]	CAI
	51,04	25,49	140,0	2,68	19,8	9,69	1,07
	51,06	25,67	140,0	2,66	16,4	7,97	1,13
	51,06	25,27	139,0	2,69	16,0	7,89	1,13
	51,10	25,41	140,0	2,69	10,3	5,05	1,12
	51,07	25,55	141,0	2,69	14,8	7,22	0,91
Minimum	51,04	25,27	139,0	2,66	10,3	5,05	0,91
Maximum	51,10	25,67	141,0	2,69	19,8	9,69	1,13
Mittelwert	**51,07**	**25,48**	**140,0**	**2,68**	**15,5**	**7,56**	**1,07**
Standardabweichung	0,02	0,15	0,7	0,01	3,4	1,68	0,09

Verhältnis-werte

$\sigma_c:\sigma_t$= 5

$E_{sec}:E_{stat}$= 1,00

$E_{stat}:\sigma_c$= 623

$W_f:\sigma_c$= 0,10

Angaben zum Untersuchungsbericht

Untersuchungsbericht Nr.:	2006 / 008
Probe Nr.:	02
Bearbeiter:	Hebenstreit
Datum:	2006-03-08
Firma:	MUL, Institut für Bergbaukunde
Staat:	A
Einsatzort:	Erzberg
Ort der Probennahme:	Haufwerk
Datum der Probennahme:	
Gesteinsbezeichnung:	Kalkstein (leicht kristallin, laminiert)

APPENDIX 9

Rock testing results: Cullinan Diamond Mine, Kimberlite

VOEST-ALPINE
Bergtechnik Ges.m.b.H.
Alpinestrasse 1
A-8740 Zeltweg/Austria
Tel.: +43 3577 755 234
+43 3577 755 823
Fax.: +43 3577 756 334
Email: uwe.restner@sandvik.com
karl-heinz.gehring@sandvik.com

RESULTS OF ROCK TEST

Test Report No.:	2003 / 039
Sample No.:	01
Report issued by:	Gehring, Hebenstreit, Restner
Date:	2003-06-11
Company / Country:	De Beers / ZA
Site:	Premier Mine
Location of Sampling:	BBIE 89 N / 70
Date of Sampling:	2003-05-15
Denomination of Rock:	Grey TKB

Zeltweg, 2003-06-11 **Signature:**

Results of Rock Test: Page 2

MECHANICAL PROPERTIES

Test Report No.:	2003 / 039	Sample No.:	01
Report issued by:	Gehring, Hebenstreit, Restner	Date:	2003-06-11

Uniaxial compressive strength σ_c (5 specimen(s) H/D = 1)

min.: 69,26 MPa max.: 84,18 MPa average: **79,08** MPa

Brazilian tensile strength σ_t (5 specimen(s) H/D = 0.5)

min.: 4,92 MPa max.: 9,23 MPa average: **6,21** MPa

Young's modulus E_{stat} (5 specimen(s) H/D = 1)

min.: 8689 MPa max.: 14390 MPa average: **12200** MPa

Secant modulus E_{sec} (5 specimen(s) H/D = 1)

min.: 8689 MPa max.: 14390 MPa average: **11399** MPa

Linear strain ε (5 specimen(s) H/D = 1)

min.: 0,0056 mm/mm max.: 0,0097 mm/mm average: **0,0073** mm/mm

Fracture energy W_f (5 specimen(s) H/D = 1)

min.: 5,81 Nm max.: 10,49 Nm average: **7,70** Nm

Related values:				**For evaluation of:**
σ_c	: σ_t	= **13**		Toughness
E_{sec}	: E_{stat}	= **0,93**		Plasticity
E_{stat}	: σ_c	= **154**		Relative elasticity
W_f	: σ_c	= **0,10**		Specific fracture energy

Specific gravity: **2,71** g/cm^3

Rock classification with regard to its mechanical behaviour:

Strength	**Toughness**	**Plasticity**	**Rel. Elasticity**	**Spec. Fract. Energy**
very high	very tough	highly plastic	very high	very high
high	tough	plastic	high	high
> average	> average	moderately plastic	average	average
moderate	brittle	> not plastic	> low	low
low	very brittle		very low	> very low

Final classification of mechanical behaviour:

Related to uniaxial compressive strength average cuttability.

Special remarks:

Results of Rock Test: Page 3

PETROGRAPHICAL ANALYSIS AND ABRASIVITY

Test Report No.:	2003 / 039	Sample No.:	01
Report issued by:	Gehring, Hebenstreit, Restner	Date:	2003-06-11

Petrographical description (based on hand rock sample):

Remarks on alteration:

fresh

Mineral content:

Average grain size of quartz: mm (fictional, if there is no quartz content)

Content of hard minerals related to quartz: %

Abrasivity values:

$F_{SCHIMAZEK}$: $F_{CERCHAR}$(CAI): **0,54** (5 specimen(s))

Classification of rock with regard to abrasivity:

based on $F_{SCHIMAZEK}$	based on $F_{CERCHAR}$(CAI)
extremely abrasive	extremely abrasive
highly abrasive	highly abrasive
very abrasive	very abrasive
abrasive	abrasive
considerably abrasive	considerably abrasive
moderately abrasive	moderately abrasive
little abrasive	=> little abrasive
not abrasive	not abrasive

VOEST-ALPINE
BERGTECHNIK

SANDVIK

VOEST-ALPINE
Bergtechnik Ges.m.b.H.
Alpinestrasse 1
A-8740 Zeltweg/Austria
Tel.: +43 3577 755 234
+43 3577 755 823
Fax.: +43 3577 756 334
Email: uwe.restner@sandvik.com
karl-heinz.gehring@sandvik.com

RESULTS OF ROCK TEST

Test Report No.:	2003 / 039
Sample No.:	05
Report issued by:	Gehring, Hebenstreit, Restner
Date:	2003-06-13
Company / Country:	De Beers / ZA
Site:	Premier Mine
Location of Sampling:	BBIE 89 N / 63
Date of Sampling:	2003-05-15
Denomination of Rock:	Hypabyssal kimberlite

Zeltweg, 2003-06-13 **Signature:**

Results of Rock Test: Page 2

MECHANICAL PROPERTIES

Test Report No.:	2003 / 039	Sample No.:	05
Report issued by:	Gehring, Hebenstreit, Restner	Date:	2003-06-13

Uniaxial compressive strength σ_c (5 specimen(s) H/D = 1)

min.: 84,30 MPa max.: 145,35 MPa average: **123,84** MPa

Brazilian tensile strength σ_t (5 specimen(s) H/D = 0.5)

min.: 6,79 MPa max.: 10,52 MPa average: **8,84** MPa

Young's modulus E_{stat} (5 specimen(s) H/D = 1)

min.: 15497 MPa max.: 23097 MPa average: **19670** MPa

Secant modulus E_{sec} (5 specimen(s) H/D = 1)

min.: 13159 MPa max.: 23097 MPa average: **18391** MPa

Linear strain ε (5 specimen(s) H/D = 1)

min.: 0,0063 mm/mm max.: 0,0080 mm/mm average: **0,0068** mm/mm

Fracture energy W_f (5 specimen(s) H/D = 1)

min.: 7,52 Nm max.: 15,54 Nm average: **11,45** Nm

Related values:				**For evaluation of:**
σ_c	:	σ_t	= **14**	Toughness
E_{sec}	:	E_{stat}	= **0,93**	Plasticity
E_{stat}	:	σ_c	= **159**	Relative elasticity
W_f	:	σ_c	= **0,09**	Specific fracture energy

Specific gravity: **2,74** g/cm^3

Rock classification with regard to its mechanical behaviour:

Strength	**Toughness**	**Plasticity**	**Rel. Elasticity**	**Spec. Fract. Energy**
> very high	very tough	highly plastic	very high	very high
high	tough	plastic	high	high
average	> average	moderately plastic	average	average
moderate	brittle	> not plastic	> low	low
low	very brittle		very low	> very low

Final classification of mechanical behaviour:

Related to uniaxial compressive strength average cuttability.

Special remarks:

Results of Rock Test: Page 3

PETROGRAPHICAL ANALYSIS AND ABRASIVITY

Test Report No.:	2003 / 039	Sample No.:	05
Report issued by:	Gehring, Hebenstreit, Restner	Date:	2003-06-13

Petrographical description (based on hand rock sample):

Remarks on alteration:

fresh

Mineral content:

Average grain size of quartz: mm (fictional, if there is no quartz content)

Content of hard minerals related to quartz: %

Abrasivity values:

$F_{SCHIMAZEK}$: $F_{CERCHAR}$(CAI): **0,74** (5 specimen(s))

Classification of rock with regard to abrasivity:

based on $F_{SCHIMAZEK}$	based on $F_{CERCHAR}$(CAI)
extremely abrasive	extremely abrasive
highly abrasive	highly abrasive
very abrasive	very abrasive
abrasive	abrasive
considerably abrasive	considerably abrasive
moderately abrasive	moderately abrasive
little abrasive	=> little abrasive
not abrasive	not abrasive

VOEST-ALPINE
BERGTECHNIK

SANDVIK

VOEST-ALPINE
Bergtechnik Ges.m.b.H.
Alpinestrasse 1
A-8740 Zeltweg/Austria
Tel.: +43 3577 755 234
+43 3577 755 823
Fax.: +43 3577 756 334
Email: uwe.restner@sandvik.com
karl-heinz.gehring@sandvik.com

RESULTS OF ROCK TEST

Test Report No.:	2003 / 039
Sample No.:	06
Report issued by:	Gehring, Hebenstreit, Restner
Date:	2003-06-13
Company / Country:	De Beers / ZA
Site:	Premier Mine
Location of Sampling:	BBIE 89 N / 51
Date of Sampling:	2003-05-15
Denomination of Rock:	TKB

Zeltweg, 2003-06-13 **Signature:**

Results of Rock Test: Page 2

MECHANICAL PROPERTIES

Test Report No.:	2003 / 039	Sample No.:	06
Report issued by:	Gehring, Hebenstreit, Restner	Date:	2003-06-13

Uniaxial compressive strength σ_c (5 specimen(s) H/D = 1)

min.: 54,37 MPa max.: 69,70 MPa average: **61,68** MPa

Brazilian tensile strength σ_t (5 specimen(s) H/D = 0.5)

min.: 4,68 MPa max.: 8,08 MPa average: **6,63** MPa

Young's modulus E_{stat} (5 specimen(s) H/D = 1)

min.: 9943 MPa max.: 20849 MPa average: **12529** MPa

Secant modulus E_{sec} (5 specimen(s) H/D = 1)

min.: 9943 MPa max.: 20849 MPa average: **12529** MPa

Linear strain ε (5 specimen(s) H/D = 1)

min.: 0,0030 mm/mm max.: 0,0067 mm/mm average: **0,0053** mm/mm

Fracture energy W_f (5 specimen(s) H/D = 1)

min.: 2,36 Nm max.: 6,03 Nm average: **4,24** Nm

Related values:				**For evaluation of:**
σ_c	: σ_t	=	**9**	Toughness
E_{sec}	: E_{stat}	=	**1,00**	Plasticity
E_{stat}	: σ_c	=	**203**	Relative elasticity
W_f	: σ_c	=	**0,07**	Specific fracture energy

Specific gravity: **2,65** g/cm^3

Rock classification with regard to its mechanical behaviour:

Strength	**Toughness**	**Plasticity**	**Rel. Elasticity**	**Spec. Fract. Energy**
very high	very tough	highly plastic	very high	very high
high	tough	plastic	high	high
> average	**>** average	moderately plastic	**>** average	average
moderate	brittle	**>** not plastic	low	low
low	very brittle		very low	**>** very low

Final classification of mechanical behaviour:

Related to uniaxial compressive strength average cuttability.

Special remarks:

Results of Rock Test: Page 3

PETROGRAPHICAL ANALYSIS AND ABRASIVITY

Test Report No.:	2003 / 039	Sample No.:	06
Report issued by:	Gehring, Hebenstreit, Restner	Date:	2003-06-13

Petrographical description (based on hand rock sample):

Remarks on alteration:

fresh

Mineral content:

Average grain size of quartz: mm (fictional, if there is no quartz content)

Content of hard minerals related to quartz: %

Abrasivity values:

$F_{SCHIMAZEK}$: $F_{CERCHAR}$(CAI): **0,44** (5 specimen(s))

Classification of rock with regard to abrasivity:

based on	$F_{SCHIMAZEK}$	based on	$F_{CERCHAR}$(CAI)
	extremely abrasive		extremely abrasive
	highly abrasive		highly abrasive
	very abrasive		very abrasive
	abrasive		abrasive
	considerably abrasive		considerably abrasive
	moderately abrasive		moderately abrasive
	little abrasive		little abrasive
	not abrasive	=>	not abrasive

VOEST-ALPINE
BERGTECHNIK

SANDVIK

VOEST-ALPINE
Bergtechnik Ges.m.b.H.
Alpinestrasse 1
A-8740 Zeltweg/Austria
Tel.: +43 3577 755 234
+43 3577 755 823
Fax.: +43 3577 756 334
Email: uwe.restner@sandvik.com
karl-heinz.gehring@sandvik.com

RESULTS OF ROCK TEST

Test Report No.:	2003 / 039
Sample No.:	07
Report issued by:	Gehring, Hebenstreit, Restner
Date:	2003-06-13
Company / Country:	De Beers / ZA
Site:	Premier Mine
Location of Sampling:	BBIE 89 N / 35
Date of Sampling:	2003-05-15
Denomination of Rock:	TKB

Zeltweg, 2003-06-13 **Signature:**

Results of Rock Test: Page 2

MECHANICAL PROPERTIES

Test Report No.:	2003 / 039	Sample No.:	07
Report issued by:	Gehring, Hebenstreit, Restner	Date:	2003-06-13

Uniaxial compressive strength σ_c (5 specimen(s) H/D = 1)

min.: 41,14 MPa max.: 56,96 MPa average: **52,89** MPa

Brazilian tensile strength σ_t (5 specimen(s) H/D = 0.5)

min.: 2,32 MPa max.: 6,84 MPa average: **4,56** MPa

Young's modulus E_{stat} (5 specimen(s) H/D = 1)

min.: 7910 MPa max.: 11762 MPa average: **10417** MPa

Secant modulus E_{sec} (5 specimen(s) H/D = 1)

min.: 6583 MPa max.: 11762 MPa average: **9103** MPa

Linear strain ε (5 specimen(s) H/D = 1)

min.: 0,0047 mm/mm max.: 0,0066 mm/mm average: **0,0059** mm/mm

Fracture energy W_f (5 specimen(s) H/D = 1)

min.: 3,33 Nm max.: 5,47 Nm average: **4,49** Nm

Related values:				**For evaluation of:**
σ_c	: σ_t	=	**12**	Toughness
E_{sec}	: E_{stat}	=	**0,87**	Plasticity
E_{stat}	: σ_c	=	**197**	Relative elasticity
W_f	: σ_c	=	**0,08**	Specific fracture energy

Specific gravity: **2,69** g/cm^3

Rock classification with regard to its mechanical behaviour:

Strength	Toughness	Plasticity	Rel. Elasticity	Spec. Fract. Energy
very high	very tough	highly plastic	very high	very high
high	tough	plastic	high	high
> average	> average	> moderately plastic	average	average
moderate	brittle	not plastic	> low	low
low	very brittle		very low	> very low

Final classification of mechanical behaviour:

Related to uniaxial compressive strength average cuttability.

Special remarks:

Results of Rock Test: Page 3

PETROGRAPHICAL ANALYSIS AND ABRASIVITY

Test Report No.:	2003 / 039	Sample No.:	07
Report issued by:	Gehring, Hebenstreit, Restner	Date:	2003-06-13

Petrographical description (based on hand rock sample):

Remarks on alteration:

fresh

Mineral content:

Average grain size of quartz: mm (fictional, if there is no quartz content)

Content of hard minerals related to quartz: %

Abrasivity values:

$F_{SCHIMAZEK}$: $F_{CERCHAR}$(CAI): **0,79** (5 specimen(s))

Classification of rock with regard to abrasivity:

based on	$F_{SCHIMAZEK}$	based on	$F_{CERCHAR}$(CAI)
	extremely abrasive		extremely abrasive
	highly abrasive		highly abrasive
	very abrasive		very abrasive
	abrasive		abrasive
	considerably abrasive		considerably abrasive
	moderately abrasive		moderately abrasive
	little abrasive	=>	little abrasive
	not abrasive		not abrasive

APPENDIX 10

Rock testing results: Concrete Block VOEST-ALPINE Bergtechnik

VOEST-ALPINE
BERGTECHNIK

SANDVIK

VOEST-ALPINE
Bergtechnik Ges.m.b.H.
Alpinestrasse 1
A-8740 Zeltweg/Austria
Tel.: +43 3577 755 234
Fax.: +43 3577 756 334
Email: uwe.restner@sandvik.com

RESULTS OF ROCK TEST

Test Report No.:	2006 / 007
Sample No.:	04
Report issued by:	Hebenstreit
Date:	2006-03-07
Company / Country:	VAB / A
Site:	Large concrete testing block outside (separate block for cutting tests)
Location of Sampling:	TUNCONSTRUCT, Block # 4
Date of Sampling:	
Denomination of Rock:	Concrete (B 50 / B 500)

Mechanical Properties and Abrasivity *Page 2*

Zeltweg, 2006-03-07 **Signature:**

Results of Rock Test: Page 2

MECHANICAL PROPERTIES AND ABRASIVITY

Test Report No.:	2006 / 007	Sample No.:	04
Report issued by:	Hebenstreit	Date:	2006-03-07

Uniaxial compressive strength σ_c (5 specimen(s) H/D = 1)

Min.: 30,28 MPa Max.: 33,95 MPa Average: **32,20** MPa

Brazilian tensile strength σ_t (5 specimen(s) H/D = 0.5)

Min.: 2,44 MPa Max.: 3,50 MPa Average: **3,13** MPa

Young's modulus E_{stat} (5 specimen(s) H/D = 1)

Min.: 6596 MPa Max.: 12466 MPa Average: **10047** MPa

Secant modulus E_{sec} (5 specimen(s) H/D = 1)

Min.: 4136 MPa Max.: 6943 MPa Average: **5731** MPa

Linear strain ε (5 specimen(s) H/D = 1)

Min.: 0,0046 mm/mm Max.: 0,0081 mm/mm Average: **0,0058** mm/mm

Fracture energy W_f (5 specimen(s) H/D = 1)

Min.: 9,46 Nm Max.: 17,05 Nm Average: **12,04** Nm

Axial USW velocity v_p (5 specimen(s) H/D = 1)

Min.: 3366 m/s Max.: 4446 m/s Average: **4032** m/s

Density: **2,25** g/cm³

Related values:

				For evaluation of:
σ_c	: σ_t	=	**10**	Toughness
E_{sec}	: E_{stat}	=	**0,57**	Plasticity
E_{stat}	: σ_c	=	**312**	Relative elasticity
W_f	: σ_c	=	**0,37**	Demanded fracture energy

Strength	Toughness	Plasticity	Rel. elasticity	Dem. fract. energy
very high	very high	very high	very high	very high
high	high	**> high**	**> high**	**> high**
average	**> average**	average	average	average
> low	low	low	low	low
very low	very low	very low	very low	very low

Final classification of mechanical behaviour:

Related to uniaxial compressive strength decreased cuttability.

Rock abrasivity $F_{CERCHAR}$**(CAI)** (5 specimen(s))

Min.: 1,01 Max.: 2,69 Average: **1,73**

Classification of rock with regard to abrasivity:

extremely abrasive	very abrasive	**> considerably abrasive**	little abrasive
highly abrasive	abrasive	moderately abrasive	not abrasive

Special remarks: